

✓ u (2)



DTIC
ALERT
DEC 10 1991



ESCAPE STRATEGIES FOR TURBOPROP AIRCRAFT IN A MICROBURST WINDSHEAR

by

Richard B. Bobbitt

March 1991

Thesis Advisor:

Richard M. Howard

Approved for public release; distribution is unlimited.

91-17265

[illegible]

Unclassified

Security Classification of this page

REPORT DOCUMENTATION PAGE

1a Report Security Classification Unclassified			1b Restrictive Markings		
2a Security Classification Authority			3 Distribution Availability of Report Approved for public release; distribution is unlimited.		
2b Declassification/Downgrading Schedule			5 Monitoring Organization Report Number(s)		
4 Performing Organization Report Number(s)			7a Name of Monitoring Organization		
6a Name of Performing Organization Naval Postgraduate School		6b Office Symbol (If Applicable) 31	7b Address (city, state, and ZIP code)		
6c Address (city, state, and ZIP code) Monterey, CA 93943-5000			9 Procurement Instrument Identification Number		
8a Name of Funding/Sponsoring Organization		8b Office Symbol (If Applicable)	10 Source of Funding Numbers		
8c Address (city, state, and ZIP code)			Program Element Number	Project No	Task No
11 Title (Include Security Classification) ESCAPE STRATEGIES FOR TURBOPROP AIRCRAFT IN MICROBURST WINDSHEAR			Work Unit Accession No		
12 Personal Author(s) Richard B. Bobbitt					
13a Type of Report Master's Thesis		13b Time Covered 14 From To		Date of Report (year, month, day) March 1991	
15 Page Count 247					
16 Supplementary Notation The views expressed in this thesis are those of the author and do not reflect the official policy or position of the Department of Defense or the U.S. Government.					
17 Cost Codes			18 Subject Terms (continue on reverse if necessary and identify by block number)		
Field	Group	Subgroup	Microburst, windshear, aircraft performance, turboprop.		
19 Abstract (continue on reverse if necessary and identify by block number) A quantitative analysis was carried out on the performance of turboprop aircraft within a microburst windshear. The objective of the analysis was to provide specific flight procedures for optimal navigation through the windshear. The microburst windshear model used in the analysis embodied the severe characteristics of the microburst encountered by Delta Flight 191 during an approach to landing at Dallas/Ft. Worth, 2 August, 1985. Different escape strategies were tested using the flight performance characteristics of the U.S. Navy's P-3 "Orion" and T-44 "Pegasus" aircraft. The three flight phases investigated were approach to landing, takeoff, and the low altitude ASW mission. Results from the analysis were coupled with the pilot's view-point from which conclusions were drawn. The results of the analysis support a constant-pitch-angle escape procedure. The same procedural steps can be used for both aircraft in any configuration or situation with the difference being the degree of pitch to employ. The conclusions are in a format for integrating specific microburst escape procedures within the NATOPS programs for the P-3 and T-44 aircraft.					
20 Distribution/Availability of Abstract <input checked="" type="checkbox"/> unclassified/unlimited <input type="checkbox"/> same as report <input type="checkbox"/> DTIC users			21 Abstract Security Classification Unclassified		
22a Name of Responsible Individual Professor Richard M. Howard			22b Telephone (Include Area code) (408) 646-2870		22c Office Symbol AA/HO

DD FORM 1473, 84 MAR

83 APR edition may be used until exhausted

All other editions are obsolete

security classification of this page

Unclassified

Approved for public release; distribution is unlimited.

Escape Strategies for Turboprop Aircraft in Microburst Windshear

by

Richard B. Bobbitt
Lieutenant Commander, United States Navy
B.S., University of South Florida, 1978

Submitted in partial fulfillment of the requirements for the
degree of

MASTER OF SCIENCE IN AERONAUTICAL ENGINEERING

from the

NAVAL POSTGRADUATE SCHOOL
March 1991

Author:

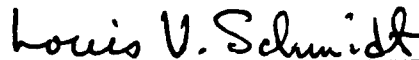


Richard B. Bobbitt

Approved by:



Richard M. Howard, Thesis Advisor



Louis V. Schmidt, Second Reader



**E. Roberts Wood, Chairman, Department of Aeronautics and
Astronautics**

ABSTRACT

A quantitative analysis was carried out on the performance of turboprop aircraft within a microburst windshear. The objective of the analysis was to provide specific flight procedures for optimal navigation through the windshear. The microburst windshear model used in the analysis embodied the severe characteristics of the microburst encountered by Delta Flight 191 during an approach to landing at Dallas/Ft. Worth, 2 August, 1985. Different escape strategies were tested using the flight performance characteristics of the U.S. Navy's P-3 "Orion" and T-44 "Pegasus" aircraft. The three flight phases investigated were approach to landing, takeoff, and the low altitude ASW mission. Results from the analysis were coupled with the pilot's view-point from which conclusions were drawn. The results of the analysis support a constant-pitch-angle escape procedure. The same procedural steps can be used for both aircraft in any configuration or situation with the difference being the degree of pitch to employ. The conclusions are in a format for integrating specific microburst escape procedures within the NATOPS programs for the P-3 and T-44.

Accession For	
DTIC TAB	
Unannounced	
Justification	
By	
Distribution/	
Availability Codes	
Avail and/or	
Dist	Special
A-1	

TABLE OF CONTENTS

I. INTRODUCTION	1
A. MICROBURSTS AND AVIATION	1
1. Microburst Definition	1
2. The Effect Of Microbursts On Aviation	4
3. Reducing The Hazard To Aviation	7
B. MICROBURST ESCAPE PROCEDURES	9
C. EFFECTS OF A MICROBURST ON FLIGHT INSTRUMENTS	11
D. PROBLEM STATEMENT	13
II. MATH MODELS AND EXPERIMENTAL DESIGN	15
A. MICROBURST WINDSHEAR MODEL	15
1. Vortex Ring Model Development	16
2. Windshear Model Fit	22
B. INERTIAL REFERENCE FRAME	29
1. Total Energy Concept	30
2. Equations of Motion	30
C. AIRCRAFT PERFORMANCE MODEL	32
D. CRITICAL FLIGHT PHASES MODELED	37
1. Landing Approach	37
2. Takeoff	39
3. P-3 On-Station	41

III. RESULTS AND DISCUSSION	43
A. WINDSHEAR AND INERTIAL REFERENCE MODEL VALIDATION ..	43
B. WEAKNESSES AND OTHER INDEPENDENT VARIABLES	48
C. DATA REDUCTION AND ANALYSIS	50
1. Approach to Landing Microburst Encounter Analysis	52
2. Takeoff Microburst Encounter Analysis	70
3. On-Station Encounter Analysis	88
D. OBSERVATIONS	90
1. Available Aircraft Flight Instruments	90
2. Optimal Escape Procedure	91
3. The Effect Of Specific Energy On Survival Probability	93
4. Stick Force vs. Off-Trim Airspeed For The P-3	94
5. Weight, Wing Loading, and Thrust to Weight Effects	95
6. Early Liftoff Speed For The P-3	96
8. Summary	97
IV. CONCLUSIONS	99
A. MICROBURST ESCAPE PROCEDURES FOR THE P-3	99
1. Approach To Landing Microburst Encounter	100
2. Takeoff Microburst Encounter	101
3. On-Station Loiter Microburst Encounter	102

B. MICROBURST ESCAPE PROCEDURES FOR THE T-44	103
1. Approach To Landing Microburst Encounter	103
2. Takeoff Microburst Encounter	105
V. RECOMMENDATIONS	106
A. ANALYSIS REFINEMENT AND CONTINUED RESEARCH	106
B. P-3 OPERATIONS AND FLIGHT CREW TRAINING	107
LIST OF REFERENCES	108
APPENDIX A. WINDSHEAR MODEL ALGORITHMS	110
APPENDIX B. PARAMETER SENSITIVITY ALGORITHM	121
APPENDIX C. LANDING APPROACH ALGORITHMS	136
APPENDIX D. TAKEOFF ALGORITHMS	158
APPENDIX E. ON-STATION ALGORITHMS	174
APPENDIX F. APPROACH TO LANDING ENCOUNTER GRAPHIC DATA ...	184
APPENDIX G. TAKEOFF ENCOUNTER GRAPHIC DATA	219
APPENDIX H. P-3 FLIGHT SIMULATOR DATA	227
INITIAL DISTRIBUTION LIST	238

TABLE OF SYMBOLS

C_D	coefficient of drag	S	aircraft lift reference area; ft ²
C_{D0}	coefficient of drag at zero angle of attack	T	thrust; lbf
C_L	coefficient of lift	t	time; sec
C_{L0}	coefficient of lift at zero angle of attack	V	equivalent airspeed; ft/s
$C_{L\alpha}$	lift curve slope; rad ⁻¹	V_{ref}	approach airspeed; KEAS
D	total drag; lbf	V_1	rotate airspeed; KEAS
E	aircraft total energy; ft-lbf	V_2	50ft target airspeed; KEAS
E_s	specific energy; ft	W	aircraft weight; lbf
g	gravitational constant; 32.175 ft/s ²	W_h	vertical wind; ft/s
h	altitude AGL; ft	W_x	horizontal wind; ft/s
K	lift drag constant	x	horizontal earth ref.; ft
KEAS	knots equivalent airspeed	α	angle of attack; rad
L	total lift; lbf	Δt	time increments; sec
m	aircraft mass; slugs	γ_a	airmass flight path angle; rad
Q	dynamic pressure; lbf/ft ²	γ_i	inertial flight path angle; rad
q	pitch rate; rad/s	θ	pitch angle; rad

I. INTRODUCTION

The microburst windshear is documented as a serious hazard to aviation. The microburst has been a contributing factor in several airline accidents in the past two decades. The seriousness of these events has lead to a significant amount of research on the effect of microbursts upon airline transport aircraft. However, little has been documented on the effect of a microburst on light-to-medium weight turbopropeller aircraft. The U.S. Navy operates a fleet of P-3 "Orion" turboprop aircraft in all-weather, long-range patrol missions. The P-3 aviation community requested a study of the effects of a microburst upon the aircraft's dynamic flight performance and the appropriate escape procedure if one were encountered. Training of the P-3 pilot starts in the T-44, a Beechcraft King Air twin turboprop. Therefore, the ultimate goal of this thesis was to derive viable microburst windshear escape procedures which can be incorporated into the Naval Air Training and Operating Procedures Standardization (NATOPS) Program for both the P-3 and the T-44 aircraft.

A. MICROBURSTS AND AVIATION

1. Microburst Definition

The microburst is a form of downburst windshear. Downbursts are associated with strong convective activity (namely

thunderstorms). Downbursts are formed by a cold air mass dropping from within a thunderstorm producing strong downdrafts. The downdraft turns outward as it approaches the earth. Fujita is a prominent pioneer in identifying and classifying this type of windshear [Ref. 1]. He defines the microburst as [Ref. 2:p. 8]:

A small downburst with its outburst, damaging winds extending only 4 km (2.5 miles) or less. In spite of its small horizontal scale, an intense microburst could induce damaging winds as high as 75 m/sec (168 mph).

Conclusions drawn from the Northern Illinois Meteorological Research on Downbursts (NIMROD) and Joint Airport Weather Studies (JAWS) [Ref. 2] programs show that the microburst structure consists of a down flow with a structure of one or more vortex rings as illustrated in Figure 1. The microburst may be wet or dry; precipitation may or may not be present in the downdraft. The design of a microburst structure was not understood, or even accepted as a viable phenomenon prior to 1982. Through the 1980s, meteorological researchers and airline accident investigators came to the conclusion that the microburst weather phenomenon is a significant hazard to aviation and has been a contributing factor in many airline accidents. The accumulation of the NIMROD and JAWS project results and inflight data conclusively shows that ring vortex flow is prevalent in microburst windshear [Ref. 3].

Microburst windshear is uniquely different from other types of windshear. The other prevalent type of windshear hazard to aviation is the thunderstorm gustfront [Ref. 4]. A gustfront windshear is associated with massive settling of rain-cooled air resulting from thunderstorm activity. A sudden wind-shift with gusty conditions that precedes a thunderstorm is characteristic of a gustfront. The main difference between a gustfront and a microburst is the size of the area effected. A gustfront is widespread

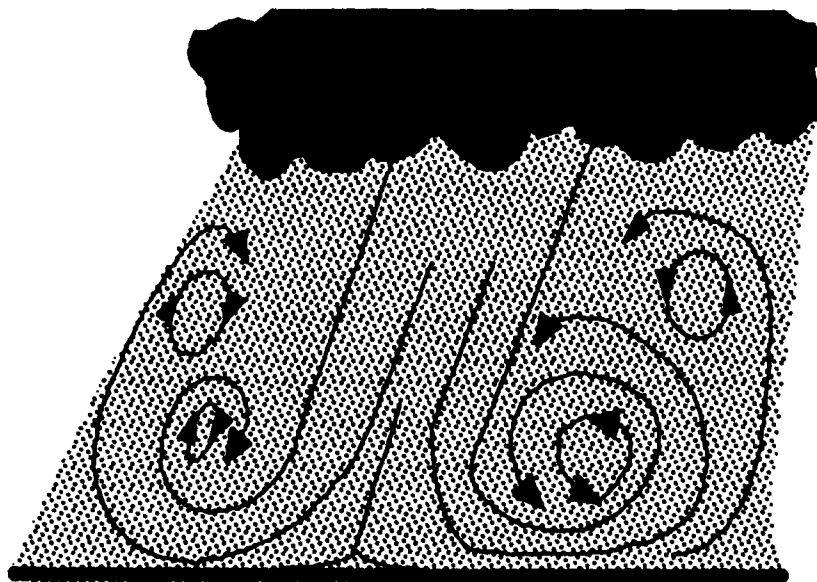


Figure 1. Wind streamlines characteristic of a microburst.

across the face of one or more thunderstorms. A microburst is small and isolated within convective activity. The local magnitude of the horizontal and vertical windshear is what matters to an aircraft penetrating convective activity. Although smaller, a microburst can be much more of a detriment to an aircraft's flight performance.

2. The Effect Of Microbursts On Aviation

The aviation community has always been aware of the potential danger of windshear. Classification of different types was not addressed until 1976, when The Federal Aviation Administration (FAA) published an advisory circular discussing the effects of windshear on flight performance. It was updated in 1979 [Ref. 5] where the term "downburst" was used to describe a strong downdraft associated with the center of a thunderstorm. There was considerable debate on the hazard of the downburst. Many argued that the downdraft rapidly weakened as it approached the ground. The research by Fujita provided overwhelming evidence to the contrary, thereby defining the microburst. By the mid-eighties, the term "microburst" was readily being used by the aviation community. However, the potential effect of a microburst upon aircraft performance was not readily understood by aircrew.

The danger of a microburst became very apparent following the crash of Delta Flight 191 (DAL 191) at Dallas/Ft. Worth, August 2, 1985. The crash ensued following the penetration of a thunderstorm during the approach to landing. The aircraft involved was a Lockheed L-1011, a three engine heavy airline transport aircraft. The National Transportation Safety Board (NTSB) investigating the DAL 191 accident published in their report the following [Ref. 6:p. 81]:

The National Transportation Safety Board determines the probable causes of the accident were the flight crew's decision to initiate and continue the approach into a cumulonimbus cloud which they observed to contain visible lightning; the lack of specific guidelines, procedures, and training for avoiding and escaping low-altitude windshear; and the lack of definitive, real-time windshear hazard information. This resulted in the aircraft's encounter at low altitude with a microburst-induced, severe windshear from a rapidly developing thunderstorm located on the final approach course.

Several pertinent questions arise from this conclusion. Airlines routinely fly through "bad" weather every day. How do a flight crew and Air Traffic Control (ATC) authorities recognize microburst type weather? Can any aircraft navigate successfully through a microburst or is it beyond the performance capabilities of the average airliner? Is there a significant departure between normal piloting techniques and microburst escape procedures? A large amount of research has been done to answer these questions. However, the focus has been directed predominantly toward airline transport aircraft.

The advent of Digital Flight Data Recorders (DFDR) provided conclusive evidence of the structure and the potential effects of a microburst windshear on aircraft. The DFDR records the last 30 minutes of voice transcripts, as well as several aircraft performance parameters. Aircraft body axis angles and accelerations, airspeed, altitude, and time are a few of the recorded parameters. These records allow the reconstruction of the wind field vectors encountered

by the aircraft [Ref. 7]. DAL 191 was equipped with a DFDR. American Airline Flight 539 (AA 539) followed DAL 191 and penetrated the same convective weather 110 seconds later [Ref. 6] as depicted in Figure 2. This second aircraft was a McDonnell/Douglas MD-80, also equipped with a DFDR. The availability of digital flight data allowed a comprehensive database to be built on the wind field generated by that microburst.

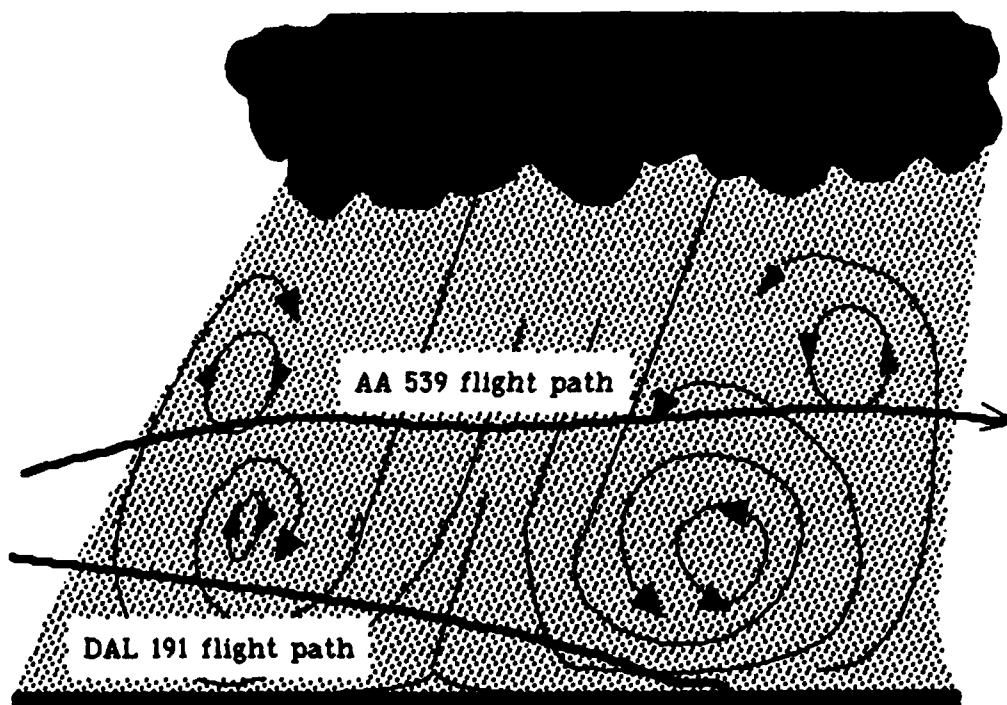


Figure 2. Flight paths of the two airlines through the Dallas/Ft. Worth microburst.

The center of the thunderstorm activity was located approximately 10,300 feet from the approach end of Runway 17L at Dallas/Ft. Worth Airport. The DFDR data show that DAL 191 initially encountered a headwind followed by a very abrupt tailwind [Ref. 7].

A significant downward airflow also accompanied the horizontal windshear which resulted in a loss of airspeed accompanied by a sharp nose down pitch. A very high sink rate resulted. The aircraft exited the bottom of the thunderstorm approximately 100 feet above ground level (AGL). Ground impact ensued with the aircraft in a slight nose up attitude and at a high airspeed [Ref 5].

In retrospect, several previous airline accidents can be attributed to windshear of this nature. Fujita had analyzed several takeoff and landing airline accidents involving windshear prior to the DAL 191 crash [Ref. 2]. However, the Dallas/Ft. Worth accident showed the need to address the microburst hazard and gain a more thorough understanding of how to alleviate the danger.

3. Reducing The Hazard To Aviation

One approach to reducing the hazard of a microburst on aviation is recognition and avoidance. This solution is very difficult given available aviation weather avoidance equipment. The primary windshear equipment available today is the aircraft weather radar and ground based Low Level Windshear Alerting System (LLWAS). On-board weather radar provides a picture of the amount of convective activity ahead, but cannot recognize microburst activity. Ground based LLWAS provides warning when wind speed sensors

located about the airfield measure significantly different wind vectors. However, the microburst must occur at the location of the LLWAS system. An LLWAS system was installed at the Dallas/Ft. Worth airport at the time of the DAL 191 accident. The microburst occurred on the final landing approach corridor two miles from the center of the airport. Because of the location of the LLWAS sensors around the airport perimeter, the system did not give any windshear warning prior to the accident. An LLWAS alert was sounded as the thunderstorm passed overhead the airfield several seconds *after* DAL 191 crashed. Neither weather radar nor LLWAS provide real-time information on microburst windshear.

Very recent technology has produced some viable, and expensive, means to recognize and avoid related microburst weather activity. Ground based Doppler Radar has been successfully proven at Denver's Stapleton airport [Ref. 8]. On-board forward looking devices such as infrared sensors, lasers, and doppler radar are being developed to provide several seconds of warning prior to a microburst encounter. But until avoidance systems are made readily available, survival of a microburst encounter will be dependent on the use of a successful escape procedure by the flight crew.

The second approach in reducing the microburst hazard is developing viable escape procedures. Research has shown that quick recognition of a microburst encounter is paramount. The reaction time of a flight crew coupled with the type of escape maneuver will govern the success of escape [Ref. 9]. The escape procedure the flight crew executes depends on the flight phase and configuration of the aircraft. Much research has been performed concerning aircraft performance and escape procedures with the focus on airline transport aircraft operations to be described below.

B. MICROBURST ESCAPE PROCEDURES

A large amount of research has been done on defining the optimal escape maneuvers for airline transport aircraft. Much of that research is based upon control theory. Comparisons of different flight strategies for microburst encounters have been addressed [Ref. 10, Ref. 11]. The total energy concept is readily used to compare the outcomes of different maneuvers [Ref. 12, Ref. 13]. One very important aspect in determining the optimal escape procedure is the ability of a flight crew to execute the appropriate maneuver utilizing the available flight performance information available.

The FAA has generated an exhaustive Windshear Training Aid [Ref. 14] aimed at modern day transport aircraft. It addresses the crew training requirements and suggests viable microburst escape strategies. Analytical research, as well as tried and tested procedures, have verified the suggestions presented by the FAA. All the major airlines have incorporated microburst recognition and escape into their recurrent training. The majority of the civil flight simulators possess some degree of windshear emulating a microburst. As of today, the aviation community recognizes the microburst as a aviation hazard and has taken significant steps in reducing the vulnerability.

The different escape strategies fall within three general categories:

- 1) Optimum aircraft performance through the airmass.
- 2) Optimum aircraft performance related to an inertial reference.
- 3) A combination of the two.

Optimum aircraft performance is defined as the performance providing the largest cushion of escape from a microburst encounter. The parameters measured for evaluating an escape strategy's outcome, are airspeed and altitude gained (or lost).

The first category includes maneuvers that trade altitude for airspeed. The second category uses measured data such as body axis

acceleration and windshear magnitude in calculating the optimal flight path [Ref. 12, Ref. 10, and Ref. 11]. Obviously the second category requires significant airborne computing capabilities not normally available. The FAA's Windshear Training Aid recommends an escape strategy that falls within the third category. The recommendation is to maintain a constant pitch attitude with maximum engine thrust applied. In general, increasing pitch attitude *toward* a 15° pitch angle shows optimal performance on most of the large airline transport aircraft. The constant pitch attitude is maintained with disregard to airspeed.

C. EFFECTS OF A MICROBURST ON FLIGHT INSTRUMENTS

How a flight crew perceives and navigates through a microburst encounter is strongly influenced by their flight instrument indications. The primary flight instruments available to pilots are:

- 1) Attitude Indicator (AI) - a gyroscopic/inertial stabilized aircraft attitude indicator. Modern design allows accurate attitude information in the highest levels of turbulence.
- 2) Airspeed Indicator - a pitot/static system instrument which displays airspeed in knots. It is sensitive to airmass pressure changes and position error.
- 3) Pressure Altimeter - a static system instrument which relates altitude, in feet, to static pressure. It is sensitive to airmass pressure changes.

- 4) Vertical Speed Indicator (VSI) - a static system instrument which measures the change in static pressure in feet per minute. It is unreliable in turbulence due to mechanical and pressure lag.

All aircraft have these primary instruments. Inertial navigation and true airspeed computers do provide other flight performance references usually through flight directors. However, the majority of the flight stations rely primarily on the basic flight instruments.

Microbursts are always associated with some degree of turbulence. Also, pressure differentials can be expected within convective activity. Ground and airborne data show that the pressure within a microburst varies about ± 3 millibar [Ref. 2, Ref. 3]. This pressure change equates to about ± 80 feet in altimeter variation.

The attitude indicator will be the flight instrument least affected by microburst atmospherics. This instrument will always give reliable aircraft attitude information. Due to the minor static pressure changes, the airspeed indicator and altimeter can still be relied upon as performance instruments. The airspeed indicator will be one of the primary instruments to indicate a windshear penetration. The VSI would probably be erratic and unreliable due to turbulence and instrument lag.

There exists a means of measuring angle-of-attack (AOA) in most larger aircraft. Transport aircraft utilize AOA as a stall warning device (stick shaker). Navy aircraft incorporate a means to read AOA in units. AOA measuring devices may have a high damping factor in their measurement, resulting in substantial lag during turbulent conditions. Therefore, AOA indication may not be a reliable performance indicator during a microburst encounter.

D. PROBLEM STATEMENT

The P-3 has no means to recognize and then avoid microburst windshear. It must rely solely on escape. The published guidelines for microburst escape are based upon airline transport aircraft which significantly differ from the P-3. In this study, the results of different escape procedures based upon the available flight instruments are compared using the parameters of altitude, airspeed, and specific energy. Characterizing the effect of a microburst windshear upon the aircraft's performance followed by the implementation of the appropriate escape procedure form the objective for the research. The final conclusions must provide viable escape procedures that are based upon the primary flight instruments.

The microburst windshear model selected must conform to a known, measured phenomenon. The windshear experienced by DAL 191 provided a suitable database for emulation.

A series of equations of motion for the aircraft were developed and designed to be controlled through pitch angle and thrust inputs. These two parameters emulate the pilot's available flight control inputs.

Three flight phases critical to a microburst encounter were considered. Approach to landing, takeoff, and on-station (P-3 only) phases require operation low to the ground in all-weather conditions. Viable escape procedures using attitude, airspeed, altitude, and angle of attack were analyzed for all three flight phases.

Three questions were considered for each flight phase:

1. What is the optimum microburst escape procedure given available flight information to the pilot?
2. Does the optimum escape procedure change with gross weight or available thrust?
3. What flight instrument indications, flight control feeling, and dynamic response would be expected during the optimum escape maneuver?

Viable microburst escape procedures were derived for the P-3 and T-44 aircraft.

II. MATH MODELS AND EXPERIMENTAL DESIGN

This analysis is based upon mathematical representations of microburst windshear and aircraft performance. Microburst windshear, inertial reference, aircraft performance, and critical flight phases form the major segments of the total algorithm suite. Most of the mathematical simulation performance was carried out on a Macintosh SE computer utilizing MatLab software.

A. MICROBURST WINDSHEAR MODEL

A double ring vortex was chosen to emulate microburst windshear. Fujita [Ref. 2:p. 14] demonstrated that the microburst was a settling airmass with vortices generated near the earth. This phenomenon produces varying degrees of three-dimensional windshear when close to the earth's surface. Figure 1 showed the general concept of a microburst.

A strong microburst windshear was experienced at Dallas/Ft. Worth on August 2, 1985. A Delta Airlines L-1011 (DAL 191) crashed while on final approach during a microburst windshear encounter. An American Airlines MD-80 (AA 539) performed a missed approach 110 seconds following the DAL 191 crash. Both aircraft were equipped with DFDRs which register a time history of the aircraft's parameters. Body axis accelerations, velocities, and Euler-angle

values were used to calculate the flow-field winds generated from the microburst. Wingrove and Bach [Ref 7] provided the analytical means to calculate the windshear. From these data, an insight was gained of the magnitude and characteristics of the windshear.

A double-vortex-ring model was chosen for the windshear model. Schultz [Ref. 15] devised a double-vortex-ring mathematical model which closely approximated the windshear experienced by the AA 539 flight. The aircraft flew through the microburst windshear at 2500 feet AGL. The original algorithm was developed and tested against recorded flight data. The double-vortex-ring algorithm was modified in the current study with the addition of source flows to better fit low altitude windshear. This modified windshear model was fit to the DAL 191 flight data by the application of a parameter sensitivity scheme. Ring location and vortex intensity were found to differ from the AA 539 model. However, a multiple microburst structure can be expected during strong convective activity [Ref. 2:p. 35]. MatLab® programing was utilized in this study and is listed in Appendix A.

1. Vortex Ring Model Development

The development of this vortex ring model comes directly from the work of Schultz [Ref. 15]. Source flow was integrated into this algorithm to more closely match the DAL 191 windshear. The wind component in the y direction was not considered in the current

model. The y component is not easily modeled by symmetric vortex rings [Ref. 15] and has no direct impact on the longitudinal dynamics of an aircraft. Figure 3 illustrates the geometric aspects of the vortex ring model. Imaging of the vortex rings leads to inviscid ground effect upon the wind field. The wind field becomes horizontal

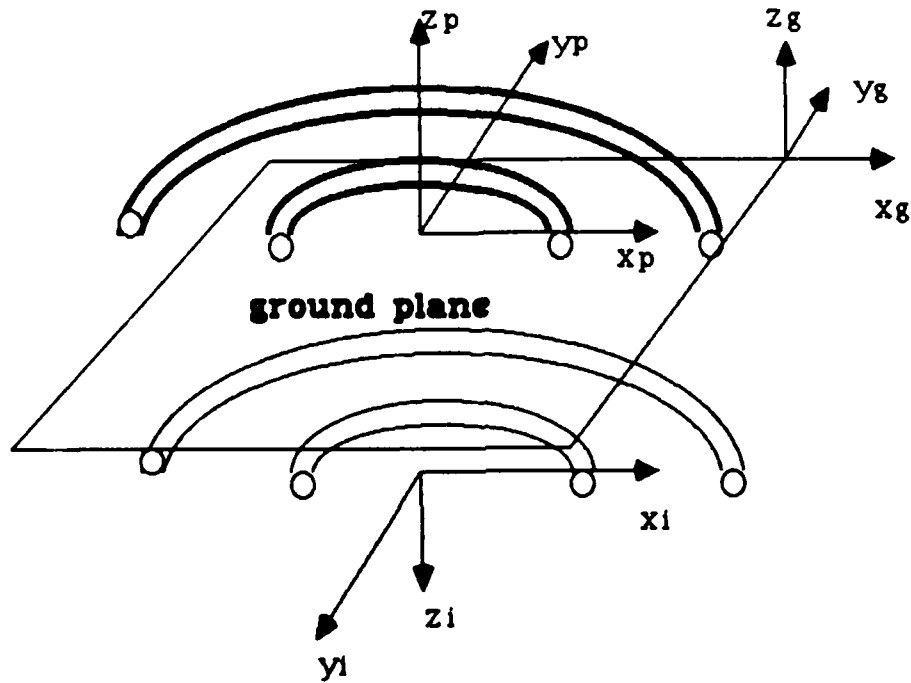


Figure 3. Vortex ring mathematical representation.

next to the ground plane as seen in nature. Boundary layer effects were neglected in this model. Bowles and Oseguera have performed research in boundary layer effects on windshear [Ref. 16]. From Figure 3, the following relationships can be seen to hold:

$$\begin{bmatrix} x \\ y \\ z \end{bmatrix}_P = \begin{bmatrix} x \\ y \\ z \end{bmatrix}_G - \begin{bmatrix} x_0 \\ y_0 \\ z_0 \end{bmatrix}_G \quad (1)$$

$$\begin{bmatrix} x \\ y \\ z \end{bmatrix}_I = \begin{bmatrix} x \\ y \\ -z \end{bmatrix}_G - \begin{bmatrix} x_0 \\ y_0 \\ z_0 \end{bmatrix}_G \quad (2)$$

$$\begin{bmatrix} v_x \\ v_y \\ v_z \end{bmatrix}_G = \begin{bmatrix} v_x \\ v_y \\ v_z \end{bmatrix}_P + \begin{bmatrix} v_x \\ v_y \\ -v_z \end{bmatrix}_I \quad (3)$$

where G, P, and I are ground, primary, and image reference respectively. The velocity components for each vortex were obtained by differentiating the vortex ring stream function ψ :

$$\begin{aligned} v_x &= \frac{x}{r} \frac{1}{r} \frac{\partial \psi}{\partial z} \\ v_y &= \frac{y}{r} \frac{1}{r} \frac{\partial \psi}{\partial z} \\ v_z &= -\frac{1}{r} \frac{\partial \psi}{\partial r} \end{aligned} \quad (4)$$

where r is the radial distance from the z axis:

$$r = \sqrt{x^2 + y^2} \quad (5)$$

The stream function for a vortex ring filament was obtained from the evaluation of an elliptical integral [Ref. 15]:

$$\psi = \frac{\kappa}{2\pi} (r_1 + r_2) \frac{0.788\lambda^2}{0.25 + 0.75\sqrt{1-\lambda^2}} \quad (6)$$

where r_1 and r_2 represent the closest and farthest distances to the point of interest from the ring's filament; κ is the ring filament

strength; and λ is a scaling term. Their algebraic relationships are as follows:

$$r_1 = \sqrt{z^2 + (r - R)^2} \quad (7)$$

$$r_2 = \sqrt{z^2 + (r + R)^2} \quad (8)$$

$$\lambda = \frac{r_2 - r_1}{r_2 + r_1} \quad (9)$$

where R is the radius of the filament.

Equation 6 was differentiated to obtain expressions for $\frac{\partial \varphi}{\partial r}$ and

$\frac{\partial \varphi}{\partial z}$:

$$\frac{\partial \varphi}{\partial r} = 0.788\delta_1(\eta_1 - \eta_2) - 0.394\lambda\delta_1(\eta_1 + \eta_2) + \delta_2[(\eta_1 - \eta_2) - \lambda(\eta_1 + \eta_2)] \quad (10)$$

$$\frac{\partial \varphi}{\partial z} = \delta_1(0.788\sigma_2 - 0.394\lambda\sigma_1) + \delta_2(\sigma_2 - \lambda\sigma_1) \quad (11)$$

where $\eta_1, \eta_2, \sigma_1, \sigma_2, \delta_1, \delta_2$, and λ are:

$$\eta_1 = \frac{r + R}{r_2} \quad (12)$$

$$\eta_2 = \frac{r - R}{r_1} \quad (13)$$

$$\sigma_1 = \frac{z}{r_2} + \frac{z}{r_1} \quad (14)$$

$$\sigma_2 = \frac{z}{r_2} - \frac{z}{r_1} \quad (15)$$

$$\delta_1 = \frac{\kappa \lambda}{\pi \tau} \quad (16)$$

$$\delta_2 = \frac{0.2955 \kappa \lambda^3}{\pi \tau^2 \sqrt{1 - \lambda^2}} \quad (17)$$

$$\tau = 0.75 \sqrt{1 - \lambda^2} + 0.25 \quad (18)$$

Equations 10 and 11 were substituted into Equation 4 to get the individual velocity components produced by each ring at a given point in space (with respect to the ground reference).

A velocity damping factor (ζ) was calculated for each ring to prevent erroneously high values of velocity near the filament cores. The value ranged from zero to one; it is zero when the point of interest is at the viscous core and approaches one at increased distances. The algebraic relationship for ζ is as follows [Ref. 15]:

$$\zeta_i = (1 - \exp\left[-\frac{r_{1i}^2}{\delta_i^2}\right]) \quad (19)$$

where r_{1i} is the closest distance from the point of interest to the i th ring's viscous core. Schultz obtained the weighting factors, ξ and ρ , by a visual comparison of the vortex ring strength and through a parameter estimation scheme [Ref. 15]. A total damping factor (Z) is obtained for the point of interest from the product of the damping factors for each of the four vortex rings:

$$Z = \prod_{i=1}^4 k_i \quad (20)$$

The low altitude windshear model required the addition of two point source flows located 10,000 feet above and below the ground plane at the center of the microburst. The radial flow is represented by the following expression:

$$V_r = \frac{\Lambda}{2\pi R_i} \quad (21)$$

where Λ is the source strength and R_i is the radial distance from the point source to the point of interest. The horizontal and vertical wind vectors contributions are estimated by:

$$\begin{aligned} V_{x_i} &= V_{r_i} \left(\frac{x}{R_i} \right) \\ V_{z_i} &= V_{r_i} \left(\frac{h}{R_i} \right) \end{aligned} \quad (22)$$

Combining the upper and lower (mirror image) sources produce:

$$\begin{aligned} V_x &= \frac{\Delta_x}{2\pi} \left(\frac{x}{R_1^2} + \frac{x}{R_2^2} \right) \\ V_z &= \frac{\Delta_z}{2\pi} \left(\frac{10,000 + h}{R_2^2} - \frac{10,000 - h}{R_1^2} \right) \end{aligned} \quad (23)$$

In summary, wind velocity for a point of interest in space referenced to earth was calculated in the following manner:

- 1) X (horizontal) and z (altitude) positions, measured in feet, are inputs for Equation 4. Calculations are made for the four vortex rings (large primary, small primary, large

image, and small image). A horizontal wind velocity (v_{x_i}) and a vertical wind velocity (v_{z_i}) are calculated for each ring.

- 2) A damping factor (ζ_i) was calculated for each ring using Equation 19.
- 3) The induced velocities for each ring were added and multiplied by the total velocity damping factor (Z):

$$W_x = \prod_{i=1}^4 \zeta_i \left[\sum_{i=1}^4 v_{x_i} \right] \quad (24)$$

$$W_h = \prod_{i=1}^4 \zeta_i \left[\sum_{i=1}^4 v_{z_i} \right] \quad (25)$$

where W_x and W_h are windshear values (ft/s).

- 4) For the low altitude model, the source flow velocities were added to the vortex velocities to give the final horizontal and vertical windshear components.

2. Windshear Model Fit

The unmodified double vortex windshear model was applied to AA 539 flight data by Schultz, using a parameter minimization scheme to fit the double-vortex-ring model to the actual DFDR data. Table 1 lists the parameters varied and the final results. Schultz concluded that the difference between the model results and recorded wind data was an rms (root mean square) of 16 ft/s for the entire system. Figure 4 shows the comparison of recorded winds to the model prediction.

The AA 539 windshear model was fit in the current study for model verification only. The windshear that DAL 191 encountered was the windshear to emulate. This windshear model was used to

TABLE 1. 2500 FEET ALTITUDE WINDSHEAR MODEL PARAMETERS

parameter	large ring	small ring
ring radius, ft	8503.3	1701.7
core radius, ft	20004.1	323.9
ring circulation, ft^2/s	431968.8	57204.9
x position, ft	0.0	50.0
y position, ft	3350.4	830.9
z position, ft	3400.6	2333.6

analyze aircraft performance during takeoff and landing flight segments. Therefore, the double-vortex-ring model was modified by the parameters listed in Table 2. The data from DAL 191 showed that

TABLE 2. LOW ALTITUDE WINDSHEAR PARAMETERS

parameter	large ring	small ring
ring radius, ft	7000	1300
core radius, ft	2004.1	323.9
ring circulation, ft^2/s	431968.8	131571.3
x position, ft	2500.0	300.0
y position, ft	-300.0	1.0
z position, ft	3400.6	800.0
x dir. source strength	1355396 ft^2/s	
z dir. source strength	3049200 ft^2/s	

the two rings were not concentric about the center [Ref. 3]. The small vortex ring was lower to the ground and displaced in the x direction from the large ring. Point source flows located 10,000 feet above and below the surface plane were added to the double-vortex-ring model to increase the outflow. A simple parameter sensitivity

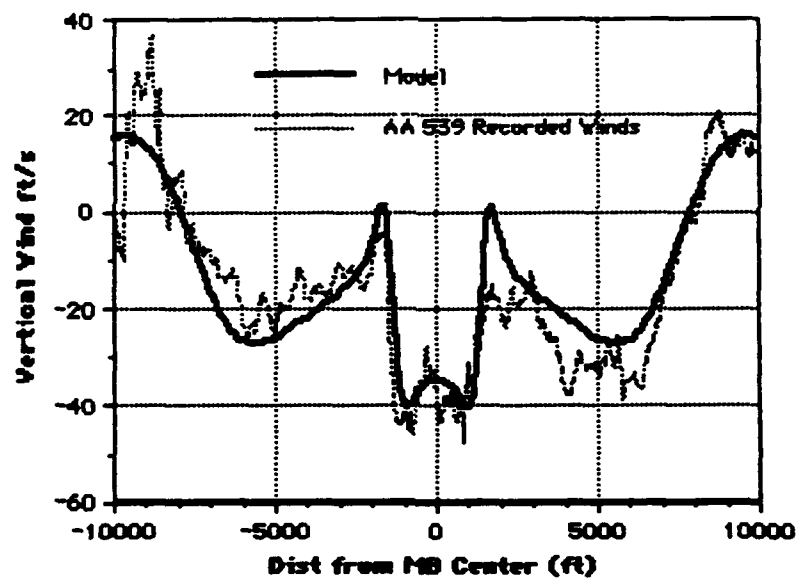
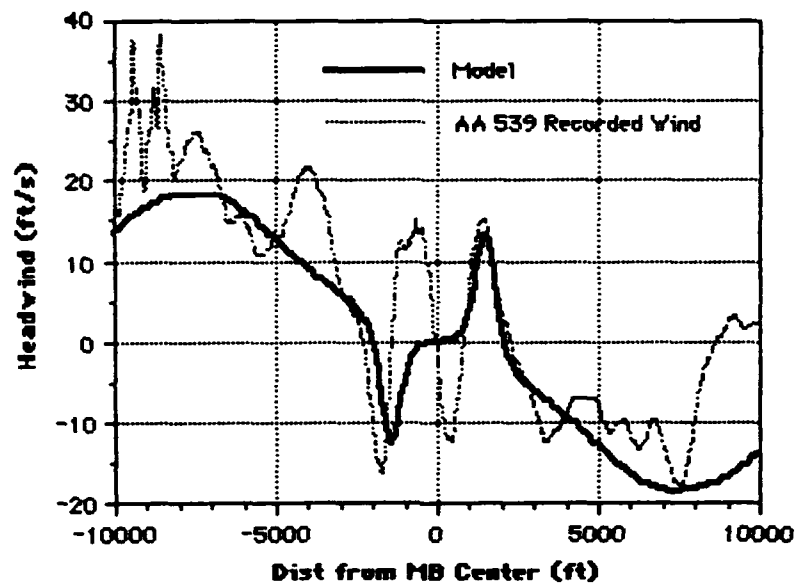


Figure 4. Vortex ring model comparison to recorded flight data [Ref. 3].

scheme was then used to estimate the parameters that best fit the modified windshear model to the recorded DAL 191 flight data.

The sensitivity scheme (listed in Appendix B) used an iterative process of varying each parameter individually, then calculating the x direction, z direction, and total system rms difference between model and recorded winds. The initial parameter matrix was built up as an 8x3 matrix. The center column was composed of the "best guess" values. Columns one and three were values obtained from an interval surrounding the initial guess value. First guess parameters, including the corresponding intervals, were obtained by graphical comparison of model and recorded data. The parameter matrix was refined after each successive run of the sensitivity scheme. Final parameter resolution was less than 3% change for the total system rms. Table 2 lists the best-fit parameters to the DAL 191 flight windshear measurements. Figure 5 is a graphical representation of the current model's vortex rings and source flow point relative locations. The wind vectors produced from the model are shown in Figure 6. Figure 7 compares the model windshear with the measured wind velocities from DAL 191.

Total system rms was calculated as 16.5 ft/s for the microburst windshear model. The final model shows a close approximation of an actual microburst, serving as a good windshear model for testing aircraft performance during low-level encounters.

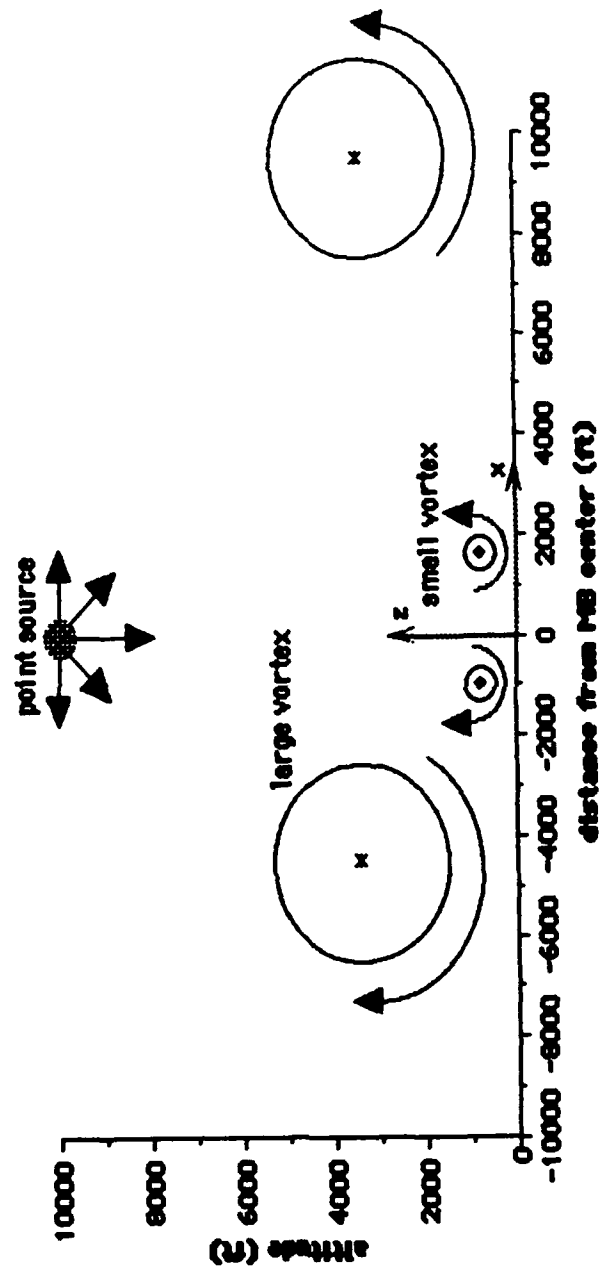


Figure 5. Geometric relationship of the vortex rings and point source within the microburst model.

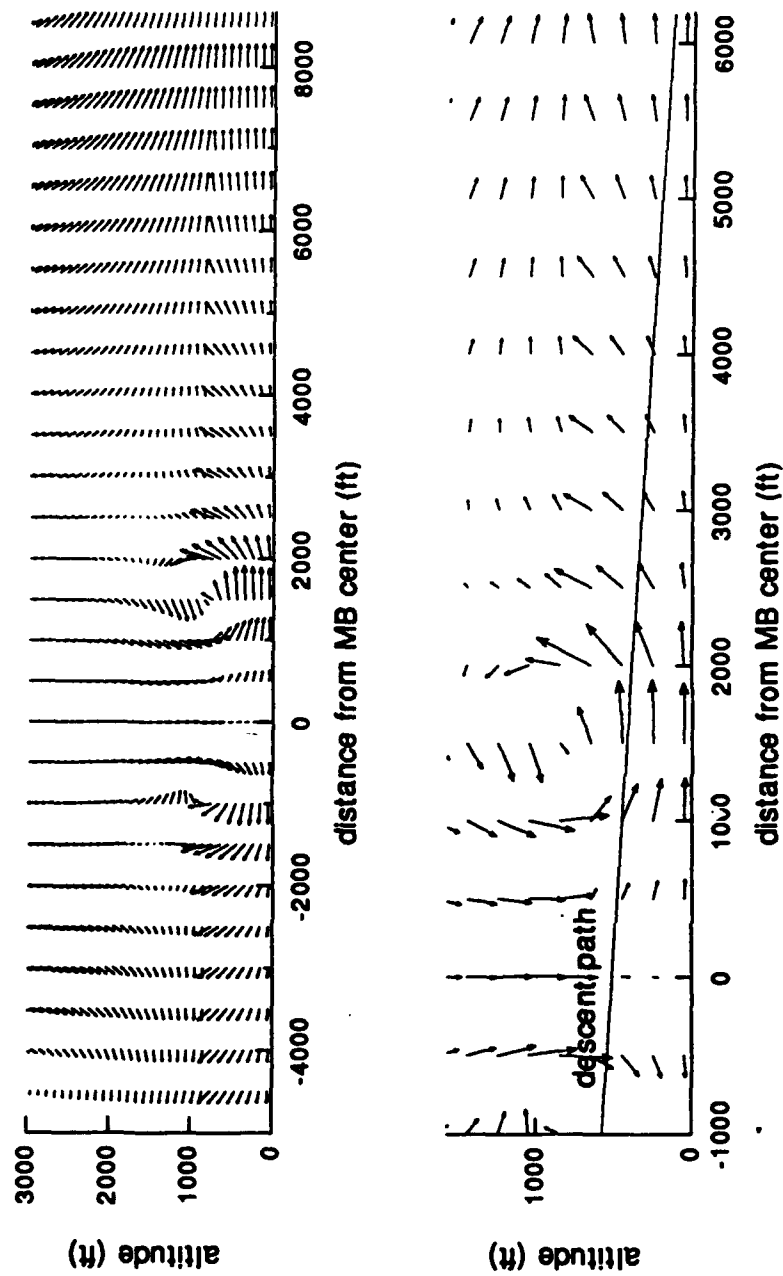


Figure 6. Vector plots of the wind-fields generated by the microburst windshear model.

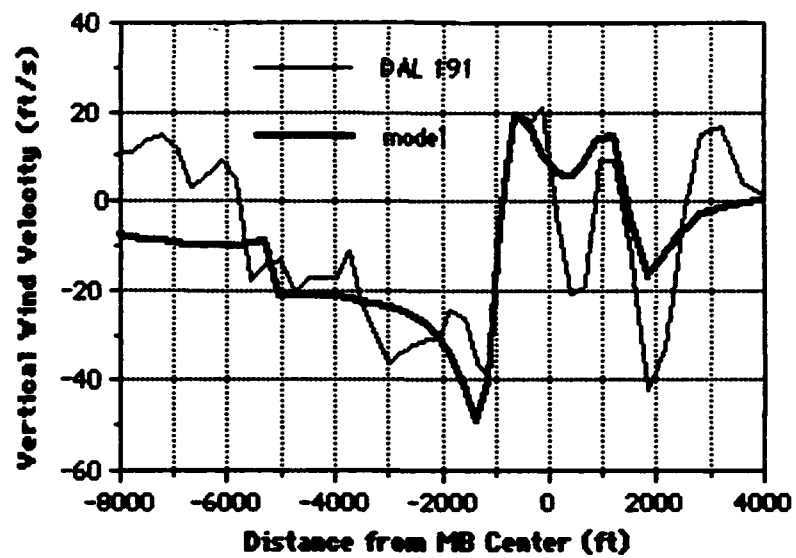
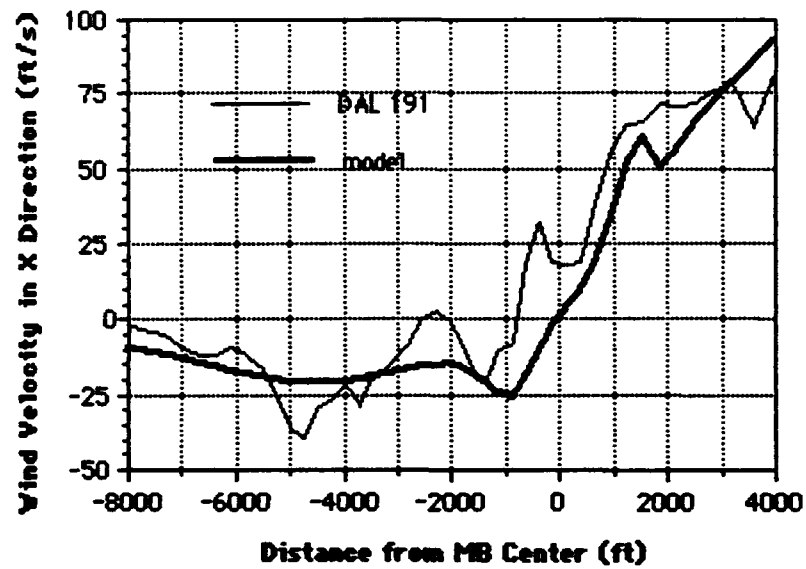


Figure 7. DAL 191 recorded winds compared to mathematical model.

B. INERTIAL REFERENCE FRAME

The concept of aircraft specific energy was used to compare the outcomes of different windshear escape strategies. The aircraft's total energy is defined as the sum of the airmass-relative kinetic energy and the inertial potential energy. A vectorial relationship of an aircraft's motion through the airmass is presented in Figure 8. A

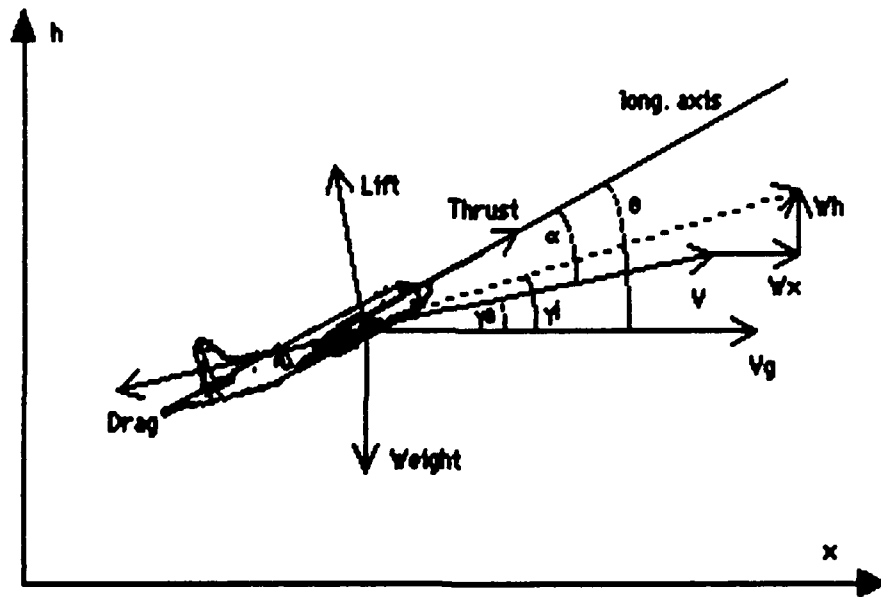


Figure 8. Inertial reference coordinate system.

set of coupled, non-linear differential equations can be developed from this vectorial relationship. These differential equations can be solved numerically where specific energy can be determined at any point in inertial space.

1. Total Energy Concept

The aircraft's altitude and airspeed at any given point can be used to determine total energy from the following relationship:

$$E = \frac{1}{2}mV^2 + mgh \quad (26)$$

where m is mass, V is airspeed, and h is the altitude. The specific energy (sometimes called energy height), E_s , is defined by:

$$E_s = \frac{V^2}{2g} + h \quad (27)$$

The time rate of change of specific energy is equal to aircraft acceleration plus rate of climb. Differentiating Equation (27) with respect to time gives specific power:

$$\dot{E}_s = V \left(\frac{\dot{V}}{g} \right) + \dot{h} \quad (28)$$

Values for V , \dot{V} , h , and \dot{h} can be obtained at any instant of time from the relevant equations of motion.

2. Equations of Motion

The relationship of an aircraft's motion through a moving air mass relative to earth leads to the development of six coupled, non-linear equations [Ref. 12]. Using the coordinate system in Figure 8, the following equations of motion evolve:

$$\dot{x} = V \cos \gamma_a + W_x \quad (29)$$

$$\dot{h} = V \sin \gamma_a + W_h \quad (29)$$

$$\dot{W}_x = \frac{\partial W_x}{\partial x}(\dot{x}) + \frac{\partial W_x}{\partial h}(\dot{h}) + \frac{\partial W_x}{\partial t} \quad (30)$$

$$\dot{W}_h = \frac{\partial W_h}{\partial x}(\dot{x}) + \frac{\partial W_h}{\partial h}(\dot{h}) + \frac{\partial W_h}{\partial t} \quad (31)$$

$$\dot{V} = \frac{T}{m} \cos \alpha - \frac{D}{m} - g \sin \gamma_a - \dot{W}_x \cos \gamma_a - \dot{W}_h \sin \gamma_a \quad (32)$$

$$\dot{\gamma}_a = \frac{T}{mV} \sin \alpha + \frac{L}{mV} - \frac{g}{V} \cos \gamma_a + \frac{\dot{W}_x}{V} \sin \gamma_a - \frac{\dot{W}_h}{V} \cos \gamma_a \quad (33)$$

Note that $\frac{\partial W_x}{\partial t}$ and $\frac{\partial W_h}{\partial t}$ were set equal to zero due to steady state conditions being assumed for the windshear model. This assumption is valid due to the minimal time the airplane is exposed to the microburst (30 to 60 sec.). Note that the equations are for point mass analysis. No dynamic cross-coupling is considered.

The equations of motion were solved using a predictor-corrector numerical scheme. Euler First-Forward, Euler Half-Step and Richardson Extrapolation [Ref. 17] were combined in the following manner:

$$y_{n+1}^{(1)} = y_n + \Delta t \dot{y}_n \quad (34)$$

$$y_{n+1/2}^{(1)} = y_n + \frac{\Delta t}{2} \dot{y}_n \quad (35)$$

$$y_{n+1}^{(2)} = y_{n+1/2}^{(1)} + \frac{\Delta t}{2} \dot{y}_{n+1/2} \quad (36)$$

$$y_{n+1} = 2y_{n+1}^{(2)} - y_{n+1}^{(1)} \quad (37)$$

Second-order accuracy is expected from this numerical scheme. By providing input values for aircraft constants and initial values for the inertial reference, the equations of motion were solved to obtain the aircraft performance.

C. AIRCRAFT PERFORMANCE MODEL

A MatLab® program was written to take aircraft performance parameters and use the set of motion equations to measure aircraft response in the windshear. Initial values were determined from aircraft performance parameters and the initial position. Iteration of the set of motion equations was based upon the time interval chosen. Values for x , h , V , \dot{V} , α , θ , γ_i , γ_a , E_s , and \dot{E}_s were tabulated after each iteration. The control of the model was taken from a pilot's point of view. The controlling variables were θ (deck angle or pitch angle) and T (thrust). Both variables can be changed between iterations.

Certain aircraft performance parameters were provided for calculating lift, drag, and AOA. The parameters were C_{L_0} , C_{L_α} , C_{D_0} , S , K , W , maximum thrust available, and maximum AOA. C_L and C_D were calculated as follows:

$$C_L = C_{L_0} + C_{L_\alpha} \alpha \quad (38)$$

$$C_D = C_{D_0} + K(C_L)^2 \quad (39)$$

Note that the lift-curve slope was referenced from the longitudinal axis of the aircraft (see Figure 8). Lift and drag were calculated using the familiar relationships:

$$L = Q S C_L \quad (40)$$

$$D = Q S C_D \quad (41)$$

where the dynamic pressure, Q , is based upon equivalent airspeed:

$$Q = \frac{1}{2} \rho_0 V^2 \quad (42)$$

Initial values for airspeed, thrust, and theta were chosen to match the aircraft requirements for the phase of flight under scrutiny. Initial values for x and h were chosen referenced to the microburst windshear center. The iteration of the model was based upon the time step, Δt .

Three aircraft were analyzed for their response in a microburst windshear. They were the U.S. Navy P-3 (Lockheed L-188), the U.S. Navy T-44 (Beechcraft King Air H-90), and a generic 3-engine "heavy" airline transport. The P-3 is a four-engine turboprop with gross weights in the medium range (75,000 to 135,000 lbs.). The T-44 is powered by two turboprop engines and falls within the category of a "light-twin" transport. The 3-engine heavy airline transport is powered by turbofans and as the name implies, is capable of high gross weights. Tables 3, 4, and 5 delineate the performance

parameters of the three aircraft. The lift curve slope for the P-3 is greater than the theoretical prediction. This result is due to the influence of the propeller induced flow-field. (Power-off $C_{L\alpha}=5.7 \text{ rad}^{-1}$.)

TABLE 3: P-3 PERFORMANCE PARAMETERS [Ref. 18].

Performance Parameters	Landing Approach Configuration	Takeoff Configuration	On-station Configuration
W (lbs)	89,500; 114,000	89,500; 120,000; 135,000	120,000
S (ft ²)	1300	1300	1300
K	0.05041	0.05041	0.05041
C _{D0} 4 engine	0.0567	0.0551	0.0213
3 engine	0.0630	-	-
C _L α (rad ⁻¹)	6.38	6.38	6.25
C _{L0}	0.800	0.800	0.350
α_{max} (rad)	0.244	0.244	0.209
T _{max} (lbf) 4 eng.	33400	33400	33400
3 eng.	25050	-	-
q (rad/s)	0.0873	0.0873	0.0873
Vref (ft/s)	236; 262	-	354
V1 (ft/s)	-	204; 214; 229	-
V2 (ft/s)	-	220; 227; 239	-

As mentioned, the AOA used in the calculations was based upon the longitudinal axis of the aircraft. Maximum thrust available and gross weight were adjusted to meet the scenario requirements.

TABLE 4. 3-ENGINE HEAVY AIRLINE TRANSPORT
PERFORMANCE PARAMETERS [Ref. 10].

Performance <u>Parameters</u>	Landing Approach <u>Configuration</u>	Takeoff <u>Configuration</u>
W (lbs)	362,000	462,000
S (ft ²)	4578	4578
K	0.059	0.059
C _{Do}	0.108	0.098
C _{Lα} (rad ⁻¹)	4.96	4.96
C _{Lo}	0.532	0.532
α _{max} (rad)	0.317	0.314
T _{max} (lbf)	126,000	126,000
q (rad/s)	0.0873	0.0873
Vref (ft/s)	227	-
V1 (ft/s)	-	238
V2 (ft/s)	-	255

TABLE 5: T-44 PERFORMANCE PARAMETERS [Ref. 19].

Performance <u>Parameters</u>	Landing Approach <u>Configuration</u>	Takeoff <u>Configuration</u>
W (lbs)	8,280	8,280
S (ft ²)	210	210
K	0.0503	0.040
C _{Do}	0.120	0.100
C _{Lα} (rad ⁻¹)	6.24	6.24
C _{Lo}	0.587	0.0523
α _{max} (rad)	0.244	0.227
T _{max} (lbf)	3,023	3,023
q (rad/s)	0.0873	0.0873
Vref (ft/s)	203	-
V1 (ft/s)	-	152
V2 (ft/s)	-	202

For each iteration of Δt , the following aircraft, inertial, and windshear model values were calculated and recorded:

- 1) x - Distance from microburst center in feet.
- 2) h - Absolute altitude in feet.
- 3) V - Equivalent airspeed in knots.
- 4) θ (theta) - Pitch angle in degrees.
- 5) α (alpha) - Angle-of-attack in degrees.
- 6) γ_a - Flight path in degrees referenced to the airmass.
- 7) γ_i - Flight path in degrees referenced to the earth.
- 8) V_g - Ground speed in knots.
- 9) ROC - Rate of climb in ft/sec. referenced to the earth.
- 10) Thrust - instantaneous thrust in lbf.
- 11) E_s - Specific energy in feet.
- 12) \dot{E}_s (Esdot) - Time rate change of specific energy in ft/sec.
- 13) W_x - Horizontal wind speed in ft/sec.
- 14) W_h - Vertical wind speed in ft/sec.

From the collection of data, plots were made of altitude, theta, alpha, airspeed, specific energy, and time with comparison to distance from microburst center.

Four basic escape maneuvers were examined for critical phase of flight. Constant airspeed, constant altitude, constant pitch angle (θ), and constant angle-of-attack (α) escape maneuvers were evaluated quantitatively (engineering standpoint) and qualitatively (piloting standpoint).

D. CRITICAL FLIGHT PHASES MODELED

There are three phases of flight in which a microburst encounter becomes critical for airplane survival. Approach to landing, initial takeoff and climb out, and low-altitude maneuvering are the three phases of flight considered in this analysis. All three phases occur at an altitude of less than 1000 feet AGL. The low-altitude maneuvering flight phase is applicable to the P-3 community. The P-3 routinely operates 200 feet above the water in all weather conditions during Anti-Submarine Warfare (ASW) missions.

1. Landing Approach

The landing approach scenario is based upon a 3 degree glideslope descent to landing. In this scenario, the microburst center is placed 10,300 feet from the end of runway. The simulation starts 500 feet ($x=-500$ feet) before the microburst center on glideslope

(h=566 feet). This situation closely represents the scenario of DAL 191. The aircraft is exposed to the windshear immediately at start, $t=0$. The simulation is run for a programmed length of time or until ground impact occurs. Five aircraft/weight combinations were analyzed for the approach to landing scenario. They were a P-3 at 89,500 pounds gross weight, a P-3 at 114,000 pounds gross weight, a 3-engine heavy airline transport, a T-44, and a P-3 at 89,500 pounds gross weight with one engine shut down.

Starting aircraft parameters were such that the given pitch angle (θ) and thrust would maintain a 3° glideslope at target approach airspeed (V_{ref}). Pitch angle and thrust were maintained until a loss of airspeed equated to V_{ref} minus 20 knots. At such time, the aircraft performed one of the following programmed escape procedures:

- 1) constant airspeed - Maximum thrust was applied and a pitch angle set to 0° . This pitch angle was maintained until the airspeed equaled V_{ref} . Pitch angle was then adjusted to maintain the airspeed at $V_{ref} \pm 5$ knots.
- 2) constant altitude - Maximum thrust was applied and a pitch angle was set to obtain a positive rate of climb. This pitch angle was maintained until the target altitude (altitude at which the maneuver began) was established. Pitch angle was then adjusted to maintain the target altitude by ± 20 feet.

- 3) constant theta - Maximum thrust was applied and a pitch angle (theta) was set and maintained. Specifically, theta values of 5°, 8°, 10°, and 15° were used.
- 4) constant alpha - Maximum thrust was applied and a pitch angle was adjusted to get a given angle-of-attack (alpha). AOA values of 12, 15, and 20 units were used for the P-3 model.

The above escape maneuvers were constrained by certain limits. Pitch rate (q) was set at 5°/sec. Thrust application rate for the P-3 model was set at 0.5 maximum thrust/sec. Thrust application rate for the generic 3-engine heavy and T-44 aircraft was set at 0.2 maximum thrust/sec. This rate accounts for engine "spool-up" time. Maximum pitch angle was limited not to exceed maximum AOA. Appendix C contains the MatLab® program used for the approach to landing scenario.

2. Takeoff

The takeoff scenarios primarily explored the effects of microburst windshear on the takeoff performance with penetration at liftoff. However, some analysis was performed on the microburst center distance from liftoff point. Generally, the simulation began with the aircraft lifting off 1200 feet from the microburst center ($x=-1200$ feet) at the appropriate liftoff speed (V_1). Initial pitch angle,

theta, was such to achieve takeoff safety speed (V_2) at 50 feet, no windshear. Maximum thrust was used for all cases. Execution of the particular escape maneuver was begun when the rate of climb (ROC) is less than or equal to zero or the airspeed fell below V_2 . Five aircraft/weight combinations were looked at. They were a P-3 at 90,000 pounds, 114,000 pounds, and 135,000 pounds gross weight, as well as a 3-engine heavy airline transport and a T-44.

Four escape methods were considered for a microburst encounter at takeoff. When the ROC was less than or equal to zero, or the airspeed fell below V_2 , one of the following programs was executed:

- 1) constant airspeed - If airspeed was less than V_2 at initiation, theta was reduced to 0° . If airspeed was greater than V_2 at initiation, theta was increased. In both cases, theta was manipulated to maintain airspeed = $V_2 \pm 5$ knots once V_2 was achieved.
- 2) constant altitude - Theta was varied to maintain altitude ± 20 feet about the target altitude. The target altitude was the altitude at which the escape maneuver began.
- 3) constant theta - Theta was held at a programmed constant value throughout the maneuver. Theta values used were 5° , 10° , and 15° .
- 4) constant alpha - Theta was varied to maintain a constant AOA value.

For the above maneuvers, a pitch rate of 5°/sec was used and maximum thrust was maintained. Also, theta was reduced any time critical AOA was exceeded.

Two variants of the takeoff scenario were analyzed for performance sensitivity. Both used the 120,000 pound P-3. For one, V_{lof} was increased 18 knots to 145 knots. This equated to an increase of the rotate speed (V_R) to 145 knots. The second variant moved the microburst center from 1200 feet to 2000 feet from the point of liftoff. This resulted in the aircraft gaining airspeed and altitude before encountering the severe horizontal windshear. The second scenario closely simulated a microburst encounter after takeoff. MatLab® programming for the takeoff scenario is listed in Appendix D.

3. P-3 On-Station

The on-station microburst encounter scenario used a P-3 at 120,000 pounds gross weight in a 4-engine loiter configuration. No wing flaps or landing gear were extended. Only aircraft reaction and performance were analyzed. No specific escape maneuver was used.

This scenario tried to emulate an autopilot maintaining altitude through pitch authority and the flight crew controlling thrust.

The microburst encounter began with the P-3 at 200 feet AGL and 5000 feet from the microburst center ($x=-5000$ feet). The initial airspeed was 210 knots (prescribed loiter airspeed). Theta was varied throughout the encounter to maintain altitude. Thrust was maintained at loiter power until 40 knots of airspeed was lost. At this point, maximum thrust was applied while still maintaining altitude. The scenario was ended at 5000 feet on the opposite side of the microburst center.

III. RESULTS AND DISCUSSION

The microburst and inertial reference math models were validated by comparing actual flight data to model data. The inertial model was further tested for the stability of the coupled differential equation scheme. Any weakness noted was considered when the results were analyzed. Each critical phase of flight was studied for aircraft response when performing a particular escape maneuver. Mathematical results were combined with other observations to build a foundation for conclusions.

A. WINDSHEAR AND INERTIAL REFERENCE MODEL VALIDATION

The windshear math model was developed from fitting a vortex/source flowfield to recorded flight data. The wind field recorded by the AA 539 DFDR (Digital Flight Data Recorder) showed a definite vortex flow. However, the flight data from the DAL 191 DFDR showed a different vortex flow arrangement. In addition, a strong outflow at the surface, and increased vertical sink, required the addition of source flows to the windshear model. This use of point source flows led to a much closer fit of the original vortex model to the wind field DAL 191 experienced. The source flows have no range damping terms. Therefore, the DAL 191 emulation windshear model

becomes invalid at distances greater than 6000 feet ($x=6000$ feet) from the microburst center. All analysis was easily done within this distance limit.

It is important to note that the aircraft performance results are insensitive to the exact modeling of a particular windshear. The rapid change of a headwind to a tailwind is the governing factor in a microburst. Secondary are the vertical down drafts that can be experienced above 100 feet AGL (above ground level). The windshear math model contains both characteristics to the same degree as the windshear experienced by DAL 191.

Validation of the inertial reference model was scrutinized for proper aircraft response to changing conditions and the effect of the time step size. Stability of the solutions obtained from the differential equation numerical scheme was the greatest concern. Results generated from the inertial model were studied for the light P-3 under stable and turbulent conditions. Also, a comparison of the 3-engine transport model was made with the DAL 191 DFDR data during the final seconds of the fateful flight.

The first approach was to check the response of a light P-3 initially stabilized on a 3° descent path with no windshear. The input came from a subroutine that would not vary pitch angle (θ) or thrust. No excursions were noted in descent path, airspeed, or α , as shown in Figure 9. The time step used was 1 second.

The second validation was to observe the stability of the inertial model solution with different size time steps. A time interval of 0.5 seconds was the target time step for running all analyses. Therefore, time steps of 1, 0.5, and 0.1 second were investigated. The light P-3 on approach to landing was again used. This time, the windshear

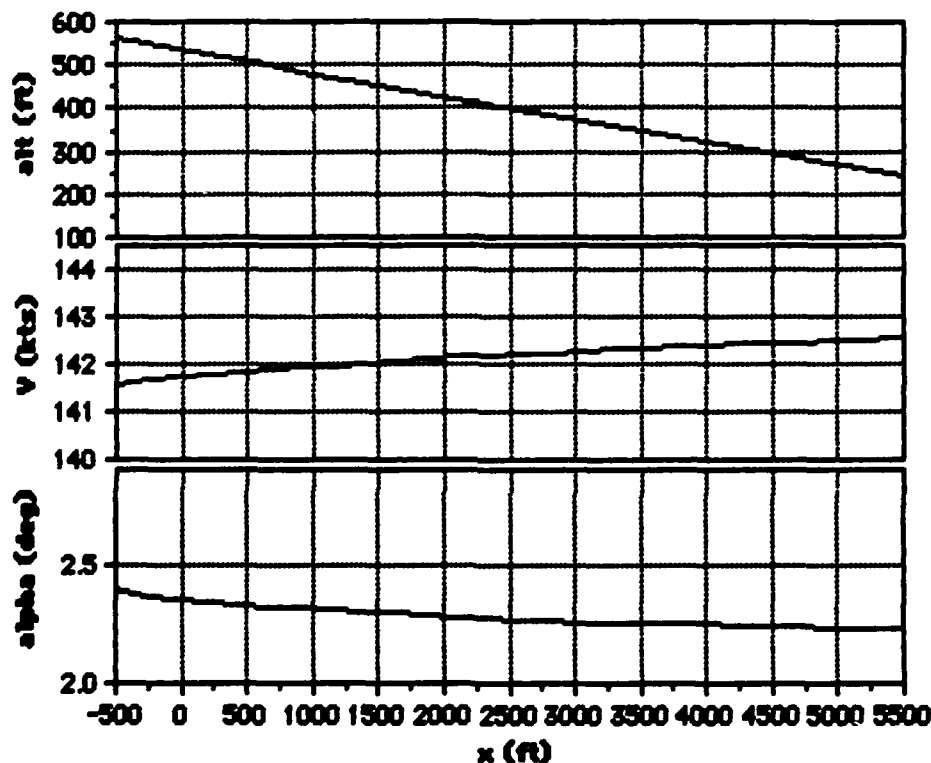


Figure 9. Light P-3 on a stabilized descent path.

model was incorporated to induce changes in the flight environment. Aircraft control was through theta and thrust inputs. Control feedback was set to vary theta to keep within ± 100 feet of the descent path and to vary thrust to maintain V_{ref} within ± 5 knots. The results are depicted in Figure 10. Note the close correlation

between the 0.1 and 0.5 second time step cases, indicating that a 0.5 second time step provides stability and adequate accuracy for the desired results.

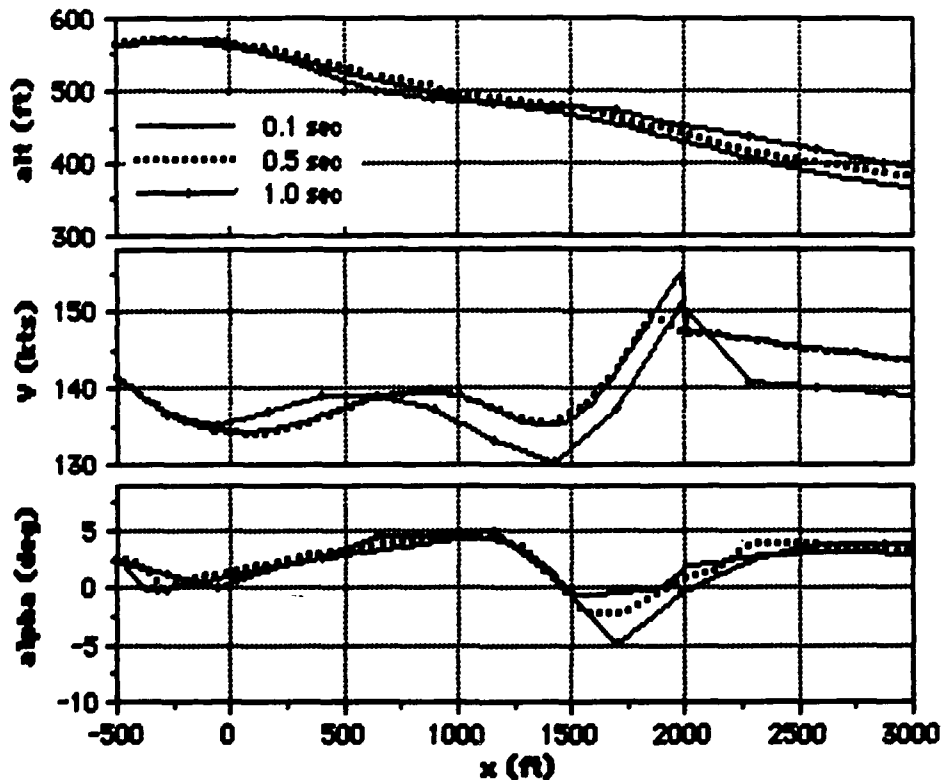


Figure 10. The effect of time step size on the inertial reference calculations.

The final validation was comparing the actual aircraft response to model predictions. DAL 191 DFDR data were used to compare an L-1011 flight path, airspeed, and alpha data to that of the 3-engine heavy airline transport model. Inputs to the aircraft control were the recorded theta and thrust of DAL 191. The windshear experienced by

DAL 191 was also incorporated for this comparison. Figure 11 graphically displays the close characterization of the actual flight path by the model. Airspeed and alpha do not reflect actual aircraft

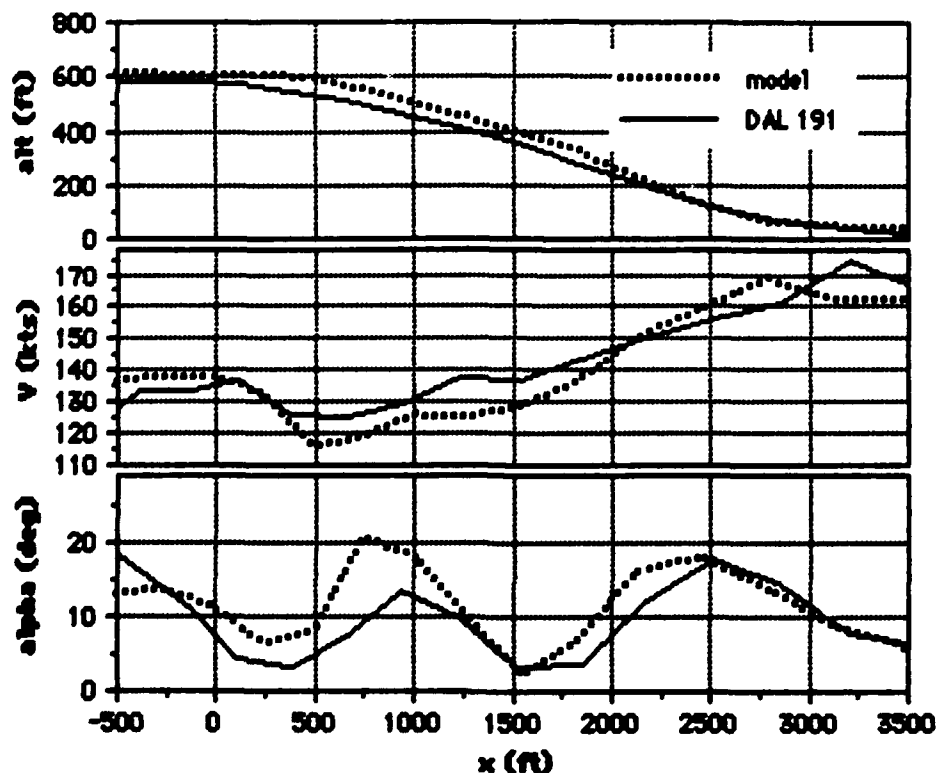


Figure 11. Comparison of aircraft response in windshear between the DAL 191 Flight L-1011 and the 3-engine transport model.

response as closely as the P-3 model, but do follow the same general response. The lag in airspeed and alpha is probably due to the model C_L and C_D equations being only of second order.

B. WEAKNESSES AND OTHER INDEPENDENT VARIABLES

Some weaknesses in the math models and unobserved independent variables exist in the total analysis. The most notable are:

- 1) C_L and C_D value errors at angle of attack near stall.
- 2) Unobserved effects of dynamic pressure and AOA upon engine thrust.
- 3) Unobserved effects of rain and turbulence on aircraft aerodynamic performance.
- 4) Unobserved effects of coupled longitudinal and lateral dynamic modes excited by turbulence and pilot induced oscillations.

None of the weaknesses or unobserved variables is believed to significantly impact the results of the analysis. The overall concept was to compare outcomes of different microburst escape strategies given the same parameters.

A weakness in the aircraft model is the ability to predict the effects of flow separation at low airspeed and high angle of attack. These effects would be an increase in drag and a decrease in generated lift. Table look-up or higher order equations could be used for the C_D and C_L expressions. The model does limit the maximum theta not to exceed maximum angle of attack for that aircraft. Keeping this weakness in mind, the results obtained from the math models are valid when determining the "best" escape maneuver.

Engine thrust is somewhat effected by airspeed and AOA. The turbojet and turbofan-type engines can be significantly effected while the turboprop is effected to a much lesser degree. Only nominal values for thrust were used in the analysis.

The effects of turbulence and rain on aircraft performance were not programmed into the models. Studies by Wingrove and Bach [Ref: 2] analytically determined that the rain had negligible effect upon DAL 191. The NTSB Report (National Transportation Safety Board) came to the same conclusion. What must be considered, is the effect of turbulence upon a pilot's ability to control the aircraft. The effect of turbulence on the ability of a pilot to execute a particular escape maneuver was kept in mind during the writing of the final conclusions.

All the aircraft models are limited to one axis of freedom. The effects of coupled lateral and directional modes upon the longitudinal response were not modeled. From past analysis and personal aviation experience, this limitation should not significantly impact aircraft performance. Again, aircraft control may become difficult if an inherent mode is excited (such as the phugoid at low airspeed and high angle of attack). Escape maneuvers that may produce such dynamic modes were noted.

The effect of changing dynamic pressure on stick forces was evaluated. This is an important consideration from the pilot's perspective. A loss of 20-30 knots airspeed can induce a significant nose-down pitch force.

C. DATA REDUCTION AND ANALYSIS

Aircraft performance for three critical flight phases was evaluated when exposed to a DAL 191 type microburst windshear. Approach to landing and takeoff flight phases were scrutinized for the best escape maneuver that could be applied. The on-station flight phase was examined for the performance of a P-3 while encountering the microburst windshear and attempting to maintain altitude. Calculated data were recorded and converted to applicable units (eg., ft/s to knots). The data were then presented in a graphical format for analytical and subjective comparison.

For all cases, tabulated data were converted to graphical form. Strip graphs for key dependent variables were produced for each aircraft performing a specific escape maneuver. They are listed in Appendices F and G. Combination graphs of flight path, airspeed, and specific energy compare escape maneuvers for each aircraft in a given microburst encounter. The abscissa axis for all the graphs represents the distance from the microburst center in feet. A

three-step approach was carried out to deduce the "best" escape maneuver for a particular encounter using these graphs.

First, the inertial reference frame of flight path performance was analyzed. This involved using the combination flight path graph. A list is generated containing the highest to lowest altitude obtained at a specific point from the microburst center. For the approach to landing scenario, only the maneuvers that resulted in flight paths staying above the descent path (landing glideslope) were chosen. Altitude values were compared for each valid escape maneuver at $x=5000$ feet. For the takeoff scenario, only the escape maneuvers that did not lead to ground impact were listed. Here, altitude values were compared at $x=4000$ feet.

The second step was to cross reference each selected maneuver's airspeed from the combination airspeed graph. This supplied an insight of the airmass reference performance. The airspeed values at the point of interest, and throughout the microburst encounter, allowed a subjective analysis of the validity of the results. Airspeeds that fell deep within the power-on stall region were scrutinized with the strip graphs comparing calculated AOA values. Any maneuver that resulted in a very low airspeed, high AOA condition was rejected from the list.

The third step evolved using the specific energy combination graph for a final resolution. Specific energy incorporates both the

inertial and the airmass reference. The eligible maneuvers that had the highest specific energy value at the point of interest analytically are the "best" escape maneuvers for that aircraft configuration, given that type of microburst encounter.

1. Approach to Landing Microburst Encounter Analysis

Figure 12, Figure 13, and Figure 14 depict the results obtained for different escape maneuvers executed by a P-3 at 89,500 pounds gross weight. Table 6 compares the results observed at x=5000 feet. The constant airspeed and 12 unit AOA escape maneuvers were rejected initially due to resulting flight trajectories below the descent path (3° landing approach glideslope) as depicted in Figure 12. The 20 unit AOA escape maneuver was subsequently rejected because of low airspeed, high AOA observed in Figure 13. Figure 14 shows that the 5° theta escape maneuver results in the highest specific energy value of the remaining list.

TABLE 6. RELATIVE VALUE RANKING FOR A P-3 AT 89,500LBS.

<u>maneuver</u>	<u>altitude</u>	<u>airspeed</u>	<u>specific energy</u>
20 unit AOA	1	rejected	- - -
const. altitude	2	5	5
15° theta	3	4	4
15 unit AOA	4	3	3
10° theta	5	2	2
5° theta	6	1	1

Figure 15, Figure 16, and Figure 17 depict the results obtained for different escape maneuvers executed by a P-3 at 114,000 pounds gross weight. Table 7 compares the results observed at x=5000 feet.

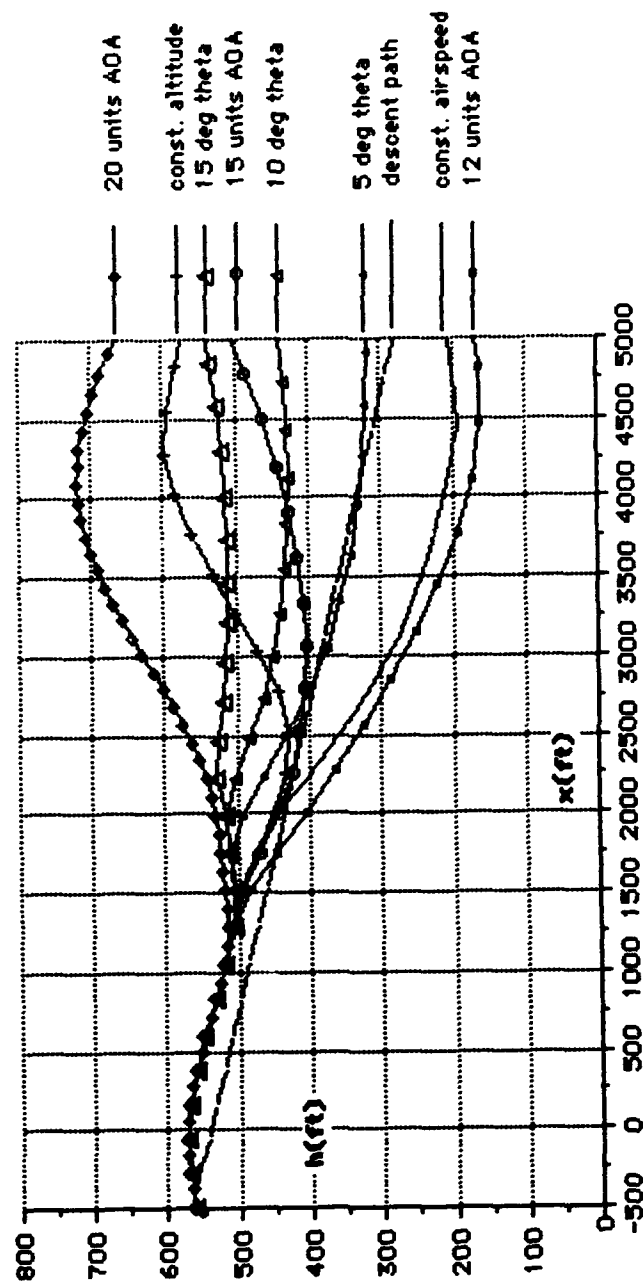


Figure 12. Flight path data comparison of a P3 at 89,500lbs performing different escape maneuvers during an approach to landing microburst encounter.

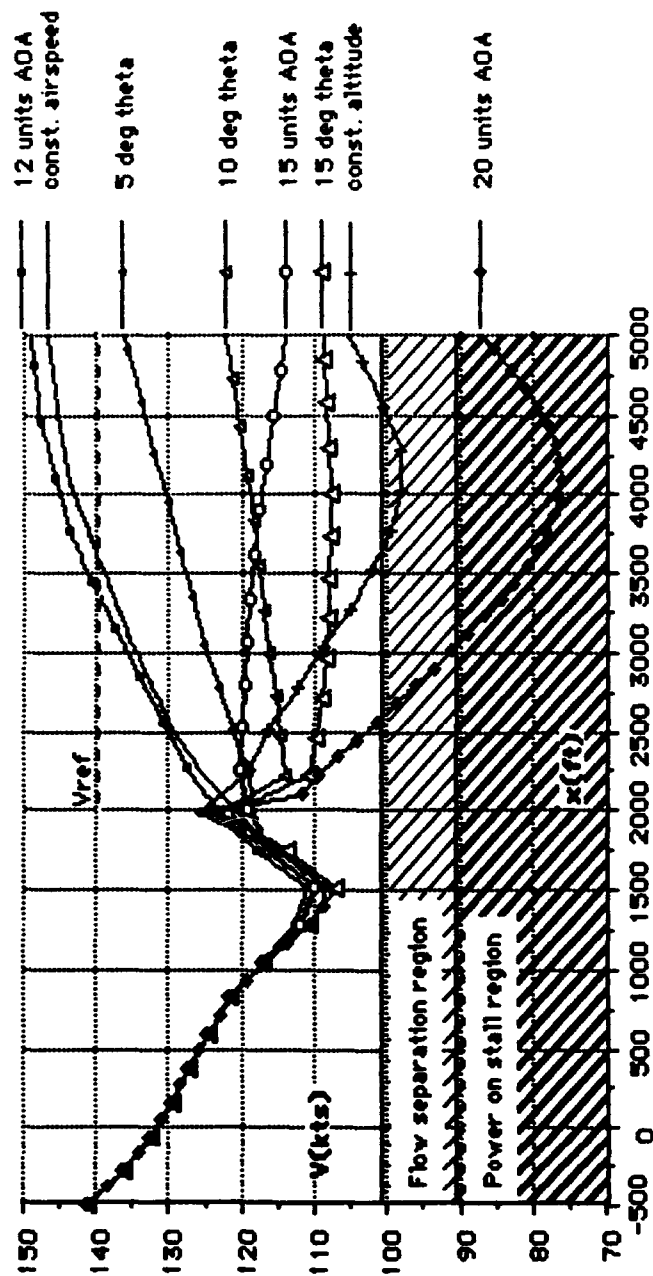


Figure 13. Airspeed data comparison of a P3 at 89,500lbs performing different escape maneuvers during an approach to landing microburst encounter.

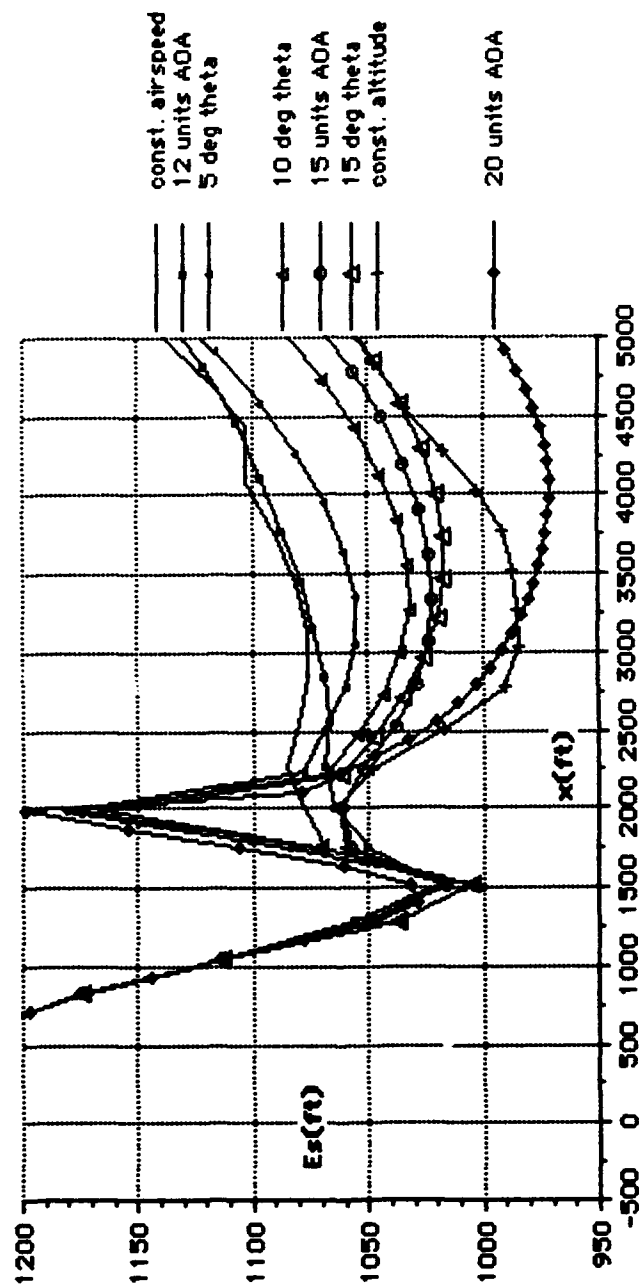


Figure 14. Specific energy data comparison of a P3 at 89,500lbs performing different escape maneuvers during an approach to landing microburst encounter.

The constant airspeed, 12 unit AOA, and 5° theta escape maneuvers were rejected initially due resulting flight trajectories below the descent path as depicted in Figure 15. The 20 unit AOA and constant altitude escape maneuvers were subsequently rejected because of low airspeeds, high AOAs observed in Figure 16. Figure 17 shows that the 15 unit AOA escape maneuver results in the highest specific energy value of the remaining list.

TABLE 7. RELATIVE VALUE RANKING FOR A P-3 AT 114,000LBS.

<u>maneuver</u>	<u>altitude</u>	<u>airspeed</u>	<u>specific energy</u>
20 unit AOA	1	rejected	- - -
const. altitude	2	rejected	- - -
15° theta	3	3	3
10° theta	4	2	2
15 unit AOA	5	1	1

Figure 18, Figure 19, and Figure 20 depict the results obtained for different escape maneuvers executed by a 3-engine heavy airline transport. Table 8 compares the results observed at x=5000 feet. The constant airspeed, 5° theta, and 10° theta escape maneuvers

TABLE 8. RELATIVE VALUE RANKING FOR A 3-ENGINE AIRLINE TRANSPORT.

<u>maneuver</u>	<u>altitude</u>	<u>airspeed</u>	<u>specific energy</u>
const. altitude	1	2	2
15° theta	2	1	1

were rejected initially due resulting flight trajectories below the descent path as depicted in Figure 18. Figure 20 shows that the 15° theta escape maneuver results in the highest specific energy value.

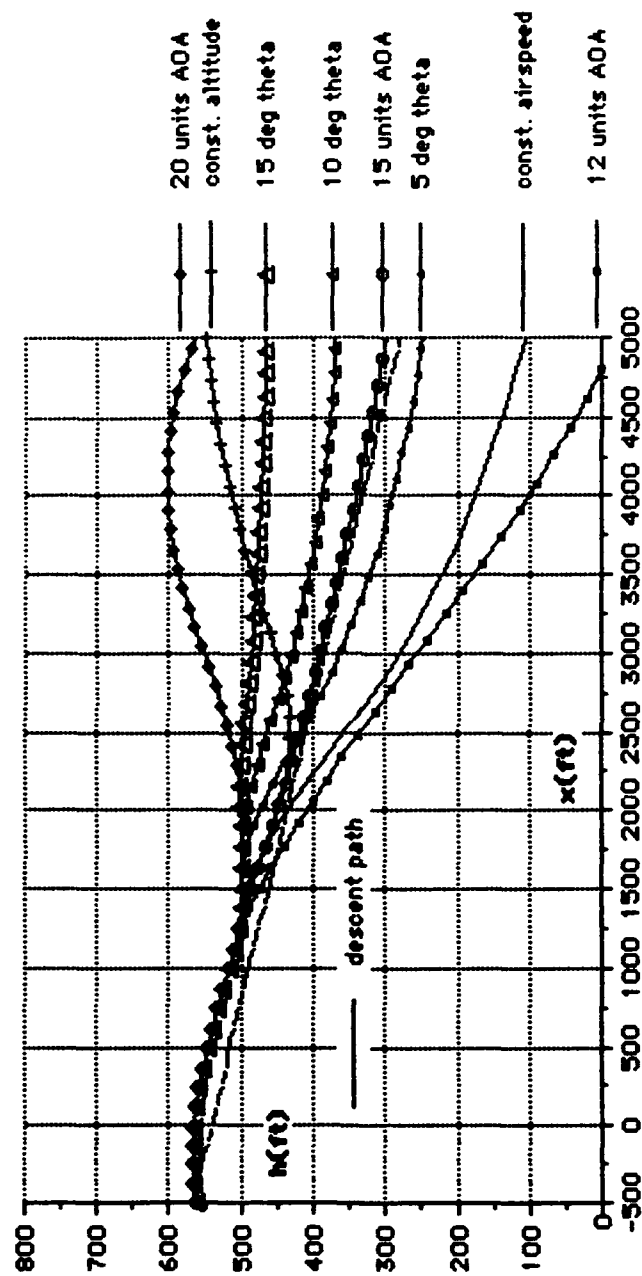


Figure 15. Flight path data comparison of a P3 at 114,000lbs performing different escape maneuvers during an approach to landing microburst encounter.

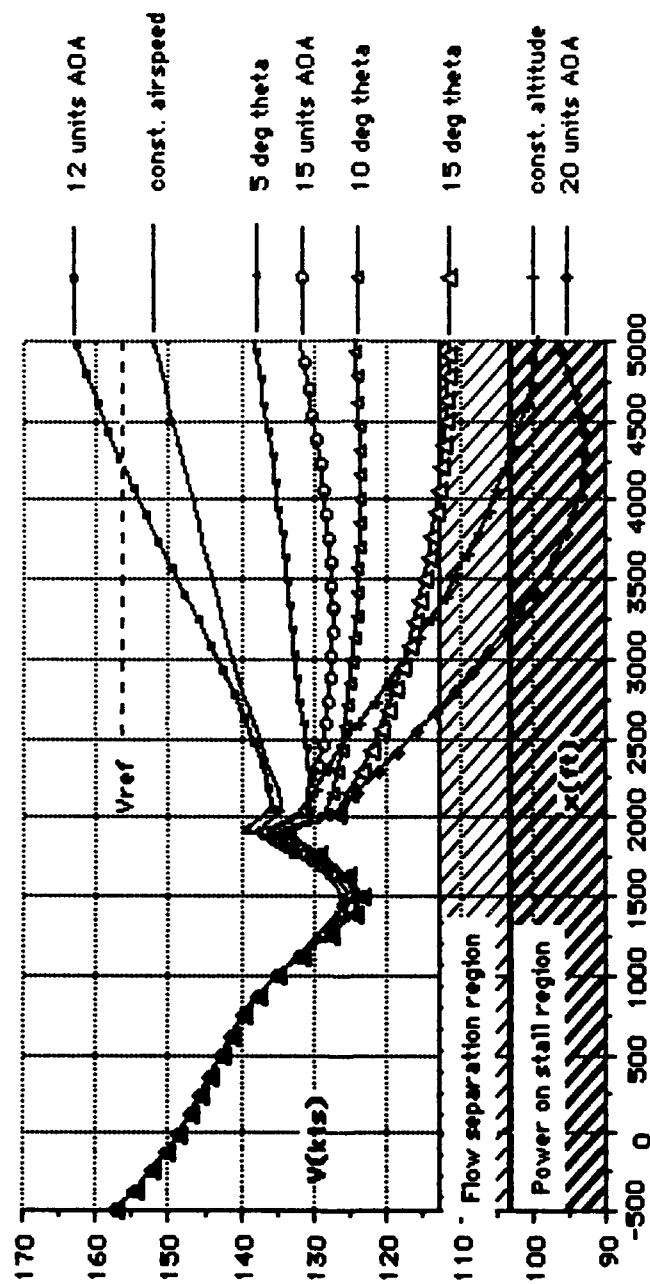


Figure 16. Airspeed data comparison of a P3 at 114,000lbs performing different escape maneuvers during an approach to landing microburst encounter.

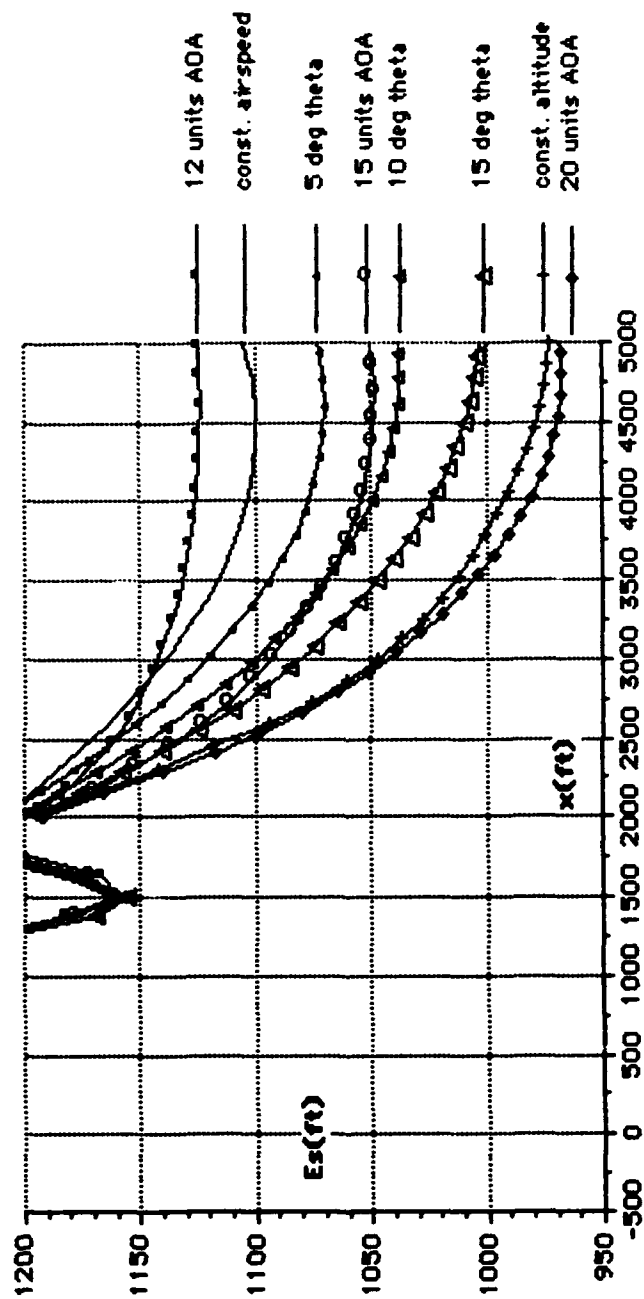


Figure 17. Specific energy data comparison of a P3 at 114,000lbs performing different escape maneuvers during an approach to landing microburst encounter.

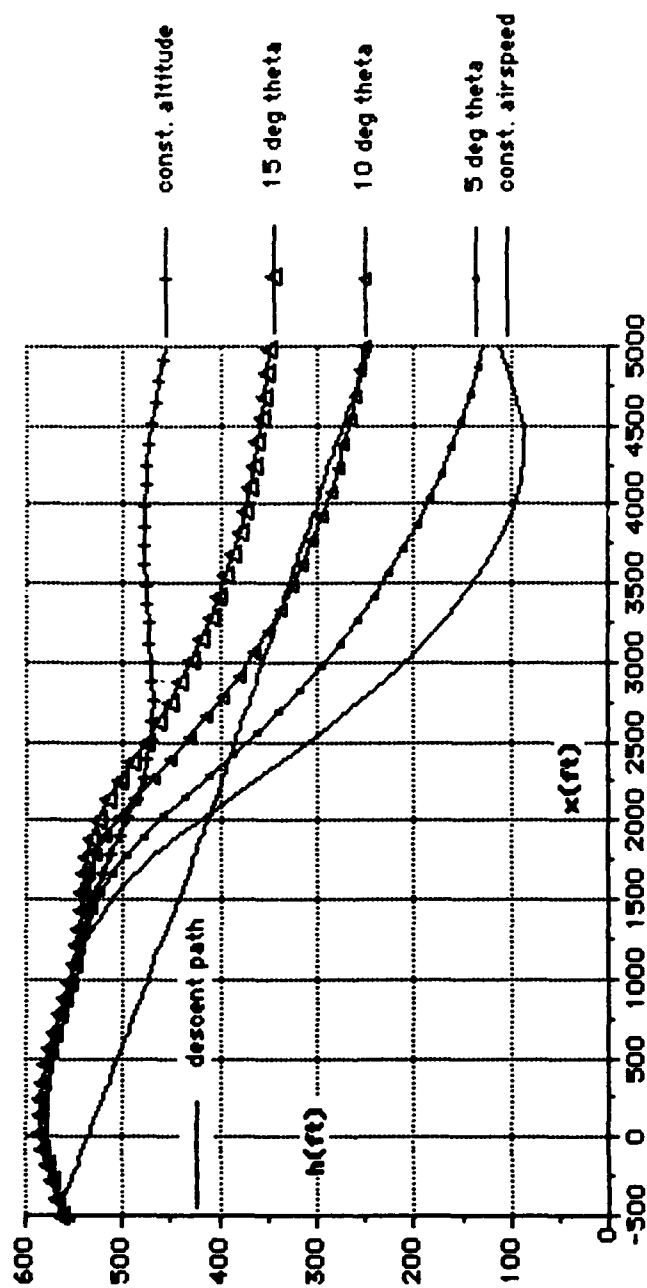


Figure 18. Altitude data comparison of a 3-engine heavy airline transport performing different escape maneuvers during an approach to landing microburst encounter.

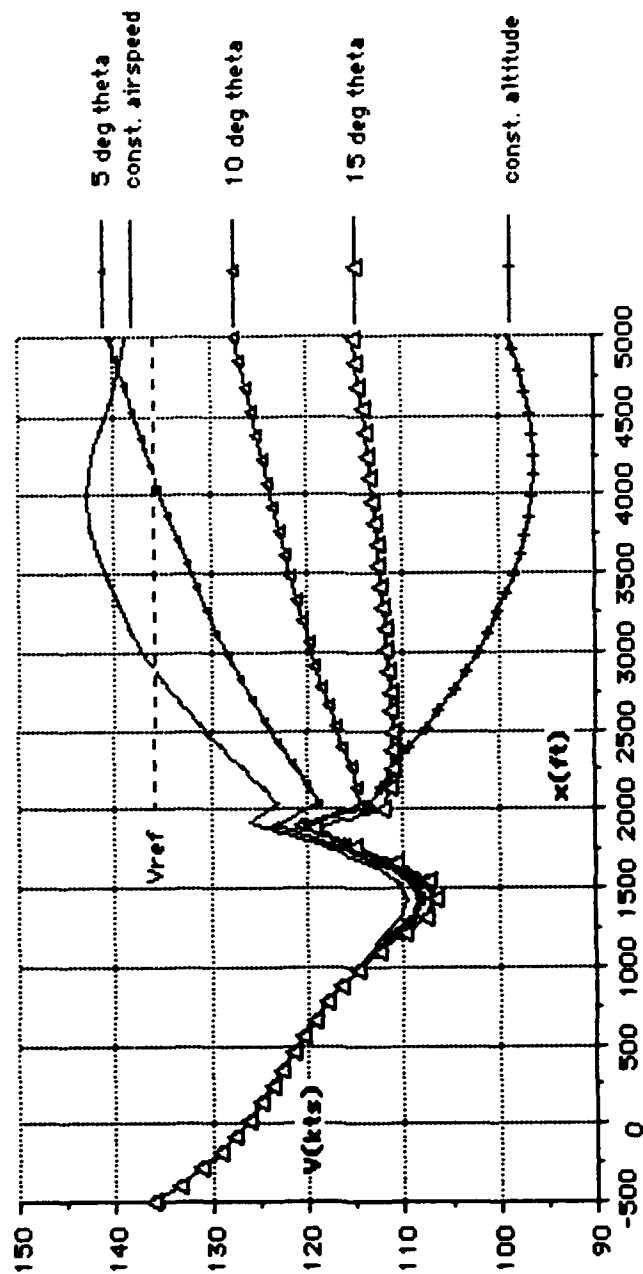


Figure 19. Airspeed data comparison of a 3-engine heavy airline transport performing different escape maneuvers during an approach to landing microburst encounter.

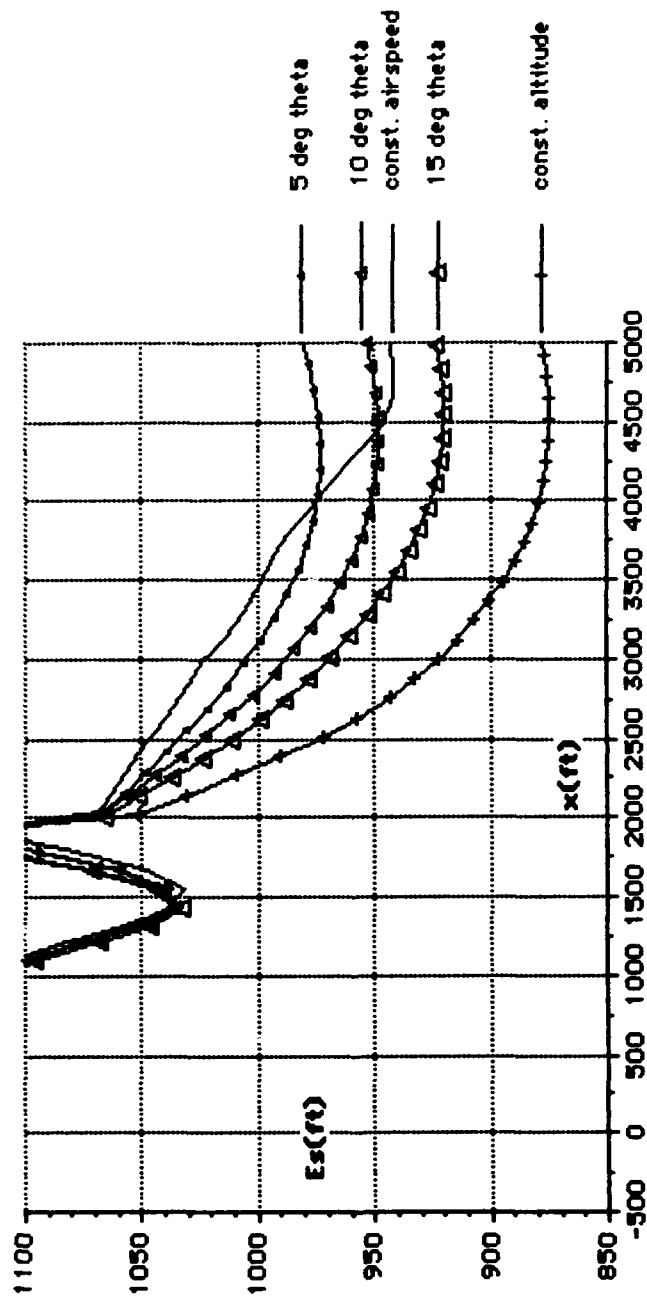


Figure 20. Specific energy data comparison of a 3-engine heavy airline transport performing different escape maneuvers during an approach to landing microburst encounter.

Figure 21, Figure 22, and Figure 23 depict the results obtained for different escape maneuvers executed by a T-44. Table 9 compares the results observed at x=5000 feet. The constant airspeed, 10 unit AOA, and 16 unit AOA escape maneuvers were rejected initially due to resulting flight trajectories below the descent path as depicted in Figure 21. The 25 unit AOA and constant altitude escape maneuvers was subsequently rejected because of low airspeeds and high AOAs observed in Figure 22. Figure 23 shows that the 5° theta escape maneuver results in the highest specific energy value of the remaining list.

TABLE 9. RELATIVE VALUE RANKING FOR A T-44.

<u>maneuver</u>	<u>altitude</u>	<u>airspeed</u>	<u>specific energy</u>
const. altitude	1	rejected	- - -
15° theta	2	3	3
25 unit AOA	3	rejected	- - -
10° theta	4	2	2
5° theta	5	1	1

Figure 24, Figure 25, and Figure 26 depict the results obtained for different escape maneuvers performed by a P-3 at 89,500 pounds gross weight operating on 3 engines. Table 10 compares the results observed at x=5000 feet. The constant airspeed, 12 unit AOA, and 5° theta escape maneuvers were rejected initially due to resulting flight trajectories below the descent path as depicted in Figure 24. The 20 unit AOA and constant altitude escape maneuvers were subsequently rejected because of low airspeeds and high AOAs observed in Figure 25. The 15° theta escape maneuver was also rejected for the

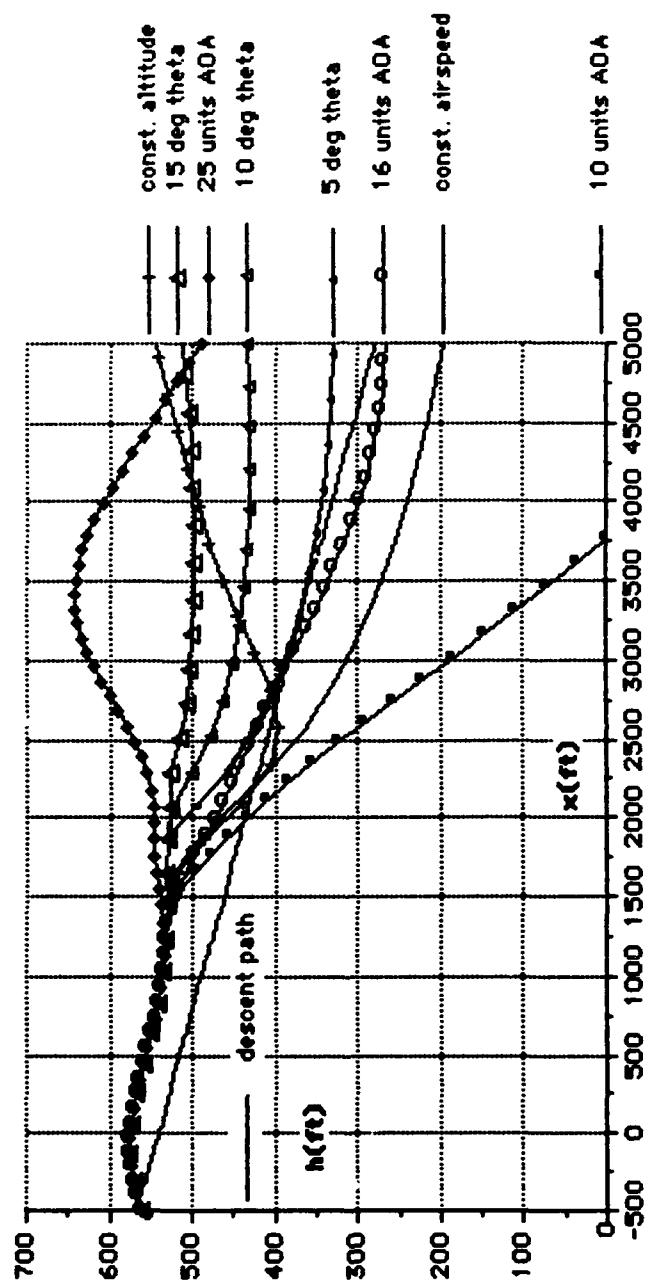


Figure 21. Altitude data comparison of a T-44 performing different escape maneuvers during an approach to landing microburst encounter.

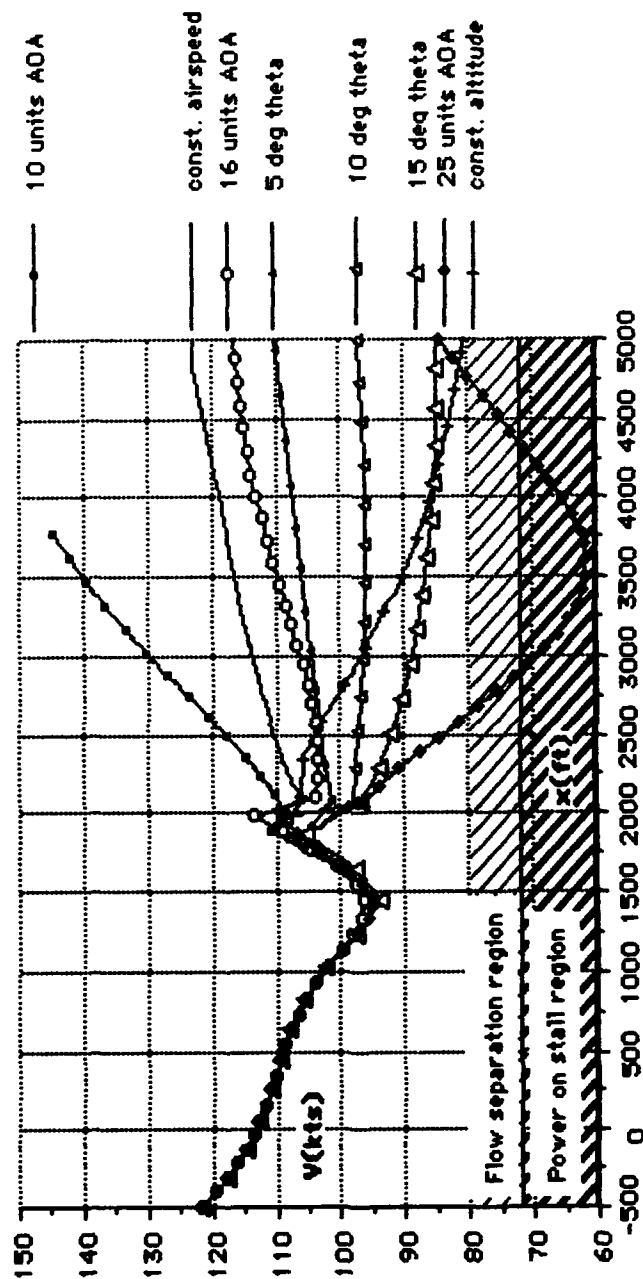


Figure 22. Airspeed data comparison of a T-44 performing different escape maneuvers during an approach to landing microburst encounter.

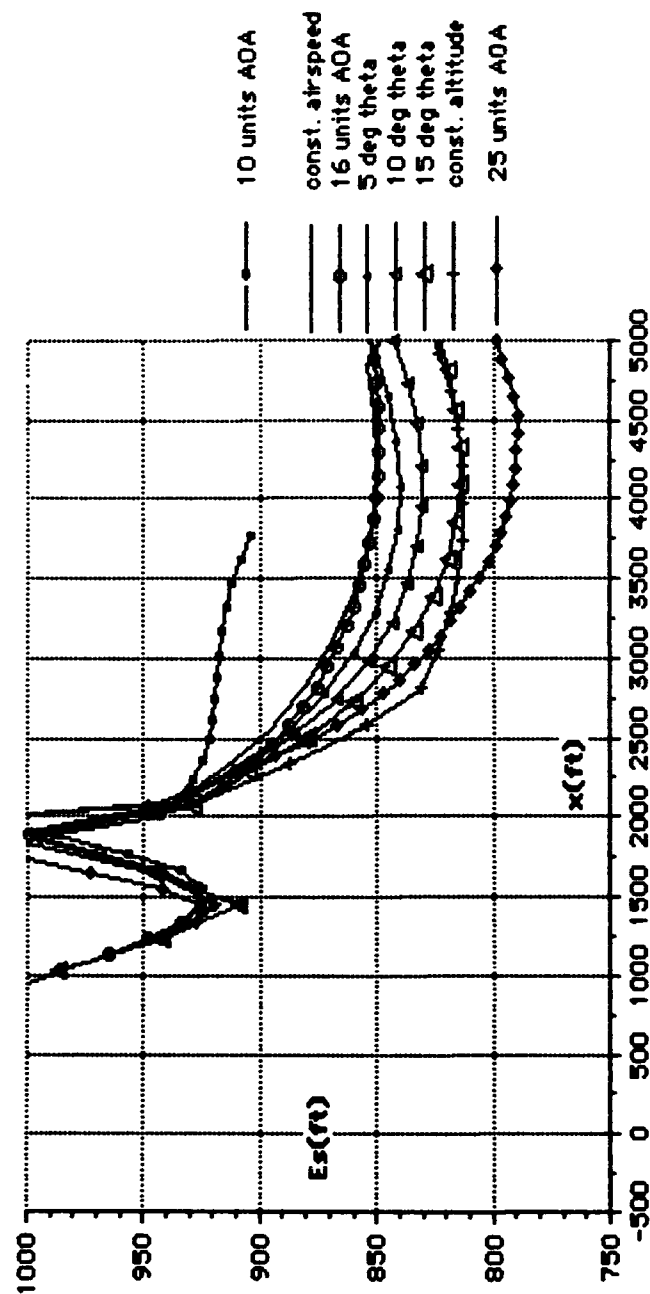


Figure 23. Specific energy data comparison of a T-44 performing different escape maneuvers during an approach to landing microburst encounter.

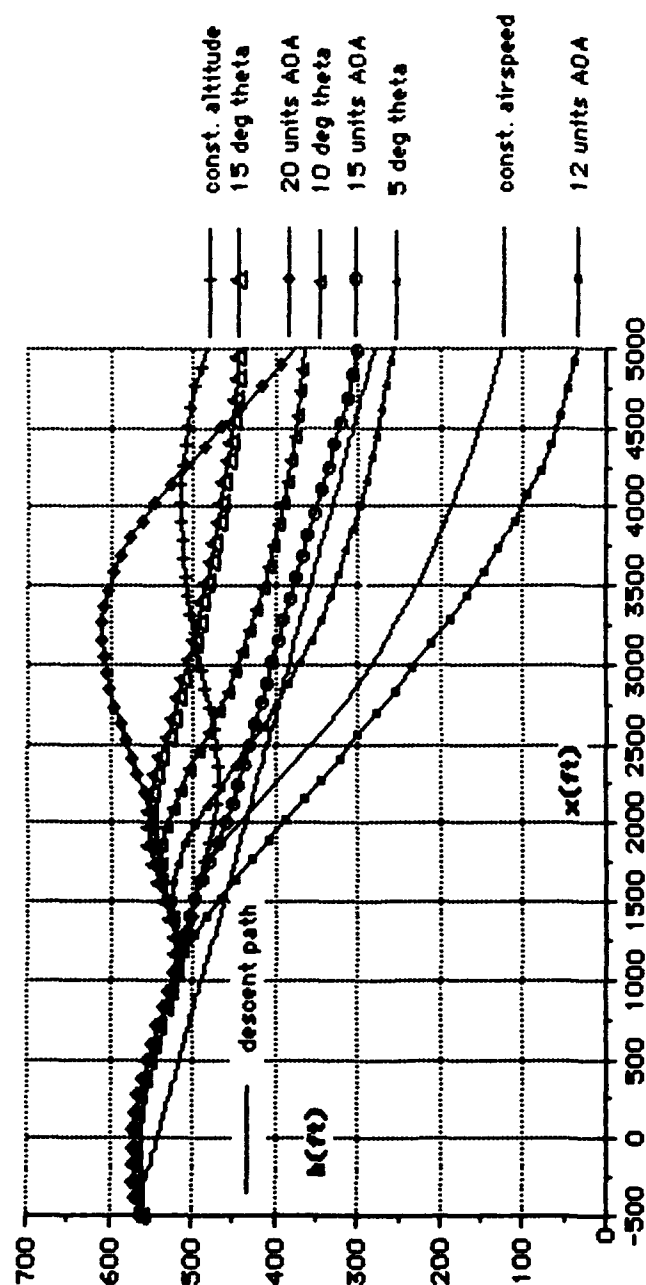


Figure 24. Altitude data comparison of a P-3 at 89,500lbs operating on 3 engines performing different escape maneuvers during an approach to landing microburst encounter.

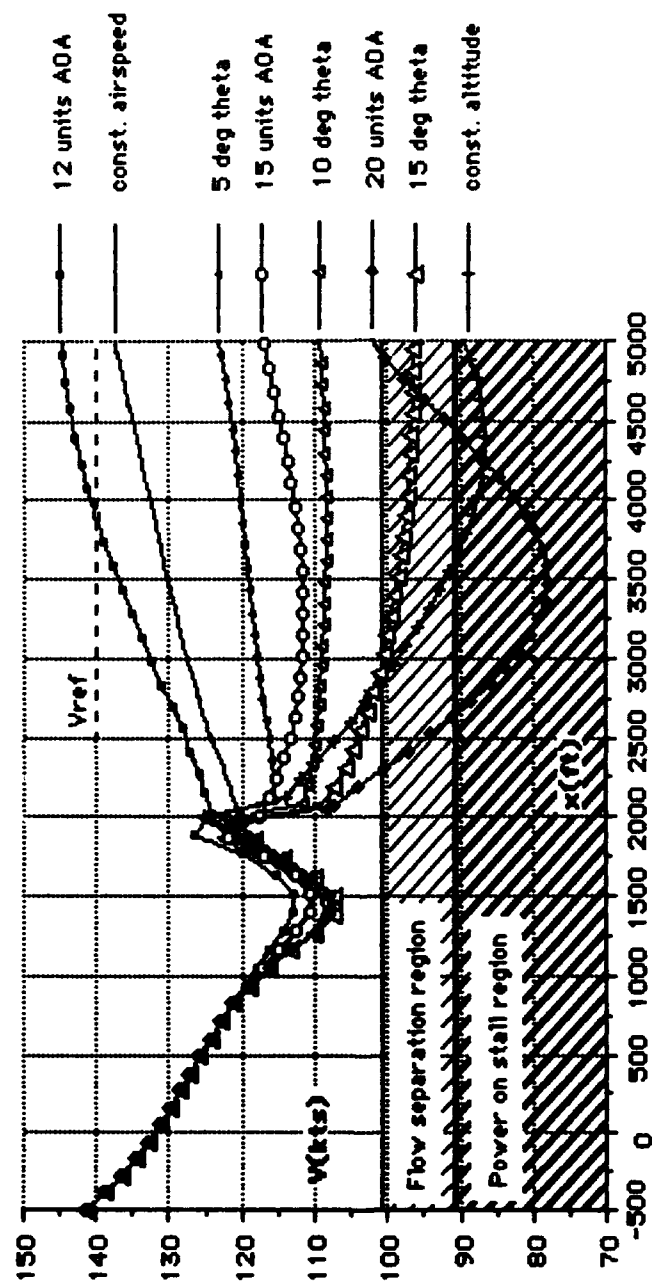


Figure 25. Airspeed data comparison of a P-3 at 89,500lbs operating on 3 engines performing different escape maneuvers during an approach to landing microburst encounter.

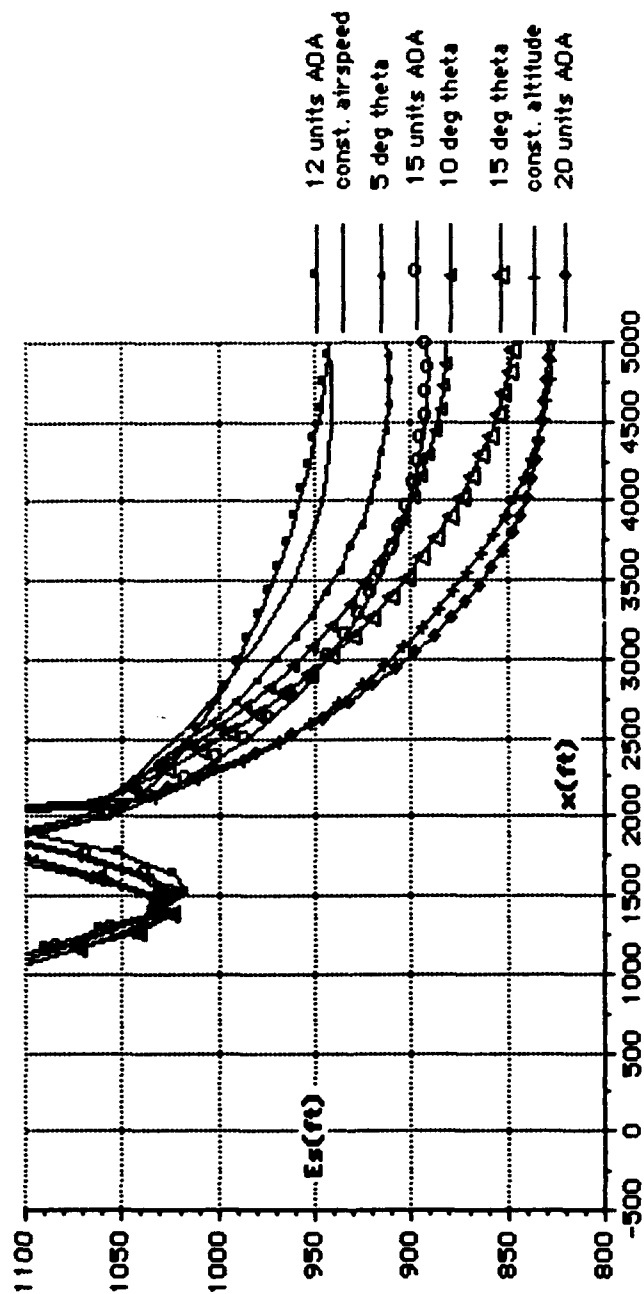


Figure 26. Specific energy data comparison of a P-3 at 89,500lbs operating on 3 engines performing different escape maneuvers during an approach to landing microburst encounter.

same reasons. Although the airspeed is only within the flow separation region (steady state stall buffet), analysis of the AOA (see Figure F34) shows that critical alpha was sustained on the latter parts of the maneuver. Figure 26 shows that the 15 unit AOA escape maneuver results in the highest specific energy value of the remaining list.

TABLE 10. RELATIVE VALUE RANKING FOR A P-3 AT 89,500LBS OPERATING ON 3 ENGINES.

<u>maneuver</u>	<u>altitude</u>	<u>airspeed</u>	<u>specific energy</u>
const. altitude	1	rejected	- - -
15° theta	2	rejected	- - -
20 unit AOA	3	rejected	- - -
10° theta	4	2	2
15 unit AOA	5	1	1

2. Takeoff Microburst Encounter Analysis

Figure 27, Figure 28, and Figure 29 depict the results obtained for different escape maneuvers performed by a P-3 at 90,000lbs gross weight. Altitude, airspeed, and specific energy values are compared at x=4000ft. All six escape maneuvers resulted in ground plane clearance as depicted in Figure 27. The 15 unit AOA escape maneuver was subsequently rejected because of low airspeed, high AOA as observed in Figure 28. Figure 29 shows that all escape maneuvers, except the 15 unit AOA escape maneuver, resulted in a grouped single value. This shows that all relevant escape maneuvers provide the same final specific energy.

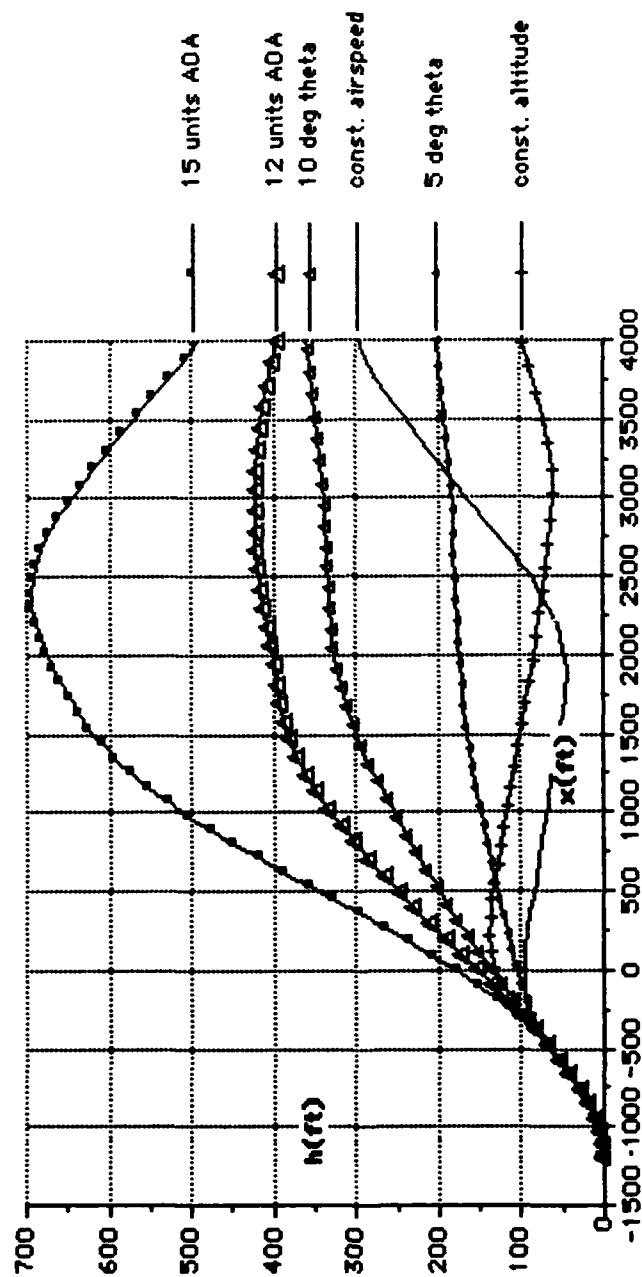


Figure 27. Flight path data comparison of a P-3 at 90,000lbs performing different escape maneuvers during a takeoff microburst encounter.

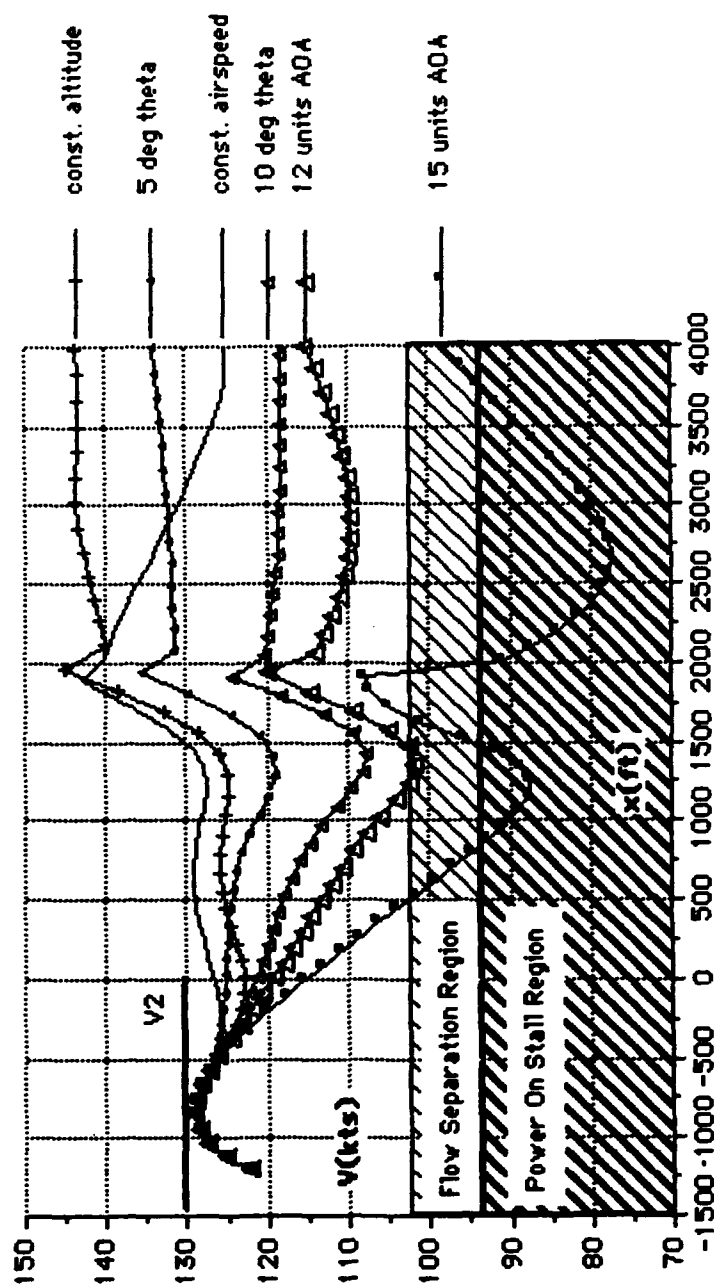


Figure 28. Airspeed comparison of a P-3 at 90,000lbs performing different escape maneuvers during a takeoff microburst encounter.

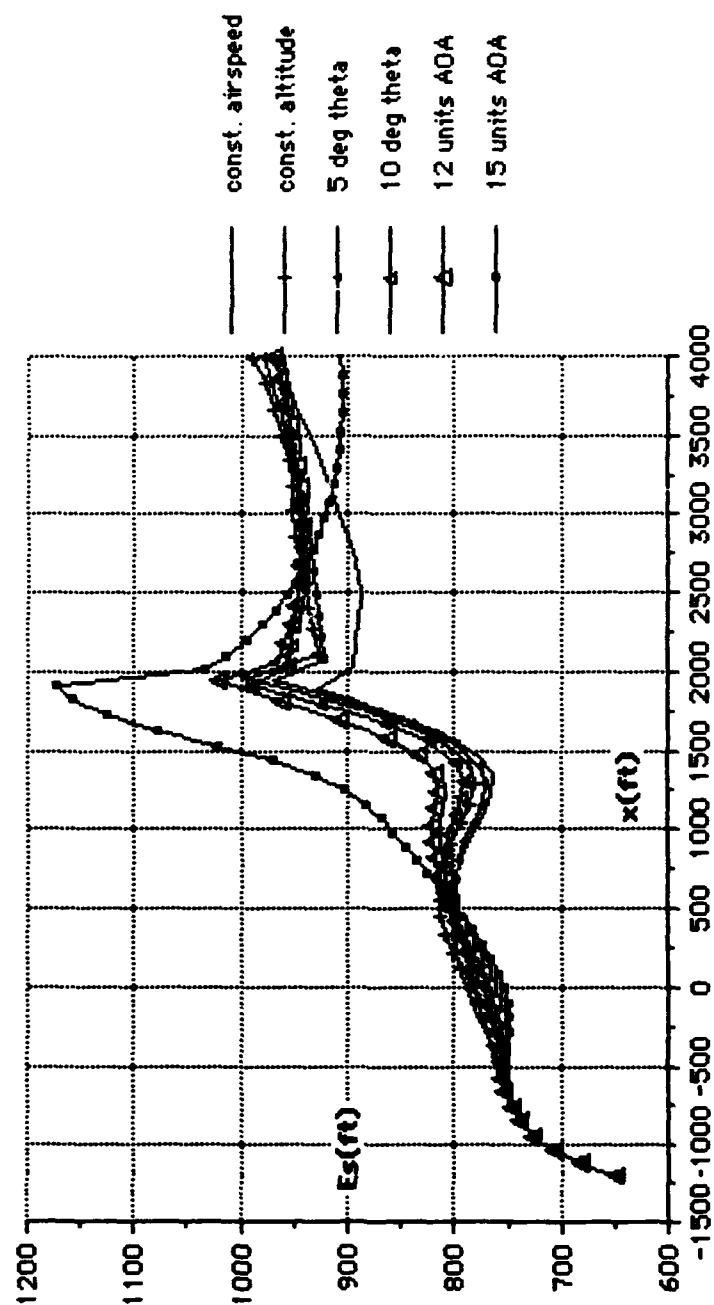


Figure 29. Specific energy comparison of a P-3 at 90,000lbs performing different escape maneuvers during a takeoff microburst encounter.

Figure 30, Figure 31, and Figure 32 depict the results obtained for different escape maneuvers performed by a P-3 at 120,000 pounds gross weight. Value comparison is made at $x=4000$ feet. The constant airspeed, constant altitude, 12 unit AOA, 15 unit AOA, and 5° theta escape maneuvers were rejected initially due ground impact as depicted in Figure 30. The 15° theta escape maneuver was subsequently rejected because of low airspeed and high AOA as observed in Figure 31. The only viable, however marginal, performance observed was for the 10° theta escape maneuver. Figure 31 shows that the 10° theta maneuver resulted in an airspeed drop of 30 knots below V_2 at one point followed by a sustained airspeed of 20 knots below V_2 .

Included with the 120,000 pound P-3 data is the resulting flight performance when V_r was increased. A large gain in altitude and specific energy over other performance profiles is observed. Increasing the rotate speed by 18 knots coupled with flying a constant 10° theta provides a 2 fold increase in altitude and a 27% increase in specific energy. This increase in specific energy is important when compared to the spread of specific energy values of different escape maneuvers.

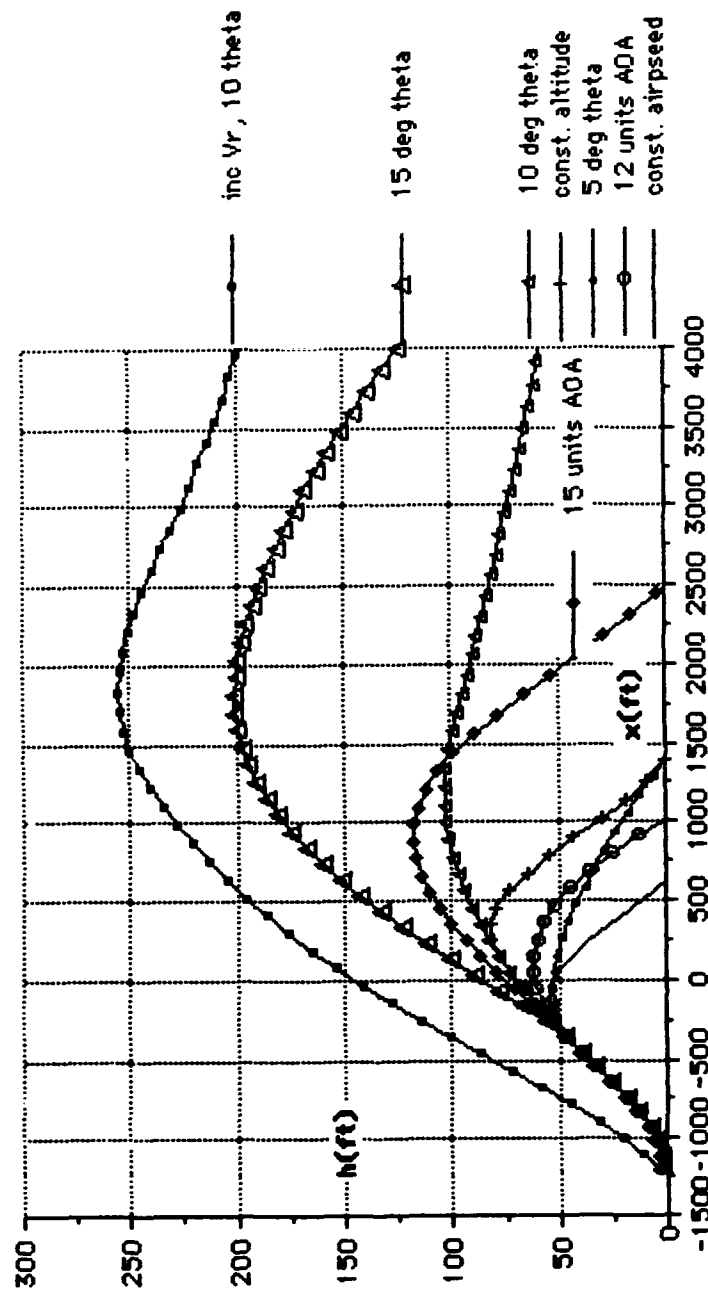


Figure 30. Flight path comparison of a P-3 at 120,000lbs performing different escape maneuvers during a takeoff microburst encounter.

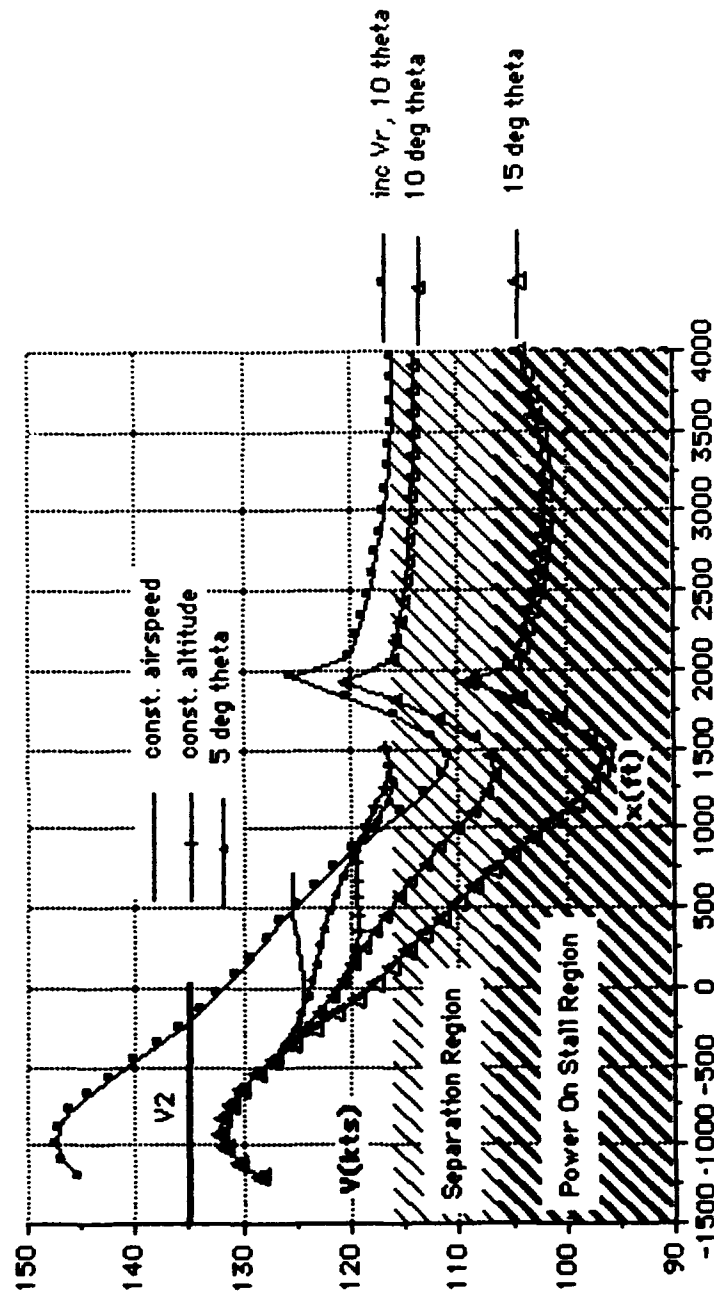


Figure 31. Airspeed comparison of a P-3 at 120,000lbs performing different escape maneuvers during a takeoff microburst encounter.

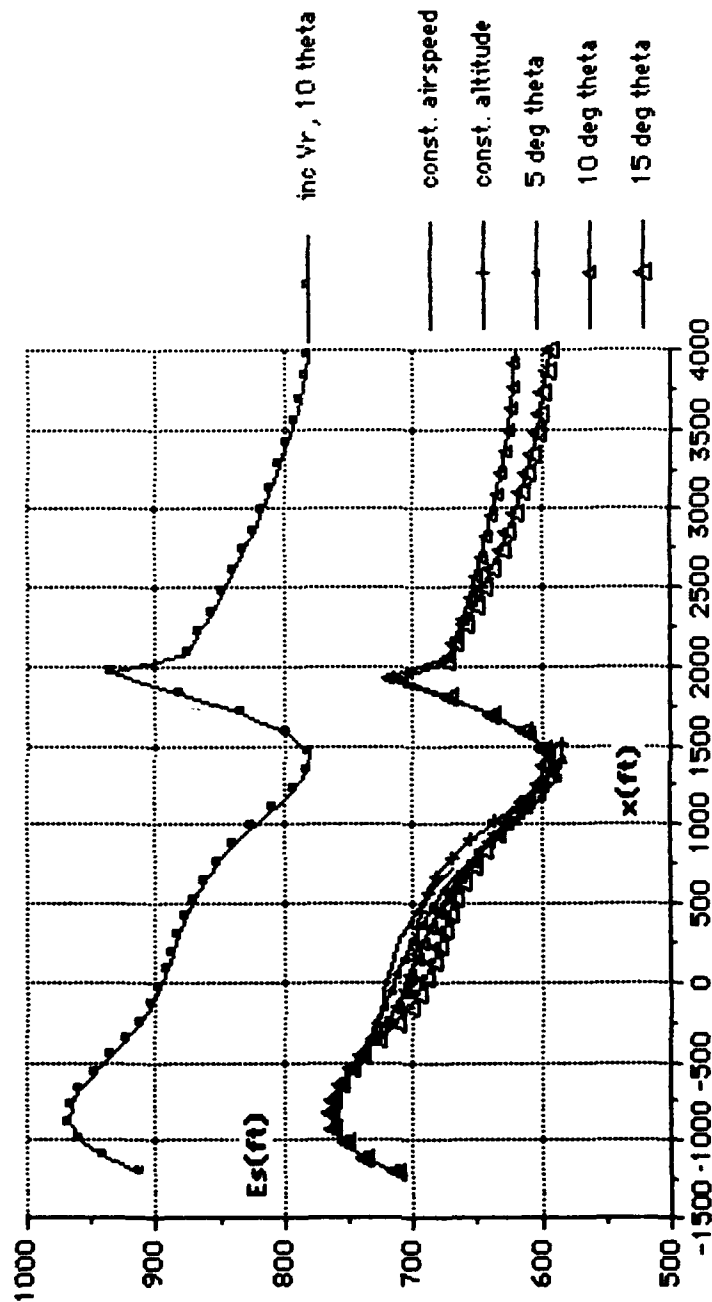


Figure 32. Specific energy comparison of a P-3 at 120,000lbs performing different escape maneuvers during a takeoff microburst encounter.

Figure 33, Figure 34, and Figure 35 depict the results obtained for different escape maneuvers performed by a P-3 at 135,000lbs gross weight. It can be graphically observed that a P-3 loaded to maximum takeoff weight is at the mercy of a strong microburst encountered at takeoff. Although the 15° theta maneuver misses the ground, the low airspeed and high AOA experienced disqualifies it as viable.

Figure 36, Figure 37, and Figure 38 depict the results obtained for different escape maneuvers performed by a T-44. Altitude, airspeed, and specific energy values are compared at x=4000 feet. All five escape maneuvers resulted in ground plane clearance as depicted in Figure 36. All five escape maneuvers provided adequate margin of airspeed and AOA as depicted in Figure 37. Note that power-on stall speed for the T-44 is less than 90 knots. Figure 38 shows that all escape maneuvers resulted in a grouped single value of specific energy. As seen above, all escape maneuvers for a given aircraft provide the same final specific energy during a takeoff microburst encounter. The only exception is when V_r is increased.

The results of one variant to the takeoff encounter are depicted in Figure 39, Figure 40, and Figure 41. Here, the microburst center is moved an added 800 feet from the liftoff point. This results in a delayed encounter with the severest part of the windshear. A P-3 at 120,00 pounds gross weight was used to perform the different

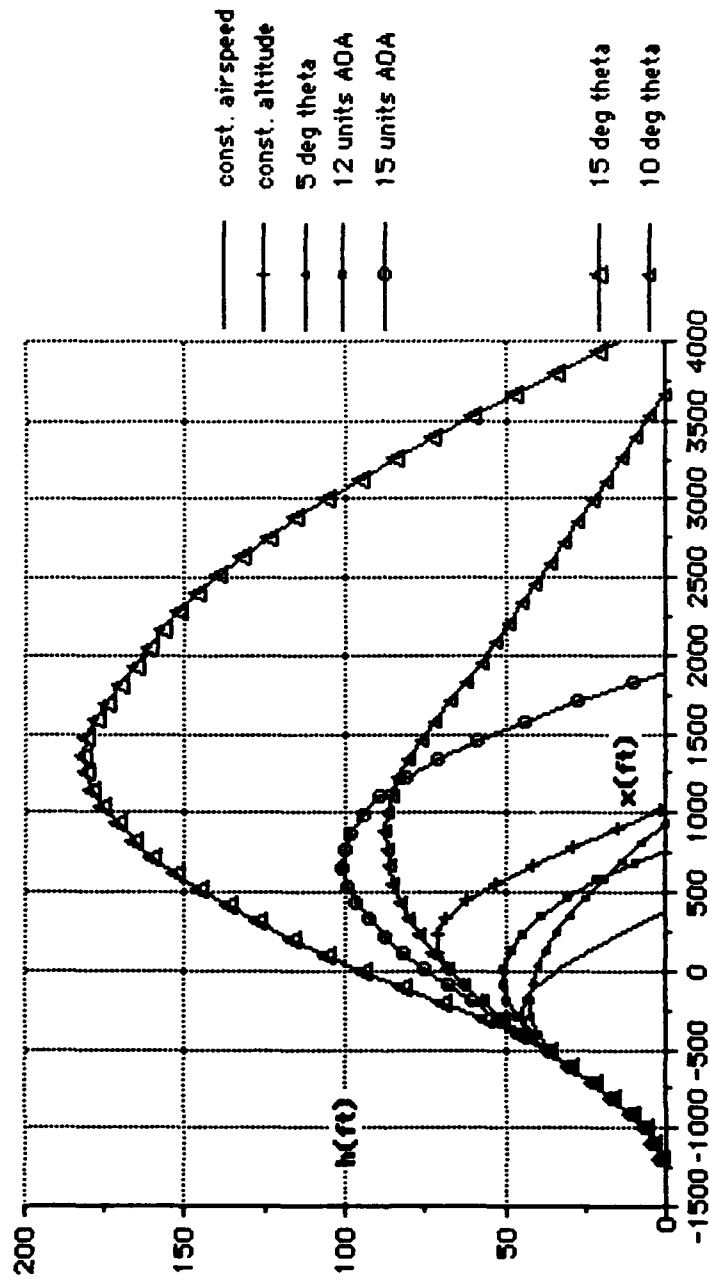


Figure 33. Flight path comparison of a P-3 at 135,000lbs performing different escape maneuvers during a takeoff microburst encounter.

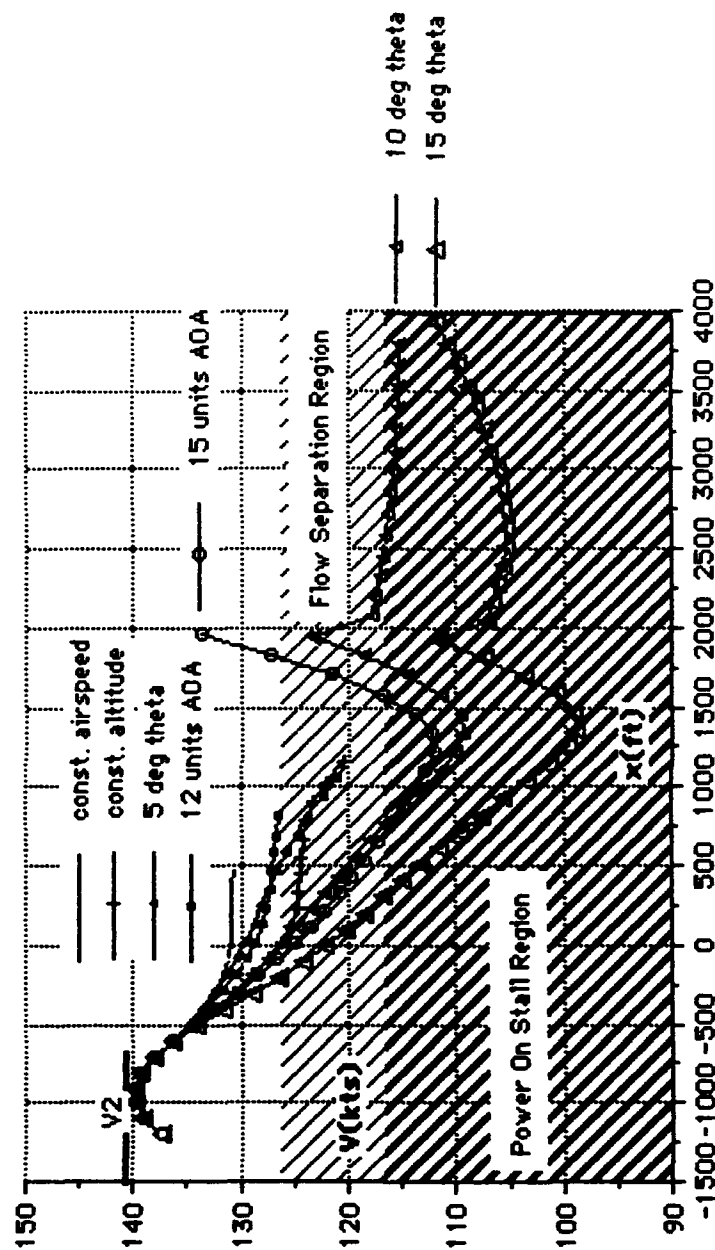


Figure 34. Airspeed comparison of a P-3 at 135,000lbs performing different escape maneuvers during a takeoff microburst encounter.

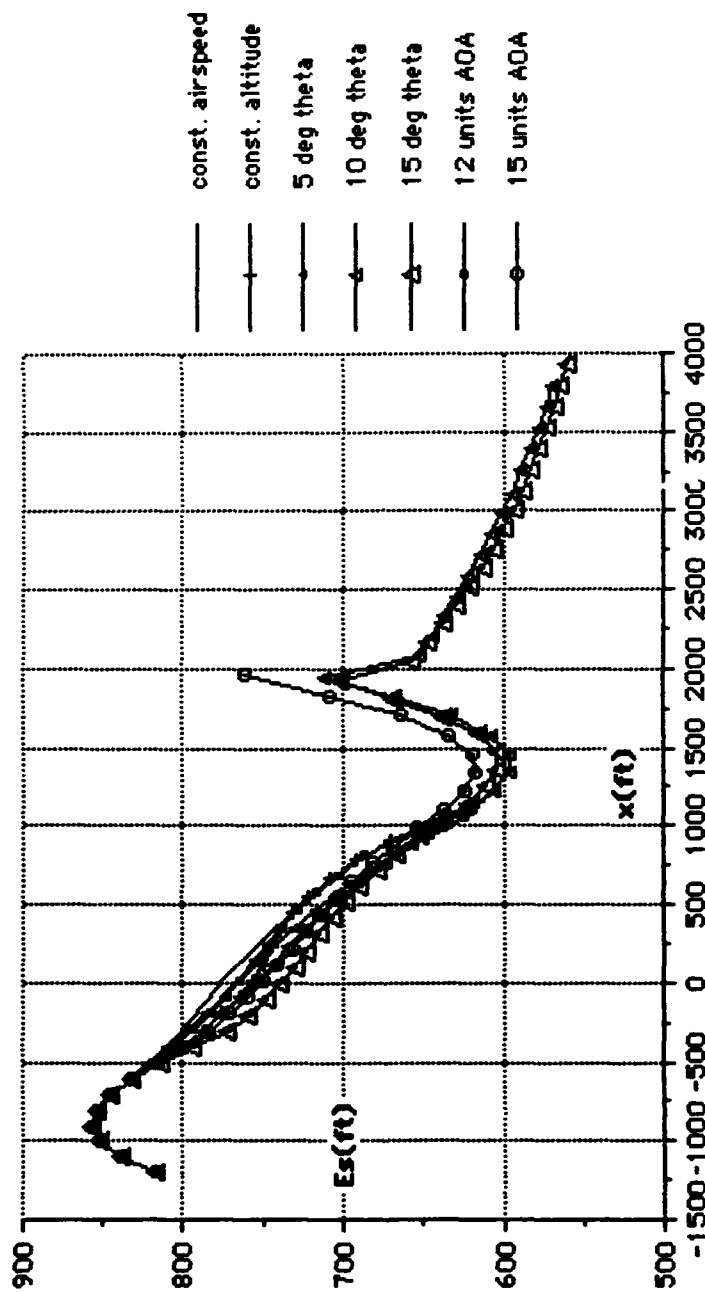


Figure 35. Specific energy comparison of a P-3 at 135,000lbs performing different escape maneuvers during a takeoff microburst encounter.

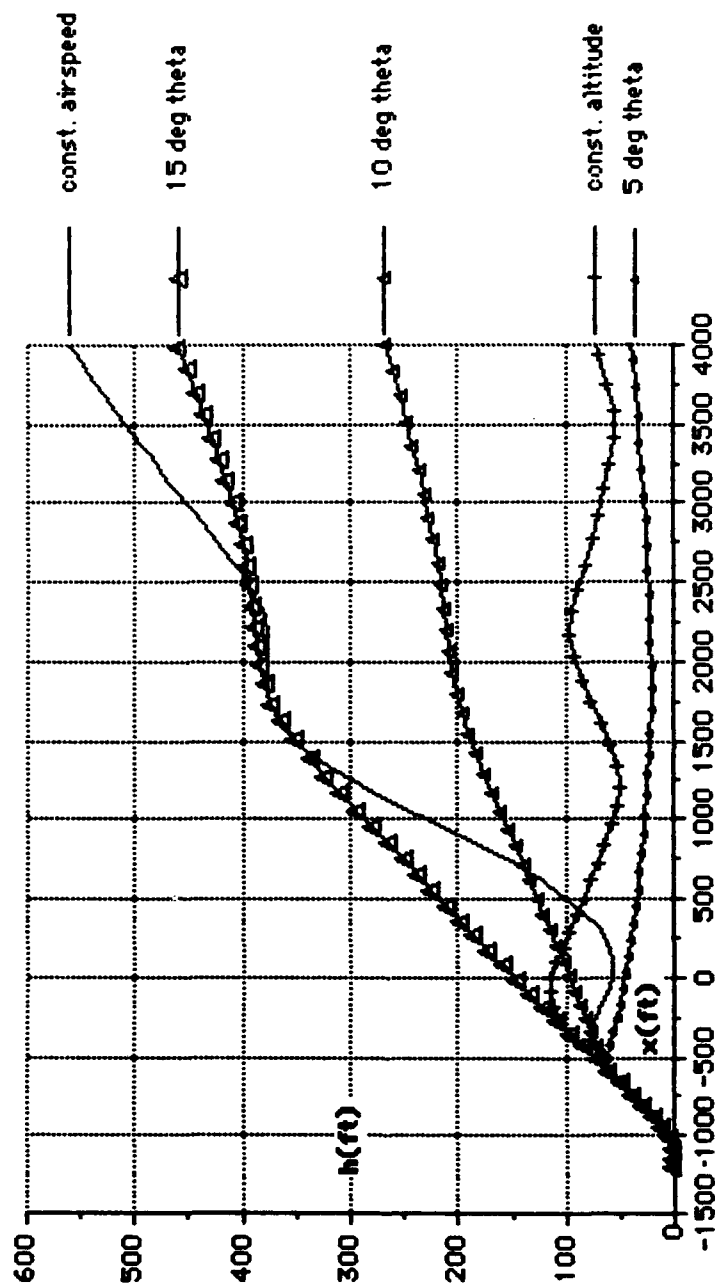


Figure 36. Flight path comparison of a T-44 performing different escape maneuvers during a takeoff microburst encounter.

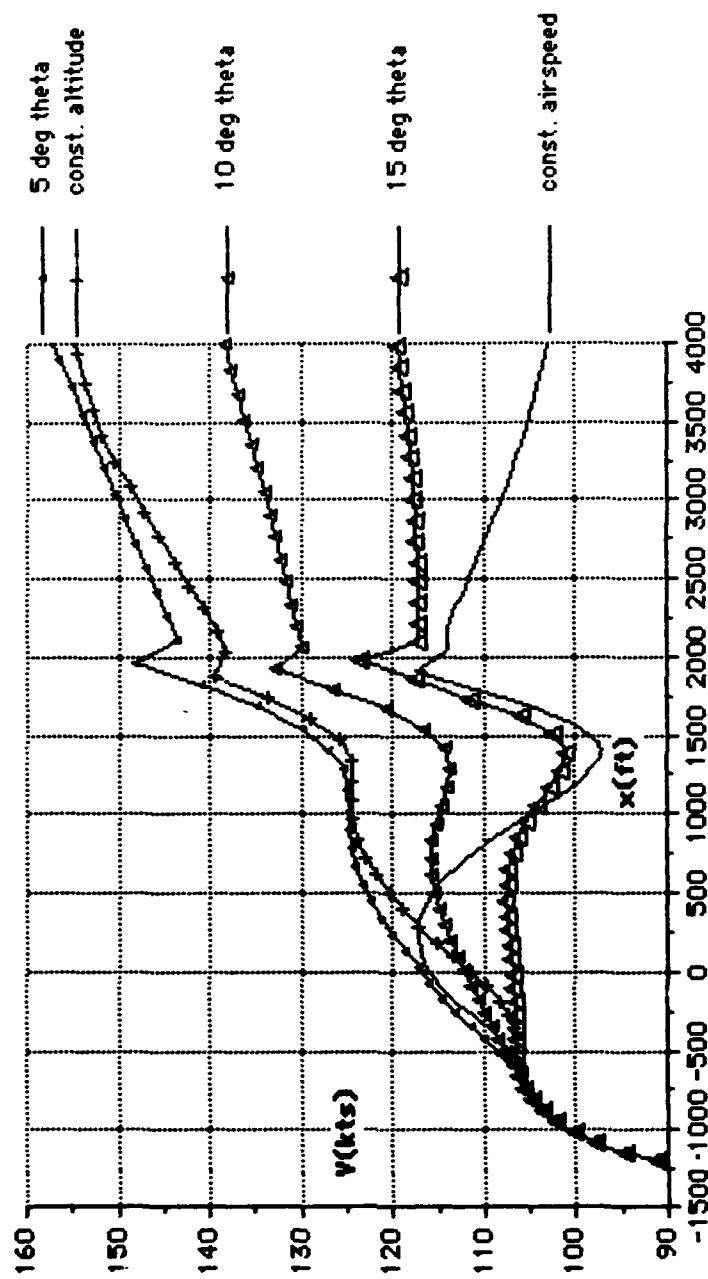


Figure 37. Airspeed comparison of a T-44 performing different escape maneuvers during a takeoff microburst encounter.

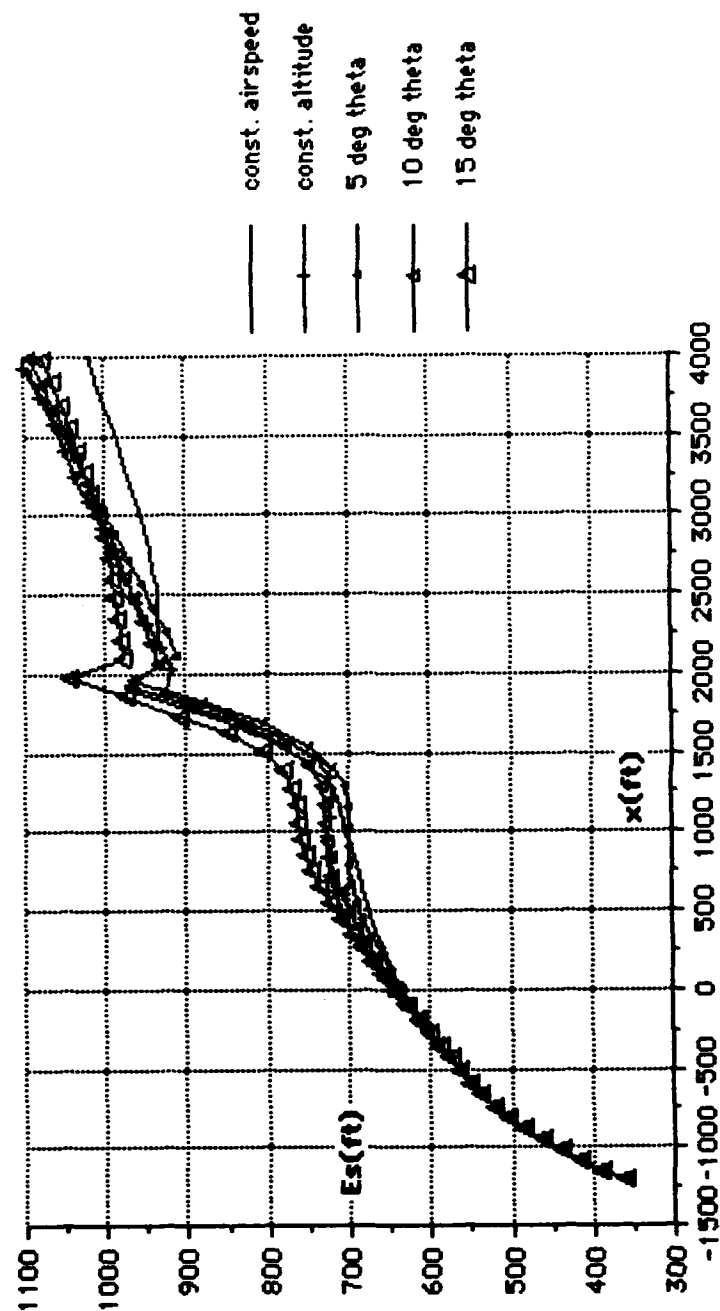


Figure 38. Specific energy comparison of a T-44 performing different escape maneuvers during a takeoff microburst encounter.

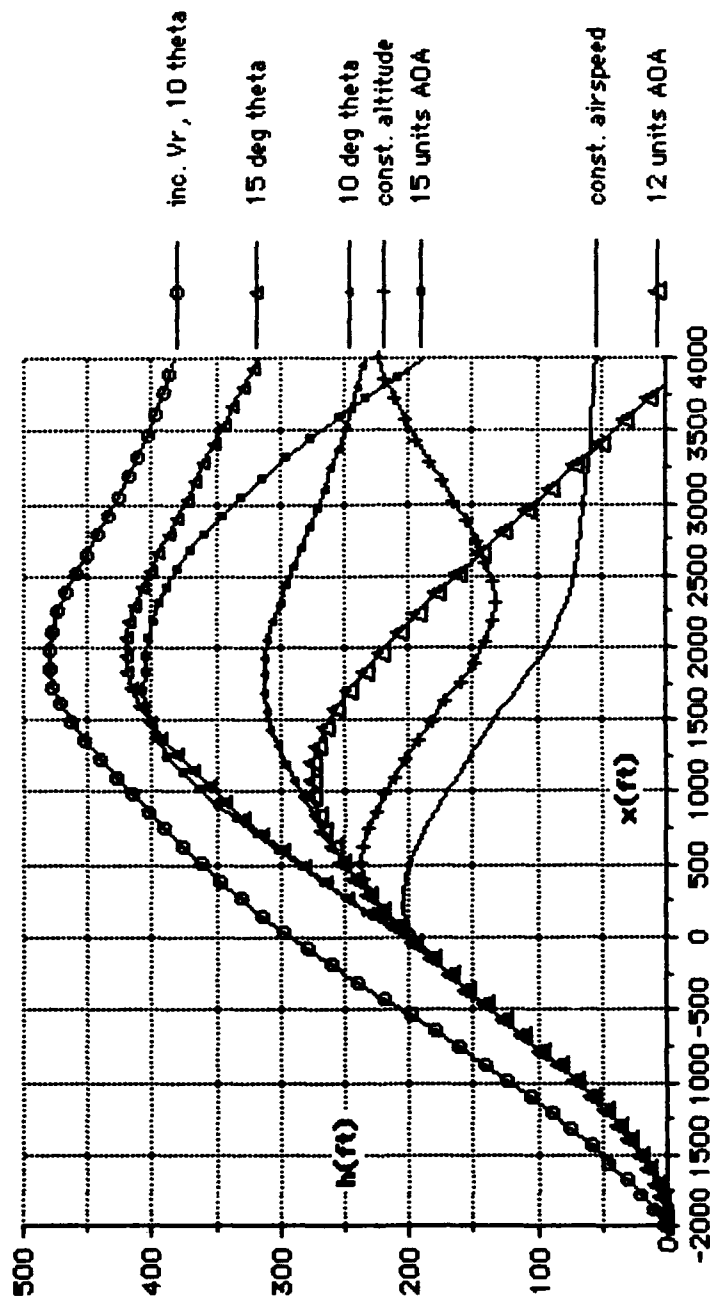


Figure 39. Flight path comparison of a P-3 at 120,000lbs performing different escape maneuvers during an after takeoff microburst encounter.

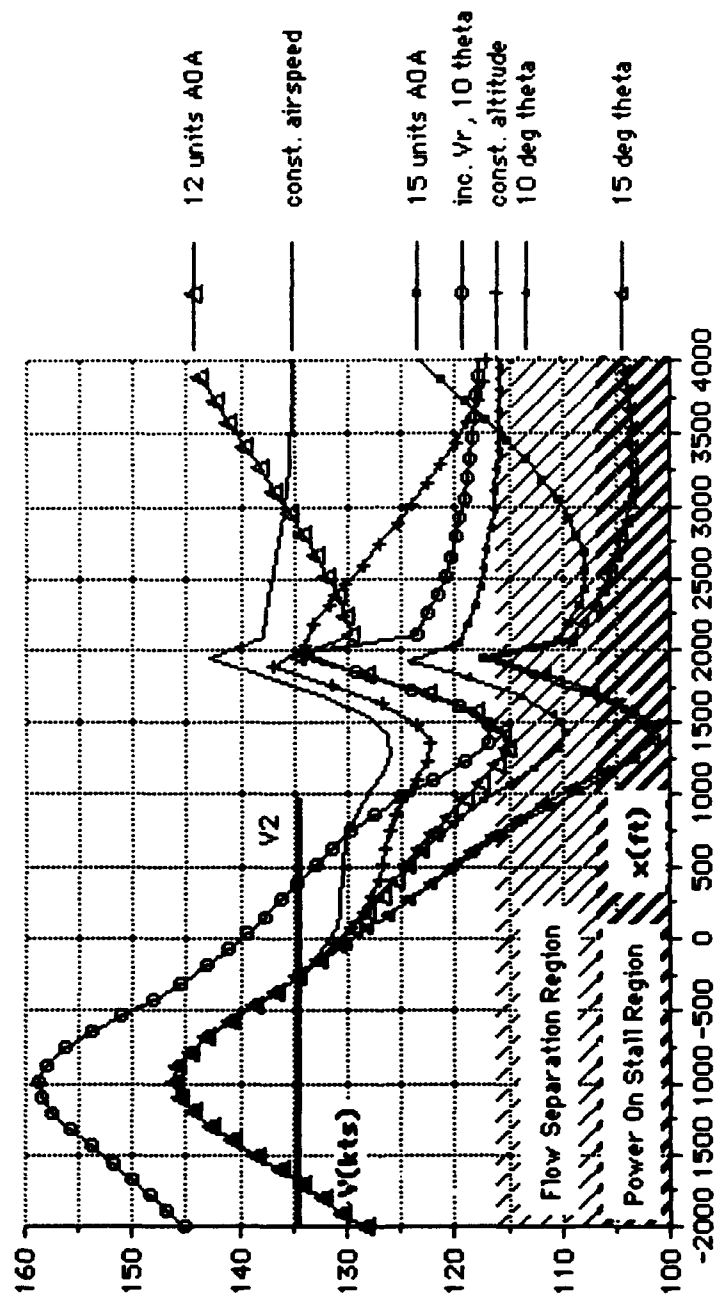


Figure 40. Airspeed comparison of a P-3 at 120,000 lbs performing different escape maneuvers during an after takeoff microburst encounter.

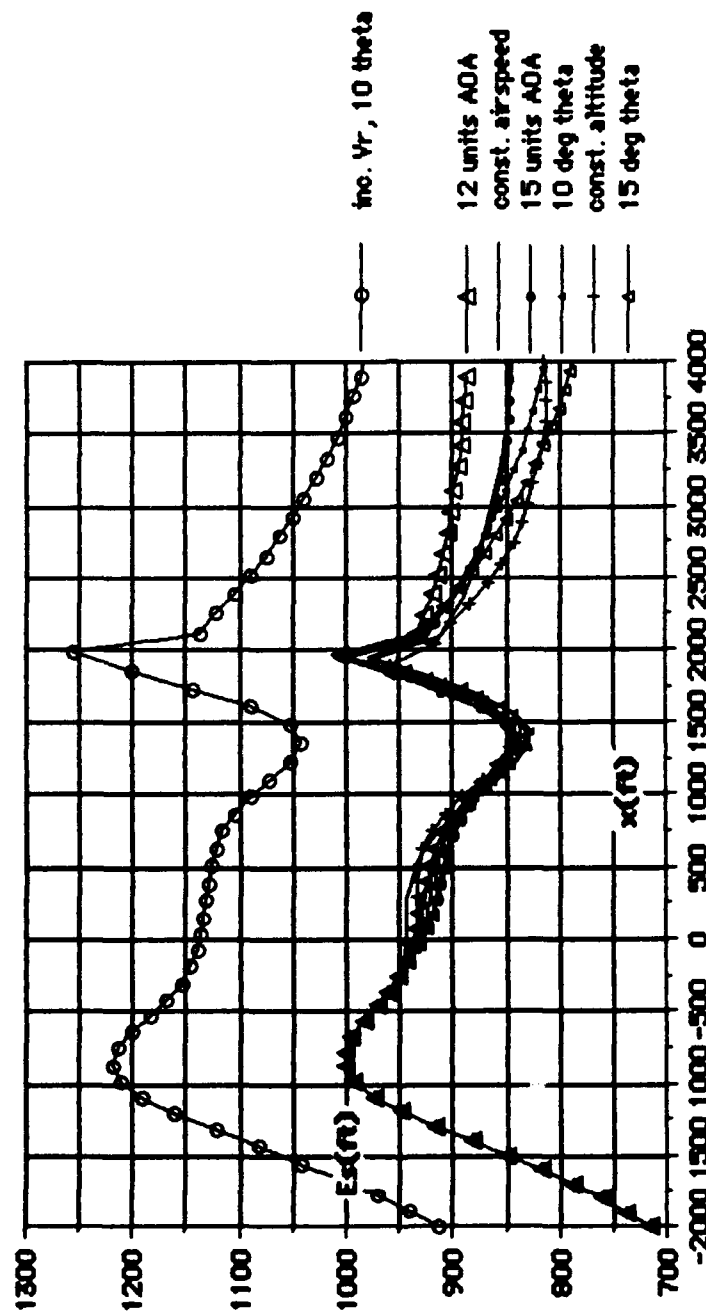


Figure 41. Specific energy comparison of a P-3 at 120,000lbs performing different escape maneuvers during an after takeoff microburst encounter.

escape maneuvers including the increased V_r technique. Table 11 compares the results observed at $x=4000$ feet. The 12 unit AOA escape maneuver was rejected initially due to ground impact as depicted in Figure 39. The 15 unit AOA and 15° theta escape maneuvers were subsequently rejected because of low airspeeds and high AOA's observed in Figure 40. Figure 41 shows that the close grouping of the specific energy values still exists for the non-increased V_r maneuvers. Again, the increased V_r resulted in a significant improvement in altitude and specific energy.

TABLE 11. RELATIVE VALUE RANKING FOR A P-3 AT 120,000LBS WITH AN AFTER TAKEOFF ENCOUNTER.

<u>maneuver</u>	<u>altitude</u>	<u>airspeed</u>	<u>specific energy</u>
increased V_r	1	2	1
15° theta	2	rejected	- - -
10° theta	3	4	2
const. altitude	4	3	3
15 unit AOA	5	rejected	- - -
const. airspeed	6	1	4

3. On-Station Encounter Analysis

The analysis showed that a P-3 at 120,000lbs gross weight successfully navigated a strong microburst during loiter operations. Figure 42 graphically depicts the results. Altitude deviation was no greater than ± 20 ft. Theta input never exceeded 10° . AOA remained below critical angle. Additional thrust was not applied until 40 knots of airspeed was lost in the encounter (a drop from 210 to 170 knots). Power was added at $x=2700$ feet and a time lapse of 23sec from the initial point of the encounter.

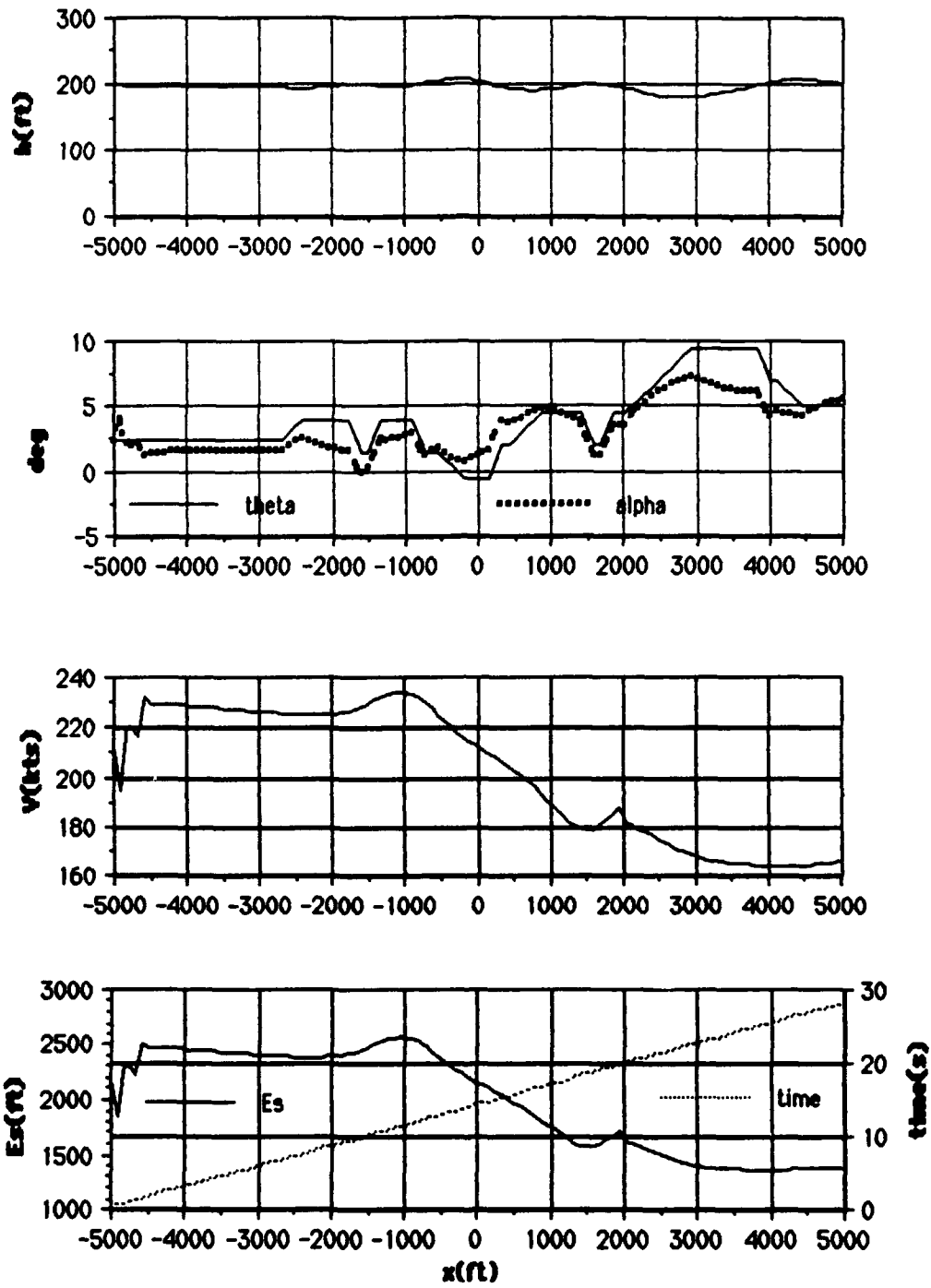


Figure 42. P-3 at 120,000lbs gross weight encountering a microburst windshear while on-station loiter.

D. OBSERVATIONS

The results obtained from the analytical analysis for each encounter are integrated with other relative information to answer the three posed questions:

- 1) What is the optimum microburst escape procedure given the type of encounter and the available flight performance information?
- 2) Is the optimum escape procedure effected by change of gross weight or available thrust?
- 3) What flight instrument indications, flight control feeling, and dynamic response would be expected during the optimum escape procedure?

The answers to these questions are directed to the P-3. However, comparison is made to the T-44 and 3-engine heavy airline transport where appropriate. Other important issues must also be addressed for comparison of results to other windshear studies. These issues include the impact of wing loading (W/S), thrust to weight (T/W), and early liftoff speeds for the P-3.

1. Available Aircraft Flight Instruments

The available flight information and type of presentation are extremely influential on the choice of the optimum escape procedure. Both the P-3 and T-44 have "conventional" flight instruments [Ref: 8 and Ref: 9]. Conventional implies gyroscopic-stabilized attitude and heading indication in combination with pitot-static airspeed, altitude, and vertical speed indication (VSI). Angle of Attack (AOA) indication

is installed on the P-3 and T-44. However, the AOA is heavily damped and is primarily designed for steady-state flight conditions. Standard radio navigation equipment is installed on both aircraft encompassing an Integrated Landing System (ILS), VHF Omni Radio (VOR), and Tactical Navigation (TACAN). The P-3 in addition has Inertial Navigation Systems (INS), but no information is presented at the flight station. Both aircraft incorporate autopilots and flight directors. The P-3 autopilot is controlled by Control Wheel Steering (CWS) input only. The T-44 autopilot is controlled through thumb wheels and can couple to the flight director. Flight directors on both aircraft can provide navigational steering. However, the primary design of the P-3 flight director is tactical while the primary design of the T-44 flight director is navigational. In summary, both the P-3 and T-44 have Attitude Indicators (AI), damped AOA indication, and pitot-static instruments for reference while executing an escape maneuver.

2. Optimal Escape Procedure

Flying a constant theta with reference to the AI seems to be the optimal escape procedure during a microburst encounter. This conclusion is supported analytically and qualitatively for the P-3 and T-44. Analytically, superior performance was obtained in a few circumstances from constant AOA maneuvers with an alpha value between approach and stall. However, qualitatively the AOA

indication in both aircraft does not lend itself as a viable reference for two reasons. First, the AOA indication may be significantly in error because of instrument lag in turbulent conditions. Second, P-3 and T-44 pilots seldom use AOA indication during the approach phase. The transition from attitude/airspeed to attitude/AOA reference during an intense situation as a microburst encounter, is more than can be expected from a pilotage standpoint. The only viable alternative to flying constant AOA was a constant theta maneuver. Note that quantitatively in all circumstances, a constant theta maneuver was superior to or closely matched with any other attempted escape maneuver.

Theta values ranging from 5° to 15° were identified as optimal for an approach to landing encounter. The theta value of 10° , if not optimal, provided suitable recovery for the P-3 in the configurations analyzed. The light, the heavy, and the 3-engine P-3 successfully navigated the microburst encounter utilizing the 10° theta escape. This result is important from the standpoint that 10° is easy to remember and easy to read on the AI. Also, 10° theta worked well for the T-44 in the approach configuration (approach flap setting). A theta of 15° was optimum for the T-44 in the takeoff configuration (flaps up). This is important because future P-3 pilots receive their first training in T44s.

3. The Effect Of Specific Energy On Survival Probability

Escaping from a takeoff microburst encounter has a lower probability for success compared to the approach to landing encounter. The type of escape maneuver selected in a takeoff encounter has a lesser effect on the outcome. This result is caused by the excess airspeed and additional altitude available during the approach phase. (Note that the P-3 community flies an unusually fast approach speed compared to their civilian counterparts. The P-3 approach V_{ref} airspeed is determined from $1.35V_s + 5$ knots [Ref. 20], which equates to $1.4V_s$ for a gross weight of 114,000 pounds. The industry standard for V_{ref} is $1.3V_s$ + an added factor as dictated by the type of aircraft.) Specific energy can be used for an interesting comparison between an approach to landing and a takeoff microburst encounter. A P-3 weighing 89,000 pounds has specific energy values of 1230 feet and 1040 feet at $x=500$ feet and $x=4000$ feet respectively during an approach to landing encounter (reference Figure 14). During a takeoff encounter, a P-3 at 90,000 pounds has a specific energy values of 810 feet and 980 feet at the same x distances from the microburst center (reference Figure 29). Both executed a 10° theta escape maneuver and both successfully navigated the microburst. Note that the approach to landing phase lost energy while the takeoff phase gained energy.

An important aspect of specific energy comparison is seen in the increased rotate speed data. Figure 41 graphically depicts a 120,000-pound P-3 starting with an additional specific energy of 200 feet compared to the normal rotate speed profiles. The exit specific energy was 175 feet greater than the comparable 10° theta maneuver. The 175 feet were translated almost completely to altitude (reference Figure 30 and Figure 31). Data support that an increased rotate speed is far more beneficial than any particular escape maneuver during a takeoff microburst encounter.

4. Stick Force vs. Off-Trim Airspeed For The P-3

The expected change in flight control "feel" for the P-3 is light compared to large aircraft. Flight tests show that stick force versus change from trim airspeed results in a shallow gradient for this size aircraft [Ref. 18:p. 37]. In the takeoff/approach flap configuration (18°), with an aft C.G. of 29% M.A.C., a stick force of an 11-pound pull is needed with a 30-knot decrease from trim airspeed. Stick force increases to a 16 pound pull with the most forward C.G. of 16% M.A.C. Flight test data [Ref. 18] also show that the stick force to trim airspeed gradient is not appreciably effected by landing gear position or gross weight. The same flap setting (takeoff/approach) is used for landing approach and takeoff. Thus, the elevator "feel" is expected to be the same for either approach to landing or takeoff microburst encounters.

The P-3 Flight Simulator (Device 2F87F) was used to confirm the flight test data relating to off-speed to stick force and landing gear drag. The simulator allows one or more flight parameters to be frozen. This feature is used by freezing the altitude to 500 feet and trimming the aircraft with maximum power at reference airspeed. The airspeed is then reset and frozen to the low airspeed value expected during a microburst encounter. The control force required to maintain a pitch attitude was then directly measured and printed out. The P-3 flight simulator data (Appendix H) showed that the elevator pull needed at V_{trim} minus 30kts decreased by 5 pounds when full power was applied. Level acceleration maneuvers were performed with the landing gear extended, retracted, and during retraction. Simulator data showed that the landing gear retraction cycle does not increase drag.

5. Weight, Wing Loading, and Thrust to Weight Effects

It is obvious from the analysis that a heavy P-3 is effected by microburst windshear to a higher degree than a light P-3. The T-44 was relatively unaffected by the windshear. The question arises whether weight, wing loading, or thrust to weight has the largest effect on microburst survival. Table 12 compares the weight (Wt), wing loading (W/S), thrust to weight (T/W), and specific energy values for three different aircraft during an approach to landing microburst encounter. The specific energy loss (E_s loss) column shows the energy

(in feet) lost during the encounter. The specific energy spread (E_s spread) column shows the spread (in feet) of the different escape techniques measured after the encounter. Apparently, the higher the thrust to weight ratio, the less energy is lost. Light wing loading equates to an individual escape procedure having less effect upon the result. Weight, as a separate parameter, is irrelevant. In other words, increased thrust to weight decreases the effect of the windshear upon the aircraft and light wing loading allows increased efficiency of energy transformation.

TABLE 12. WEIGHT, WING LOADING, AND THRUST TO WEIGHT EFFECTS ON P_s VALUES.

<u>aircraft</u>	<u>Wt (lbs)</u>	<u>W/S</u>	<u>T/W</u>	<u>E_s loss</u>	<u>E_s spread</u>
P-3	89,500	68.85	0.37	380	145
P-3	114,000	88.08	0.29	455	155
T-44	8,280	39.43	0.37	285	50
3-eng. hvy.	362,000	79.07	0.35	345	100

6. Early Liftoff Speed For The P-3

The analyses did not look at the effect of a microburst windshear encountered during a takeoff roll. The FAA Windshear Training Aid [Ref. 14] points out that if windshear is encountered past V_1 , the aircraft should be committed to flight no later than with 2000 feet of runway remaining. Although the airspeed may fall and stay below V_R , most aircraft can go airborne. In this regard, a theoretical liftoff speed was calculated for the P-3. Equations 38, 40, and 42 were used in conjunction to solve for V . The $C_{L\alpha}$ data were

extrapolated from flight test data [Ref. 18]. Table 13 compares the recommended V_r speed [Ref. 20] to the theoretical liftoff speed for a rotate pitch attitude of 10° . Ground effect was not considered in the calculations.

TABLE 13. THEORETICAL LIFTOFF SPEEDS

<u>weight (lbs)</u>	<u>V_r (kts)</u>	<u>theoretical liftoff (kts)</u>
80,000	115	90
90,000	115	95
100,000	115	101
110,000	117	105
120,000	123	110
130,000	129	115
140,000	134	119

8. Summary

The original three questions are answered for the P-3:

- 1) The optimum approach to landing microburst escape procedure is to set and maintain maximum power while simultaneously setting a 10° pitch attitude. For the takeoff microburst encounter, increase rotate speed to 140 knots then pitch to and maintain 10° .
- 2) The optimum escape procedures remain the same for all gross weights. The approach to landing encounter escape procedure is the same for four or three operating engines.
- 3) The airspeed will rapidly decay and remain abnormally low during a microburst penetration. An elevator force of 5 to 10 pounds can be expected to maintain a 10° pitch attitude with full power. Flight tests show that the P-3 has no unusual short period, phugoid, nor cross-couple dynamics to contend with.

The answers for the T-44 should be similar to the P-3. The 10° pitch attitude was optimal for the approach to landing encounter. A pitch attitude of 15° is optimal for takeoff, the difference being that the flaps are up in the takeoff configuration. Not enough performance data were available to predict the expected stick forces. However, personal flight experience has shown that the T-44 exhibits longitudinal forces and responses very similar to the P-3.

IV. CONCLUSIONS

The aim of this thesis was to analytically produce microburst escape flight procedures. Study was directed at two turboprop aircraft the Navy routinely operates. The P-3 and T-44 were closely scrutinized for the optimal escape procedure if confronted with a microburst penetration. The microburst modeled was patterned after that encountered by a Delta Airlines L-1011 at Dallas/Ft. Worth on August 2, 1985. The conclusions drawn are presented within the format of the FAA Windshear Training Aid [Ref. 14]. Viable flight procedures and associated precautions are presented for both aircraft. The precautions should be adhered to if an encounter with a microburst windshear is a possible expectation. NATOPS change recommendations reflecting these conclusions will be forwarded to the appropriate aircraft model managers.

A. MICROBURST ESCAPE PROCEDURES FOR THE P-3

A target pitch attitude of 10° is optimal for all weights and with four or three engines operating. This target pitch attitude is used for approach to landing and takeoff microburst encounters with the flaps in the Takeoff/Approach position. The airspeed at which the P-3 lifts off is the critical factor in the takeoff scenario.

1. Approach To Landing Microburst Encounter

Precautions:

- 1) Avoid thunderstorm conditions. Delay the approach if possible.
- 2) Use Takeoff/Approach flap setting. Do not extend flaps to Land position until the runway is made.
- 3) Use a precision approach procedure.
- 4) The approach speed, V_{ref} , should be equal to $1.35V_3 + 5$ knots. Additional airspeed is not normally warranted. This V_{ref} will provide a comfortable margin above stall speed. Note that additional airspeed increases landing distance (5 knots faster, 10% farther).
- 5) Determine expected descent rate.
- 6) Consider using the autopilot (ASW-31) with the altitude hold switch in the off position. The autopilot will provide wing rock damping and pitch attitude augmentation in the face of turbulence. It will also provide pitch attitude hold if a microburst escape maneuver is warranted. Insure autopilot disconnect passing 200 feet AGL.
- 7) Attain a stabilized airspeed approach before passing 1000 feet AGL. Minimize power lever movement beyond this point. Maintain glideslope with pitch. The airspeed indicator will serve as a windshear indicator.
- 8) Strong consideration should be given to executing the microburst escape procedure if one of the indications is observed:
 - a) a rapid and sustained airspeed loss of 20 knots below V_{ref} ;
 - b) a descent rate 500 feet per minute greater than the predetermined value;
 - c) greater than 1 dot low on the ILS glideslope associated with airspeed 10 knots below V_{ref} ; or
 - d) a "well below glideslope" call on a PAR associated with airspeed 10 knots below V_{ref} .

Escape procedure:

- 1) Apply maximum power (power levers to the stops).
- 2) Set and maintain a pitch attitude of 10° on the AI. *Do not* attempt to recover airspeed.
- 3) Once a positive rate of climb is established, select landing gear up.
- 4) Do not raise the flaps until the airspeed has increased above 140 knots indicating exit from the windshear.

2. Takeoff Microburst Encounter

Precautions:

- 1) Delay the takeoff if able.
- 2) Select the longest suitable runway.
- 3) Perform takeoff planning for adverse conditions as prescribed by the NATOPS Flight Manual.
- 4) Increase rotate airspeed to 140 knots, or the airspeed that is attained with 2000 feet of runway remaining. This is determined by using the Four Engine Acceleration Chart in NATOPS and following this procedure:
 - a) Subtract two thousand feet from the available runway length.
 - b) Enter the chart with the adjusted runway length, pressure altitude, temperature and gross weight. Exit the chart with the corresponding airspeed value. Use 140 knots if the chart value is higher.
 - c) Corrections for runway slope, winds, or standing water is not required for THIS prediction.
- 5) Thoroughly brief the takeoff procedure, voice calls, and windshear indications among the flight crew. Penetration of a windshear during takeoff will be indicated by a loss of airspeed or no airspeed acceleration.

Procedure:

- 1) Abort the takeoff if windshear is indicated before reaching refusal airspeed. Reaching refusal speed ground roll distance with airspeed significantly below OR above refusal speed indicates windshear.
- 2) Continue the takeoff if windshear is experienced after refusal speed. Rotate the nose when:
 - a) predicted increased rotate speed, usually 140 knots, is attained, or
 - b) 2000 feet of runway remain.
- 3) Rotate to a pitch attitude of 10°. DO NOT delay rotating the nose because of low airspeed.
- 4) Increase pitch attitude toward 15° if ground impact is imminent.
- 5) Raise the landing gear when above 100 feet AGL with a positive rate of climb.
- 6) Do not raise the flaps until normal climb airspeed is regained, indicating clear of the microburst.

3. On-Station Loiter Microburst Encounter

No immediate effect on the aircraft performance was observed. However, certain precautions should be taken and procedures followed if flying through convective activity at low altitude:

- 1) Use the autopilot altitude hold in dual axis mode. Note that if the autopilot is not used, the pilot can expect abnormal elevator control force changes.
- 2) Minimize power lever movement. Do not pull off power for high airspeed indication.

- 3) A penetration of a microburst will be indicated by a significant loss of airspeed. The first and foremost reaction should be the addition of full power. Monitor autopilot input and altitude hold.
- 4) If a climb is deemed warranted, set 10° pitch attitude using the CWS function of the autopilot.

B. MICROBURST ESCAPE PROCEDURES FOR THE T-44

Target pitch attitude escape procedures are just as effective for a light turboprop as the T-44. In its case, the target pitch values are different between takeoff and landing. This change is owed to different flap settings. Many of the same precautions and procedures are the same between the T-44 and P-3.

1. Approach To Landing Microburst Encounter

Precautions:

- 1) Avoid thunderstorm conditions. Delay the approach if possible.
- 2) Use Approach flap setting. Do not extend flaps to full down position unless required and until the runway is made.
- 3) Use a precision approach procedure.
- 4) The approach speed, V_{ref} , should be equal to 120 knots. Additional airspeed is not warranted. This V_{ref} will provide a comfortable margin above stall speed. Note that additional airspeed increases landing distance (5 knots faster, 10% farther).
- 5) Determine expected descent rate.

- 6) Consider using the autopilot in the coupled mode if executing an ILS. However, close monitoring of the autopilot is required because of abnormal elevator pitch forces expected in a windshear. Insure autopilot disconnect passing 200 feet AGL.
- 7) Attain a stabilized airspeed approach before passing 1000 feet AGL. Minimize power lever movement beyond this point. Maintain glideslope with pitch. The airspeed indicator will serve as a windshear indicator.
- 8) Strong consideration should be given to executing the microburst escape procedure if one of the indications is observed:
 - a) a rapid and sustained airspeed loss of 15 knots below V_{ref} ;
 - b) a descent rate 500 feet per minute greater than the predetermined value;
 - c) greater than 1 dot low on the ILS glideslope associated with airspeed 10 knots below V_{ref} ; or
 - d) a "well below glideslope" call on a PAR associated with airspeed 10 knots below V_{ref} .

Escape procedure:

- 1) Apply maximum power (power levers to the stops).
- 2) Set and maintain a pitch attitude of 10° on the AI. DO NOT attempt to recover airspeed.
- 3) Once a positive rate of climb is established, select landing gear up.
- 4) Do not raise the flaps until the airspeed has increased above 120 knots, indicating exit from the windshear.

2. Takeoff Microburst Encounter

Precautions:

- 1) Delay the takeoff if able.
- 2) Select the longest suitable runway.
- 3) Perform takeoff planning for adverse conditions as prescribed by the NATOPS Flight Manual.
- 4) Increase rotate airspeed to 120 knots, or the airspeed that is attained with 2000 feet of runway remaining.
- 5) Thoroughly brief the takeoff procedure, voice calls, and windshear indications among the flight crew. Penetration of a windshear during takeoff will be indicated by a loss of airspeed or no airspeed acceleration.

Procedure:

- 1) Abort the takeoff if windshear is indicated before reaching 91 knots airspeed.
- 2) Continue the takeoff if windshear is experienced after 91 knots airspeed. Rotate the nose when:
 - a) 120 knots; or
 - b) 2000 feet of runway remain.
- 3) Rotate to a pitch attitude of 15°. DO NOT delay rotating the nose because of low airspeed.
- 4) Increase pitch attitude toward 20° if ground impact is imminent.
- 5) Raise the landing gear when above 100 feet AGL with a positive rate of climb.

V. RECOMMENDATIONS

Recommendations are broken into two sections. The first set are for analysis refinement and further research. The second set are directed to the P-3 operators.

A. ANALYSIS REFINEMENT AND CONTINUED RESEARCH

There were some weak areas of this analysis that were pointed out earlier. Although valid results were obtained, refinement of the windshear model and the aircraft equations of motion would further explore the edges of the operating envelopes. The following recommendations are provided for the microburst windshear model:

- 1) Vortex wind field models seem to provide the closest representation of a microburst windshear, short of applying Navier-Stokes principles. Schultz's multiple vortex model combined with source flows should be combined and fitted to other previously recorded microbursts.
- 2) A more sophisticated parameter estimation scheme should be applied to enhance and accelerate parameter fits of recorded data to the vortex/source flow model.
- 3) Realistic boundary conditions to the windshear model should be defined. This would help explore the entry/exit aircraft response.

The following recommendations are for the aircraft performance models:

- 1) The lift and drag equations should be improved from second to fourth order equations. This change will enhance the representation of the aircraft performance at low airspeed/high angle of attack.
- 2) An available thrust algorithm should be integrated into the aircraft performance model. Comparison of turbojet, turbofan, turboprop, and reciprocating engine propulsion may lead to significant effects on performance through windshear.
- 3) A state-space matrix of aircraft dynamics should be integrated into the performance algorithm. Some aircraft may exhibit unexpected dynamics associated with microburst windshear and escape maneuvers.

B. P-3 OPERATIONS AND FLIGHT CREW TRAINING

An engineering analysis provides the performance specifications for penetrating a microburst and escaping. However, certain issues must be addressed by the P-3 community so as to successfully employ the results:

- 1) Flight crew coordination training is essential for successful employment of microburst escape procedures. All members of the flight deck must understand the teamwork required to execute these procedures. Therefore, comprehensive windshear training should be developed. The FAA Windshear Training Aid and this thesis provides an initial foundation.
- 2) A windshear algorithm should be developed for the P-3 Flight Simulators. There is no effective inflight means to expose flight crews to microburst effects. Nor can escape procedure be effectively practiced. The only proven instructional means are with a flight simulator.
- 3) A brief dissertation on microburst and gust front windshear should be provided in the flight station NATOPS manual. NATOPS change recommendations reflecting the conclusions of this study should be adopted.

LIST OF REFERENCES

1. Fujita, T.T., *Microbursts as an Aviation Wind Shear Hazard*, AIAA-81-0368 Paper, January 1981.
2. Fujita, T.T., *The Downburst-Microburst and Macrobust*, SMRP-RP-210, University of Chicago, 1985.
3. Fujita, T.T., *DFW Microburst*, SMRP-RP-217, University of Chicago, 1986.
4. Caracena, F., Holle, R.L., Doswell III, C.A., *Microbursts - A Handbook for Visual Identification*, U.S. Department of Commerce, U.S. Government Printing Office, Washington, D.C., February 1990.
5. Federal Aviation Administration, *Low-Level Wind Shear*, Advisory Circular 00-50A, Washington, D.C., January 1979.
6. Aircraft Accident Report, *Delta Airlines, Inc., Lockheed 1-1011-385-1, N726D, Dallas/Fort Worth International Airport, Texas, August 2, 1985*, National Transportation Safety Board, Washington, DC, Report AAR-86/05, August, 1986.
7. Wingrove, R.C., and Bach, R.E., *Severe Winds in the Dallas/Ft. Worth Microburst Measured from Two Aircraft*, J. Aircraft, Vol. 26, No. 3, March 1989.
8. Schlickenmaier, H.W., *Windshear Case Study: Denver, Colorado, July 11, 1988*, National Technical Information Service, DOT/FAA/DS-89/19, November, 1989.
9. Hinton, D.A., *Relative Merits of Reactive and Forward-Look Detection for Wind-Shear Encounters During Landing Approach for Various Microburst Escape Strategies*, NASA Technical Memorandum 4158, DOT/FAA/DS-89/35, 1990.
10. Bray, R.S., *Aircraft Performance and Control in Downburst Wind Shear*, NASA TM-861698, 1986.

11. Miele, A., Wang, T., Tzeng, C.Y., Melvin, W.W., *Optimization and Guidance of Abort Landing Trajectories in Windshears*, AIAA Guidance, Navigation, and Control Conference, Vol. 1, 1987.
12. Hinton, D.A., *Flight-Management Strategies for Escape From Microburst Encounters*, NASA TM-4057, August, 1988.
13. Baily, J.E., Krishnakumar, K., *Total Energy Control Concepts, Applied to Flight in Windshear*, AIAA Guidance, Navigation, and Control Conference, Vol. 1, 1987.
14. Federal Aviation Administration, *Windshear Training Aid*, National Archives, Washington, D.C., 1987.
15. Schultz, T.A., *A Multiple-Vortex-Ring Model of the DFW Microburst*, AIAA-88-0685 Paper, January, 1988.
16. Oseguera, R.M., Bowles, R.L., *A Simple, Analytical 3-Dimensional Downburst Model Based On Boundary Layer Stagnation Flow*, NASA Technical Memorandum 100632, July, 1988.
17. Ferziger, J.H., *Numerical Methods for Engineering Applications*, John Wiley & Sons, Inc., 1981.
18. Lockheed Aircraft Corporation Report 13133, *Lockheed P3V-1 Flying Qualities*, unclassified, 19 November, 1959.
19. Naval Air Test Center Technical Report AT-71R-81, *Flight Fidelity Evaluation of the T44 Operational Flight Trainer (2F129)*, by LCDR T.J. Lee, 5 June 1982.
20. Naval Air Systems Command Publication, *NATOPS Flight Manual, Navy Model P-3C Aircraft*, NAVAIR 01-75PAC-1, official use only, 1 December, 1983.
21. Naval Air Systems Command Publication, *NATOPS Flight Manual, Navy Model T-44A Aircraft*, NAVAIR 01-T44AAA-1, official use only, 1 March, 1985.

APPENDIX A

WINDSHEAR MODEL ALGORITHMS

The following are MatLab® functions which model the winds experienced at DFW on August 2, 1985 by two separate aircraft. AA539 penetrated the microburst at 2500 feet. DAL191 penetrated the same microburst while attempting a landing.

A. AA539 WINDSHEAR MODEL ALGORITHM

```
function [vx,vz]=microburst(ze,x)
```

```
% INITIAL VALUES AND INPUTS
```

```
% Earth position
```

```
%ze = altitude (ft)
```

```
%x horizontal position (ft)
```

```
% Vortex Ring Dimensions
```

```
RL=8503.3;
```

```
%radius of ring filament (ft)
```

```
riL=2004.1;
```

```
%core radius (ft)
```

```
kL=431968.8;
```

```
%vortex strength of the ring
```

```
%filament(ft^2/sec)
```

```
rowL=riL/0.371;
```

```
%related core radius
```

```
yL=3350.4;
```

```
%large ring y lateral position (ft)
```

```
LVoralt=3400.6;
```

```
%large vortex altitude AGL (ft)
```

```
Rs=1701.7;
```

```
%radius of ring filament (ft)
```

```
ris=323.9;
```

```
%core radius (ft)
```

```
ks=57204.9;
```

```
%vortex strength of the ring
```

```
%filament (ft^2/sec)
```

```
rowS=ris/0.371;
```

```
%related core radius
```

```
ys=830.9;
```

```
%small ring y lateral position (ft)
```

```
sVoralt=2333.6;
```

```
%small vortex altitude AGL (ft)
```

% PRIMARY LARGE RING CALCULATIONS

```

z=ze-LUoralt;
if x==0,
    if yL==0,
        vxL=0;
        vzL=-kL*RL^2/(2*(RL^2+z^2)^1.5);
        zerock=0;
    end
else
    zerock=999;
    r=sqrt(x^2+yL^2);           %radial distance from the z axis
    r1=sqrt(z^2+(r-RL)^2);      %closest distance to the point of
                                %interest from the ring filament.
    r2=sqrt(z^2+(r+RL)^2);      %farthest distance to the point of
                                %interest from the ring filament.
    lambda=(r2-r1)/(r2+r1);     %scaling term
    n1=(r+RL)/r2;
    n2=(r-RL)/r1;
    sig1=z/r2+z/r1;
    sig2=z/r2-z/r1;
    tow=0.75*sqrt(1-lambda^2)+0.25;
    delta1=(kL*lambda)/(pi*tow);
    delta2=(0.2955*kL*lambda^3)/(pi*tow^2*sqrt(1-lambda^2));
    dSidr=0.788*delta1*(n1-n2)-0.394*lambda*delta1*(n1+n2)
           +delta2*((n1-n2)-lambda*(n1+n2));
                                %derivative of the stream function wrt r
    dSidz=delta1*(0.788*sig2-0.394*lambda*sig1)
           +delta2*(sig2-lambda*sig1);
                                %derivative of the stream function wrt z
    dampL=(1-exp(-r1^2/(0.1*rowL^2)));
                                %velocity damping factor
    vxL=(x/r)*(1/r)*dSidz;     %horizontal velocity in x direction
    vzL=-(1/r)*dSidr;          %vertical velocity
end %if

```

```

% PRIMARY SMALL RING CALCULATIONS
z=ze-sUoralt;
if x==0,
    if ys==0,
        vxs=0;
        vzs=-ks*Rs^2/(2*(Rs^2+z^2)^1.5);
    end
else
    r=sqrt((x-50)^2+ys^2);           %radial distance from the z axis
    r1=sqrt(z^2+(r-Rs)^2);           %closest distance to the point of
                                     %interest from the ring filament.
    r2=sqrt(z^2+(r+Rs)^2);           %farthest distance to the point of
                                     %interest from the ring filament.
    lambda=(r2-r1)/(r2+r1);           %scaling term
    n1=(r+Rs)/r2;
    n2=(r-Rs)/r1;
    sig1=z/r2+z/r1;
    sig2=z/r2-z/r1;
    tow=0.75*sqrt(1-lambda^2)+0.25;
    delta1=(ks*lambda)/(pi*tow);
    delta2=(0.2955*ks*lambda^3)/(pi*tow^2*sqrt(1-lambda^2));
    dSldr=0.788*delta1*(n1-n2)-0.394*lambda*delta1
            *(n1+n2)+delta2*((n1-n2)-lambda*(n1+n2));
                                     %derivative of the stream function wrt r
    dSldz=delta1*(0.788*sig2-0.394*lambda*sig1)
            +delta2*(sig2-lambda*sig1);
                                     %derivative of the stream function wrt z
    if (r1^2/(0.1*rows^2))>444,
        daps=1;
    else
        %velocity damping factor
        daps=1-exp(-r1^2/(0.1*rows^2));
    end
    vxs=(x/r)*(1/r)*dSldz;           %horizontal velocity x direction
    vzs=-(1/r)*dSldr;                 %vertical velocity
end %if

```



```

% IMAGE LARGE RING CALCULATIONS
x=x;
z=-ze-LUoralt;
if x==0,
    if yL==0,
        vxLi=0;
        vzLi=-kL*RL^2/(2*(RL^2+z^2)^1.5);
    end
else
    r=sqrt(x^2+yL^2);           %radial distance from the z axis
    r1=sqrt(z^2+(r-RL)^2);      %closest distance to the point of
                                %interest from the ring filament.
    r2=sqrt(z^2+(r+RL)^2);      %farthest distance to the point of
                                %interest from the ring filament.
    lambda=(r2-r1)/(r2+r1);     %scaling term
    n1=(r+RL)/r2;
    n2=(r-RL)/r1;
    sig1=z/r2+z/r1;
    sig2=z/r2-z/r1;
    tow=0.75*sqrt(1-lambda^2)+0.25;
    delta1=(kL*lambda)/(pi*tow);
    delta2=(0.2955*kL*lambda^3)/(pi*tow^2*sqrt(1-lambda^2));
    dSldr=0.788*delta1*(n1-n2)-0.394*lambda*delta1
        *(n1+n2)+delta2*((n1-n2)-lambda*(n1+n2));
                                %derivative of the stream function wrt r
    dSldz=delta1*(0.788*sig2-0.394*lambda*sig1)
        +delta2*(sig2-lambda*sig1);
                                %derivative of the stream function wrt z
    dapLi=(1-exp(-r1^2/(0.1*rowL^2)));
                                %velocity damping factor
    vxLi=(x/r)*(1/r)*dSldz;    %horizontal velocity in x direction
    vzLi=-(1/r)*dSldr;         %vertical velocity
end %if

```

```

% IMAGE SMALL RING CALCULATIONS
z=-ze-sUoralt;
if x==0,
    if ys==0,
        vxsi=0;
        uzsi=-ks*Rs^2/(2*(Rs^2+z^2)^1.5);
    end
else
    r=sqrt((x+50)^2+ys^2);           %radial distance from the z axis
    r1=sqrt(z^2+(r-Rs)^2);           %closest distance to the point of
                                     %interest from the ring filament.
    r2=sqrt(z^2+(r+Rs)^2);           %farthest distance to the point of
                                     %interest from the ring filament.
    lambda=(r2-r1)/(r2+r1);          %scaling term
    n1=(r+Rs)/r2;
    n2=(r-Rs)/r1;
    sig1=z/r2+z/r1;
    sig2=z/r2-z/r1;
    tow=0.75*sqrt(1-lambda^2)+0.25;
    delta1=(ks*lambda)/(pi*tow);
    delta2=(0.2955*ks*lambda^3)/(pi*tow^2*sqrt(1-lambda^2));
    dSidr=0.788*delta1*(n1-n2)-0.394*lambda*delta1
           *(n1+n2)+delta2*((n1-n2)-lambda*(n1+n2));
                                     %derivative of the stream function wrt r
    dSidz=delta1*(0.788*sig2-0.394*lambda*sig1)
           +delta2*(sig2-lambda*sig1);
                                     %derivative of the stream function wrt z
    if (r1^2/(0.1*rows^2))>444,
        dapsi=1;
    else
        %velocity damping factor
        dapsi=1-exp(-r1^2/(0.1*rows^2));
    end

    vxsi=(x/r)*(1/r)*dSidz;          %horizontal velocity x direction
    vzsi=-(1/r)*dSidr;               %vertical velocity
end %if

```

```

%      SUMMATION
if zerock==999,
    dap=dapL*daps*dapLi*dapsi;
    ux=-(dap*(uxL+uxs+uxLi+uxsi));
    vz=dap*(vzL+vzs-vzLi-vzsi);
else
    ux=-(uxL+uxs+uxLi+uxsi);
    vz=vzL+vzs-vzLi-vzsi;
end

```

B. DAL191 WINDSHEAR MODEL ALGORITHM

```
function [ux,vz]=microburst(ze,x)
```

```
%      INITIAL VALUES AND INPUTS
```

```
% Earth position
```

```
%ze = altitude (ft)
```

```
%x horizontal position (ft)
```

```
% Vortex Ring Dimensions
```

```
RL=7000;
```

```
%radius of ring filament (ft)
```

```
riL=2004.1;
```

```
%core radius (ft)
```

```
kL=431968.8*1;
```

```
%vortex strength of the ring
```

```
%filament (ft^2/sec)
```

```
rowL=riL/0.371;
```

```
%related core radius
```

```
yL=-300;
```

```
%large ring y lateral position (ft)
```

```
LUoralt=3400;
```

```
%large vortex altitude AGL (ft)
```

```
Lxdisp=2500;
```

```
%large ring displacement in x (ft)
```

```
Rs=1300;
```

```
%radius of ring filament (ft)
```

```
ris=323.9;
```

```
%core radius (ft)
```

```
ks=57204.9*2.3;
```

```
%vortex strength of the ring
```

```
%filament (ft^2/sec)
```

```
rows=ris/0.371;
```

```
%related core radius
```

```
ys=1;
```

```
%small ring y lateral position (ft)
```

```
sUoralt=800;
```

```
%small vortex altitude AGL (ft)
```

```
sxdisp=300;
```

```
%small ring displacement in x (ft)
```

```

% PRIMARY LARGE RING CALCULATIONS
z=ze-LUoralt;
if x==0,
    if yL==0,
        vxL=0;
        vzL=-kL*RL^2/(2*(RL^2+z^2)^1.5);
        zerock=0;
    end
else
    zerock=999;
    r=sqrt(x^2+yL^2); %radial distance from the z axis
    r1=sqrt(z^2+(r-RL)^2); %closest distance to the point of
    %interest from the ring filament.
    r2=sqrt(z^2+(r+RL)^2); %farthest distance to the point of
    %interest from the ring filament.
    lambda=(r2-r1)/(r2+r1); %scaling term
    n1=(r+RL)/r2;
    n2=(r-RL)/r1;
    sig1=z/r2+z/r1;
    sig2=z/r2-z/r1;
    tow=0.75*sqrt(1-lambda^2)+0.25;
    delta1=(kL*lambda)/(pi*tow);
    delta2=(0.2955*kL*lambda^3)/(pi*tow^2*sqrt(1-lambda^2));
    dSldr=0.788*delta1*(n1-n2)-0.394*lambda*delta1*(n1+n2)
        +delta2*((n1-n2)-lambda*(n1+n2));
    %derivative of the stream function wrt r
    dSldz=delta1*(0.788*sig2-0.394*lambda*sig1)
        +delta2*(sig2-lambda*sig1);
    %derivative of the stream function wrt z
    dmpL=(1-exp(-r1^2/(0.1*rowL^2)));
    %velocity damping factor
    vxL=(x/r)*(1/r)*dSldz; %horizontal velocity in x direction
    vzL=-(1/r)*dSldr; %vertical velocity
end %if

```

```

% PRIMARY SMALL RING CALCULATIONS
z=ze-sUoralt;
if x==0,
    if ys==0,
        vx=0;
        vz=-ks*Rs^2/(2*(Rs^2+z^2)^1.5);
    end
else
    r=sqrt((x-50)^2+ys^2);           %radial distance from the z axis
    r1=sqrt(z^2+(r-Rs)^2);           %closest distance to the point of
                                     %interest from the ring filament.
    r2=sqrt(z^2+(r+Rs)^2);           %farthest distance to the point of
                                     %interest from the ring filament.
    lambda=(r2-r1)/(r2+r1);          %scaling term
    n1=(r+Rs)/r2;
    n2=(r-Rs)/r1;
    sig1=z/r2+z/r1;
    sig2=z/r2-z/r1;
    tow=0.75*sqrt(1-lambda^2)+0.25;
    delta1=(ks*lambda)/(pi*tow);
    delta2=(0.2955*ks*lambda^3)/(pi*tow^2*sqrt(1-lambda^2));
    dSldr=0.788*delta1*(n1-n2)-0.394*lambda*delta1
            *(n1+n2)+delta2*((n1-n2)-lambda*(n1+n2));
                                     %derivative of the stream function wrt r
    dSldz=delta1*(0.788*sig2-0.394*lambda*sig1)
            +delta2*(sig2-lambda*sig1);
                                     %derivative of the stream function wrt z
    if (r1^2/(0.1*rows^2))>444,
        daps=1;
    else
        %velocity damping factor
        daps=1-exp(-r1^2/(0.1*rows^2));
    end
    vx=(x/r)*(1/r)*dSldz;           %horizontal velocity x direction
    vz=-(1/r)*dSldr;                %vertical velocity
end %if

```

```

% IMAGE LARGE RING CALCULATIONS
x=x;
z=-ze-LVoralt;
if x==0,
    if yL==0,
        vxLi=0;
        vzLi=-kL*RL^2/(2*(RL^2+z^2)^1.5);
    end
else
r=sqrt(x^2+yL^2);           %radial distance from the z axis
r1=sqrt(z^2+(r-RL)^2);      %closest distance to the point of
                             %interest from the ring filament.
r2=sqrt(z^2+(r+RL)^2);      %farthest distance to the point of
                             %interest from the ring filament.

lambda=(r2-r1)/(r2+r1);     %scaling term
n1=(r+RL)/r2;
n2=(r-RL)/r1;
sig1=z/r2+z/r1;
sig2=z/r2-z/r1;
tow=0.75*sqrt(1-lambda^2)+0.25;
delta1=(kL*lambda)/(pi*tow);
delta2=(0.2955*kL*lambda^3)/(pi*tow^2*sqrt(1-lambda^2));
dSidr=0.788*delta1*(n1-n2)-0.394*lambda*delta1
        *(n1+n2)+delta2*((n1-n2)-lambda*(n1+n2));
                             %derivative of the stream function wrt r
dSidz=delta1*(0.788*sig2-0.394*lambda*sig1)
        +delta2*(sig2-lambda*sig1);
                             %derivative of the stream function wrt z
dnpLi=(1-exp(-r1^2/(0.1*rouL^2)));
                             %velocity damping factor
vxLi=(x/r)*(1/r)*dSidz;    %horizontal velocity in x direction
vzLi=-(1/r)*dSidr;         %vertical velocity
end %if

```

```

% IMAGE SMALL RING CALCULATIONS
z=-ze-sUoralt;
if x==0,
    if ys==0,
        vxsi=0;
        vzsi=-ks*Rs^2/(2*(Rs^2+z^2)^1.5);
    end
else
    r=sqrt((x+50)^2+ys^2);           %radial distance from the z axis
    r1=sqrt(z^2+(r-Rs)^2);           %closest distance to the point of
                                     %interest from the ring filament.
    r2=sqrt(z^2+(r+Rs)^2);           %farthest distance to the point of
                                     %interest from the ring filament.
    lambda=(r2-r1)/(r2+r1);          %scaling term
    n1=(r+Rs)/r2;
    n2=(r-Rs)/r1;
    sig1=z/r2+z/r1;
    sig2=z/r2-z/r1;
    tow=0.75*sqrt(1-lambda^2)+0.25;
    delta1=(ks*lambda)/(pi*tow);
    delta2=(0.2955*ks*lambda^3)/(pi*tow^2*sqrt(1-lambda^2));
    dSidr=0.788*delta1*(n1-n2)-0.394*lambda*delta1
        *(n1+n2)+delta2*((n1-n2)-lambda*(n1+n2));
                                     %derivative of the stream function wrt r
    dSidz=delta1*(0.788*sig2-0.394*lambda*sig1)
        +delta2*(sig2-lambda*sig1);
                                     %derivative of the stream function wrt z
    if (r1^2/(0.1*rows^2))>444,
        dapsi=1;
    else
        %velocity damping factor
        dapsi=1-exp(-r1^2/(0.1*rows^2));
    end

    vxsi=(x/r)*(1/r)*dSidz;         %horizontal velocity x direction
    vzsi=-(1/r)*dSidr;               %vertical velocity
end %if

```

```

%    SOURCE PROFILE FOR VZ CORRECTION
Salt=10000;                %source altitude
gagaz=2772000;             %source strength/2π
gagax=1355396;             %source strength/2π far
vzsource=0.0;
vxsource=0.0;

if ze>800,
vzsource=-15*(LUoralt-ze)/((LUoralt-ze)^2+x^2)^0.5;
else
Radius1=(x^2+(Salt-ze)^2)^0.5;
                    %radius from primary source to the flight pt
Radius2=(x^2+(Salt+ze)^2)^0.5;
                    %radius from image source to the flight pt
vzsource=gagaz*((Salt+ze)/Radius2^2-(Salt-ze)/Radius1^2);
end
vxsource=gagax*x*(1/Radius1^2+1/Radius2^2);

%    SUMMATION
if zerock==999,
    dap=dapL*daps*dapLi*dapsi;
    if x<=2000,
        vx=(dap*(vxL+vxs+vxLi+vxi));
    else
        vx=vxsource;
    end
    vz=-(dap*(vzL+vzs-vzLi-vzi)-vzsource);
else
    vx=-(vxL+vxs+vxLi+vxi);
    vz=vzL+vzs-vzLi-vzi;
end

```


APPENDIX B

PARAMETER SENSITIVITY ALGORITHM

The following are MatLab® m-file and function algorithms used to determine the parameters for the windshear model that approximates the DAL191 recorded winds.

A. M-FILE DRIVER

```
%Parameter sensitivity program for the DAL191 wind model.
clear
clc
%Recorded flight data from DAL191.
%[ref number, altitude(ft AGL), dist from MB center(ft), x wind
(ft/s), y wind (ft/s)].
DAL=[1 987 -8642 2 10;
2 975 -8361 -1 11;
3 962 -8080 -3 11;
4 948 -7799 -4 11;
5 935 -7518 -6 14;
6 922 -7237 -9 15;
7 909 -6956 -12 12;
8 894 -6676 -12 3;
9 875 -6396 -9 6;
10 856 -6117 -11 9;
11 842 -5838 -16 4;
12 823 -5561 -25 -18;
13 807 -5287 -36 -14;
14 790 -5016 -39 -13;
15 777 -4749 -29 -20;
16 764 -4486 -26 -17;
17 755 -4229 -22 -17;
```

```

18 747 -3977 -29 -17;
19 742 -3730 -20 -11;
20 738 -3487 -17 -23;
21 730 -3249 -12 -30;
22 714 -3013 -8 -36;
23 698 -2778 0 -34;
24 680 -2542 3 -32;
25 662 -2306 0 -31;
26 647 -2069 -8 -31;
27 635 -1831 -18 -24;
28 627 -1593 -20 -26;
29 620 -1355 -10 -36;
30 608 -1117 -8 -40;
31 592 -880 18 -4;
32 585 -639 32 19;
33 582 -391 19 16;
34 580 -139 18 21;
35 573 120 19 -3;
36 548 385 38 -21;
37 511 656 54 -19;
38 462 936 65 9;
39 411 1228 66 9;
40 351 1531 72 -13;
41 277 1845 71 -42;
42 193 2169 72 -33;
43 119 2504 76 -2;
44 70 2851 78 15;
45 42 3211 64 17;
46 20 3579 81 4;
47 0 3954 85 2];

```

%Parameter matrix:

```

Ps=[2300      2500      2800;      %Large ring x displacement
    1250      1300      1350;      %Small ring core radius
    57204.9*2  57204.9*2.3  57204.9*2.5; %Small ring vortex strength
    -400      -300      -200;      %Large ring y posit
     300      500      700;      %Small ring x displacement
    -150      1      150;      %Small ring y displacement

```

```

1386000*1.8 1386000*2 1386000*2.2; %Source z strength
193628*6.5 193628*7 193628*7.5]; %Source x strength

```

```

uxerr=0.0;uzerr=0.0;an=0;bestms=999; %initialization
i=1;
z=1;
for k=1:3,
home
i
z
k
bestms
for l=1:3, for m=1:3, for n=1:3,
for o=1:3, for p=1:3,
uxerr=0.0;uzerr=0.0;
for c=1:47,
[ux,uh]=pmicroburst(DAL(c,2),DAL(c,3),Ps(1,i),Ps(2,z),
Ps(3,k),Ps(4,l),Ps(5,m),Ps(6,n),Ps(7,o),Ps(8,p));
uxerr=uxerr+(DAL(c,4)-ux)^2;
uzerr=uzerr+(DAL(c,5)-uh)^2;
end
rmsux=(uxerr/40)^0.5;
rmsuz=(uzerr/40)^0.5;
rmstot=((uxerr+uzerr)/80)^0.5;
an=an+1;
PM(an,:)=[Ps(1,i),Ps(2,z),Ps(3,k),Ps(4,l),
Ps(5,m),Ps(6,n),Ps(7,o),Ps(8,p),rmsux,rmsuz,rmstot];
if bestms>rmstot,
BESTP=PM(an,:);
bestms=rmstot;
save BEST
end
end, end, end, end, end, end,
save parameters11
clear ux uh rmsux rmstot an PM BESTP

```

```

uxerr=0.0;uzerr=0.0;an=0; %initialization

```

```

i=1;
z=2;
for k=1:3,
home
i
z
k
bestrms
for l=1:3, for m=1:3, for n=1:3,
for o=1:3, for p=1:3,
uxerr=0.0;uzerr=0.0;
for c=1:47,
[ux,uh]=pamicroburst(DAL(c,2),DAL(c,3),Ps(1,l),Ps(2,z),
    Ps(3,k),Ps(4,l),Ps(5,m),Ps(6,n),Ps(7,o),Ps(8,p));
uxerr=uxerr+(DAL(c,4)-ux)^2;
uzerr=uzerr+(DAL(c,5)-uh)^2;
end
rmsux=(uxerr/40)^0.5;
rmsuz=(uzerr/40)^0.5;
rmstot=((uxerr+uzerr)/80)^0.5;
mn=mn+1;
PM(mn,:)=[Ps(1,l),Ps(2,z),Ps(3,k),Ps(4,l),
    Ps(5,m),Ps(6,n),Ps(7,o),Ps(8,p),rmsux,rmsuz,rmstot];
if bestrms>rmstot,
    BESTP=PM(mn,:);
    bestrms=rmstot;
    save BEST
end
end, end, end, end, end, end,
save parameters12
clear ux uh rmsux rmstot mn PM BESTP

uxerr=0.0;uzerr=0.0;mn=0; %initialization
i=1;
z=3;
for k=1:3,
home
i

```

```

z
k
bestres
for l=1:3, for m=1:3, for n=1:3,
for o=1:3, for p=1:3,
uxerr=0.0;uzerr=0.0;
for c=1:47,
[ux,uh]=pmicroburst(DAL(c,2),DAL(c,3),Ps(1,i),Ps(2,z),
    Ps(3,k),Ps(4,l),Ps(5,m),Ps(6,n),Ps(7,o),Ps(8,p));
uxerr=uxerr+(DAL(c,4)-ux)^2;
uzerr=uzerr+(DAL(c,5)-uh)^2;
end
rmsux=(uxerr/40)^0.5;
rmsuz=(uzerr/40)^0.5;
rmstot=((uxerr+uzerr)/80)^0.5;
mn=mn+1;
PM(mn,:)= [Ps(1,i),Ps(2,z),Ps(3,k),Ps(4,l),
    Ps(5,m),Ps(6,n),Ps(7,o),Ps(8,p),rmsux,rmsuz,rmstot];
if bestres>rmstot,
    BESTP=PM(mn,:);
    bestres=rmstot;
    save BEST
end
end, end, end, end, end, end,
save parameters13
clear ux uh rmsux rmstot mn PM BESTP

uxerr=0.0;uzerr=0.0;mn=0;    %initialization
i=2;
z=1;
for k=1:3,
home
i
z
k
bestres
for l=1:3, for m=1:3, for n=1:3,
for o=1:3, for p=1:3,

```

```

uxerr=0.0;uzerr=0.0;
for c=1:47,
[ux,uh]=pmicroburst(DAL(c,2),DAL(c,3),Ps(1,i),Ps(2,z),
    Ps(3,k),Ps(4,l),Ps(5,m),Ps(6,n),Ps(7,o),Ps(8,p));
uxerr=uxerr+(DAL(c,4)-ux)^2;
uzerr=uzerr+(DAL(c,5)-uh)^2;
end
rmsux=(uxerr/40)^0.5;
rmsuz=(uzerr/40)^0.5;
rmstot=((uxerr+uzerr)/80)^0.5;
mn=mn+1;
PM(mn,:)=[Ps(1,i),Ps(2,z),Ps(3,k),Ps(4,l),
    Ps(5,m),Ps(6,n),Ps(7,o),Ps(8,p),rmsux,rmsuz,rmstot];
if bestrms>rmstot,
    BESTP=PM(mn,:);
    bestrms=rmstot;
    save BEST
end
end, end, end, end, end, end,
save parameters21
clear ux uh rmsux rmstot mn PM BESTP

uxerr=0.0;uzerr=0.0;mn=0; %initialization
l=2;
z=2;
for k=1:3,
home
l
z
k
bestrms
for l=1:3, for m=1:3, for n=1:3,
for o=1:3, for p=1:3,
uxerr=0.0;uzerr=0.0;
for c=1:47,
[ux,uh]=pmicroburst(DAL(c,2),DAL(c,3),Ps(1,l),Ps(2,z),
    Ps(3,k),Ps(4,l),Ps(5,m),Ps(6,n),Ps(7,o),Ps(8,p));
uxerr=uxerr+(DAL(c,4)-ux)^2;

```

```

uzerr=uzerr+(DAL(c,5)-Wh)^2;
end
rmsux=(uxerr/40)^0.5;
rmsuz=(uzerr/40)^0.5;
rmstot=((uxerr+uzerr)/80)^0.5;
mn=mn+1;
PM(mn,:)= [Ps(1,i),Ps(2,z),Ps(3,k),Ps(4,l),
            Ps(5,m),Ps(6,n),Ps(7,o),Ps(8,p),rmsux,rmsuz,rmstot];
if bestrms>rmstot,
    BESTP=PM(mn,:);
    bestrms=rmstot;
    save BEST
end
end, end, end, end, end, end,
save parameters22
clear ux wh rmsux rmstot mn PM BESTP

uxerr=0.0;uzerr=0.0;mn=0;    %initialization
i=2;
z=3;
for k=1:3,
    home
    i
    z
    k
    bestrms
    for l=1:3, for m=1:3, for n=1:3,
        for o=1:3, for p=1:3,
            uxerr=0.0;uzerr=0.0;
            for c=1:47,
                [Ux,Uh]=pmicroburst(DAL(c,2),DAL(c,3),Ps(1,i),Ps(2,z),
                                    Ps(3,k),Ps(4,l),Ps(5,m),Ps(6,n),Ps(7,o),Ps(8,p));
                uxerr=uxerr+(DAL(c,4)-Ux)^2;
                uzerr=uzerr+(DAL(c,5)-Uh)^2;
            end
            rmsux=(uxerr/40)^0.5;
            rmsuz=(uzerr/40)^0.5;
            rmstot=((uxerr+uzerr)/80)^0.5;

```

```

mn=mn+1;
PM(mn,:)=[Ps(1,i),Ps(2,z),Ps(3,k),Ps(4,l),
          Ps(5,m),Ps(6,n),Ps(7,o),Ps(8,p),rmsux,rmsuz,rstot];
if bestms>rstot,
    BESTP=PM(mn,:);
    bestms=rstot;
    save BEST
end
end, end, end, end, end, end,
save parameters23
clear ux uh rmsux rstot mn PM BESTP

uxerr=0.0;uzerr=0.0;mn=0;    %initialization
i=3;
z=1;
for k=1:3,
    home
    i
    z
    k
    bestms
    for l=1:3, for m=1:3, for n=1:3,
        for o=1:3, for p=1:3,
            uxerr=0.0;uzerr=0.0;
            for c=1:47,
                [Ux,Uh]=pmicroburst(DAL(c,2),DAL(c,3),Ps(1,i),Ps(2,z),
                                   Ps(3,k),Ps(4,l),Ps(5,m),Ps(6,n),Ps(7,o),Ps(8,p));
                uxerr=uxerr+(DAL(c,4)-Ux)^2;
                uzerr=uzerr+(DAL(c,5)-Uh)^2;
            end
            rmsux=(uxerr/40)^0.5;
            rmsuz=(uzerr/40)^0.5;
            rstot=((uxerr+uzerr)/80)^0.5;
            mn=mn+1;
            PM(mn,:)=[Ps(1,i),Ps(2,z),Ps(3,k),Ps(4,l),
                      Ps(5,m),Ps(6,n),Ps(7,o),Ps(8,p),rmsux,rmsuz,rstot];
            if bestms>rstot,
                BESTP=PM(mn,:);

```



```

    bestres=rstot;
    save BEST
end
end, end, end, end, end, end,
save parameters31
clear ux uh rsux rstot mn PM BESTP

uxerr=0.0;uzerr=0.0;mn=0;    %initialization
i=3;
z=2;
    for k=1:3,
    home
    j
    z
    k
    bestres
    for l=1:3, for m=1:3, for n=1:3,
    for o=1:3, for p=1:3,
    uxerr=0.0;uzerr=0.0;
    for c=1:47,
    [Ux,Uh]=pmburst(DAL(c,2),DAL(c,3),Ps(1,i),Ps(2,z),
        Ps(3,k),Ps(4,l),Ps(5,m),Ps(6,n),Ps(7,o),Ps(8,p));
    uxerr=uxerr+(DAL(c,4)-Ux)^2;
    uzerr=uzerr+(DAL(c,5)-Uh)^2;
    end
    rsux=(uxerr/40)^0.5;
    rsuz=(uzerr/40)^0.5;
    rstot=((uxerr+uzerr)/80)^0.5;
    mn=mn+1;
    PM(mn,:)=[Ps(1,i),Ps(2,z),Ps(3,k),Ps(4,l),
        Ps(5,m),Ps(6,n),Ps(7,o),Ps(8,p),rsux,rsuz,rstot];
    if bestres>rstot,
        BESTP=PM(mn,:);
        bestres=rstot;
        save BEST
    end
    end, end, end, end, end, end,
    save parameters32

```

```

clear mx mh rmsux rstot mn PM BESTP

uxerr=0.0;uzerr=0.0;mn=0;    %initialization
i=3;
z=3;
for k=1:3,
home
i
z
k
bestrms
for l=1:3, for m=1:3, for n=1:3,
for o=1:3, for p=1:3,
uxerr=0.0;uzerr=0.0;
for c=1:47,
[wx,wh]=pmburst(DAL(c,2),DAL(c,3),Ps(1,i),Ps(2,z),
                Ps(3,k),Ps(4,l),Ps(5,m),Ps(6,n),Ps(7,o),Ps(8,p));
uxerr=uxerr+(DAL(c,4)-wx)^2;
uzerr=uzerr+(DAL(c,5)-wh)^2;
end
rmsux=(uxerr/40)^0.5;
rmsuz=(uzerr/40)^0.5;
rstot=((uxerr+uzerr)/80)^0.5;
mn=mn+1;
PM(mn,:)=[Ps(1,i),Ps(2,z),Ps(3,k),Ps(4,l),
          Ps(5,m),Ps(6,n),Ps(7,o),Ps(8,p),rmsux,rmsuz,rstot];
if bestrms>rstot,
    BESTP=PM(mn,:);
    bestrms=rstot;
    save BEST
end
end, end, end, end, end, end,
save parameters33
clear

load BEST
uxerr=0.0;uzerr=0.0;
for l=1:47,

```

```

home
i
X=DAL(i,3);
[ux,uh]=pmburst(DAL(i,2),DAL(i,3),BESTP(1),BESTP(2),
    BESTP(3),BESTP(4),BESTP(5),BESTP(6),BESTP(7),BESTP(8));
    model(i,:)=[i,ux,uh];
    uxerr=uxerr+(DAL(i,4)-ux)^2;
    uzerr=uzerr+(DAL(i,5)-uh)^2;
end
rmsux=(uxerr/40)^0.5;
rmsuz=(uzerr/40)^0.5;
rmstot=((uxerr+uzerr)/80)^0.5;
answer=0;
while answer~=999,
    disp('The horizontal RMS is: ')
    disp(rmsux)
    disp('The vertical RMS is:')
    disp(rmsuz)
    disp('The total system RMS is:')
    disp(rmstot)
    disp('The following plots are available:')
    disp(' 1=horizontal winds')
    disp(' 2=vertical winds')
    disp(' 999=end')
    answer=input('plot number ');
    if answer==1,
        plot(DAL(:,3),DAL(:,4))
        hold
        plot(DAL(:,3),model(:,2),'--')
        pause
        hold
    elseif answer==2,
        plot(DAL(:,3),DAL(:,5))
        hold
        plot(DAL(:,3),model(:,3),'--')
        pause
        hold
    end,end

```

B. WINDSHEAR FUNCTION

```
function [vx,vz]=pmburst(ze,x,Lxdisp,Ra,ka,yL,sxdisp,RL,kL)
```

```
% INITIAL VALUES AND INPUTS
```

```
% Earth position
```

```
%ze = altitude (ft)
```

```
%x horizontal position (ft)
```

```
% Vortex Ring Dimensions
```

```
%RL
```

```
%radius of ring filament (ft)
```

```
r1L=2004.1;
```

```
%core radius (ft)
```

```
%kL
```

```
%vortex strength of the ring
```

```
%filament (ft^2/sec)
```

```
rowL=r1L/0.371;
```

```
%related core radius
```

```
%yL
```

```
%large ring y lateral position (ft)
```

```
LUoralt=3400;
```

```
%large vortex altitude AGL (ft)
```

```
%Lxdisp
```

```
%large ring displacement in x (ft)
```

```
%Ra
```

```
%radius of ring filament (ft)
```

```
r1a=323.9;
```

```
%core radius (ft)
```

```
%ka
```

```
%vortex strength of the ring
```

```
%filament (ft^2/sec)
```

```
rowa=r1a/0.371;
```

```
%related core radius
```

```
ya=830.9/830.9;
```

```
%small ring y lateral position (ft)
```

```
sUoralt=800;
```

```
%small vortex altitude AGL (ft)
```

```
%sxdisp
```

```
%small ring displacement in x (ft)
```

```
% PRIMARY LARGE RING CALCULATIONS
```

```
z=ze-LUoralt;
```

```
zerock=999;
```

```
r=sqrt((x-Lxdisp)^2+yL^2);
```

```
r1=sqrt(z^2+(r-RL)^2);
```

```
r2=sqrt(z^2+(r+RL)^2);
```

```
lambda=(r2-r1)/(r2+r1);
```

```
n1=(r+RL)/r2;
```

```
n2=(r-RL)/r1;
```

```

sig1=z/r2+z/r1;
sig2=z/r2-z/r1;
tow=0.75*sqrt(1-lambda^2)+0.25;
delta1=(kL*lambda)/(pi*tow);
delta2=(0.2955*kL*lambda^3)/(pi*tow^2*sqrt(1-lambda^2));
dSidr=0.788*delta1*(n1-n2)-0.394*lambda*delta1
      *(n1+n2)+delta2*((n1-n2)-lambda*(n1+n2));
dSidz=delta1*(0.788*sig2-0.394*lambda*sig1)
      +delta2*(sig2-lambda*sig1);
dapL=(1-exp(-r1^2/(0.1*rowL^2)));
uxL=(x/r)*(1/r)*dSidz;
uzL=-(1/r)*dSidr;

```

X PRIMARY SMALL RING CALCULATIONS

```

z=ze-sUoralt;
r=sqrt((x-sxdisp)^2+ys^2);
r1=sqrt(z^2+(r-Rs)^2);
r2=sqrt(z^2+(r+Rs)^2);
lambda=(r2-r1)/(r2+r1);
n1=(r+Rs)/r2;
n2=(r-Rs)/r1;
sig1=z/r2+z/r1;
sig2=z/r2-z/r1;
tow=0.75*sqrt(1-lambda^2)+0.25;
delta1=(ks*lambda)/(pi*tow);
delta2=(0.2955*ks*lambda^3)/(pi*tow^2*sqrt(1-lambda^2));
dSidr=0.788*delta1*(n1-n2)-0.394*lambda*delta1
      *(n1+n2)+delta2*((n1-n2)- lambda*(n1+n2));
dSidz=delta1*(0.788*sig2-0.394*lambda*sig1)
      +delta2*(sig2-lambda*sig1);
if (r1^2/(0.1*rows^2))>444,
    daps=1;
else
    daps=1-exp(-r1^2/(0.15*rows^2));
end
uxs=(x/r)*(1/r)*dSidz;
uzs=-(1/r)*dSidr;

```

% IMAGE LARGE RING CALCULATIONS

z=-ze-LVoralt;

r=sqrt((x-Lxdisp)^2+yL^2);

r1=sqrt(z^2+(r-RL)^2);

r2=sqrt(z^2+(r+RL)^2);

lambda=(r2-r1)/(r2+r1);

n1=(r+RL)/r2;

n2=(r-RL)/r1;

sig1=z/r2+z/r1;

sig2=z/r2-z/r1;

tau=0.75*sqrt(1-lambda^2)+0.25;

delta1=(kL*lambda)/(pi*tau);

delta2=(0.2955*kL*lambda^3)/(pi*tau^2*sqrt(1-lambda^2));

dSldr=0.788*delta1*(n1-n2)-0.394*lambda*delta1*(n1+n2)+delta2*((n1-n2)-lambda*(n1+n2));

dSidz=delta1*(0.788*sig2-0.394*lambda*sig1)
+delta2*(sig2-lambda*sig1);

dnpLi=(1-exp(-r1^2/(0.1*rowL^2)));

vxLi=(x/r)*(1/r)*dSidz;

vzLi=-(1/r)*dSldr;

% IMAGE SMALL RING CALCULATIONS

z=-ze-sVoralt;

r=sqrt((x-sxdisp)^2+ys^2);

r1=sqrt(z^2+(r-Rs)^2);

r2=sqrt(z^2+(r+Rs)^2);

lambda=(r2-r1)/(r2+r1);

n1=(r+Rs)/r2;

n2=(r-Rs)/r1;

sig1=z/r2+z/r1;

sig2=z/r2-z/r1;

tau=0.75*sqrt(1-lambda^2)+0.25;

delta1=(ks*lambda)/(pi*tau);

delta2=(0.2955*ks*lambda^3)/(pi*tau^2*sqrt(1-lambda^2));

dSldr=0.788*delta1*(n1-n2)-0.394*lambda*delta1
(n1+n2)+delta2((n1-n2)-lambda*(n1+n2));

dSidz=delta1*(0.788*sig2-0.394*lambda*sig1)

```

        +delta2*(sig2-lambda*sig1);
if (r1^2/(0.1*rows^2))>444,
    dapsi=1;
else
    dapsi=1-exp(-r1^2/(0.15*rows^2));
end
uxsi=(x/r)*(1/r)*dSidz;
vzsi=-(1/r)*dSidr;

% SOURCE PROFILE FOR VZ CORRECTION
Salt=10000;           %source altitude
%gagaz                %source strength/2π
%gagax                %source strength/2π far
vzsource=0.0;
vxsource=0.0;

if ze>800,
vzsource=-15*(LUoralt-ze)/((LUoralt-ze)^2+x^2)^0.5;
else
Radius1=(x^2+(Salt-ze)^2)^0.5;
Radius2=(x^2+(Salt+ze)^2)^0.5;
vzsource=gagaz*((Salt+ze)/Radius2^2-(Salt-ze)/Radius1^2);
end
vxsource=gagax*x*(1/Radius1^2+1/Radius2^2);

% SUMMATION
dap=dapL*daps*dapLi*dapsi;
if x<=2000,
    vx=(dap*(vxL+vxs+vxLi+vxsi));
else
    vx=vxsource;
end
vz=-(dap*(vzL+vzs-vzLi-vzsi)-vzsource);

```

APPENDIX C

LANDING APPROACH ALGORITHMS

Contained in this appendix are the MatLab® programs utilized in calculating the aircraft response given a windshear and a particular escape maneuver. They are listed in three sections. The first section contains the driver routine and the functions required to solve the differential equations. The second and third sections contain the specific aircraft parameter functions and escape maneuver functions respectively. The windshear function is listed in Appendix A.

A. DRIVER AND DIFFERENTIAL EQUATION SOLVER

```
*****
%   Descent Profile Model   *
*****
%   This program will calculate the inertial flight path angle for
%   a given aircraft. It utilizes the function 'microburst' which
%   models the wind shear encountered during the DFW Delta Accident.
%   This program uses energy height theory to calculate inertial space
%   position.

clear
clc
format bank
format compact

%-----
%INITIALIZATION AND ENVIRONMENTAL CONSTANTS
% The following initialize constants and variables for the model.
```


%AIRCRAFT CONSTANTS

% The following constants are for the particular aircraft being studied.

```
disp('    LANDING APPROACH MODEL')
disp(' ')
answer=0.0;
disp('Type aircraft:')
disp('  1. P3 at 89,500lb')
disp('  2. P3 at 114,500lb')
disp('  3. P3 at 89,500lb 3 engine')
disp('  4. L1011')
disp('  5. T44')
answer=input(' Enter desired aircraft by number: ');
if answer==1,
    [S,K,CDo,Tmax,Wt,CLo,CLalpha,alphamax,q,U1,T,theta]=P3LtApp;
                                     %P3 @ 89,500lbs, app config.
elseif answer==2,
    [S,K,CDo,Tmax,Wt,CLo,CLalpha,alphamax,q,U1,T,theta]=P3HvApp;
                                     %P3 @ 114,500lbs, app config.
elseif answer==3,
    [S,K,CDo,Tmax,Wt,CLo,CLalpha,alphamax,q,U1,T,theta]=P3Eout;
                                     %P3 with one engine out.
elseif                                     answer==4,
    [S,K,CDo,Tmax,Wt,CLo,CLalpha,alphamax,q,U1,T,theta]=L1011App;%L1011
elseif answer==5,
    [S,K,CDo,Tmax,Wt,CLo,CLalpha,alphamax,q,U1,T,theta]=T44App;%T44
end
```

%S=plane form surface area in ft²
%K=coefficient for CD calculation
%CDo=coefficient of drag
%Tmax=max thrust available in ft-lbs
%Wt=aircraft weight in lbs
M=Wt/32.174; % mass in slugs
%CLo=zero AOA lift coefficient
%CLalpha=lift curve slope
%alphamax=stall buffet alpha w/ approach flaps

```

%q=nominal pitch rate of 5deg/sec
%U1=approach equivalent airspeed in ft/s
%T=initial thrust in lbf
%-----
%***programed initial values*****
iters=30;                                %number of iterations
deltat=1.0;                              %time increment in sec
MBcenter=10300;                          %distance MB center is
                                         %from runway
xstart=-500;                             %starting distance from
                                         %MB center
%*****
hstart=(MBcenter-xstart)*tan(0.052);      %starts on a 3deg
glideslope
disp(' Initial Input Section')
disp(' ')
disp('The following values are preprogrammed:')
disp(' a. The approach is based upon a 3deg glideslope.')
disp(' b. The starting distance (distance from MB center) is:')
disp(xstart)
disp(' c. The MB center is this from the end of the runway:')
disp(MBcenter)
disp(' d. The starting altitude is:')
disp(hstart)
disp(' e. The time step in sec:')
disp(deltat)
disp(' f. The number of iterations is:')
disp(iters)
disp(' ')

TW=Tmax/Wt;                             %thrust/weight ratio
WL=Wt/S;                                 %wing loading
disp('The following values were supplied/calculated from aircraft
constants')
disp(' a. Uref in ft/s (1.35Uso+5kts for P3 and 1.3Uso for other
aircraft:')
disp(U1)
disp(' b. Thrust to weight is:')

```

```

disp(TW)
disp(' c. Wing loading is:')
disp(WL)
disp(' ')

maneuver=0.0;
disp('Select the escape maneuver:')
disp(' 1. Stay on glide slope, go missed at 200ft AGL; NO
windshear')
disp(' 2. Stay on glide slope, go missed at 200ft AGL;WITH
windshear')
disp(' 3. Escape with constant airspeed')
disp(' 4. Escape with constant altitude')
disp(' 5. Escape with constant theta')
disp(' 6. Escape with constant alpha')
disp(' 7. Escape with max alpha')
disp(' 8. Emulate DAL191 final few seconds using recorded theta')
disp(' 9. Emulate DAL191 final few seconds using recorded theta and
winds')
maneuver=input(' Enter selection number: ');

if maneuver==5,
    disp('What value for escape theta?')
    thetaaim=input(' Enter in radians: ');
elseif maneuver==6,
    disp('What value for escape alpha?')
    alphaaim=input(' Enter in radians: ');
elseif maneuver==7,
    alphaaim=alphamax;
elseif maneuver>=8,
    hstart=hstart+50;
end

x1=xstart;           %initialization
h1=hstart;           %initialization
Ug=U1;               %ground speed initialization in ft/s
gamma1=-.052;        %initial inertial flight path angle in
rad (-3deg)

```

```

row=0.002377;           %air density in slugs/ft^3 @ S.L.
trigger=0.0;            %utility check number
check1=0.0;             %utility check number
check2=0.0;             %utility check number
X-----
%ALGORITHM
% The actual algorithm is broken into several smaller divisions and
functions:
%   starting values - as it implies
%   loop - beginning of iterating process
%   windshear inputs - uses the function 'microburst' to give
%                       point x and z axis wind speeds
%   predictor - first guess at the solution of the governing DEs
%   corrector - corrected solutions to the governing DEs and
%               final point values.
%   output file management - as it implies
%   aircraft control - uses multiple control functions for
%                       control inputs to theta, thrust, and AOA
%   final output - as it implies
X-----
%starting values:
pt=1;                   %counter
Q=0.5*row*U1^2;         %dynamic pressure
CL=Wt/(Q*S);            %coefficient of lift
CD=CD0+K*CL^2;          %coefficient of drag
alpha=(CL-CL0)/CLalpha; %AOA required for 1g flight
gammaa=theta-alpha;     %airmass flight path angle
Es=U1^2/(2*32.174)+h1;  %specific energy in ft
Esdot=-12.32;           %time rate change in specific energy

y(1)=x1;                %y(1)=x position in ft
y(2)=h1;                %y(2)=aircraft altitude in ft
y(5)=U1;                %y(5)=aircraft airspeed in ft/s
y(6)=gammaa;            %y(6)=aircraft airmass flt. path (rad)
Aircraft(1,:)=[x1,h1,U1,-12.36,theta,alpha,1,T];
Inertial(1,:)=[Ug,0,gamaa,gama1,0,0,1,Es,Esdot];
% starting output files
X-----

```

```

%loop:
clc
while theta~=999,           %loop control
pt=pt+1;                   %present pt in space
%-----
%wind shear inputs:
x2=Ug*deltat+x1;           %approximate horizontal displacement
h2=tan(gama1)*(x2-x1)+h1;   %approximate vertical displacement

if maneuver==1,
    Ux11=0;Ux21=0;Ux12=0;Ux22=0;Uh11=0;Uh21=0;Uh12=0;Uh22=0;
elseif maneuver==9,
    [Ux11,Uh11]=recwinds(pt); %recorded winds from DAL191
    [Ux22,Uh22]=recwinds(pt+1);
    Ux12=(Ux11+Ux22)/2;
    Ux21=Ux12;
    Uh12=(Uh11+Uh22)/2;
    Uh21=Uh12;
else
    [Ux11,Uh11]=microburst(h1,x1); %These four calls to the function
    [Ux21,Uh21]=microburst(h2,x1); %microburst finds the point wind
    [Ux12,Uh12]=microburst(h1,x2); %shear for determination of the
    [Ux22,Uh22]=microburst(h2,x2); %average block wind shear.
                                %The above is used in conjunction
                                %other calls when no wind shear is
                                %desired.
end
WindX(pt)=Ux11;               %Wind shear matrices
WindH(pt)=Uh11;

dUxdx=((Ux12-Ux11)+(Ux22-Ux21))/(2*(x2-x1)); %These formulas
dUxdh=((Ux22-Ux12)+(Ux21-Ux11))/(2*(h2-h1)); %calculate the
dUhdh=((Uh12-Uh11)+(Uh22-Uh21))/(2*(x2-x1)); %differential change
dUhdh=((Uh22-Uh12)+(Uh21-Uh11))/(2*(h2-h1)); %in wind shear.

y(3)=Ux11;                   %y(3)=wind shear in the x dir. ft/s
y(4)=Uh11;                   %y(4)=wind shear in the z dir. ft/s
%-----

```

```

    %predictor and intermediate values
    ydot=yprimes(y,dWxdx,dWxdh,dWhdx,dWhdh,theta,T,S,M,Q,CL,CD,
                alpha,alphamax);
                %call to the DE function

    for n=1:6,
        y1(n)=y(n)+deltat*ydot(n);      %Euler first step fwd predictor
        yhalf(n)=y(n)+deltat/2*ydot(n); %Euler half step fwd predictor
    end

    alpha=theta-y(6);                  %AOA
    CL=CLo+alpha*CLalpha;              %coefficient of lift
    CD=CDo+K*CL^2;                     %coefficient of drag
    Q=0.5*row*yhalf(5)^2;              %dynamic pressure
    %-----

    %corrector and new value formulation
    ydot=yprimes(yhalf,dWxdx,dWxdh,dWhdx,dWhdh,theta,T,S,M,Q,CL,CD,
                alpha,alphamax);

    for n=1:6,
        y2(n)=yhalf(n)+deltat/2*ydot(n); %Richardson extrapolation
        y(n)=2*y2(n)-y1(n);              %corrector scheme.
    end

    x1=y(1);                           %new x posit in ft
    h1=y(2);                           %new altitude in ft AGL
    Ug=y(5)*cos(y(6))+y(3);             %ground speed in ft/sec
    ROC=y(5)*sin(y(6))+y(4);            %Rate of Climb in ft/sec
    gamai=atan(ROC/Ug);                 %new airmass FP angle in rad
    Es=y(5)^2/64.348+y(2);              %new specific energy
    Esdot=y(5)*ydot(5)/32.174+ydot(2); %new trc of specific energy

    alpha=theta-y(6);                  %new AOA
    CL=CLo+alpha*CLalpha;              %new coefficient of lift
    CD=CDo+K*CL^2;                     %new coefficient of drag
    Q=0.5*row*y(5)^2;                  %new dynamic pressure
    %-----

```

```

%output file management:
Aircraft(pt,:)= [y(1),y(2),y(5),ydot(5),theta,alpha,pt,T];
Inertial(pt,:)= [Ug,ROC,y(6),gamma,y(3),y(4),pt,Es,Esdot];

home
disp('          pt          x          h          U
airspeed accel  ')
op1=[pt,Aircraft(pt,1),Aircraft(pt,2),Aircraft(pt,3),
      Aircraft(pt,4)];
disp(op1)

disp(' pt          theta          alpha          gamma          gamma')
op2=[pt,Aircraft(pt,5),Aircraft(pt,6),Inertial(pt,3),
      Inertial(pt,4)];
disp(op2)

disp('          pt          Ug          ROC          Thrust')
op3=[pt,Inertial(pt,1),Inertial(pt,2),Aircraft(pt,8)];
disp(op3)

disp('          pt          Es          Esdot')
op5=[pt,Inertial(pt,8),Inertial(pt,9)];
disp(op5)

disp('          pt          Wx          Wh')
op4=[pt,Inertial(pt,5),Inertial(pt,6)];
disp(op4)
%-----

```

%aircraft control:

%functions called for theta, thrust
 %and alpha control.

```

if maneuver <= 2,
    if y(2)<200,
        trigger=1;
        [theta,T]=MAcontrol(q,deltat,Tmax,theta,T,alpha,alphamax,y);
    elseif trigger ~= 1,

```

```

[theta,T]=GPcontrol(q,deltat,ROC,Tmax,theta,T,alpha,alphamax,U1,
                    hstart,xstart,y);
elseif trigger == 1,
    [theta,T]=MAcontrol(q,deltat,Tmax,theta,T,alpha,alphamax,y);
end
elseif maneuver<8,
    if y(5) < (U1-33.33),
        trigger=1;
    end
else
    if y(2)<=1004,
        [theta,T,check1]=DALtheta(Tmax,theta,T,U1,y,check1);
    else
[theta,T]=GPcontrol(q,deltat,ROC,Tmax,theta,T,alpha,alphamax,U1,
                    hstart,xstart,y);

        end
    end

if maneuver >=3,
    if trigger == 1,
        if maneuver == 3,
            [theta,T,check1]=CASesc(q,deltat,Tmax,theta,T,alpha,alphamax,
                                    U1,y,check1)

        elseif maneuver == 4,
            [theta,T,check1]=CALTesc(q,deltat,Tmax,theta,T,alpha,alphamax,
                                    y,check1,ydot)

        elseif maneuver == 5,
            [theta,T]=CTHesc(q,deltat,Tmax,theta,T,alpha,alphamax,thetaaim)
        elseif maneuver == 6,
            [theta,T]=CAOAesc(q,deltat,Tmax,theta,T,alpha,alphamax,alphaaim)
        elseif maneuver == 7,
            [theta,T]=MAXesc(q,deltat,Tmax,theta,T,alpha,alphaaim)
        end
    end
end

if pt==iters,
    theta=999;
    %number of iterations
end

```



```

elseif y(2)<0,                %stop at ground impact
    theta=999;
else
end

end                            %while algorithm loop
%-----
    %output files:
    answer=input('Do you want a flight path plot? 1=YES ');
    if answer==1,
        plot(Aircraft(:,1),Aircraft(:,2))
        pause
        answer=0.0;

    end
    answer=input('Do you want x, h, U, and airspeed accel? 1=YES ');
    if answer==1,
        disp('      pt      x      h      U      airspeed accel ')
        op1=[Aircraft(:,7),Aircraft(:,1),Aircraft(:,2),Aircraft(:,3),
            Aircraft(:,4)];
        disp(op1)
    else
    end

    answer=input('Do you want theta, alpha, gamma, and gamma_i? 1=YES ');
    if answer==1,
        disp('      pt      theta      alpha      gamma      gamma_i')
        op2=[Aircraft(:,7),Aircraft(:,5),Aircraft(:,6),Inertial(:,3),
            Inertial(:,4)];
        disp(op2)
    else
    end

    answer=input('Do you want U_g, ROC, and Thrust? 1=YES ');
    if answer==1,
        disp('      pt      U_g      ROC      Thrust')
        op3=[Aircraft(:,7),Inertial(:,1),Inertial(:,2),Aircraft(:,8)];
        disp(op3)
    end

```

```
else  
end
```

```
answer=input('Do you want Es and Esdot? 1=YES ');  
if answer==1,  
disp('          pt          Es          Esdot')  
op5=[Aircraft(:,7),Inertial(:,8),Inertial(:,9)];  
disp(op5)  
else  
end
```

```
answer=input('Do you want Wx and Wh? 1=YES ');  
if answer==1,  
disp('          pt          Wx          Wh')  
op4=[Aircraft(:,7),Inertial(:,5),Inertial(:,6)];  
disp(op4)  
else  
end
```

```

function [ydot]=yprimes(y,dWxdx,dWxdh,dWhdx,dWhdh,theta,
                        T,S,M,Q,CL,CD,alpha,alphamax)
% This function calculates the y' solutions to the
% coupled system equations:
%  $y(1)' = \dot{x} = U \cos(\gamma) + W_x$ 
%  $y(2)' = \dot{h} = U \sin(\gamma) + W_h$ 
%  $y(3)' = \dot{W}_x = dW_x/dx \cdot \dot{x} + dW_x/dh \cdot \dot{h}$ 
%  $y(4)' = \dot{W}_h = dW_h/dx \cdot \dot{x} + dW_h/dh \cdot \dot{h}$ 
%  $y(5)' = \dot{U} = (T \cos(\alpha)) / (M - D/M - g \sin(\gamma)) - W_x \dot{x} \cos(\gamma) - W_h \dot{h} \sin(\gamma)$ 
%  $y(6)' = T \sin(\alpha) / (M \cdot U) + L / (M \cdot U) - g \cos(\gamma) / U + W_x \dot{x} \sin(\gamma) / U - W_h \dot{h} \cos(\gamma) / U$ 

ydot(1)=y(5)*cos(y(6))+y(3);
ydot(2)=y(5)*sin(y(6))+y(4);
ydot(3)=dWxdx*ydot(1)+dWxdh*ydot(2);
ydot(4)=dWhdx*ydot(1)+dWhdh*ydot(2);
if alpha<alphamax,
ydot(5)=T/M*cos(theta-y(6))-Q*S*CD/M-32.174*sin(y(6))
-ydot(3)*cos(y(6))-ydot(4)*sin(y(6));
ydot(6)=T/(M*y(5))*sin(theta-y(6))+Q*S*CL/(M*y(5))
-32.174/y(5)*cos(y(6))+ydot(3)*sin(y(6))/y(5)-
ydot(4)/y(5)*cos(y(6));
else
ydot(5)=T/M*cos(alphamax)-Q*S*CD/M-32.174*sin(y(6))
-ydot(3)*cos(y(6))-ydot(4)*sin(y(6));
ydot(6)=T/(M*y(5))*sin(alphamax)+Q*S*CL/(M*y(5))-32.174/y(5)
*cos(y(6))+ydot(3)*sin(y(6))/y(5)-ydot(4)/y(5)*cos(y(6));
end

```

B. AIRCRAFT PERFORMANCE PARAMETER FUNCTIONS

```
function[S,K,CDo,Tmax,Wt,CLo,CLalpha,alphamax,q,U1,T,theta]
    =P3LtApp()
%P3 at 89,500lbs, app flaps, gear down
S=1300;                %plane form surface area in ft^2
K=0.05041;            %coefficient for CD calculation
CDo=0.0567;           %coefficient of drag
Tmax=33400;           %max thrust available in ft-lbs
Wt=89500;             %aircraft weight in lbs
CLo=0.800;            %zero AOA lift coefficient
CLalpha=5.73;         %lift curve slope
alphamax=0.244;       %stall buffet alpha w/ approach flaps
q=0.0873;             %nominal pitch rate of 5deg/sec
U1=236;               %approach equivalent airspeed in ft/s
T=5000;               %initial thrust in lbf
theta=-0.013;         %initial water line deck angle in rad
```

```
function[S,K,CDo,Tmax,Wt,CLo,CLalpha,alphamax,q,U1,T,theta]
    =P3HvApp()
%P3 at 114,000lbs, app flaps, gear down
S=1300;                %plane form surface area in ft^2
K=0.05041;            %coefficient for CD calculation
CDo=0.0567;           %coefficient of drag
Tmax=33400;           %max thrust available in ft-lbs
Wt=114500;            %aircraft weight in lbs
CLo=0.800;            %zero AOA lift coefficient
CLalpha=5.73;         %lift curve slope
alphamax=0.244;       %stall buffet alpha w/ approach flaps
q=0.0873;             %nominal pitch rate of 5deg/sec
U1=262;               %approach equivalent airspeed in ft/s
T=8000;               %initial thrust in lbf
theta=-0.013;         %initial water line deck angle in rad
```

```

function[S,K,CDo,Tmax,Wt,CLo,CLalpha,alphamax,q,U1,T,theta]
=L1011App()
%L1011 at 362,000lbs, App flaps, gear down
S=4578;           %plane form surface area in ft^2
K=0.059;          %coefficient for CD calculation
CDo=0.108;        %coefficient of drag
Tmax=126000;      %max thrust available in ft-lbs
Wt=362000;        %aircraft weight in lbs
CLo=0.532;        %zero AOA lift coefficient
CLalpha=4.96;     %lift curve slope
alphamax=0.314;   %stall warning alpha w/ approach flaps
                  % (18deg)
q=0.0873;         %nominal pitch rate of 5deg/sec
U1=227;           %approach equivalent airspeed in ft/s
                  % (136kts)
T=44500;          %initial thrust in lbf
theta=0.118;      %initial water line deck angle in rad

```

```

function[S,K,CDo,Tmax,Wt,CLo,CLalpha,alphamax,q,U1,T,theta]
=T44App()
%T44 at 8280lbs, app flaps, gear down
S=210;           %plane form surface area in ft^2
K=0.0503;        %coefficient for CD calculation
CDo=0.120;        %coefficient of drag
Tmax=3023;       %max thrust available in ft-lbs
Wt=8280;         %aircraft weight in lbs
CLo=0.587;       %zero AOA lift coefficient
CLalpha=6.24;    %lift curve slope
alphamax=0.244;  %stall buffet alpha w/ approach flaps
q=0.0873;        %nominal pitch rate of 5deg/sec
U1=203;          %approach equivalent airspeed in ft/s
T=1250;          %initial thrust in lbf
theta=-0.02;     %initial water line deck angle in rad

```

```

function[S,K,CDo,Tmax,Wt,CLo,CLalpha,alphamax,q,U1,T,theta]
    =P3Eout()
%P3 at 89,500lbs, app flaps, gear down, one engine out.
S=1300;           %plane form surface area in ft^2
K=0.05041;       %coefficient for CD calculation
CDo=0.0630;      %coefficient of drag (inc for eng. out)
Tmax=33400*(3/4); %max thrust available in ft-lbs
Wt=89500;        %aircraft weight in lbs
CLo=0.800;       %zero AOA lift coefficient
CLalpha=5.73;    %lift curve slope
alphamax=0.244;  %stall buffet alpha w/ approach flaps
q=0.0873;        %nominal pitch rate of 5deg/sec
U1=236;          %approach equivalent airspeed in ft/s
T=5000;          %initial thrust in lbf
theta=-0.013;    %initial water line deck angle in rad

```

C. FLIGHT PATH CONTROL AND ESCAPE MANEUVER FUNCTIONS

```

function[thetaout,Tout]=GPcontrol(q,deltat,ROC,Tmax,theta,T,
                                alpha,alphamax,U1,hstart,xstart,y)
%This control function tries to maintain a 3deg glide path.
Tout=T;
thetaout=theta;
wantedh=hstart-(abs(xstart-y(1))*0.0524);
                                %desired altitude for 3deg GP
hdiff=y(2)-wantedh;            %alt difference (neg when low)
Udiff=y(5)-U1;                 %airspeed diff (neg when slow)
% theta input:
if alpha<0,                     %(1)check for negative AOA
    thetaout=theta-alpha;
elseif alpha<alphamax,         %(2)check for max available AOA
    if ROC>0,                   %(3)check for ROC > 0fpm
        thetaout=theta-q*deltat;    %if so pitch dwn q*time
    elseif ROC<-25.0,          %(4)check for ROC < 1500fpm
        thetaout=theta+q*deltat;    %if so pitch up q*time
    elseif hdiff>100,          %(5)check for alt >100 diff
        thetaout=theta-q/2*deltat;  %if so pitch dwn 1/2*q*time
    elseif hdiff<-100,         %(6)check for alt <100 diff
        thetaout=theta+q/2*deltat;  %if so pitch up 1/2*q*time
    end
    if thetaout>0.524,          %now check for theta limit of
        thetaout=0.524;          % -10deg to +30 deg
    elseif thetaout<-0.175,
        thetaout=-0.175;
    end
else
    thetaout=theta-(alpha-alphamax);
end
%Thrust input:
if Udiff>8.5,                   %check speed diff
    Tout=T-0.20*Tmax*deltat;    %if diff > 5kts above app speed
    if Tout<0,                  %reduce thrust by 20% of Tmax
        Tout=0;                 %but not less than 0.
    else

```

```

    end
elseif Udiff<-8.5,
    Tout=T+0.25*Tmax*deltat;      %if diff < 5kts below app speed
    if Tout>Tmax,                  %inc thrust by 25% of Tmax
        Tout=Tmax;                %but not more than Tmax.
    else
    end
end
end

```

```

function[thetaout,Tout]=MAcontrol(q,deltat,Tmax,theta,T,alpha,
                                alphanax,y)
%This control function initiates a normal missed approach.
% Max power is added and theta increased to 10deg. Max AOA
%is applied when required.
Tout=T;
thetaout=theta;
% theta input:
if alpha<alphanax,                %(1)check for max available AOA
    if thetaout>=0.175,            %(2)check for 10deg deck angle
        thetaout=0.175;
    else
        thetaout=theta+q/2*deltat;  %(3)if theta not 10deg, pitch to
10deg
    end
else
    thetaout=theta-(alpha-alphanax);
end
%Thrust input:
if Tout<Tmax,
    Tout=T+Tmax/2*deltat;
    if Tout>Tmax,
        Tout=Tmax;
    end
else
end
end

```



```

function[thetaout,Tout,check1]=CRSesc(q,deltat,Tmax,theta,T,
                                     alpha,alphamax,U1,y,check1)
%Aircraft escape maneuver consisting of constant airspeed.
thetaout=theta;
if check1==0,
    if y(5)<U1,
        thetaout=0;
    else
        thetaout=q*deltat;
        check1=1;
    end
else
    if y(5)>=(U1+8.4),
        thetaout=theta+q*deltat;
    elseif y(5)<=(U1-8.4)
        thetaout=theta-q*deltat;
    end
end
if alpha>alphamax,
    thetaout=theta-(alpha-alphamax);
end
if T<Tmax,
    Tout=T+Tmax*0.2*deltat;
else
    Tout=Tmax;
end

```

```

function[thetaout,Tout,check1]=CALTesc(q,deltat,Tmax,theta,T,
                                     alpha,alphamax,y,check1,ydot)
%Aircraft control using constant altitude escape maneuver.
thetaout=theta;
if check1==0;
    check1=y(2);
end
if y(2)<check1-20,
    if ydot(2)<=0,
        thetaout=theta+q*deltat;
    end
elseif y(2)>check1+20,
    if ydot(2)>=0,
        thetaout=theta-q*deltat;
    end
end
if alpha>alphamax,
    thetaout=theta-(alpha-alphamax);
end
if T<Tmax,
    Tout=T+Tmax*0.2*deltat;
else
    Tout=Tmax;
end
end

```

```
function[thetaout,Tout]=CTHesc(q,deltat,Tmax,theta,T,
                                alpha,alpha_max,thetaaim)
```

```
%Constant theta escape maneuver.
```

```
if theta<thetaaim,
    thetaout=theta+q*deltat;
else
    thetaout=thetaaim;
end
if alpha>alpha_max,
    thetaout=theta-(alpha-alpha_max);
end
if T<Tmax,
    Tout=T+Tmax*0.2*deltat;
else
    Tout=Tmax;
end
```

```
function[thetaout,Tout]=CAOAesc(q,deltat,Tmax,theta,T,
                                alpha,alpha_max,alphaaim)
```

```
%Constant alpha escape maneuver.
```

```
if alpha<alphaaim,
    thetaout=theta+(alphaaim-alpha);
    if thetaout>(theta+q*deltat),
        thetaout=theta+q*deltat;
    end
else
    thetaout=theta-(alpha-alphaaim);
    if thetaout<(theta-q*deltat),
        thetaout=theta-q*deltat;
end, end
if alpha>alpha_max,
    thetaout=theta-(alpha-alpha_max);
end
if T<Tmax,
    Tout=T+Tmax*0.2*deltat;
else, Tout=Tmax; end
```

```

function[thetaout,Tout]=MAXesc(q,deltat,Tmax,theta,T,alpha,alphaaim)
%Maximum alpha escape maneuver.
if alpha<alphaaim,
    thetaout=theta+(alphaaim-alpha);
    if thetaout>(theta+q*deltat),
        thetaout=theta+q*deltat;
    end
else
    thetaout=theta-(alpha-alphaaim);
    if thetaout<(theta-q*deltat),
        thetaout=theta-q*deltat;
    end
end
if T<Tmax,
    Tout=T+Tmax*0.2*deltat;
else
    Tout=Tmax;
end

```

```

function[thetaout,Tout,checkout]=DALtheta(Tmax,theta,T,U1,y,check1)
% This control function tries to emulate DAL191
%last 48 sec of flight.
if check1==0,           %starting point
    check1=32;
end
% theta input:(theta,%power)
DAL191=[0.069813170071;
0.0628318530 71; 0.054105206871;
0.0471238898 72; 0.047123889873; 0.038397243573;
0.0314159265 71; 0.022689280271; 0.038397243569;
0.0541052068 69; 0.054105206869; 0.054105206870;
0.0785398163 68; 0.123918376867; 0.132645023167;
0.1623156204 67; 0.185004900767; 0.191986217767;
0.2007128639 67; 0.200712863969; 0.200712863971;
0.2234021442 72; 0.253072741585; 0.267035375589;
0.2740166925 92; 0.274016692592; 0.267035375595;
0.2600540585 92; 0.237364778292; 0.237364778292;
0.2530727415 87; 0.253072741587; 0.223402144292;
0.1553343034 93; 0.062831853098; 0.031415926596;
0.0226892802 99; -0.005235987100; -0.068067840100;
-0.144862327 100; -0.130899693100; -0.020943951100;
0.0698131700 100; 0.0925024503100; 0.0314159265100;
-0.005235987 100; 0.0541052068100; 0.0314159265100];
thetaout=DAL191(check1+1,1);
Tout=DAL191(check1+1,2)/100*Tmax;
checkout=check1+1;

```

APPENDIX D

TAKEOFF ALGORITHMS

Contained in this appendix are the MatLab® programs utilized in calculating the aircraft response given a windshear and a particular escape maneuver. They are listed in three sections. The first section contains the driver routine. The second and third sections contain the specific aircraft parameter functions and escape maneuver functions respectively. The windshear function is listed in Appendix A. The differential equation solving routine is listed in Appendix C.

A. DRIVER

```
x*****
%   Takeoff Profile Model   *
x*****
%   This program will calculate the inertial flight path angle for
%   a given aircraft. It utilizes the function 'microburst' which
%   models the wind shear encountered during the DFW Delta Accident.
%   This program uses energy height theory to calculate inertial space
%   position.

clear
clc
format bank
format compact

%-----
%INITIALIZATION AND ENVIRONMENTAL CONSTANTS
% The following initialize constants and variables for the model.
```

%AIRCRAFT CONSTANTS

% The following constants are for the particular aircraft being studied.

disp(' TAKEOFF MODEL')

disp(' ')

answer=0.0;

disp('Type aircraft:')

disp(' 1. P3 at 90,000lb')

disp(' 2. P3 at 120,000lb')

disp(' 3. P3 at 135,000lb')

disp(' 4. L1011')

disp(' 5. T44')

disp(' 6. P3 at 120,000lb, Ur=140')

answer=input(' Enter desired aircraft by number: ');

if answer==1,

[S,K,CDo,Wt,CLo,CLalpha,alphamax,q,U1,U2,T,thetacimb]=P3LtToff;

theta=0.087; %initialization

elseif answer==2,

[S,K,CDo,Wt,CLo,CLalpha,alphamax,q,U1,U2,T,thetacimb]=P3HvToff;

theta=0.130; %initialization

elseif answer==3,

[S,K,CDo,Wt,CLo,CLalpha,alphamax,q,U1,U2,T,thetacimb]=P3HvHvToff;

theta=0.133; %initialization

elseif answer==4,

[S,K,CDo,Wt,CLo,CLalpha,alphamax,q,U1,U2,T,thetacimb]=L1011Toff;%L1011

theta=0.2; %initialization

elseif answer==5,

[S,K,CDo,Wt,CLo,CLalpha,alphamax,q,U1,U2,T,thetacimb]=T44Toff;

%T44

theta=0.200; %initialization

elseif answer==6,

[S,K,CDo,Wt,CLo,CLalpha,alphamax,q,U1,U2,T,thetacimb]=modP3HvTo;

theta=0.130; %initialization

end

```

%S=plane form surface area in ft^2
%K=coefficient for CD calculation
%CD0=coefficient of drag
%Wt=aircraft weight in lbs
    M=Wt/32.174; % mass in slugs
%CL0=zero AOA lift coefficient
%CLalpha=lift curve slope
%alpha_max=stall buffet alpha w/ approach flaps
%q=nominal pitch rate of 5deg/sec
%U1=rotate speed in ft/s
%U2=takeoff safety airspeed in ft/s
%T=thrust in lbf
%-----
%***programed initial values*****
    iters=65;                %number of iterations
    deltat=0.5;              %time increment in sec
    xstart=-1200;            %starting distance from
                              MB center
    hstart=2.0;              %starts at rotate
%*****
disp(' Initial Input Section')
disp(' ')
disp('The following values are preprogrammed:')
disp(' a. The flight path is based on max power.')
disp(' b. The starting distance (distance from MB center) is:')
disp(xstart)
disp(' c. The MB center is this from the end of the runway:')
disp(abs(xstart))
disp(' d. The time step in sec:')
disp(deltat)
disp(' e. The number of iterations is:')
disp(iters)
disp(' ')

TW=T/Wt;                    %thrust/weight ratio
WL=Wt/S;                    %wing loading
disp('The following values were supplied/calculated from aircraft
constants')

```



```

disp(' a. Takeoff Safety Speed:')
disp(U2)
disp(' b. Thrust to weight is:')
disp(TW)
disp(' c. Wing loading is:')
disp(WL)
disp(' ')

```

```

maneuver=0.0;
disp('Select the escape maneuver:')
disp(' 1. Takeoff flight path; NO windshear')
disp(' 2. Takeoff flight path; WITH windshear')
disp(' 3. Escape with constant airspeed')
disp(' 4. Escape with constant altitude')
disp(' 5. Escape with constant theta')
disp(' 6. Escape with constant alpha')
maneuver=input(' Enter selection number: ');

```

```

if maneuver==5,
    disp('What value for escape theta?')
    thetaaim=input(' Enter in radians: ');
elseif maneuver==6,
    disp('What value for escape alpha?')
    alphaaim=input(' Enter in radians: ');
end

```

```

x1=xstart;           %initialization
h1=hstart;           %initialization

```

```

Ug=U1;               %ground speed initialization in ft/s
gamai=0.001;         %initial inertial flight path angle in
rad (1deg)
rho=0.002377;        %air density in slugs/ft^3 @ S.L.
trigger=0.0;         %utility check number
check1=0.0;          %utility check number
check2=0.0;          %utility check number

```

```

%-----
%ALGORITHM

```

% The actual algorithm is broken into several smaller divisions and functions:

```
%      starting values - as it implies
%      loop - beginning of iterating process
%      windshear inputs - uses the function 'microburst' to give
%                          point x and z axis wind speeds
%      predictor - first guess at the solution of the governing DEs
%      correcter - corrected solutions to the governing DEs and
%                  final point values.
%      output file management - as it implies
%      aircraft control - uses multiple control functions for
%                          control inputs to theta, thrust, and AOA
%      final output - as it implies
```

%starting values:

```
pt=1;                %counter
Q=0.5* $\rho$ *U1^2;        %dynamic pressure
CL=Wt/(Q*S);         %coefficient of lift
CD=CDo+K*CL^2;       %coefficient of drag
alpha=(CL-CLo)/CLalpha; %AOA required for 1g flight
gamma=theta-alpha;   %airmass flight path angle
Es=U1^2/(2*32.174)+h1; %specific energy in ft
Esdot=-12.32;        %time rate change in specific energy
```

```
y(1)=x1;             %y(1)=x position in ft
y(2)=h1;             %y(2)=aircraft altitude in ft
y(5)=U1;             %y(5)=aircraft airspeed in ft/s
y(6)=gamma;          %y(6)=aircraft airmass flight path in
rad
```

```
Aircraft(1,:)=[x1,h1,U1,-12.36,theta,alpha,1,T];
```

```
Inertial(1,:)=[Ug,0,gamma,gamaI,0,0,1,Es,Esdot];
```

% starting output files

%loop:

clc

```
while theta~=999,    %loop control
pt=pt+1;            %present pt in space
```

```

    %wind shear inputs:
    x2=Ug*deltat+x1;           %approximate horizontal displacement
    h2=tan(gamai)*(x2-x1)+h1;   %approximate vertical displacement

    if maneuver~=1,
        [Wx11,Wh11]=microburst(h1,x1); %These four calls to the function
        [Wx21,Wh21]=microburst(h2,x1); %microburst finds the point wind
        [Wx12,Wh12]=microburst(h1,x2); %shear for determination of the
        [Wx22,Wh22]=microburst(h2,x2); %average block wind shear.
    else
        Wx11=0;Wx21=0;Wx12=0;Wx22=0;Wh11=0;Wh21=0;Wh12=0;Wh22=0;
        %The above is used in conjunction
        %other calls when no wind shear is
        %desired.

    end
    WindX(pt)=Wx11;           %Wind shear matrices
    WindH(pt)=Wh11;

    dWxdx=((Wx12-Wx11)+(Wx22-Wx21))/(2*(x2-x1)); %These formulas
    dWxdh=((Wx22-Wx12)+(Wx21-Wx11))/(2*(h2-h1)); %calculate the
    dWhdx=((Wh12-Wh11)+(Wh22-Wh21))/(2*(x2-x1)); %differential change
    dWhdh=((Wh22-Wh12)+(Wh21-Wh11))/(2*(h2-h1)); %in wind shear.

    y(3)=Wx11;                %y(3)=wind shear in the x direction
    ft/s
    y(4)=Wh11;                %y(4)=wind shear in the z direction
    ft/s
    %-----
    %predictor and intermediate values
    ydot=yprimes(y,dWxdx,dWxdh,dWhdx,dWhdh,theta,T,S,M,Q,CL,CD,alpha,alp
    hamax);

    %call to the DE function

    for n=1:6,
        y1(n)=y(n)+deltat*ydot(n);      %Euler first step fwd predictor
        yhalf(n)=y(n)+deltat/2*ydot(n); %Euler half step fwd predictor
    end

```

```

alpha=theta-y(6);          %ROA
CL=CLo+alpha*CLalpha;      %coefficient of lift
CD=CDo+K*CL^2;             %coefficient of drag
Q=0.5*row*yhalf(5)^2;      %dynamic pressure
%-----

%corrector and new value formulation
ydot=yprimes(yhalf,dWxdx,dWxdh,dWhdx,dWhdh,theta,T,S,M,Q,CL,CD,alpha
,alpha_max);

for n=1:6,
    y2(n)=yhalf(n)+deltat/2*ydot(n); %Richardson extrapolation
    y(n)=2*y2(n)-y1(n);             %corrector scheme.
end

x1=y(1);                      %new x posit in ft
h1=y(2);                      %new altitude in ft AGL
Ug=y(5)*cos(y(6))+y(3);        %ground speed in ft/sec
ROC=y(5)*sin(y(6))+y(4);       %Rate of Climb in ft/sec
gamma1=atan(ROC/Ug);           %new airmass FP angle in rad
Es=y(5)^2/64.348+y(2);         %new specific energy
Esdot=y(5)*ydot(5)/32.174+ydot(2); %new trc of specific energy

alpha=theta-y(6);            %new ROA
CL=CLo+alpha*CLalpha;        %new coefficient of lift
CD=CDo+K*CL^2;               %new coefficient of drag
Q=0.5*row*y(5)^2;            %new dynamic pressure
%-----

%output file management:
Aircraft(pt,:)=[y(1),y(2),y(5),ydot(5),theta,alpha,pt,T];
Inertial(pt,:)=[Ug,ROC,y(6),gamma1,y(3),y(4),pt,Es,Esdot];

home
disp('          pt          x          h          U
airspeed accel ')
opl=[pt,Aircraft(pt,1),Aircraft(pt,2),Aircraft(pt,3),Aircraft(pt,4)]
;

```

```

disp(op1)

disp('          pt          theta          alpha          gamma')
disp('gamma1')
op2=[pt,Aircraft(pt,5),Aircraft(pt,6),Inertial(pt,3),Inertial(pt,
4)];
disp(op2)

disp('          pt          Ug          ROC          Thrust')
op3=[pt,Inertial(pt,1),Inertial(pt,2),Aircraft(pt,8)];
disp(op3)

disp('          pt          Es          Eadot')
op5=[pt,Inertial(pt,8),Inertial(pt,9)];
disp(op5)

disp('          pt          Ux          Uh')
op4=[pt,Inertial(pt,5),Inertial(pt,6)];
disp(op4)
%-----

%aircraft control:
%functions called for theta, thrust
%and alpha control.
if y(2)>50,
    if ROC <=0,
        trigger=1;
    elseif y(5)<U2,
        trigger=1;
    end
elseif y(5)<U1,
    trigger=1;
end

if trigger==0,
    theta=theta+q*0.8*deltat;
    if theta>thetaclimb,
        theta=thetaclimb;
    end
end

```

```

else
    if maneuver==3,

[theta,check1]=ToffCAS(q,deltat,theta,alpha,alphamax,U2,y,check1)
    elseif maneuver==4,

[theta,check1]=ToffCALT(q,deltat,theta,alpha,alphamax,y,check1,ydot)
    elseif maneuver==5,
        [theta]=ToffCTH(q,deltat,theta,alpha,alphamax,thetaaim)
    elseif maneuver==6,
        [theta]=ToffCAOA(q,deltat,theta,alpha,alphamax,alphaaim)
    end
end

if pt==iters,                %number of iterations
    theta=999;
elseif pt>5,
    if y(2)<0.0,
        theta=999;
    end
end

end                            %while algorithm loop
%-----
    %output files:
answer=input('Do you want a flight path plot? 1=YES ');
if answer==1,
    plot(Aircraft(:,1),Aircraft(:,2))
    pause
    answer=0.0;

end
answer=input('Do you want x, h, U, and airspeed accel? 1=YES ');
if answer==1,
    disp('          pt          x          h          U
    airspeed accel ')
    op1=[Aircraft(:,7),Aircraft(:,1),Aircraft(:,2),Aircraft(:,3),Aircraft(:,4)];

```

```

disp(op1)
else
end

answer=input('Do you want theta, alpha, gamma, and gamai? 1=YES ');
if answer==1,
disp('          pt          theta          alpha          gamma
gai')
op2=[Aircraft(:,7),Aircraft(:,5),Aircraft(:,6),Inertial(:,3),Inertia
l(:,4)];
disp(op2)
else
end

answer=input('Do you want Ug, ROC, and Thrust? 1=YES ');
if answer==1,
disp('          pt          Ug          ROC          Thrust')
op3=[Aircraft(:,7),Inertial(:,1),Inertial(:,2),Aircraft(:,8)];
disp(op3)
else
end

answer=input('Do you want Es and Esdot? 1=YES ');
if answer==1,
disp('          pt          Es          Esdot')
op5=[Aircraft(:,7),Inertial(:,8),Inertial(:,9)];
disp(op5)
else
end

answer=input('Do you want Wx and Wh? 1=YES ');
if answer==1,
disp('          pt          Wx          Wh')
op4=[Aircraft(:,7),Inertial(:,5),Inertial(:,6)];
disp(op4)
else
end

```

B. AIRCRAFT PERFORMANCE PARAMETER FUNCTIONS

```
function[S,K,CD0,Wt,CL0,CLalpha,alphamax,q,U1,U2,T,thetaclimb]
    =P3LtToff()
%P3 at 90,000lbs, app flaps, gear up
S=1300;                %plane form surface area in ft^2
K=0.05041;            %coefficient for CD calculation
CD0=0.0551;           %coefficient of drag
Wt=90000;              %aircraft weight in lbs
CL0=1.000;            %zero AOA lift coefficient
CLalpha=5.73;         %lift curve slope
alphamax=0.244;       %stall buffet alpha w/ approach flaps
q=0.0673;             %nominal pitch rate of 5deg/sec
U1=204;               %Liftoff speed (121kts)
U2=220;               %takeoff safety airspeed in ft/s
T=33400;              %thrust in lbf
thetaclimb=0.175;     %water line deck angle in rad
```

```
function[S,K,CD0,Wt,CL0,CLalpha,alphamax,q,U1,U2,T,thetaclimb]
    =P3HvToff()
%P3 at 120,000lbs, app flaps, gear up
S=1300;                %plane form surface area in ft^2
K=0.05041;            %coefficient for CD calculation
CD0=0.0551;           %coefficient of drag
Wt=120000;             %aircraft weight in lbs
CL0=1.000;            %zero AOA lift coefficient
CLalpha=5.73;         %lift curve slope
alphamax=0.244;       %stall buffet alpha w/ approach flaps
q=0.0673;             %nominal pitch rate of 5deg/sec
U1=214;               %Liftoff speed (127kts)
U2=227;               %takeoff safety airspeed in ft/s
T=33400;              %thrust in lbf
thetaclimb=0.175;     %water line deck angle in rad
```



```

function[S,K,CDo,Wt,CLo,CLalpha,alphamax,q,U1,U2,T,thetaclimb]
    =P3HuHuToff()
%P3 at 135,000lbs, app flaps, gear up
S=1300;                %plane form surface area in ft^2
K=0.05041;            %coefficient for CD calculation
CDo=0.0551;           %coefficient of drag
Wt=135000;             %aircraft weight in lbs
CLo=1.000;             %zero AOA lift coefficient
CLalpha=5.73;         %lift curve slope
alphamax=0.244;       %stall buffet alpha w/ approach flaps
q=0.0673;             %nominal pitch rate of 5deg/sec
U1=229;               %Liftoff speed (136kts)
U2=239;               %takeoff safety airspeed in ft/s
T=33400;              %thrust in lbf
thetaclimb=0.1745;    %water line deck angle in rad

```

```

function[S,K,CDo,Wt,CLo,CLalpha,alphamax,q,U1,U2,T,thetaclimb]
    =modP3HuTo()
%P3 at 120,000lbs, app flaps, gear up. Increased rotate speed.
S=1300;                %plane form surface area in ft^2
K=0.05041;            %coefficient for CD calculation
CDo=0.0551;           %coefficient of drag
Wt=120000;             %aircraft weight in lbs
CLo=1.000;             %zero AOA lift coefficient
CLalpha=5.73;         %lift curve slope
alphamax=0.244;       %stall buffet alpha w/ approach flaps
q=0.0673;             %nominal pitch rate of 5deg/sec
U1=242;               %Liftoff speed (145kts)
U2=254;               %takeoff safety airspeed in ft/s
T=33400;              %thrust in lbf
thetaclimb=0.175;     %water line deck angle in rad

```

```

function[S,K,CD0,Wt,CL0,CLalpha,alpha_max,q,U1,U2,T,theta_climb]
    =L1011Toff()
%L1011 at 462,000lbs, App flaps, gear up
S=4578;                %plane form surface area in ft^2
K=0.059;               %coefficient for CD calculation
CD0=0.098;             %coefficient of drag
Wt=462000;             %aircraft weight in lbs
CL0=0.532;             %zero AOA lift coefficient
CLalpha=4.96;          %lift curve slope
alpha_max=0.314;       %stall warning alpha w/ approach flaps
                        %(18deg)
q=0.0873;              %nominal pitch rate of 5deg/sec
U1=238;                %rotate speed in ft/sec (141kts)
U2=255;                %takeoff safety airspeed ft/s (151kts)
T=126000;              %thrust in lbf
theta_climb=0.209;     %initial deck angle rad(12deg)

```

```

function[S,K,CD0,Wt,CL0,CLalpha,alpha_max,q,U1,U2,T,theta_climb]
    =T44Toff()
%T44 at 7817lbs, app flaps, gear down
S=210;                 %plane form surface area in ft^2
K=0.040;               %coefficient for CD calculation
CD0=0.010;             %coefficient of drag
Wt=7817;               %aircraft weight in lbs
CL0=0.0524;            %zero AOA lift coefficient
CLalpha=6.24;          %lift curve slope
alpha_max=0.227;       %stall buffet alpha w/flaps up
q=0.0873;              %nominal pitch rate of 5deg/sec
U1=152;                %liftoff airspeed in ft/s(90kts)
U2=180;                %takeoff safety speed ft/s (107kts)
T=3023;                %initial thrust in lbf
theta_climb=0.262;     %initial deck angle in rad (15 deg)

```

C. FLIGHT PATH CONTROL AND ESCAPE MANEUVER FUNCTIONS

```
function[thetaout,check1]
    =ToffCRS(q,deltat,theta,alpha,alphamax,U2,y,check1)
%Aircraft escape maneuver consisting of constant airspeed.
thetaout=theta;
if check1==0,
    if y(5)<U2,
        thetaout=theta-q*deltat;
        if thetaout<0.0,
            thetaout=0.0;
        end
    else
        thetaout=theta+q*deltat;
        check1=1;
    end
else
    if y(5)>=(U2+8.4),
        thetaout=theta+q*deltat;
    elseif y(5)<=(U2-8.4)
        thetaout=theta-q*deltat;
    end
end
if alpha>alphamax,
    thetaout=theta-(alpha-alphamax);
end
```

```

function[thetaout,check1]
    =ToffCALT(q,deltat,theta,alpha,alphamax,y,check1,ydot)
%Aircraft control using constant altitude escape maneuver.
thetaout=theta;
if check1==0;
    check1=y(2)+20;
end
if y(2)<check1-10,
    if ydot(2)<=0,
        thetaout=theta+q*deltat;
    end
elseif y(2)>check1+10,
    if ydot(2)>=0,
        thetaout=theta-q*deltat;
    end
end
if thetaout<0,
    thetaout=0;
end
if alpha>alphamax,
    thetaout=theta-(alpha-alphamax);
end

function[thetaout]=ToffCTH(q,deltat,theta,alpha,alphamax,thetaaim)
%Constant theta escape maneuver.
if theta<thetaaim,
    thetaout=theta+q*deltat;
else
    thetaout=thetaaim;
end
if alpha>alphamax,
    thetaout=theta-(alpha-alphamax);
end

```

```

function[thetaout]=ToffCORA(q,deltat,theta,alpha,alphamax,alphaaim)
%Constant alpha escape maneuver.
if alpha<alphaaim,
    thetaout=theta+(alphaaim-alpha);
    if thetaout>(theta+q*deltat),
        thetaout=theta+q*deltat;
    end
else
    thetaout=theta-(alpha-alphaaim);
    if thetaout<(theta-q*deltat),
        thetaout=theta-q*deltat;
    end
end
if alpha>alphamax,
    thetaout=theta-(alpha-alphamax);
end

```

APPENDIX E

ON-STATION ALGORITHMS

Contained in this appendix are the MatLab® programs utilized in calculating the response of a P-3 encountering a windshear while operating close to the surface. They are listed in three sections. The first section contains the driver routine. The second and third sections contain the aircraft parameter function and flight path control function respectively. The windshear function is listed in Appendix A. The differential equation solving routine is listed in Appendix C.

A. DRIVER

```
*****
% P3 Loiter Profile Model  *
*****

clear
clc
format bank
format compact
%-----
%INITIALIZATION AND ENVIRONMENTAL CONSTANTS
% The following initialize constants and variables for the model.
%AIRCRAFT CONSTANTS
% The following constants are for the particular aircraft being
studied.
disp('      P3 ON-STATION')
```

```

disp(' ')
check1=0.0;
U=0.0;
answer =1.0;
check1=input(' Enter on-station loiter altitude(ft): ');
U=input(' Enter loiter airspeed in knots: ');
U=U*1.687; %convert knots to ft/sec
answer=input('Enter 0 for no windshear: ');

[S,K,CDo,Wt,CLo,CLalpha,alphamax,q,T,theta]=P3onsta(U);
%initialization

%S=plane form surface area in ft^2
%K=coefficient for CD calculation
%CDo=coefficient of drag
%Wt=aircraft weight in lbs
M=Wt/32.174; % mass in slugs
%CLo=zero ROR lift coefficient
%CLalpha=lift curve slope
%alphamax=stall buffet alpha w/ approach flaps
%q=nominal pitch rate of 5deg/sec
%U1=rotate speed in ft/s
%U2=takeoff safety airspeed in ft/s
%T=thrust in lbf
%-----
%***programed initial values*****
iters=145; %number of iterations
deltat=0.25; %time increment in sec
xstart=-5000; %starting distance from
%NB center
%*****
disp(' Initial Input Section')
disp(' ')
disp('The following values are preprogrammed:')
disp(' a. The flight path is based on constant power.')
disp(' b. The starting distance (distance from NB center) is:')
disp(xstart)
disp(' c. The time step in sec:')

```

```

disp(deltat)
disp(' d. The number of iterations is:')
disp(iters)
disp(' ')
TW=T/Wt;                                %thrust/weight ratio
WL=Wt/S;                                %wing loading
disp('The following values were supplied/calculated from aircraft
constants')
disp(' a. Loiter Air Speed:')
disp(U)
disp(' b. Thrust to weight is:')
disp(TW)
disp(' c. Wing loading is:')
disp(WL)
disp(' ')
x1=xstart;                               %initialization
h1=check1;                               %initialization
U1=U;                                    %initialization
Ug=U;                                    %ground speed initialization in ft/s
gamai=0.001;                             %initial inertial flight path angle in
rad (1deg)
rho=0.002377;                            %air density in slugs/ft^3 @ S.L.
trigger=0.0;                             %utility check number
check2=0.0;                              %utility check number
%-----
%ALGORITHM
% The actual algorithm is broken into several smaller divisions and
functions:
%   starting values - as it implies
%   loop - beginning of iterating process
%   windshear inputs - uses the function 'microburst' to give
%                       point x and z axis wind speeds
%   predictor - first guess at the solution of the governing DEs
%   corrector - corrected solutions to the governing DEs and
%               final point values.
%   output file management - as it implies
%   aircraft control - uses multiple control functions for
%                       control inputs to theta, thrust, and AOA

```



```

%      final output - as it implies
%-----
%starting values:
pt=1;                                %counter
Q=0.5* $\rho$ *U1^2;                      %dynamic pressure
CL=Wt/(Q*S);                         %coefficient of lift
CD=CD0+K*CL^2;                       %coefficient of drag
alpha=(CL-CL0)/CLalpha;              %AOA required for 1g flight
gamma=theta-alpha;                   %airmass flight path angle
Es=U1^2/(2*32.174)+h1;               %specific energy in ft
Esdot=U;                             %time rate change in specific energy

y(1)=x1;                             %y(1)=x position in ft
y(2)=h1;                             %y(2)=aircraft altitude in ft
y(5)=U1;                             %y(5)=aircraft airspeed in ft/s
y(6)=gamma;                          %y(6)=aircraft airmass flight path in
rad
Aircraft(1,:)=[x1,h1,U1,0,theta,alpha,1,T];
Inertial(1,:)=[Ug,0,gamma,gamaI,0,0,1,Es,Esdot];
% starting output files
%-----
%loop:
clc
while theta~=999,
pt=pt+1;                             %present pt in space
%-----
%wind shear inputs:
x2=Ug*deltat+x1;                     %approximate horizontal displacement
h2=tan(gamaI)*(x2-x1)+h1;             %approximate vertical displacement

if answer~=0,
[Ux11,Wh11]=microburst(h1,x1); %These four calls to the function
[Ux21,Wh21]=microburst(h2,x1); %microburst finds the point wind
[Ux12,Wh12]=microburst(h1,x2); %shear for determination of the
[Ux22,Wh22]=microburst(h2,x2); %average block wind shear.
if pt<=8,                             %These next if logic commands
Ux11=Ux11*pt/8;Wh11=Wh11*pt/8; %control the entry and exit
Ux12=Ux12*pt/8;Wh12=Wh12*pt/8; %windshear effects.

```

```

elseif y(1)>=abs(xstart),
    if check2==0,
        check2=pt;
    end
    if (8-pt+check2)>=0,
        Ux21=Ux21*(8-(pt-check2))/8;Uh21=Uh21*(8-(pt-check2))/8;
        Ux22=Ux22*(8-(pt-check2))/8;Uh22=Uh22*(8-(pt-check2))/8;
    else
        Ux11=0;Ux21=0;Ux12=0;Ux22=0;Uh11=0;Uh21=0;Uh12=0;Uh22=0;
    end
end
else
    Ux11=0;Ux21=0;Ux12=0;Ux22=0;Uh11=0;Uh21=0;Uh12=0;Uh22=0;
    %The above is used in conjunction
    %other calls when no wind shear is
    %desired.

end %answer
WindX(pt)=Ux11; %Wind shear matrices
WindH(pt)=Uh11;

dUxdx=((Ux12-Ux11)+(Ux22-Ux21))/(2*(x2-x1));%These formulas
dUxdh=((Ux22-Ux12)+(Ux21-Ux11))/(2*(h2-h1));%calculate the
dUhdh=((Uh12-Uh11)+(Uh22-Uh21))/(2*(x2-x1));%differential change
dUhdh=((Uh22-Uh12)+(Uh21-Uh11))/(2*(h2-h1));%in wind shear.

y(3)=Ux11; %y(3)=wind shear in the x direction
ft/s
y(4)=Uh11; %y(4)=wind shear in the z direction
ft/s
%-----
%predictor and intermediate values
ydot=yprimes(y,dUxdx,dUxdh,dUhdh,dUhdh,theta,T,S,M,Q,CL,CD,
    alpha,alphamax); %call to the DE function
for n=1:6,
    y1(n)=y(n)+deltat*ydot(n); %Euler first step fud predictor
    yhalf(n)=y(n)+deltat/2*ydot(n); %Euler half step fud predictor
end

```

```

alpha=theta-y(6);          %AOA
CL=CLo+alpha*CLalpha;      %coefficient of lift
CD=CDo+K*CL^2;             %coefficient of drag
Q=0.5*row*yhalf(5)^2;       %dynamic pressure
%-----
    %corrector and new value formulation
ydot=yprimes(yhalf,dWxdx,dWxdh,dWhdx,dWhdh,theta,T,S,M,Q,
            CL,CD,alpha,alphamax);
for n=1:6,
    y2(n)=yhalf(n)+deltat/2*ydot(n); %Richardson extrapolation
    y(n)=2*y2(n)-y1(n);             %corrector scheme.
end

x1=y(1);                    %new x posit in ft
h1=y(2);                    %new altitude in ft AGL
Ug=y(5)*cos(y(6))+y(3);      %ground speed in ft/sec
ROC=y(5)*sin(y(6))+y(4);     %Rate of Climb in ft/sec
gamai=atan(ROC/Ug);          %new airmass FP angle in rad
Es=y(5)^2/64.348+y(2);       %new specific energy
Esdot=y(5)*ydot(5)/32.174+ydot(2); %new trc of specific energy

alpha=theta-y(6);          %new AOA
CL=CLo+alpha*CLalpha;      %new coefficient of lift
CD=CDo+K*CL^2;             %new coefficient of drag
Q=0.5*row*y(5)^2;          %new dynamic pressure
%-----
    %output file management:
Aircraft(pt,:)= [y(1),y(2),y(5),ydot(5),theta,alpha,pt,T];
Inertial(pt,:)= [Ug,ROC,y(6),gamai,y(3),y(4),pt,Es,Esdot];
home
disp('          pt          x          h          U
airspeed accel  ')
op1=[pt,Aircraft(pt,1),Aircraft(pt,2),Aircraft(pt,3),
    Aircraft(pt,4)];
disp(op1)
disp('          pt          theta          alpha          gamaa
gamai')
op2=[pt,Aircraft(pt,5),Aircraft(pt,6),Inertial(pt,3),

```

```

        Inertial(pt, 4)];
disp(op2)
disp('          pt          Ug          ROC          Thrust')
op3=[pt, Inertial(pt, 1), Inertial(pt, 2), Aircraft(pt, 8)];
disp(op3)
disp('          pt          Es          Esdot')
op5=[pt, Inertial(pt, 8), Inertial(pt, 9)];
disp(op5)
disp('          pt          Ux          Uh')
op4=[pt, Inertial(pt, 5), Inertial(pt, 6)];
disp(op4)
%-----
%aircraft control:
[theta, T]=CALT(q, deltat, theta, alpha, alphamax, y, check1,
               ydot, T, U)
if pt==iters,          %number of iterations
    theta=999;
elseif y(1)>5000,
    theta=999;
end
end                    %while algorithm loop
%-----
%output files:
answer=input('Do you want a flight path plot? 1=YES ');
if answer==1,
    plot(Aircraft(:, 1), Aircraft(:, 2))
    pause
    answer=0.0;
end
answer=input('Do you want x, h, U, and a/speed accel? 1=YES ');
if answer==1,
disp('          pt          x          h          U
a/speed accel ')
op1=[Aircraft(:, 7), Aircraft(:, 1), Aircraft(:, 2), Aircraft(:, 3),
      Aircraft(:, 4)];
disp(op1)
else
end

```

```

answer=input('Do you want theta, alpha, gamma, and gamai? 1=YES ');
if answer==1,
disp('          pt          theta          alpha          gamma
gamma')
op2=[Aircraft(:,7),Aircraft(:,5),Aircraft(:,6),Inertial(:,3),
      Inertial(:,4)];
disp(op2)
else
end
answer=input('Do you want Ug, ROC, and Thrust? 1=YES ');
if answer==1,
disp('          pt          Ug          ROC          Thrust')
op3=[Aircraft(:,7),Inertial(:,1),Inertial(:,2),Aircraft(:,8)];
disp(op3)
else
end
answer=input('Do you want Es and Estdot? 1=YES ');
if answer==1,
disp('          pt          Es          Estdot')
op5=[Aircraft(:,7),Inertial(:,8),Inertial(:,9)];
disp(op5)
else
end
answer=input('Do you want Wx and Wh? 1=YES ');
if answer==1,
disp('          pt          Wx          Wh')
op4=[Aircraft(:,7),Inertial(:,5),Inertial(:,6)];
disp(op4)
else
end

```

B. AIRCRAFT PERFORMANCE PARAMETER FUNCTION

```
function[S,K,CDo,Wt,CLo,CLalpha,alphamax,q,T,theta]=P3onsta(U)
%P3 at 120,000lbs, flaps and gear up.
S=1300;                %plane form surface area in ft^2
K=0.05041;             %coefficient for CD calculation
CDo=0.0213;            %coefficient of drag
Wt=120000;              %aircraft weight in lbs
CLo=0.350;              %zero AOA lift coefficient
CLalpha=6.25;          %lift curve slope
alphamax=0.209;        %stall buffet alpha w/ flaps up
q=0.0873;              %nominal pitch rate of 5deg/sec
T=.5*0.002377*U^2*S*(CDo+K*(Wt/(.5*.002377*U^2*S))^2);
                        %thrust in lbf
theta=(Wt/(.5*.002377*U^2*S)-CLo)/CLalpha;
                        %water line deck
                        angle in rad
```

C. FLIGHT PATH CONTROL FUNCTION

```
function[thetaout,Tout]=CALT(q,deltat,theta,alpha,alphamax,y,  
                             check1,ydot,T,U)  
%Aircraft control using constant altitude escape maneuver.  
thetaout=theta;  
Tout=T;  
if y(2)<check1-5,  
    if ydot(2)<=0,  
        thetaout=theta+q/2.5*deltat;  
    end  
elseif y(2)>check1+5,  
    if ydot(2)>=0,  
        thetaout=theta-q/2.5*deltat;  
    end  
end  
if abs(ydot(2)*deltat)>abs(y(2)-check1),  
    thetaout=thetaout-sign(ydot(2))*q/1*deltat;  
end  
if alpha>alphamax,  
    thetaout=theta-(alpha-alphamax);  
end  
if y(5)<=(U-67.5),  
    Tout=T+deltat/2*33400;  
end  
if Tout>33400,  
    Tout=33400;  
end
```

APPENDIX F

APPROACH TO LANDING ENCOUNTER GRAPHIC DATA

This appendix contains the calculated performance of different aircraft and weight combinations upon encountering a microburst windshear during an approach to landing. Each figure is for a particular aircraft performing a specified escape maneuver. Each figure contains four graphs depicting altitude, theta, alpha, airspeed, specific energy, and time. The abscissa in all graphs is x (distance from microburst center).

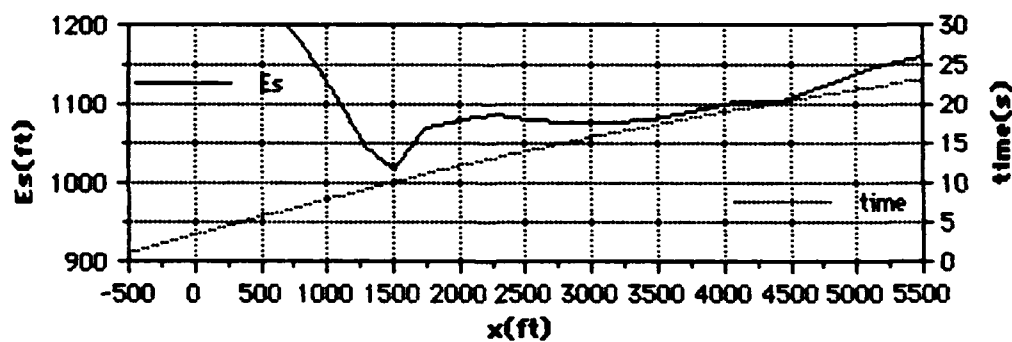
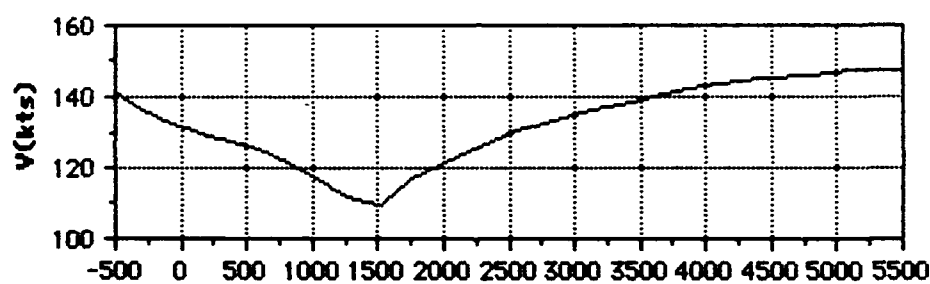
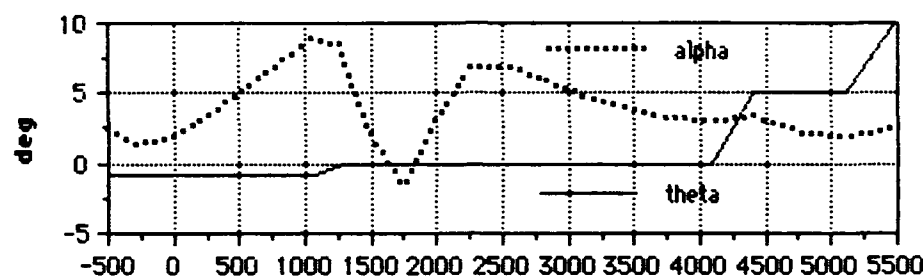
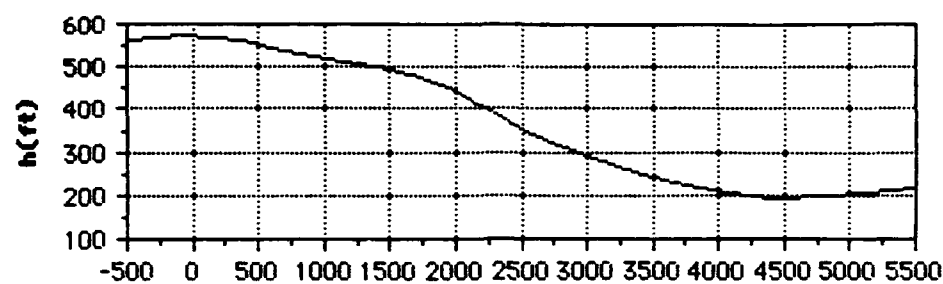


Figure F1. P-3 at 89,500lbs gross weight performing a constant airspeed escape.

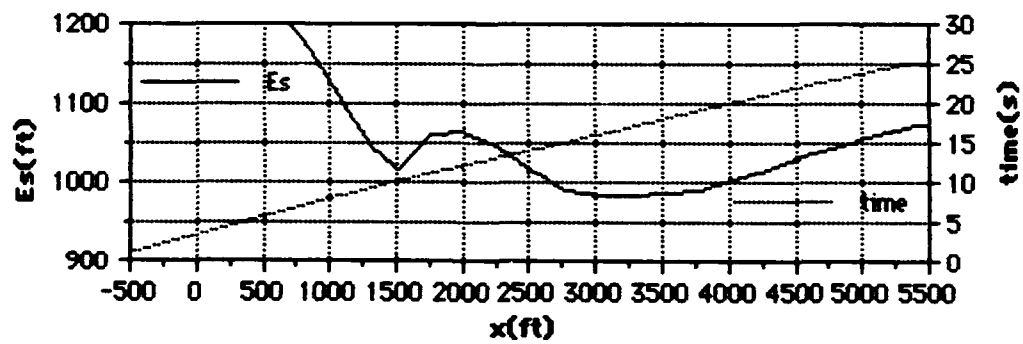
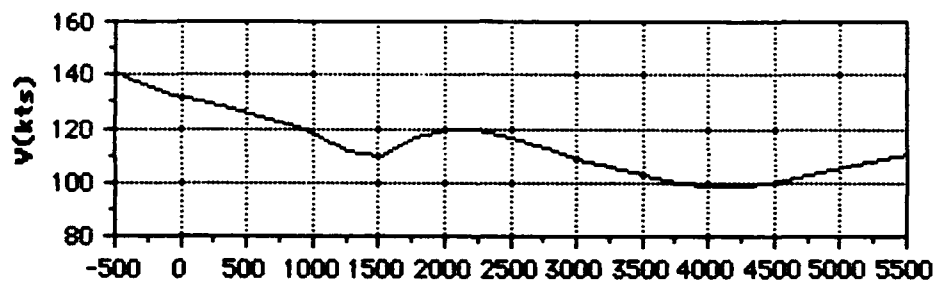
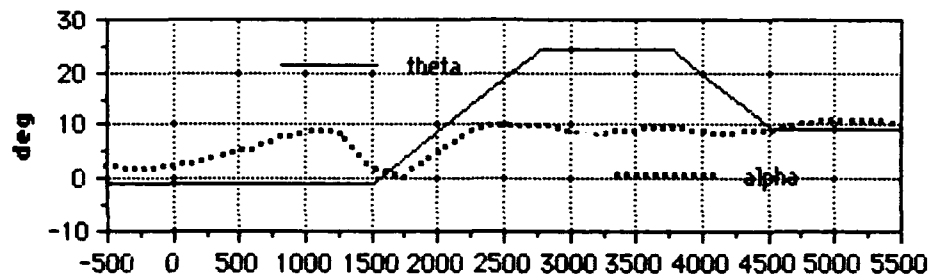
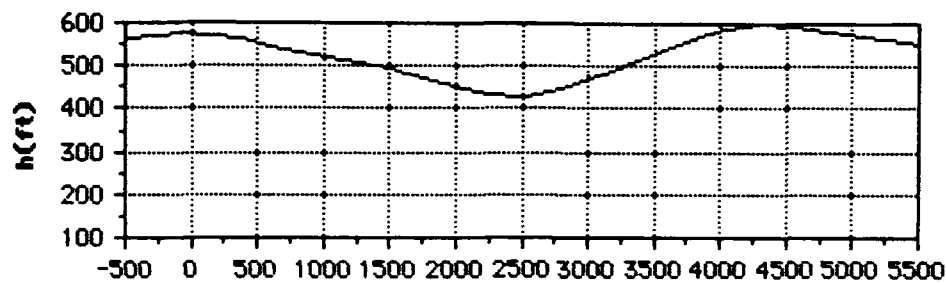


Figure F2. P-3 at 89,500lbs gross weight performing a constant altitude escape.

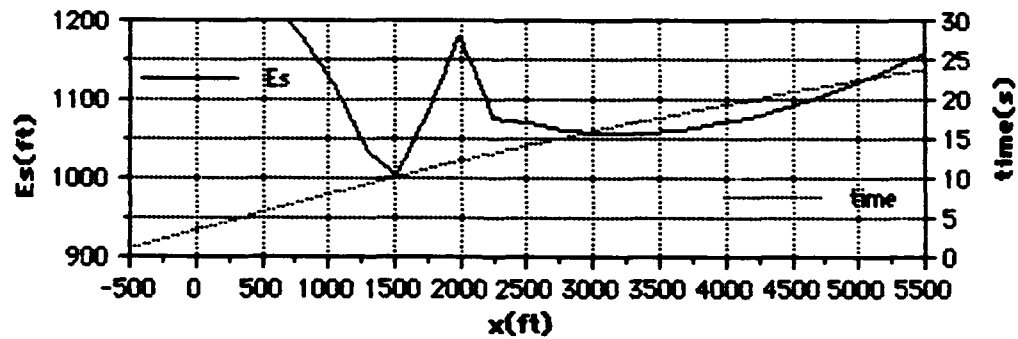
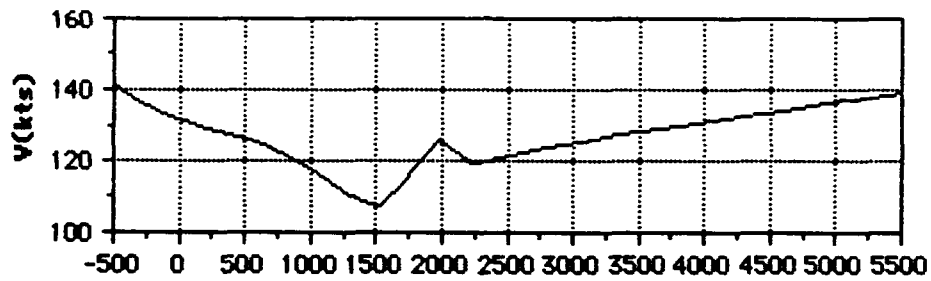
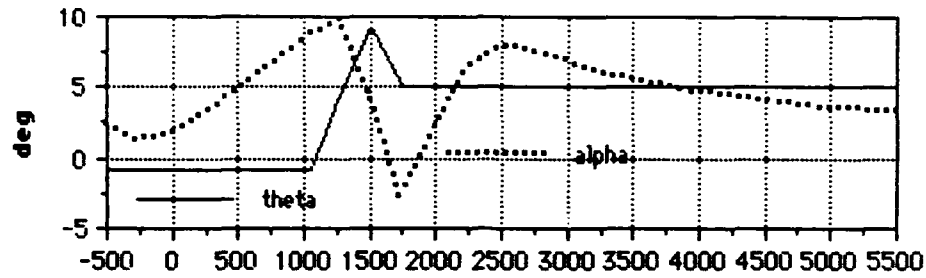
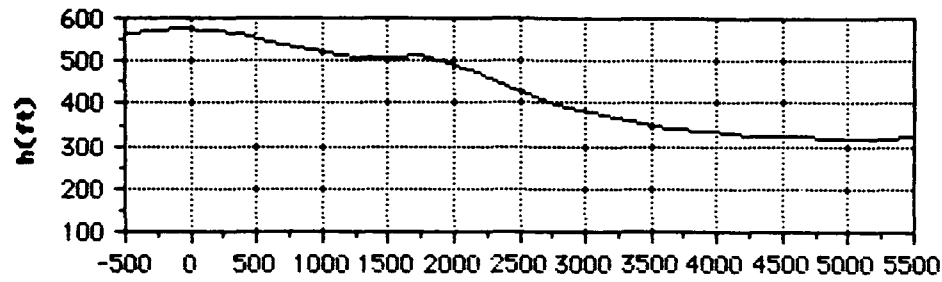


Figure F3. P-3 at 89,500lbs gross weight performing a constant 5° theta escape.

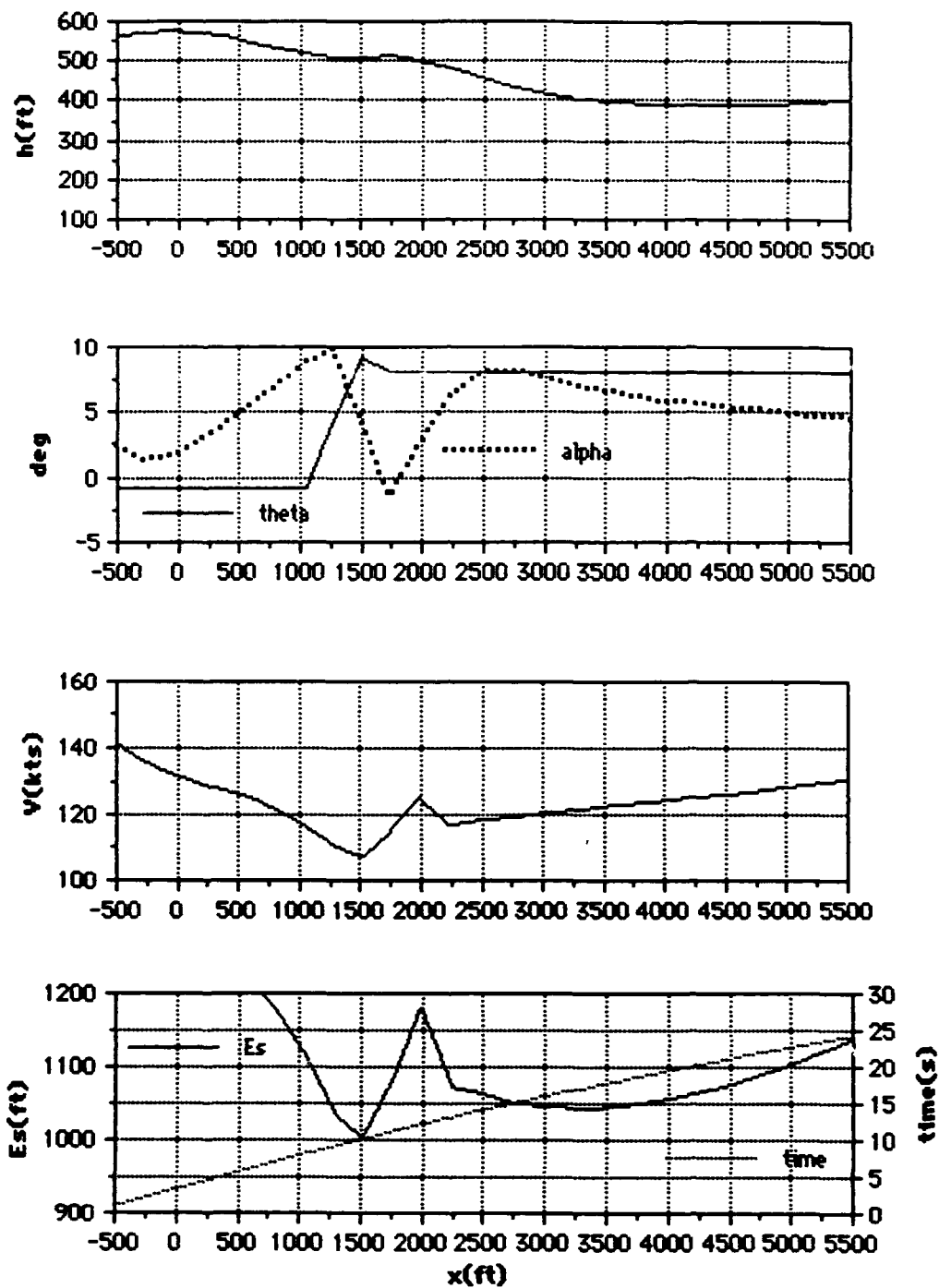


Figure F4. P-3 at 89,500lbs gross weight performing a constant 8° theta escape.

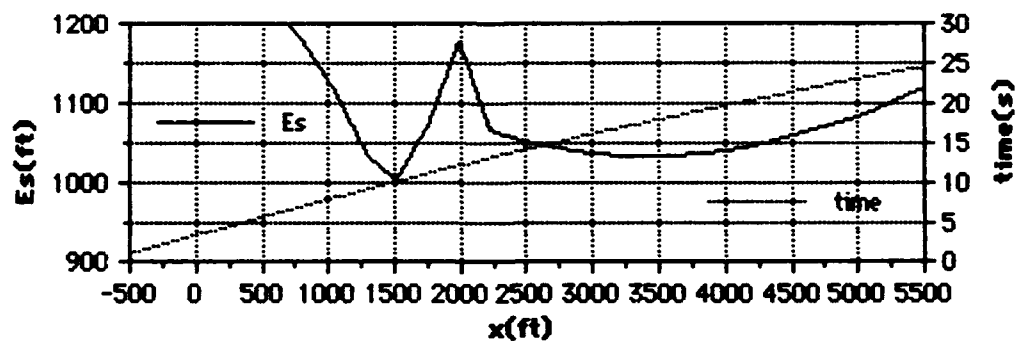
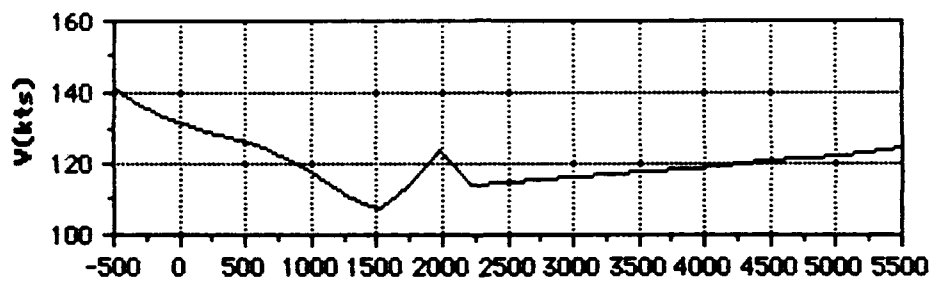
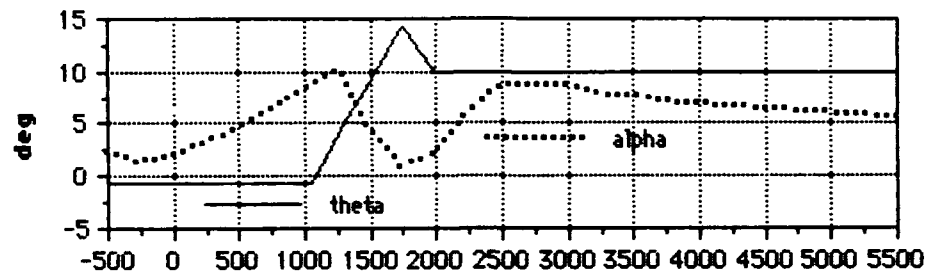
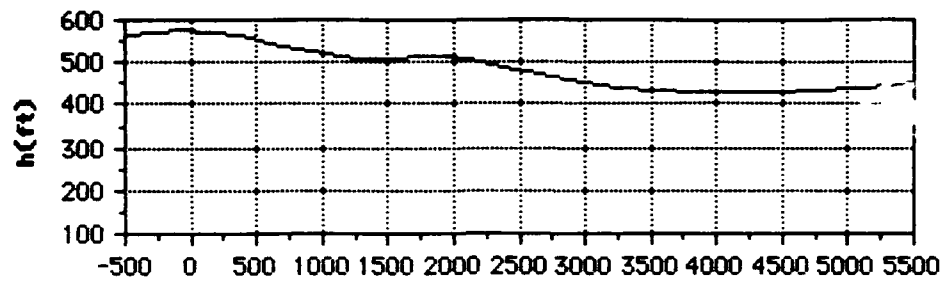


Figure F5. P-3 at 89,500lbs gross weight performing a constant 10° theta escape.

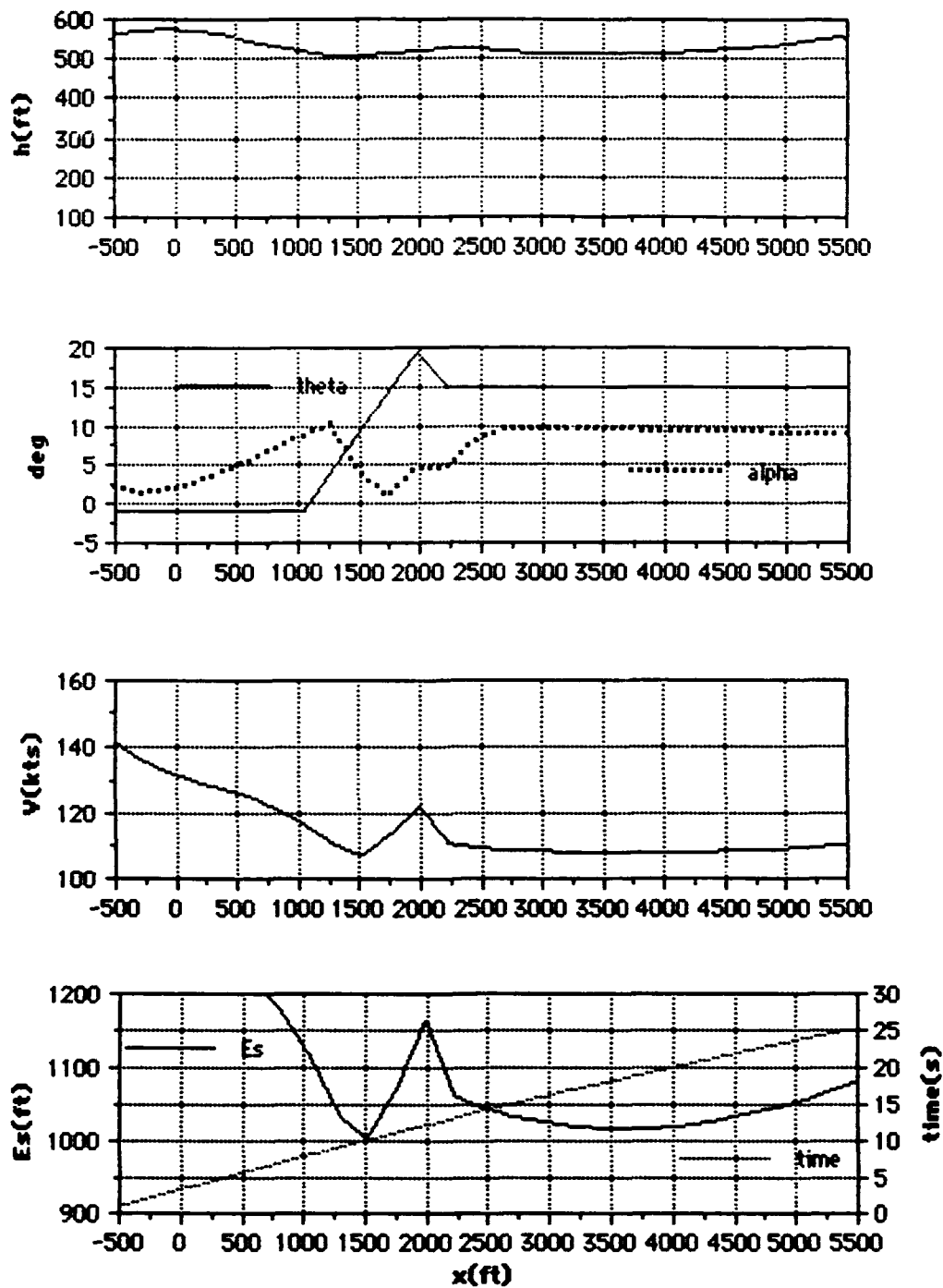


Figure F6. P-3 at 89,500lbs gross weight performing a constant 15° theta escape.

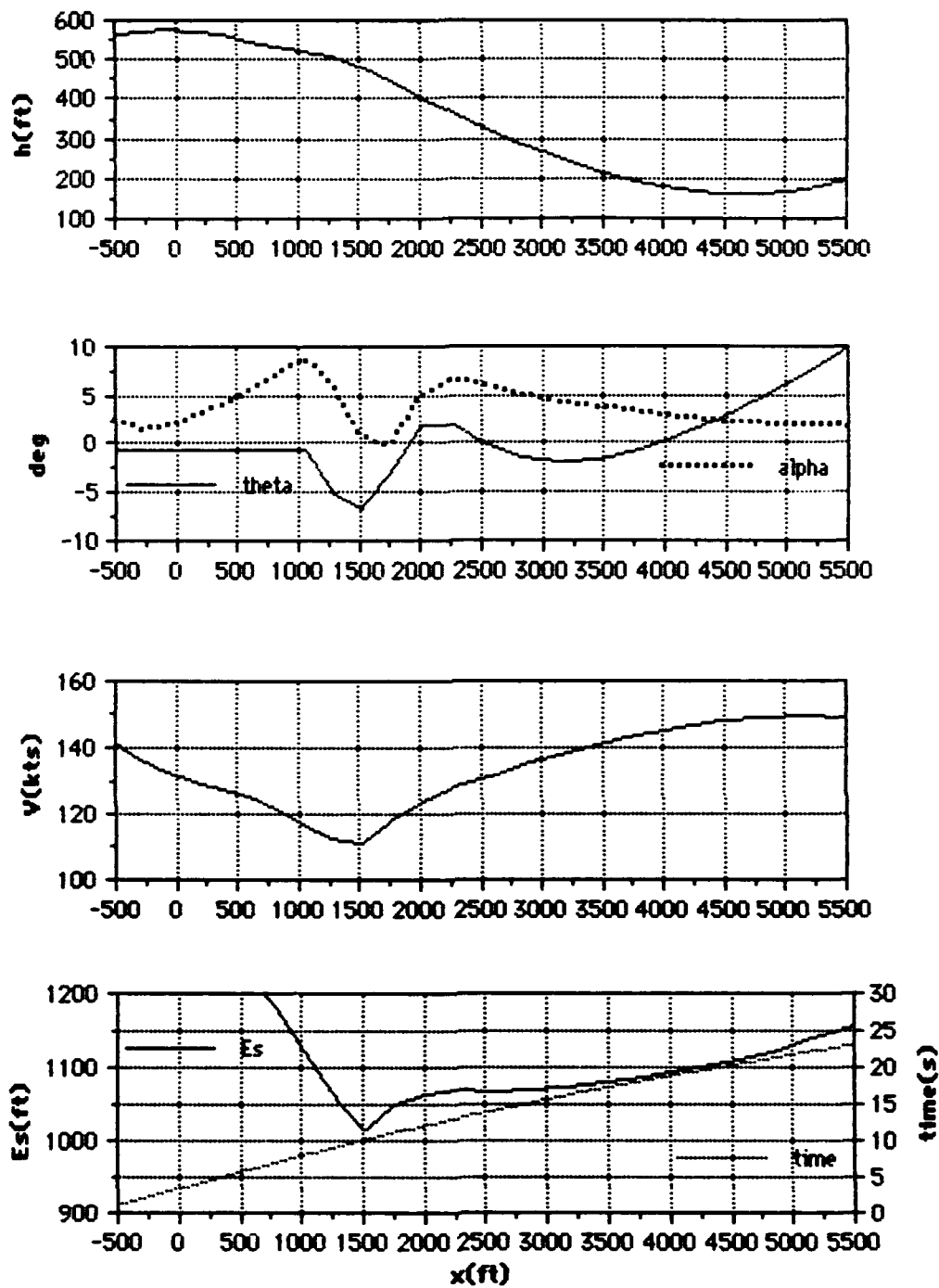


Figure F7. P-3 at 89,500lbs gross weight performing a constant 12 unit AOA escape.

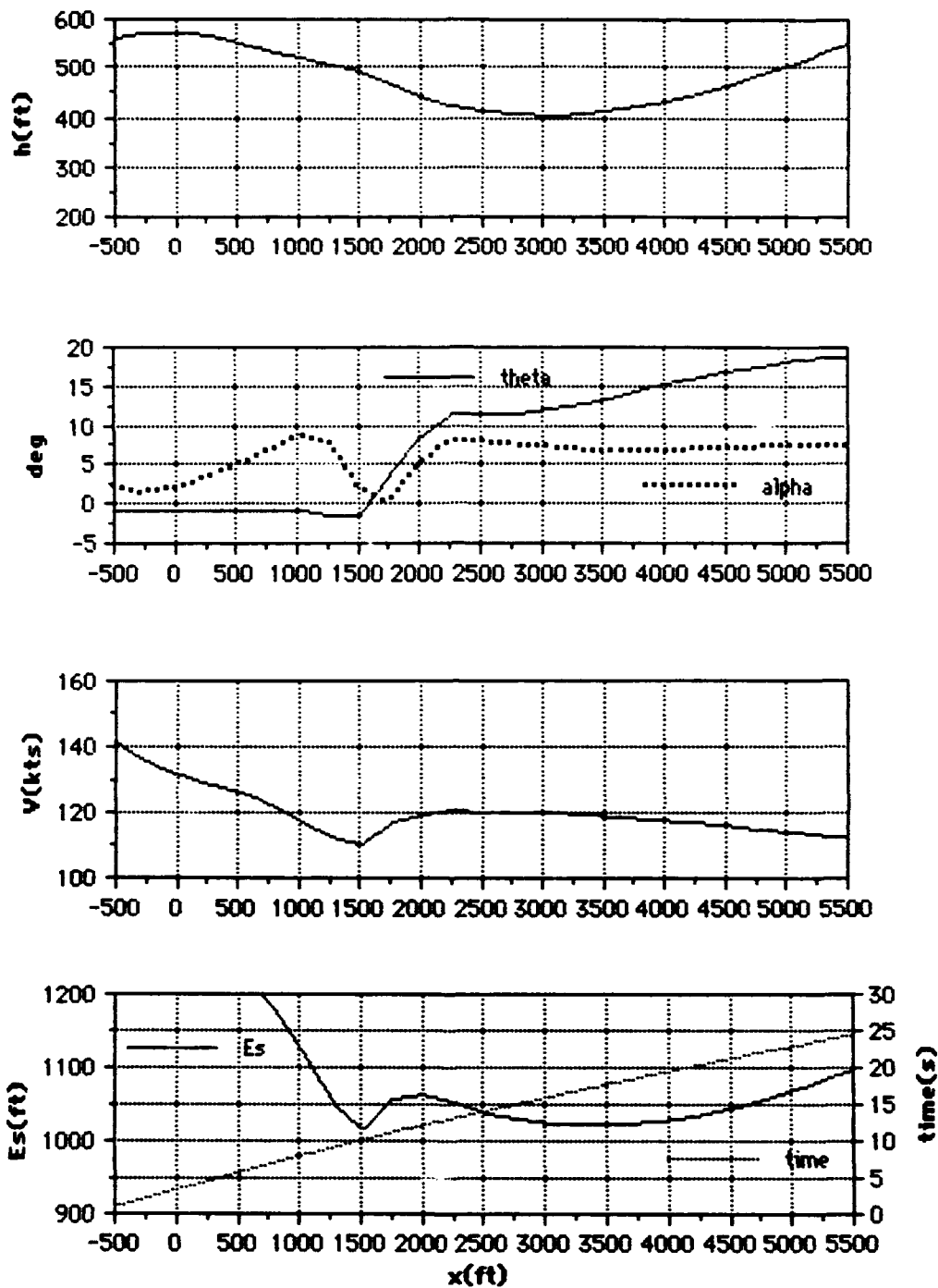


Figure F8. P-3 at 89,500lbs gross weight performing a constant 15 unit AOA escape.

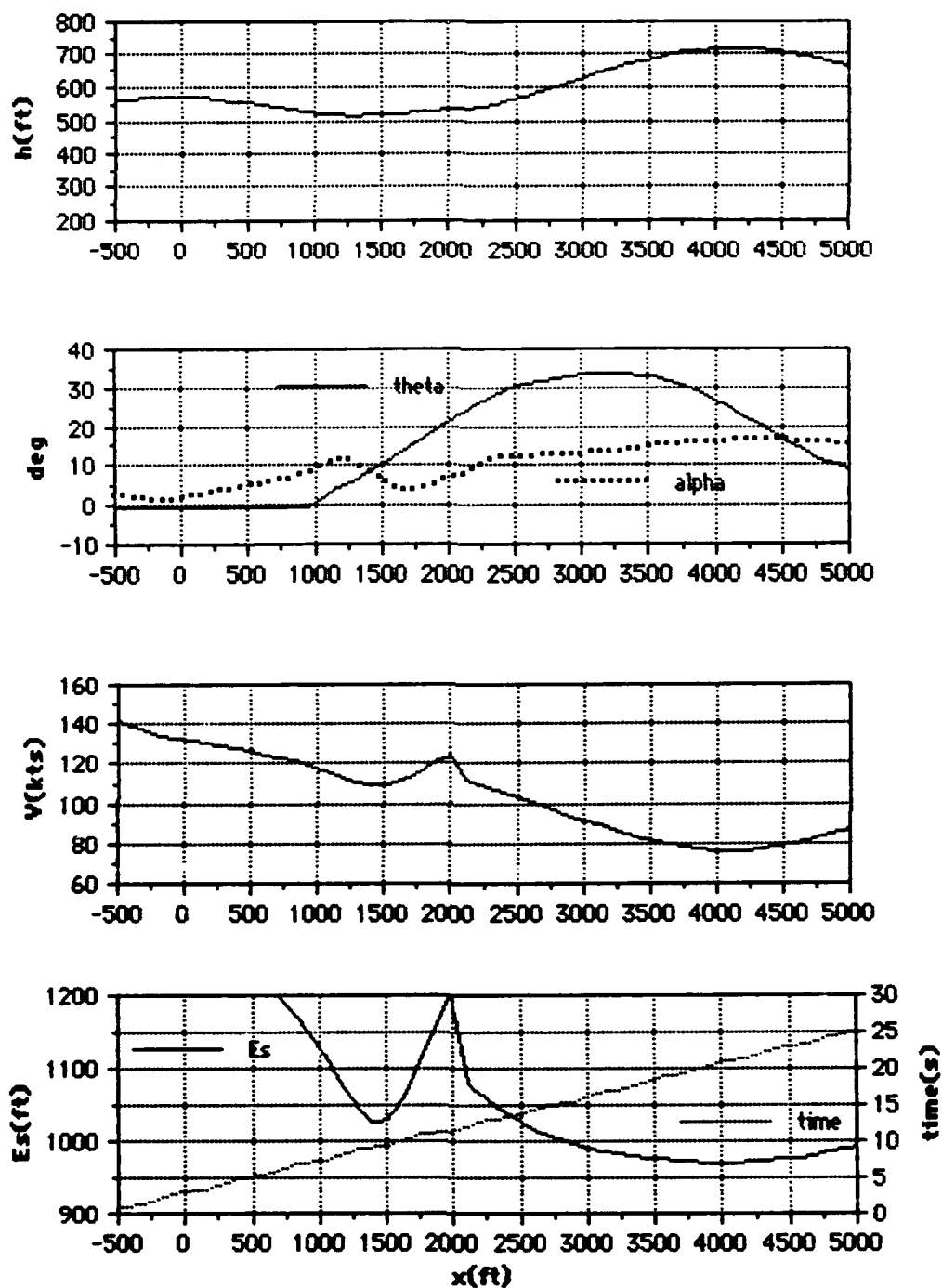


Figure F9. P-3 at 89,500lbs gross weight performing a constant 20 unit AOA escape.

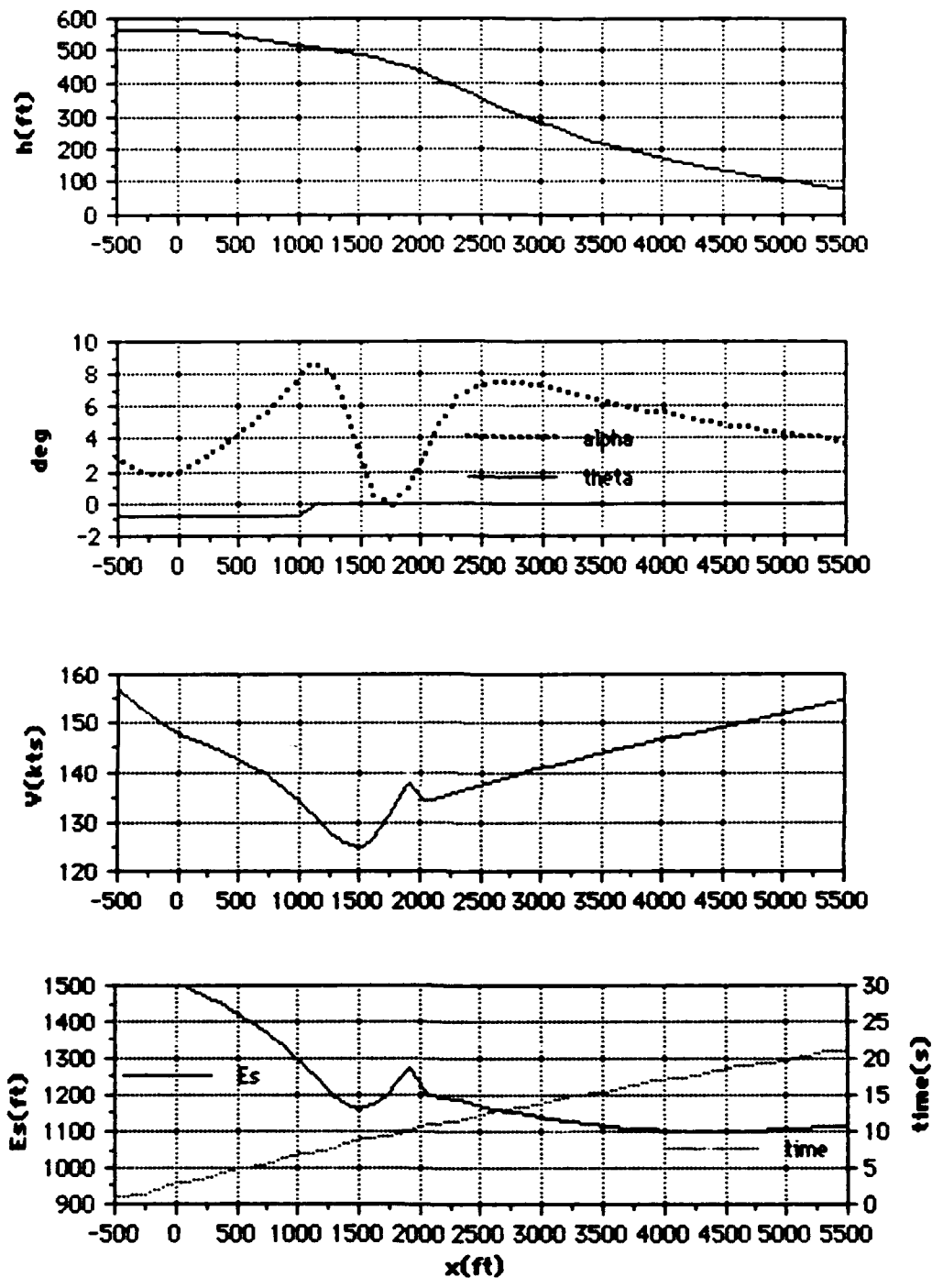


Figure F10. P-3 at 114,000lbs gross weight performing a constant airspeed escape.

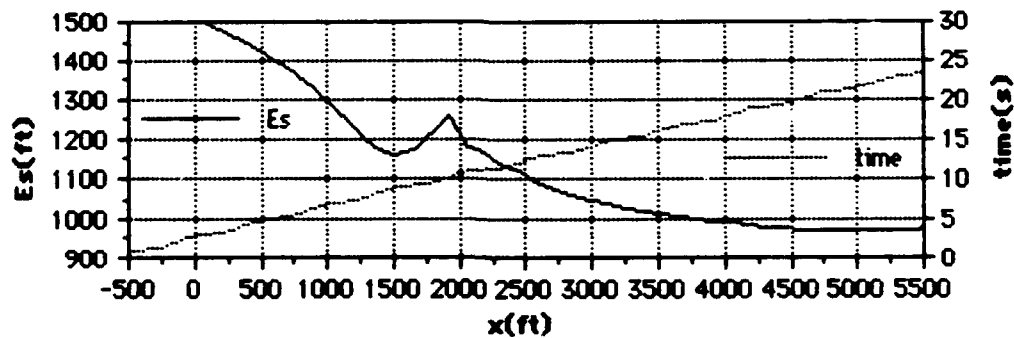
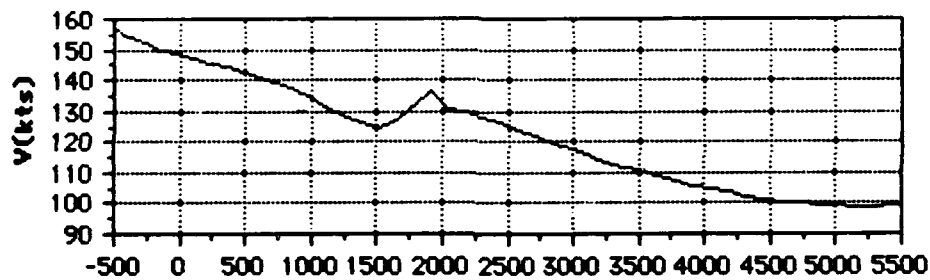
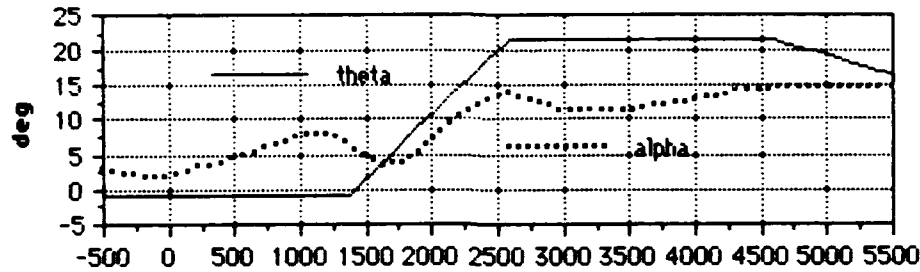
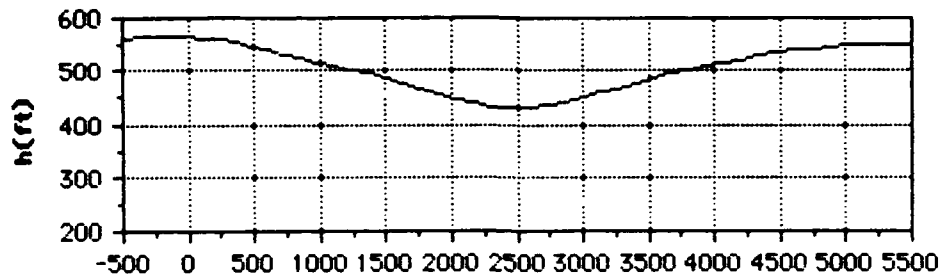


Figure F11. P-3 at 114,000lbs gross weight performing a constant altitude escape.

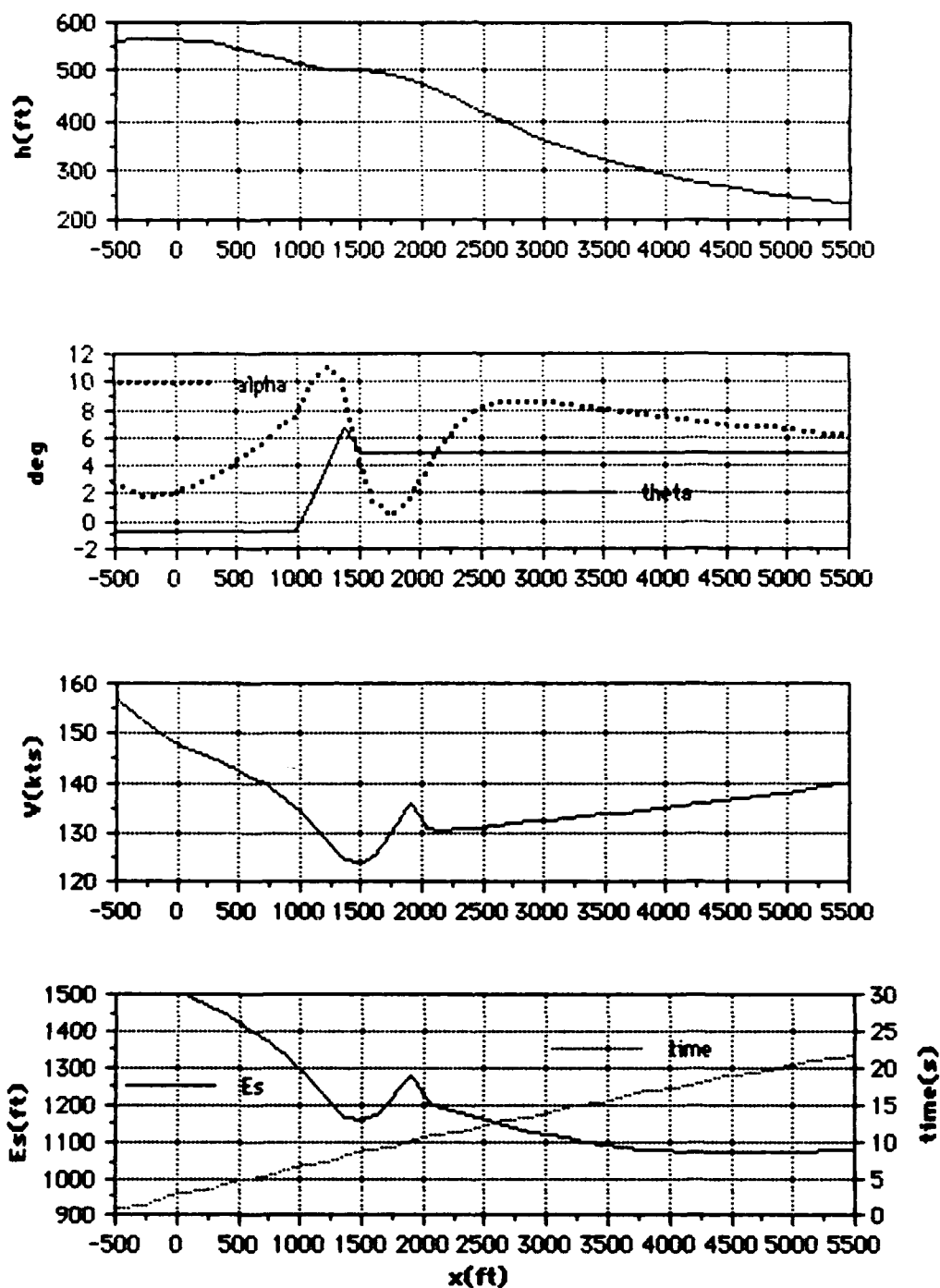


Figure F12. P-3 at 114,000lbs gross weight performing a constant 5° theta escape.

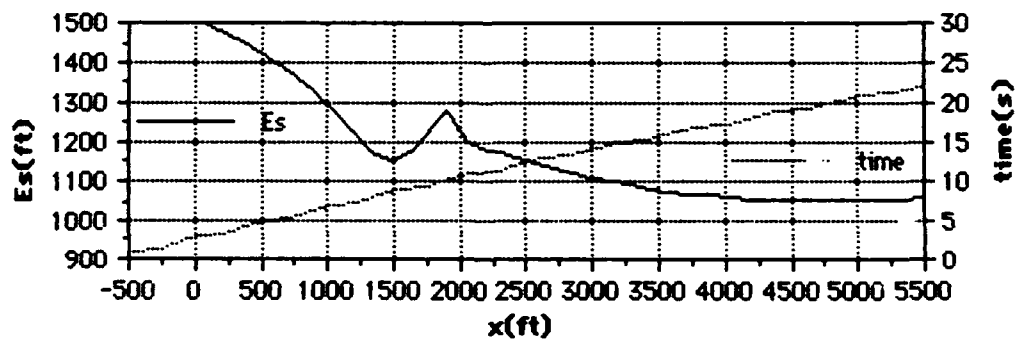
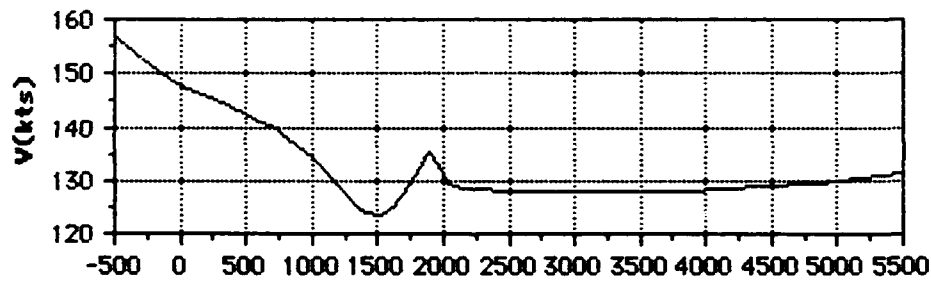
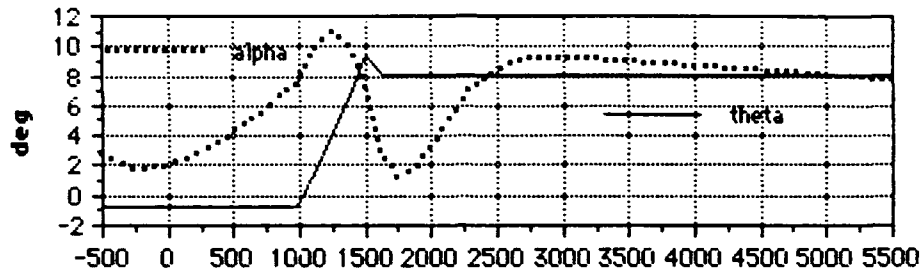
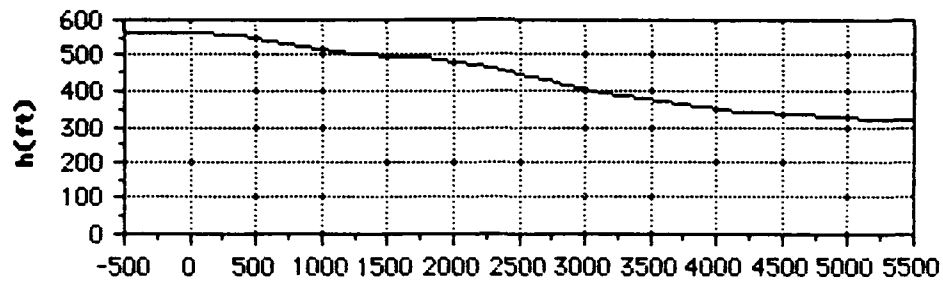


Figure F13. P-3 at 114,000lbs gross weight performing a constant 8° theta escape.

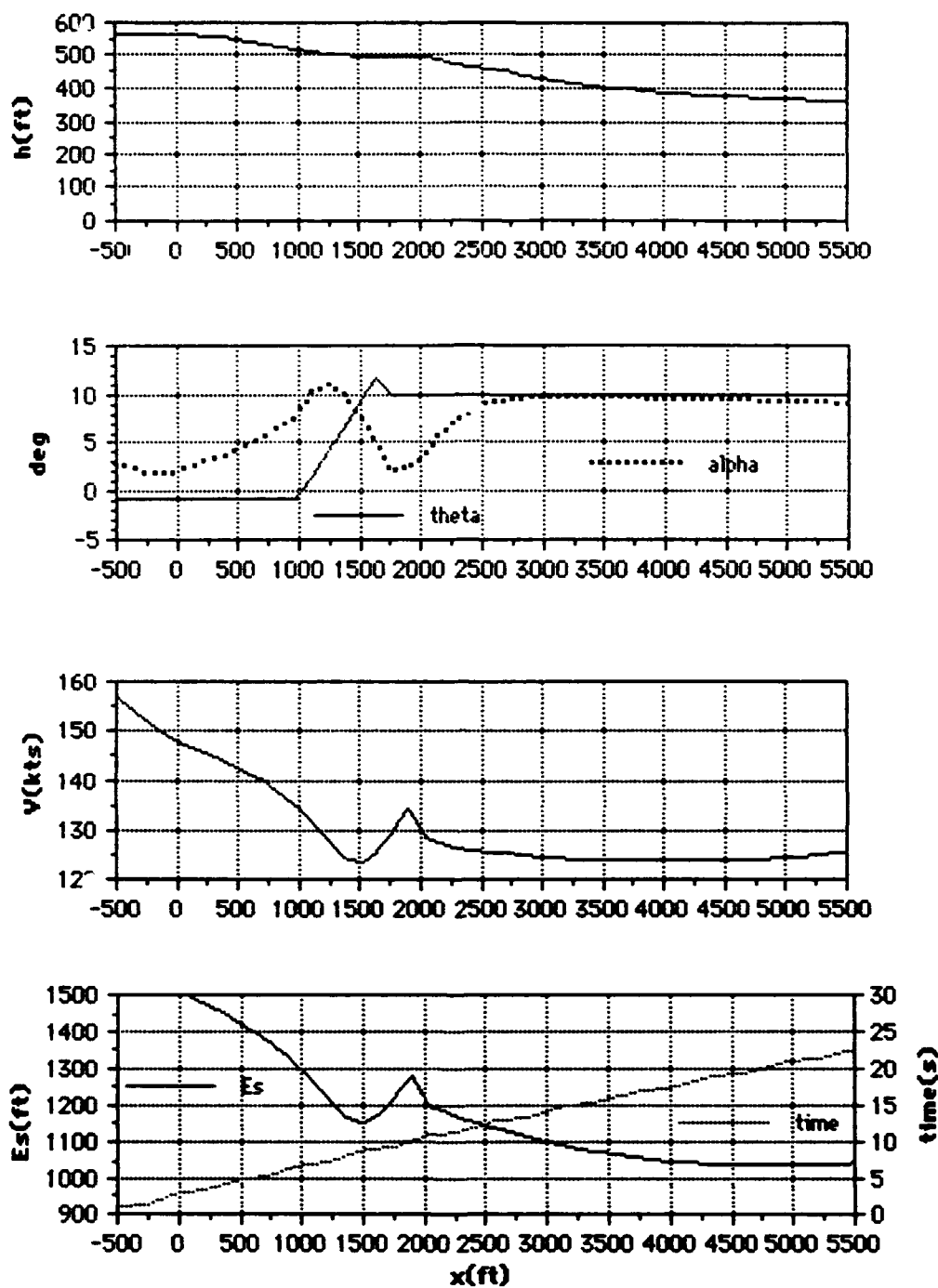


Figure F14. P-3 at 114,000lbs gross weight performing a constant 10° theta escape.

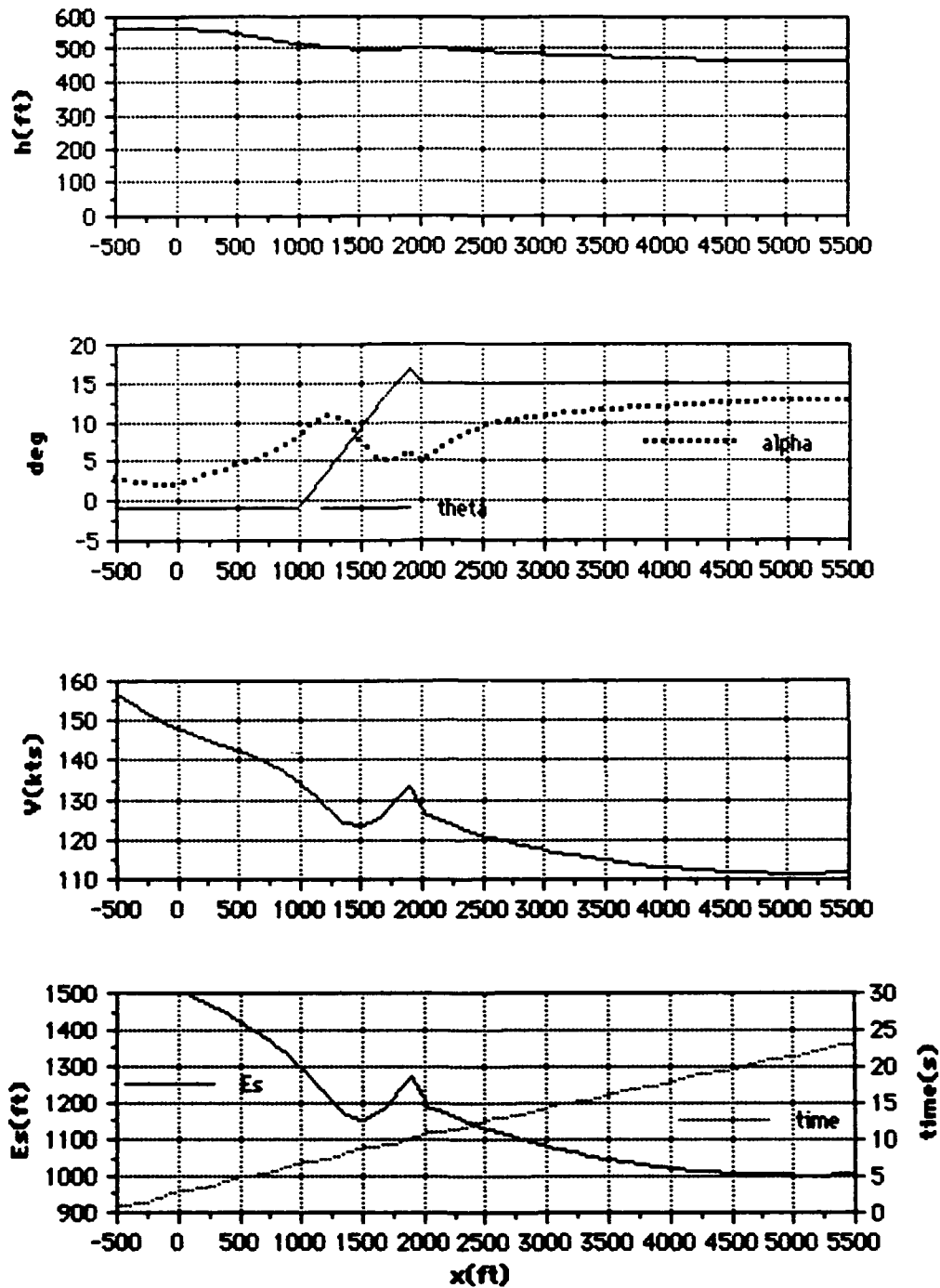


Figure F15. P-3 at 114,000lbs gross weight performing a constant 15° theta escape.

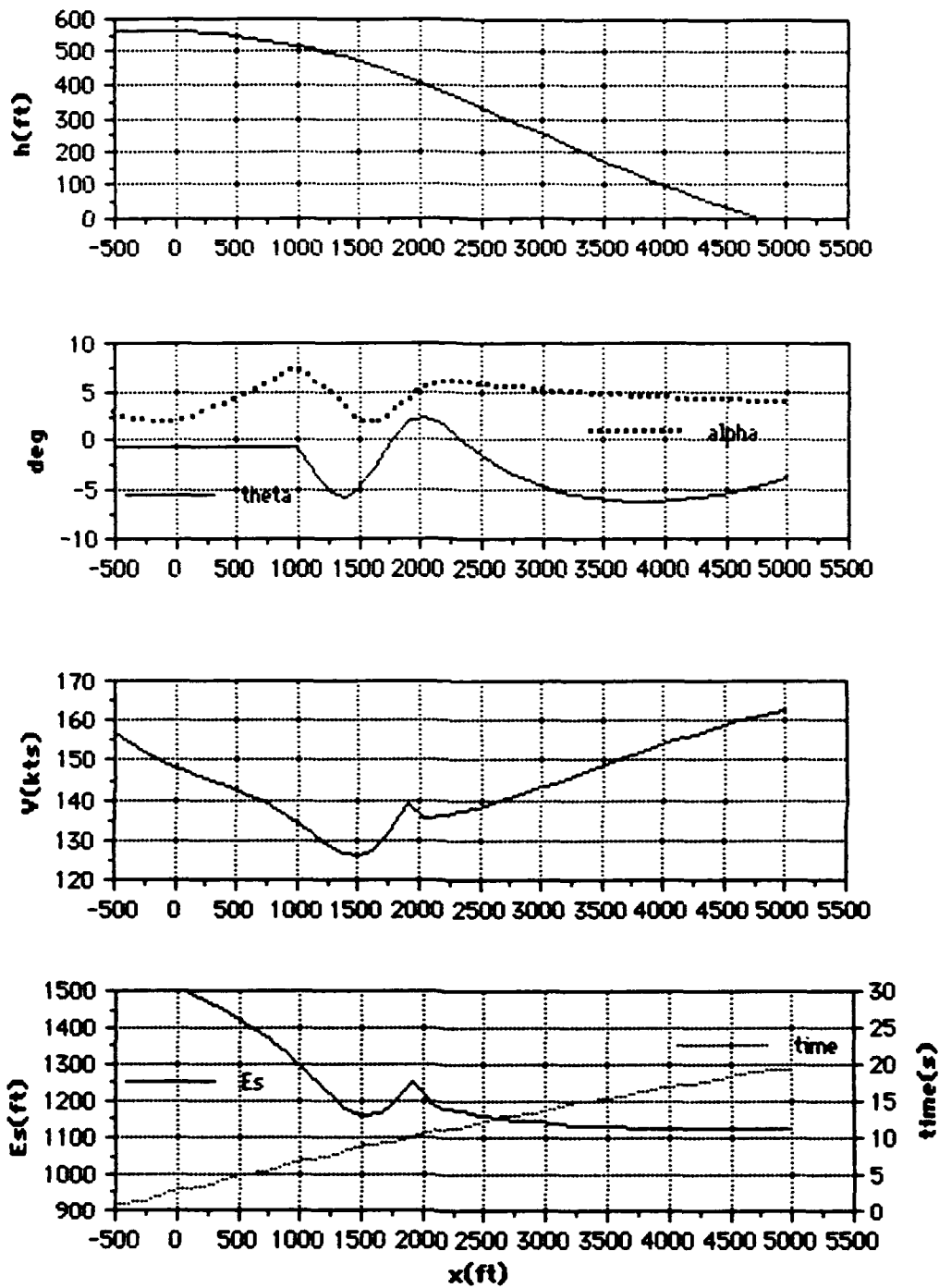


Figure F16. P-3 at 114,000lbs gross weight performing a constant 12 unit AOA escape.

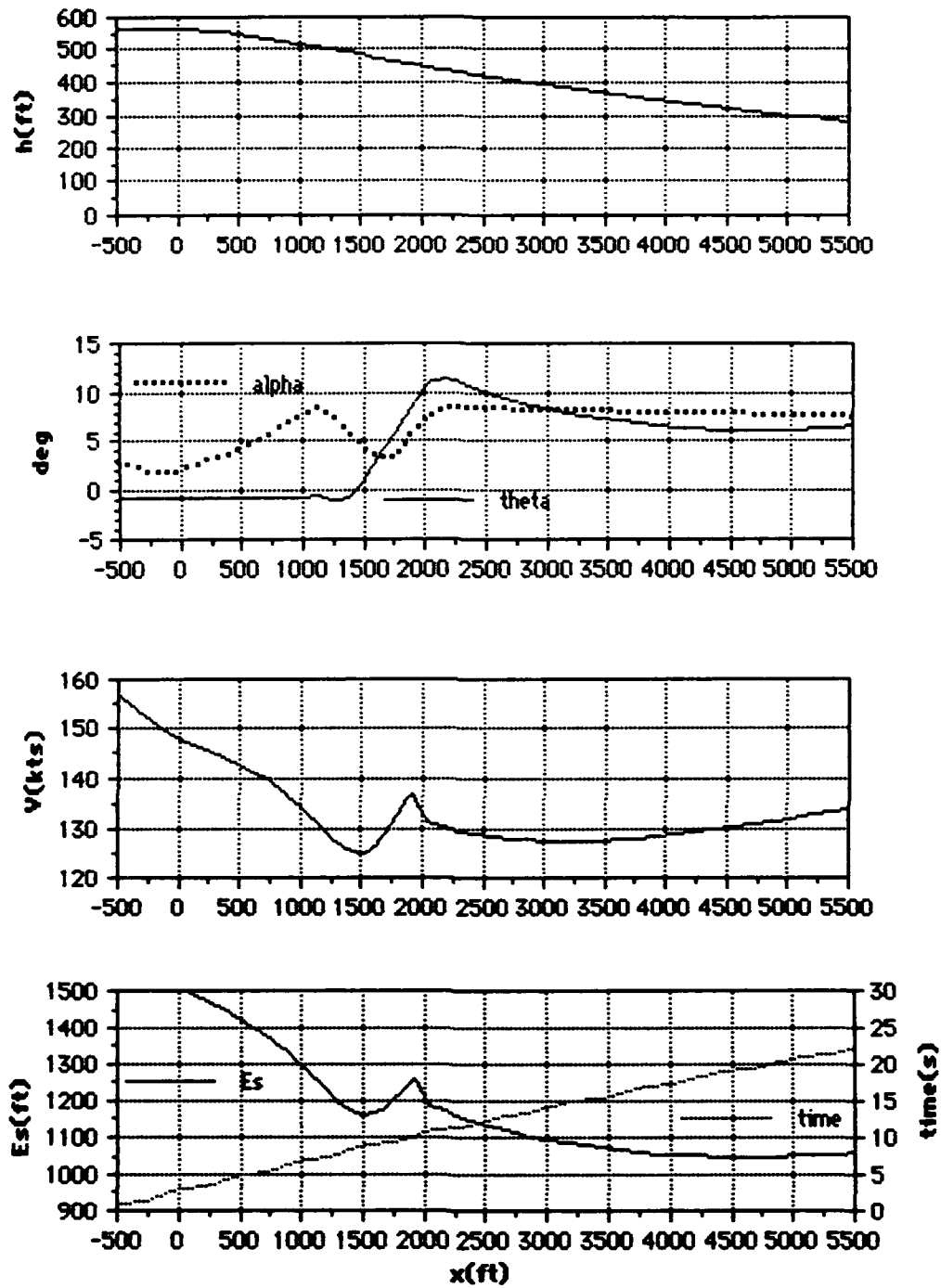


Figure F17. P-3 at 114,000lbs gross weight performing a constant 15 unit AOA escape.

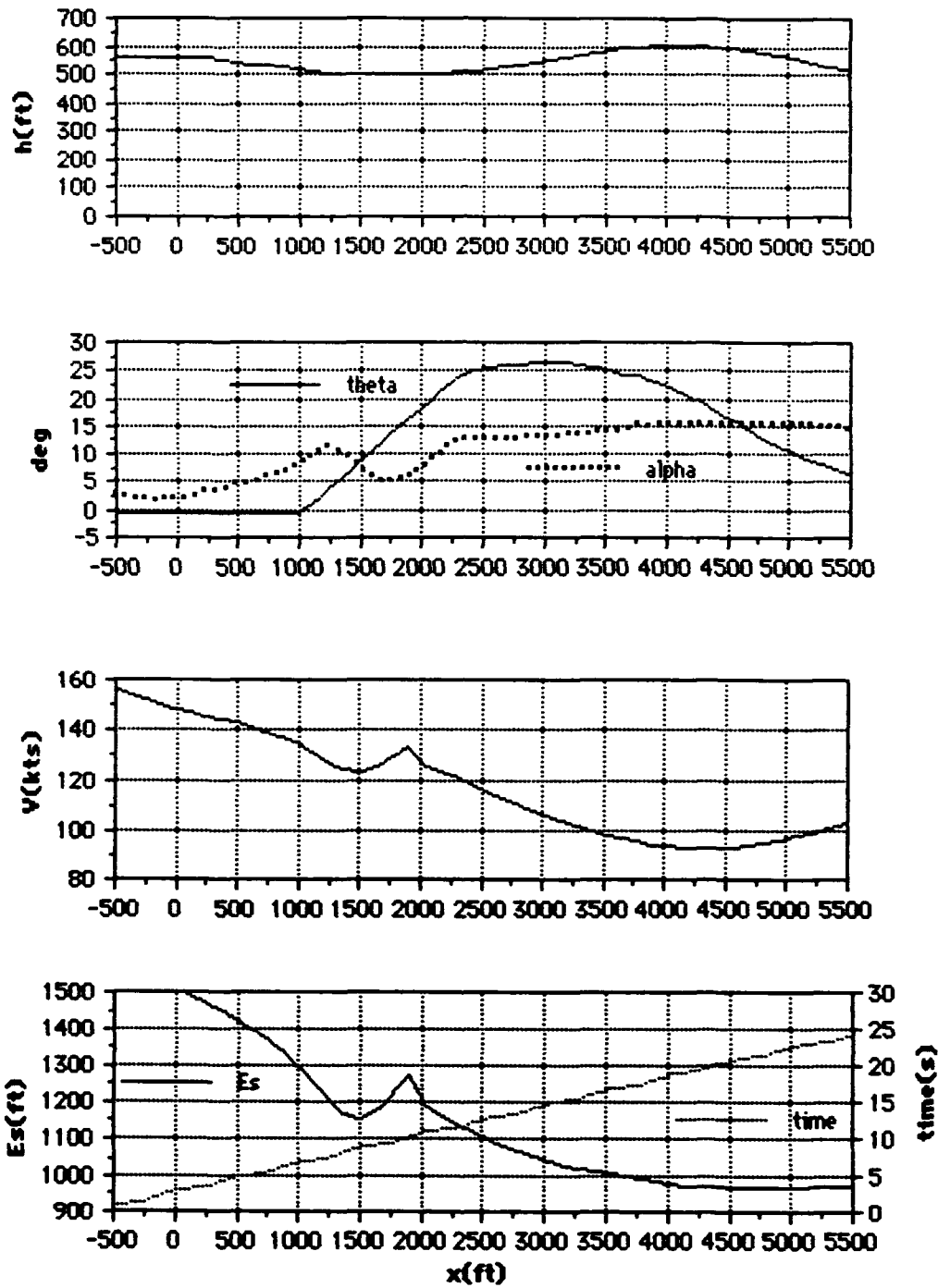


Figure F18. P-3 at 114,000lbs gross weight performing a constant 20 unit AOA escape.

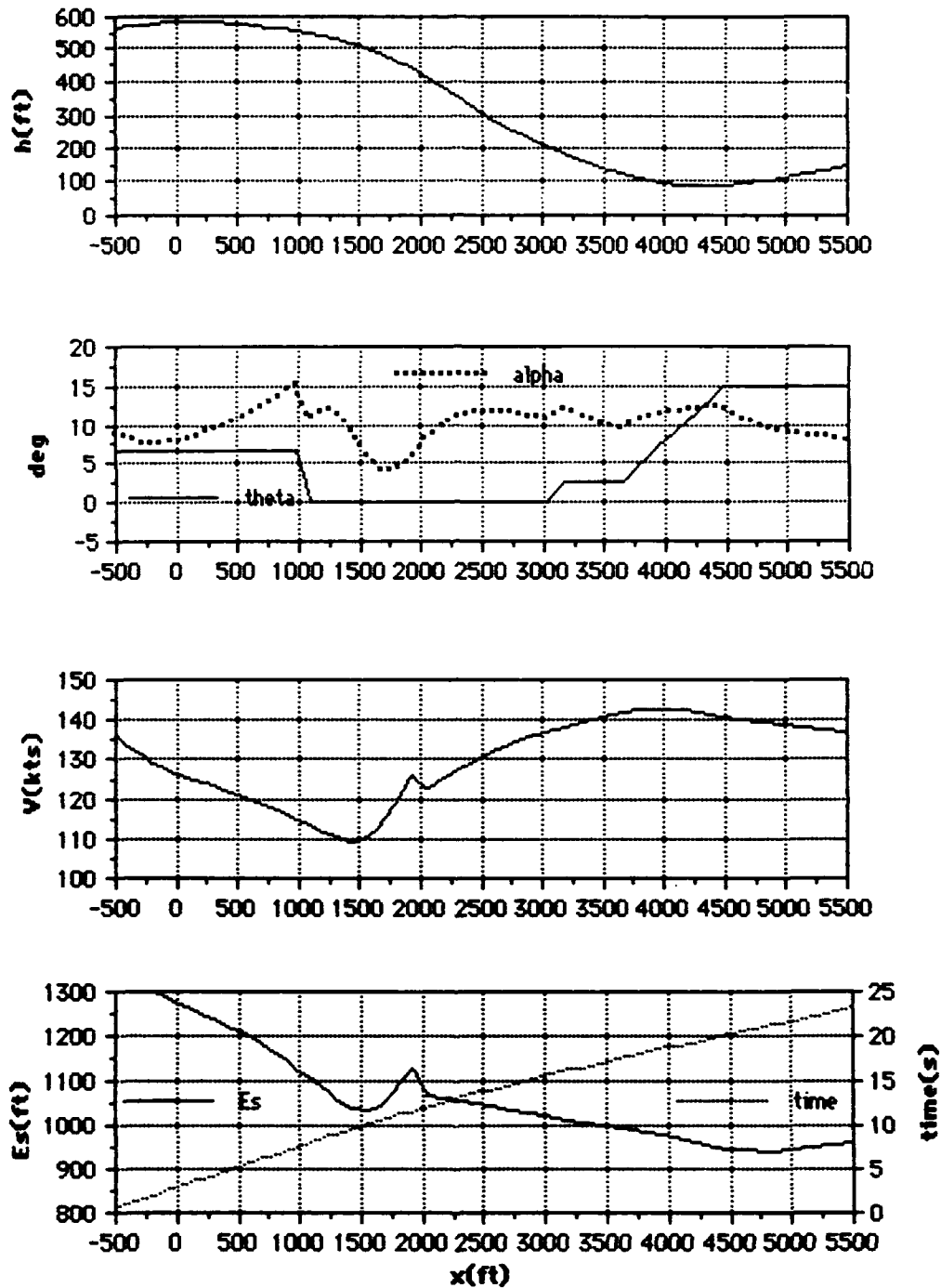


Figure F19. Three-engine heavy airline transport performing a constant airspeed escape.

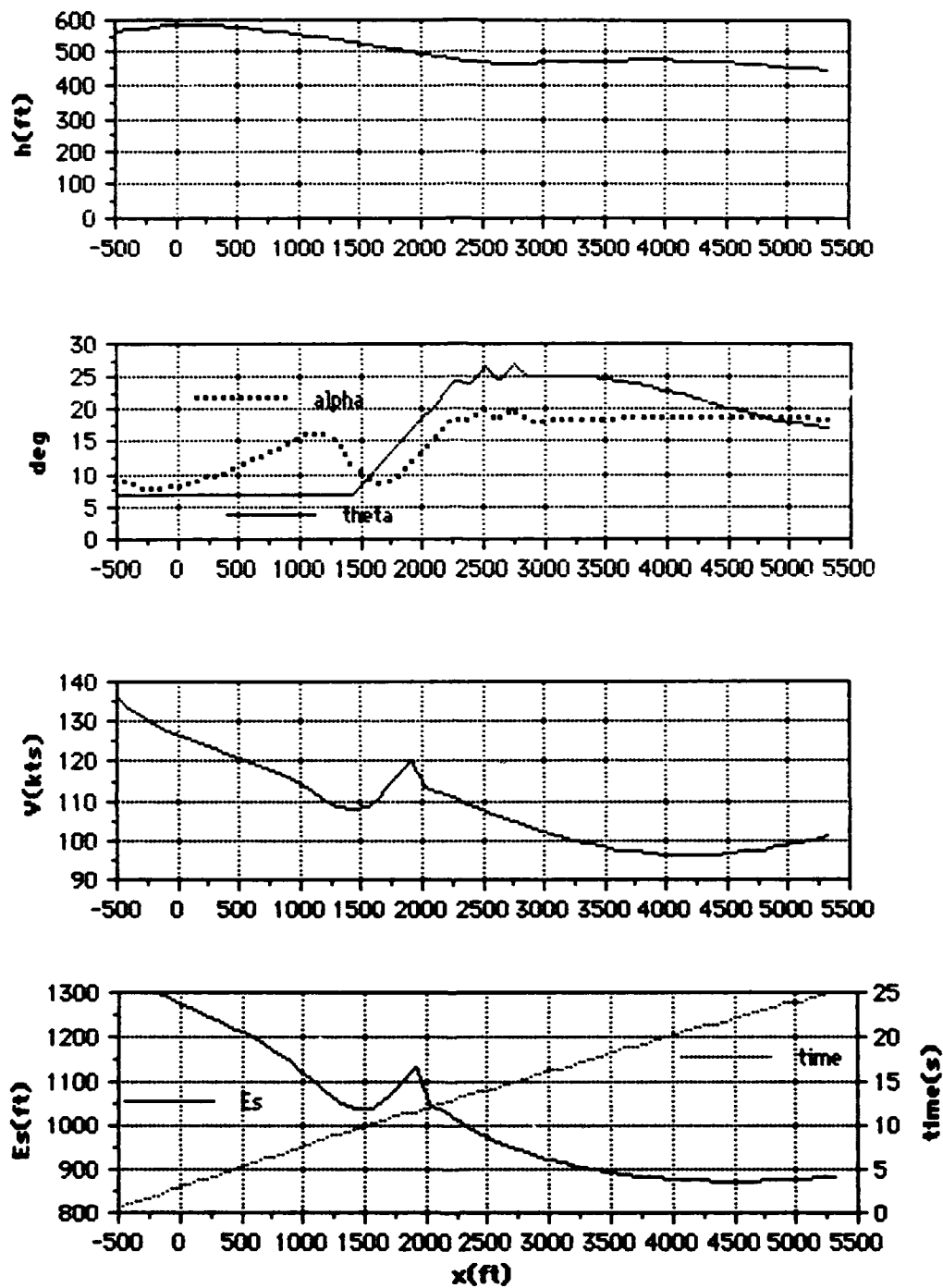


Figure F20. Three-engine heavy airline transport performing a constant altitude escape.

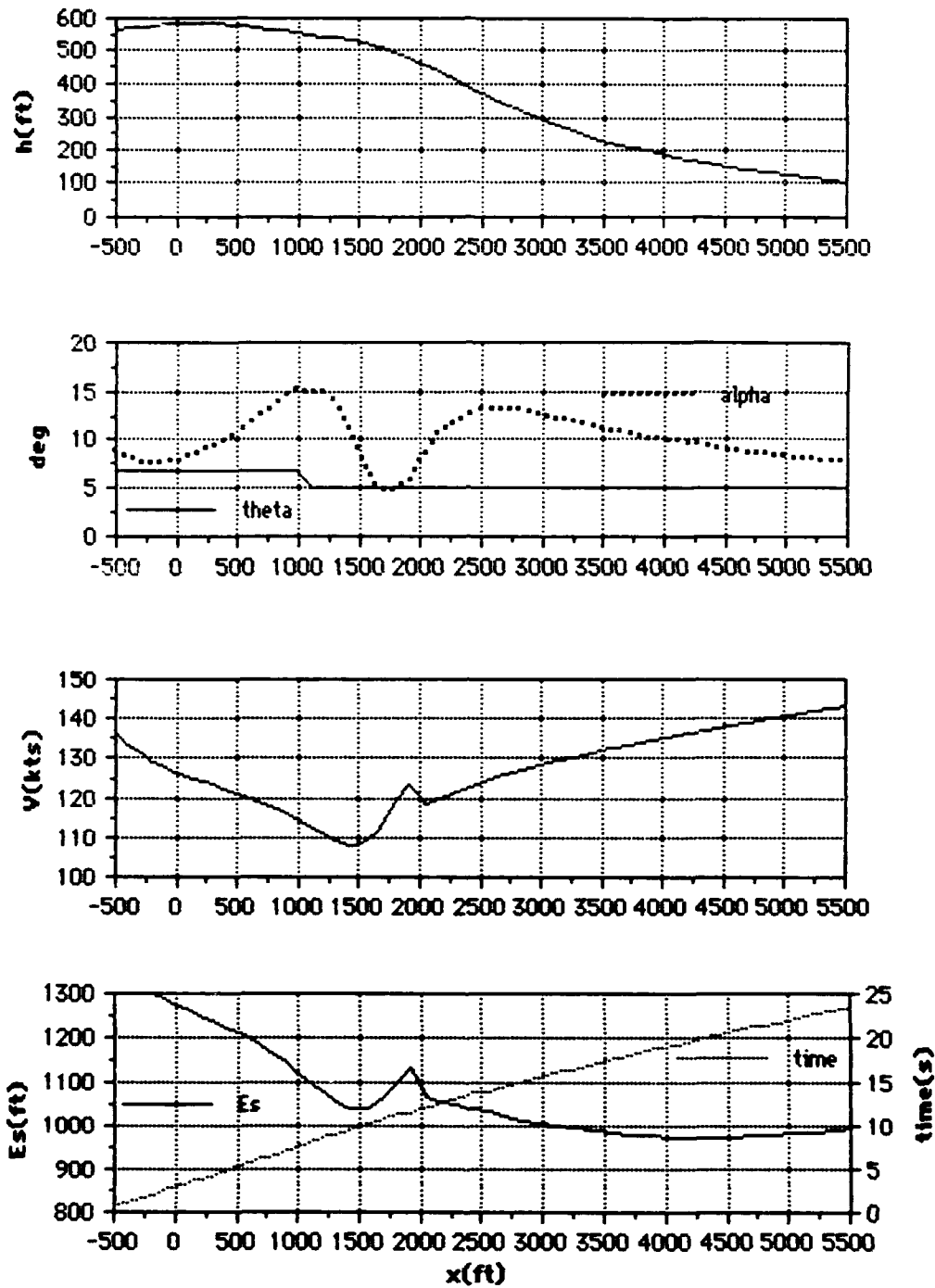


Figure F21. Three-engine heavy airline transport performing a constant 5° theta escape.

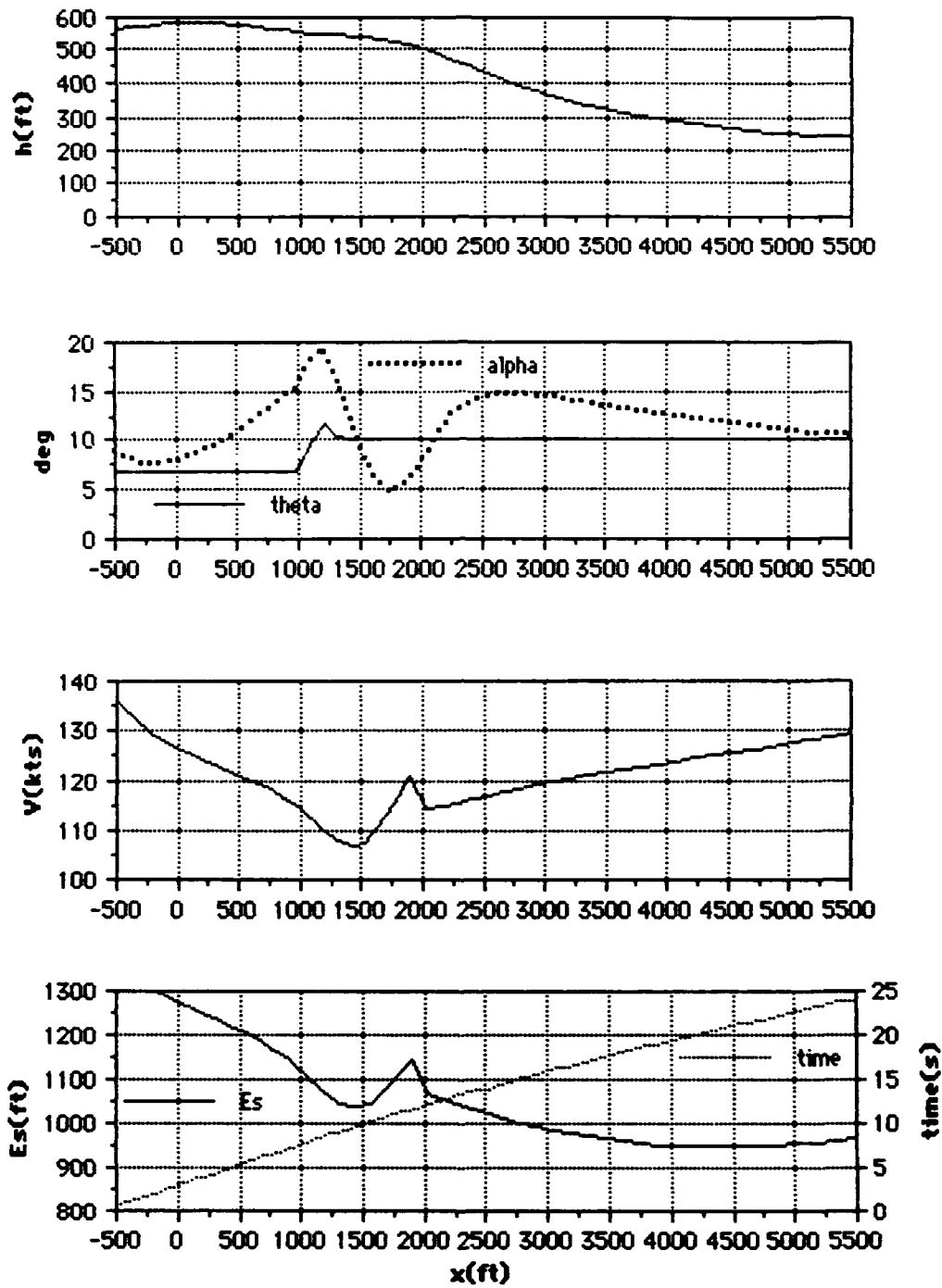


Figure F22. Three-engine heavy airline transport performing a constant 10° theta escape.

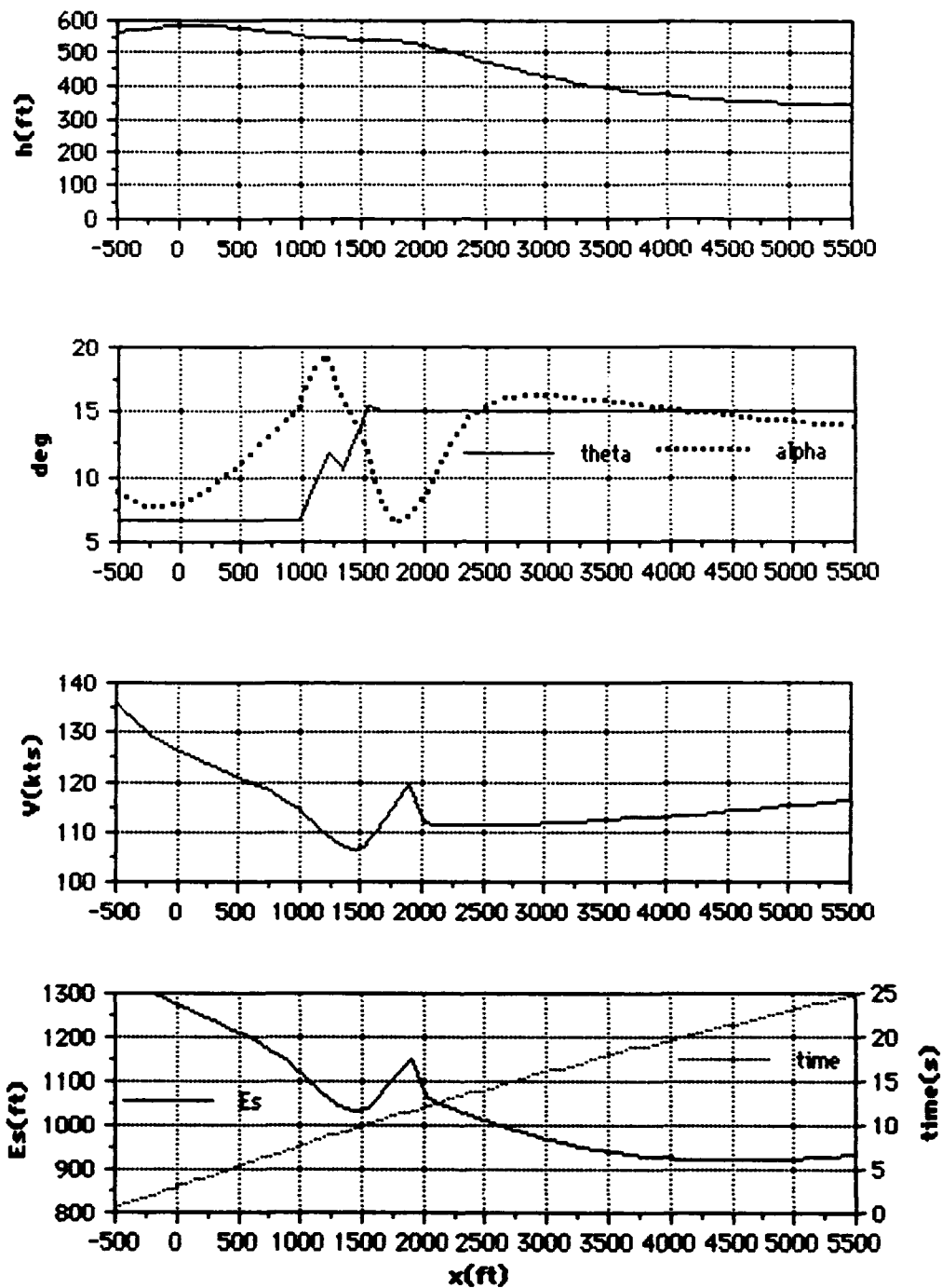


Figure F23. Three-engine heavy airline transport performing a constant 15° theta escape.

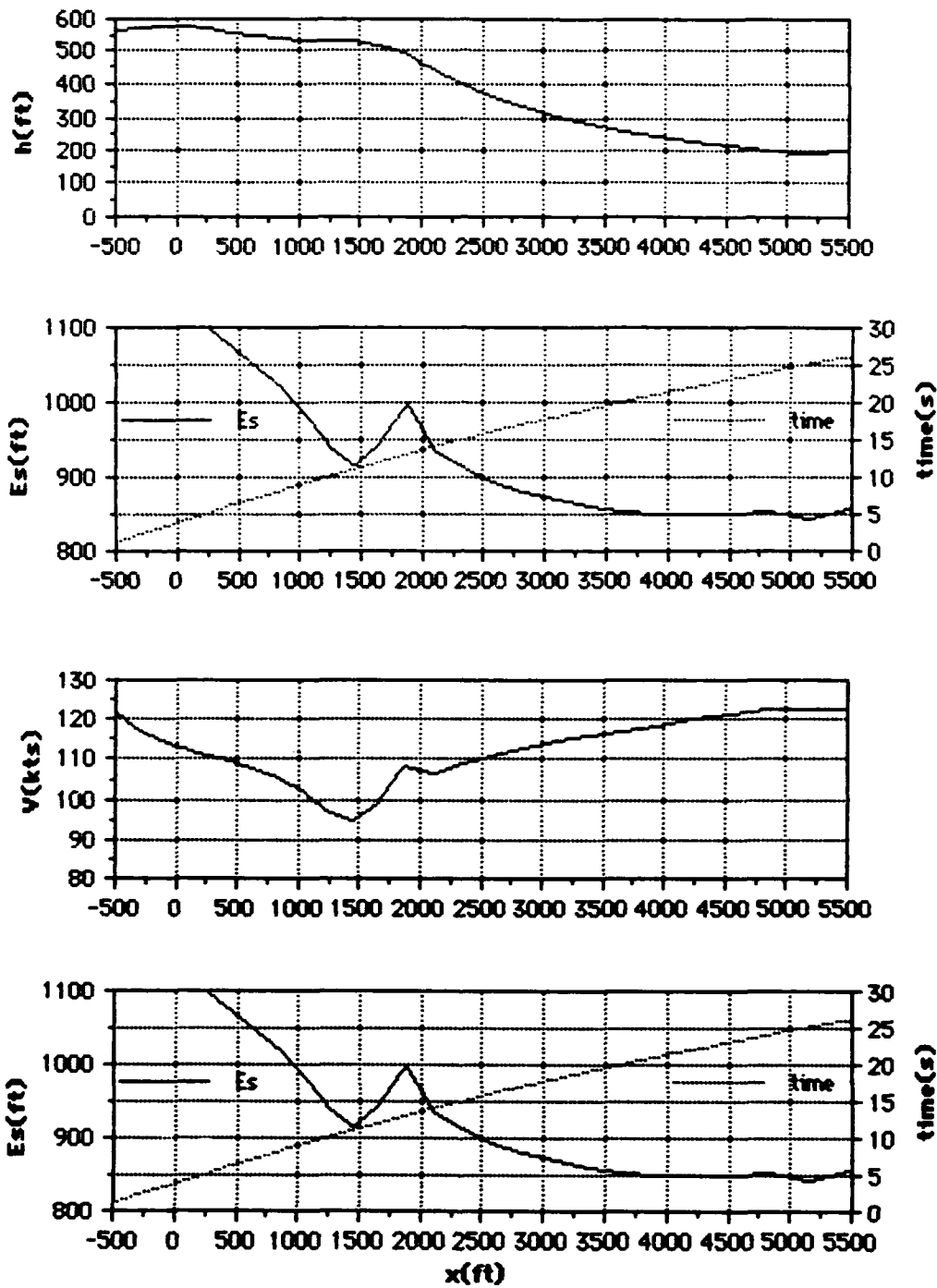


Figure F24. T-44 performing a constant airspeed escape.

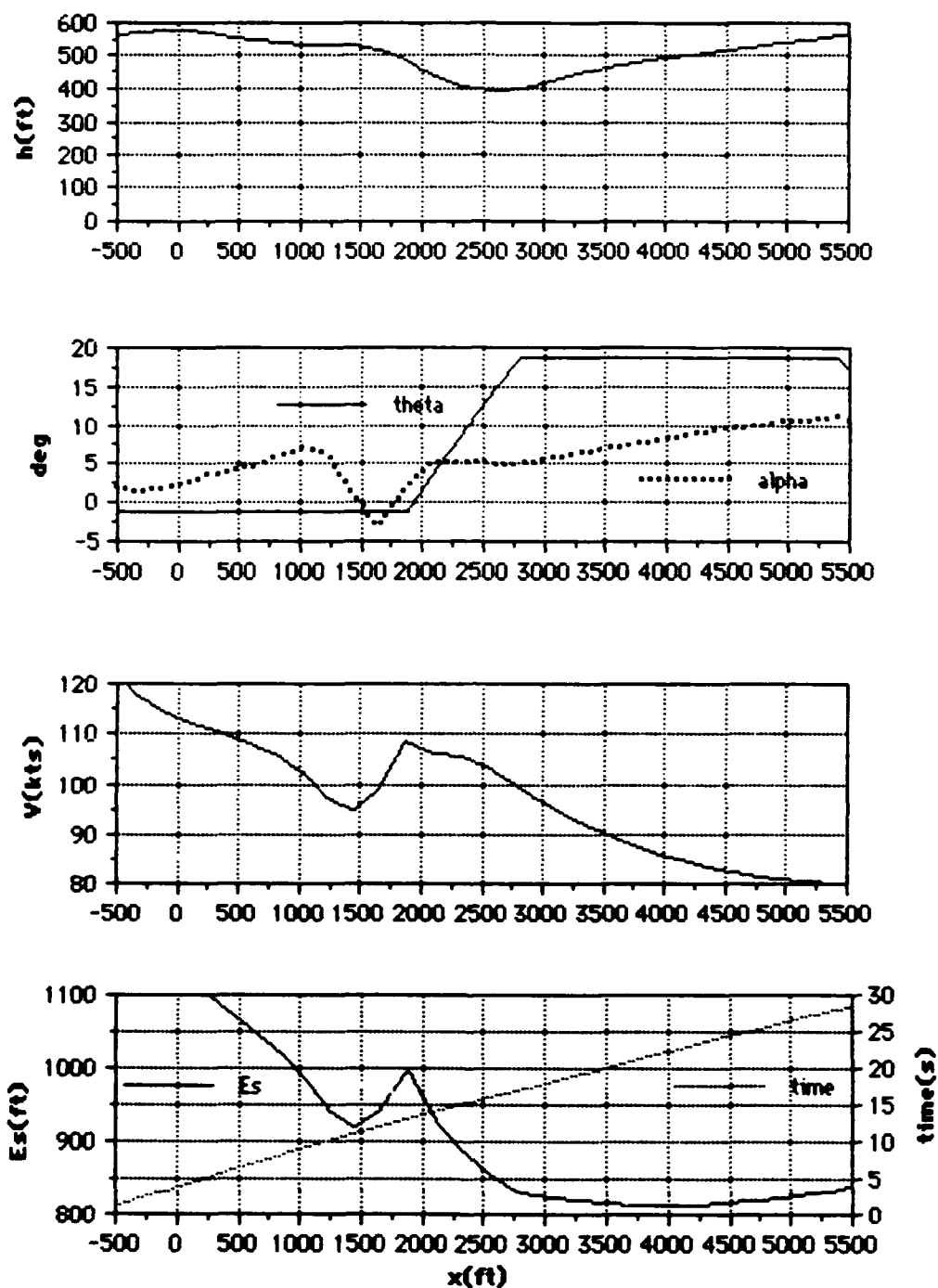


Figure F25. T-44 performing a constant altitude escape.

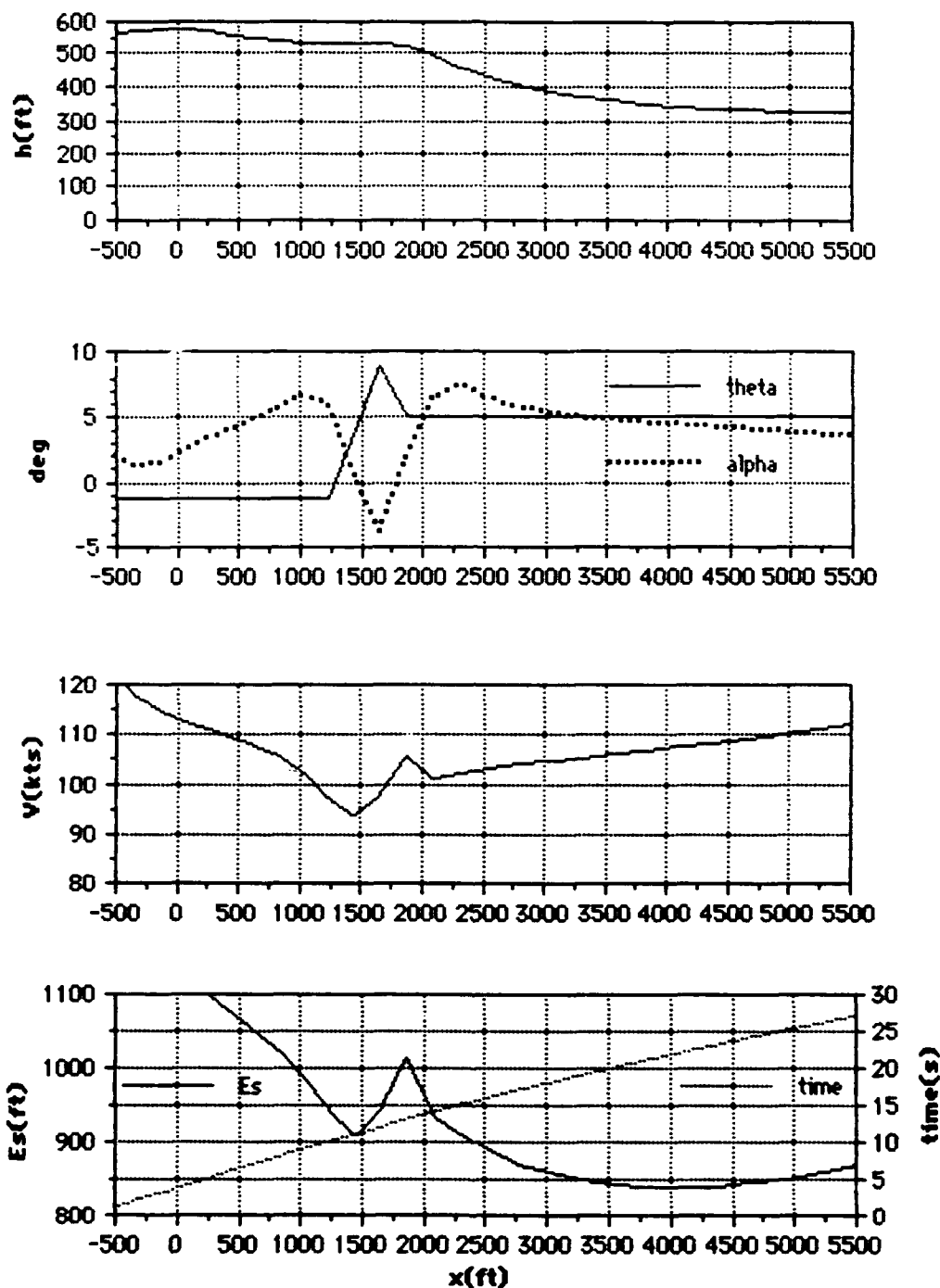


Figure F26. T-44 performing a constant 5° theta escape.

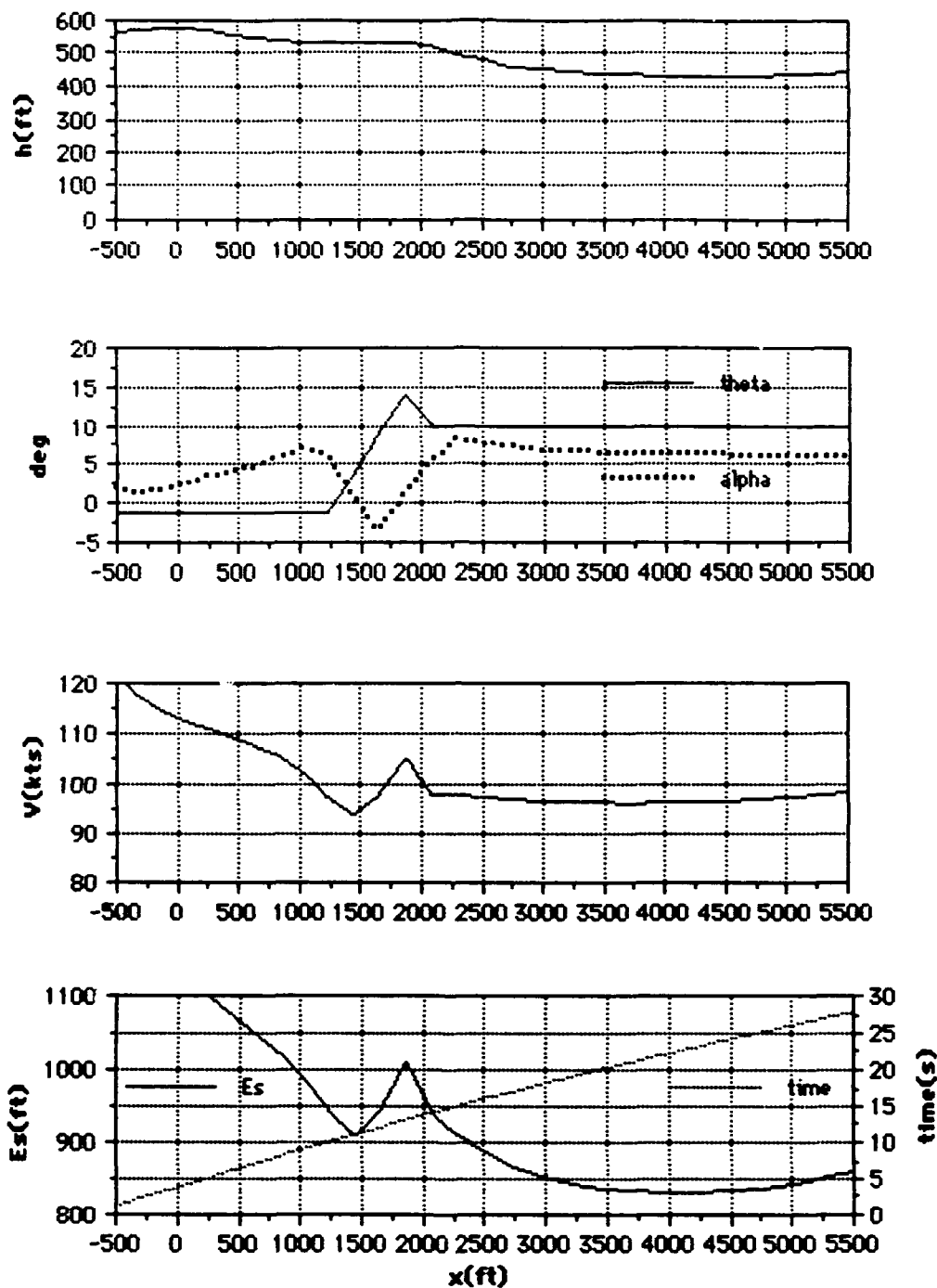


Figure F27. T-44 performing a constant 10° theta escape.

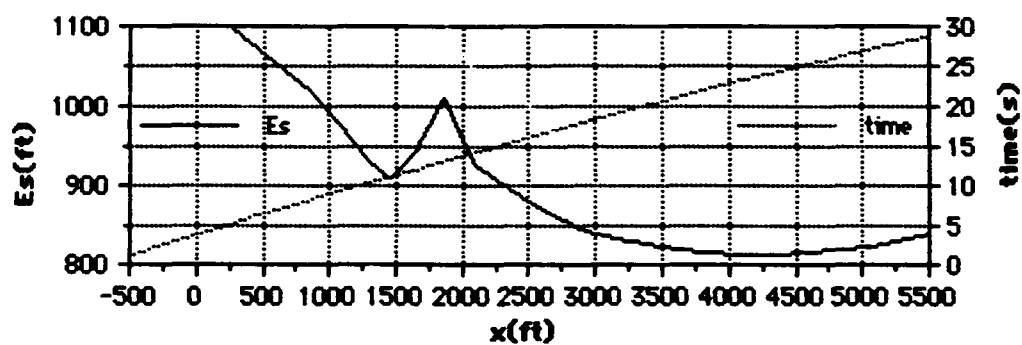
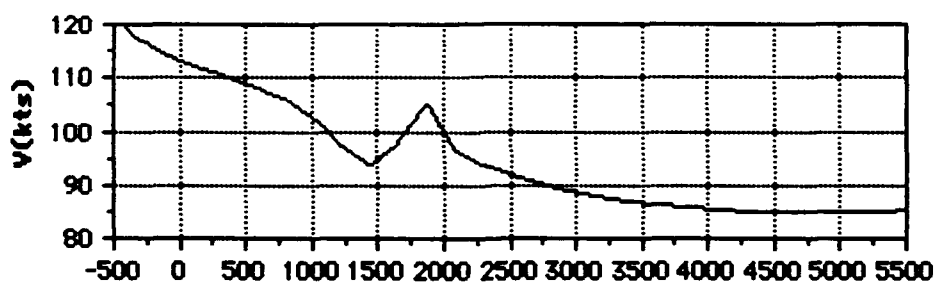
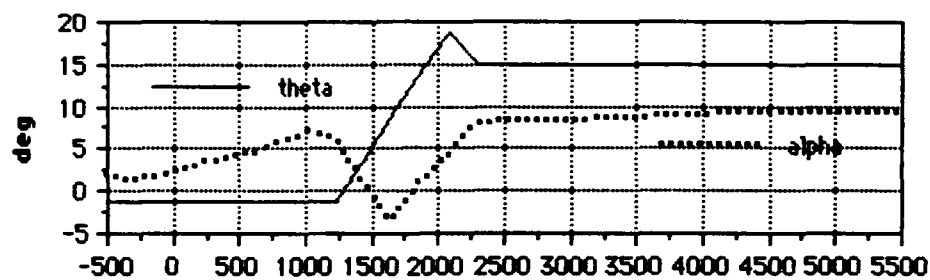
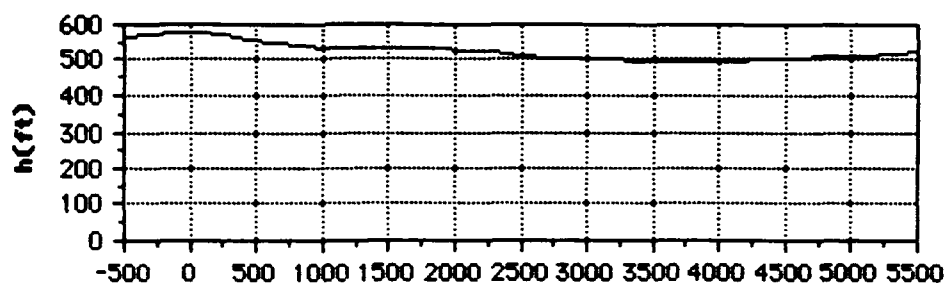


Figure F28. T-44 performing a constant 15° theta escape.

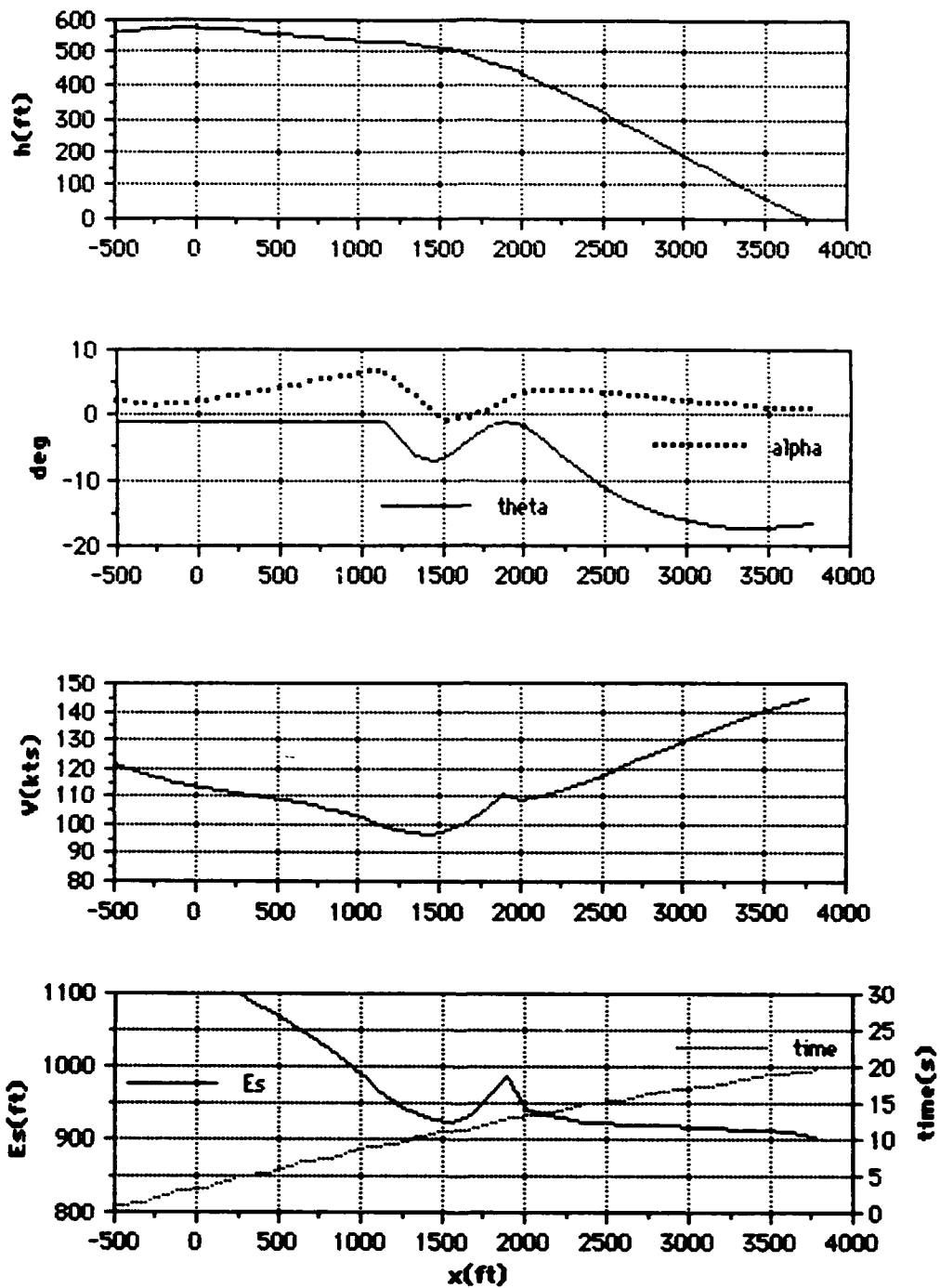


Figure F29. T-44 performing a constant 10 unit AOA escape.

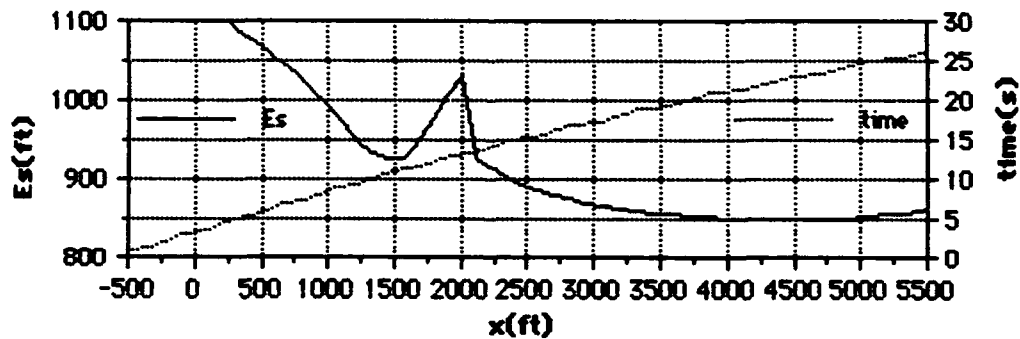
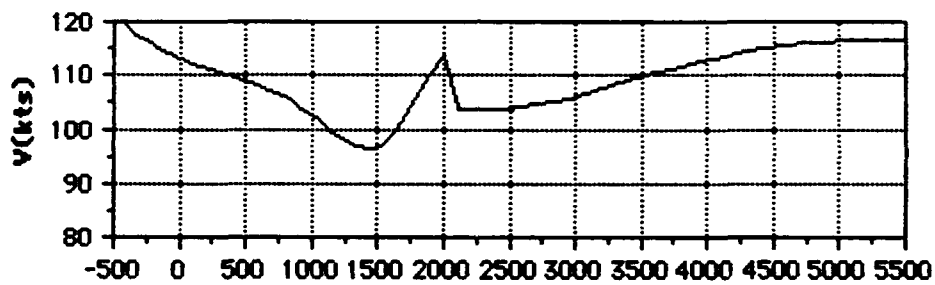
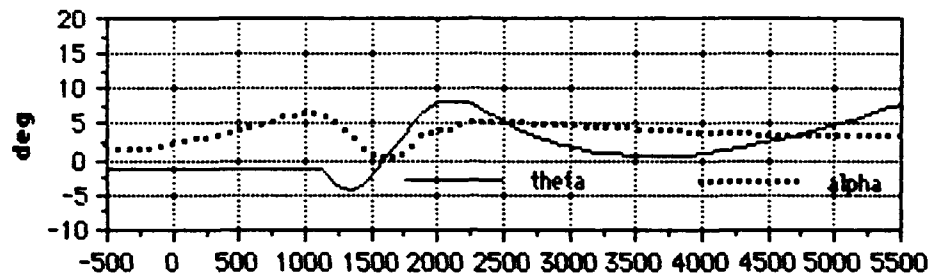
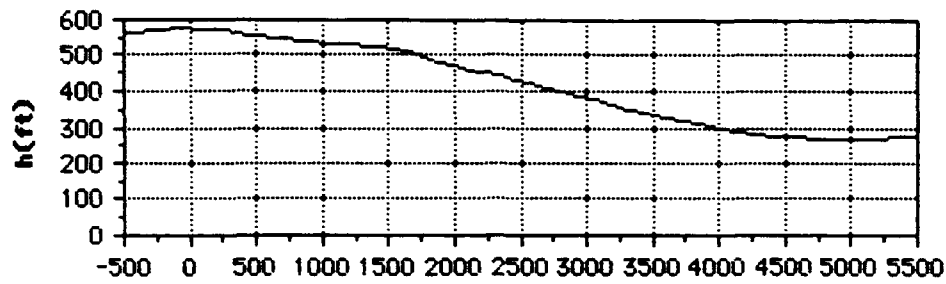


Figure F30. T-44 performing a constant 16 unit AOA escape.

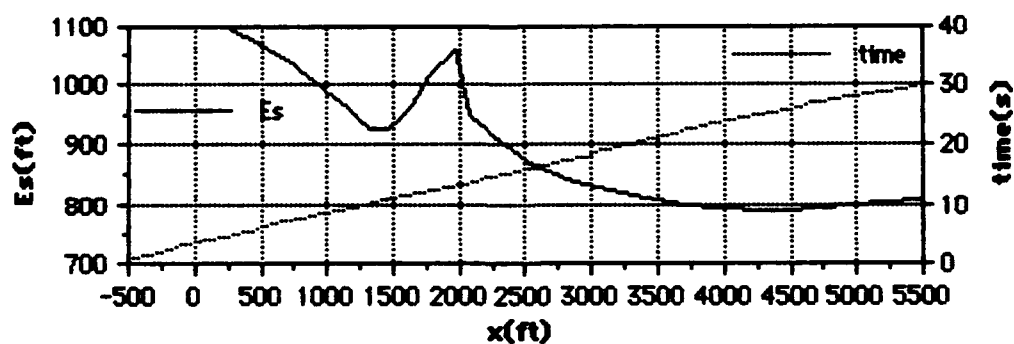
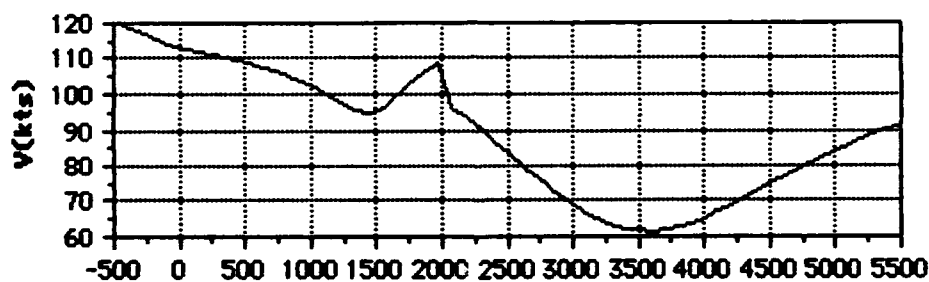
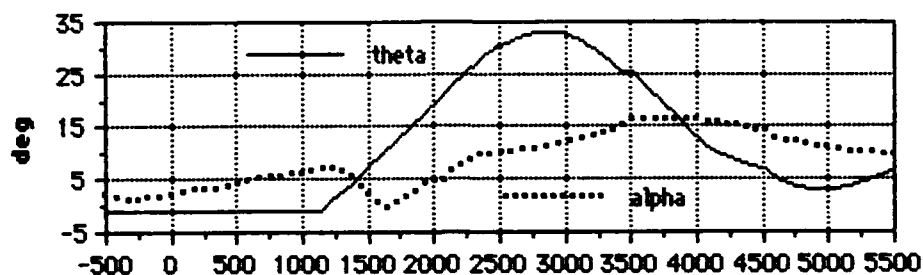
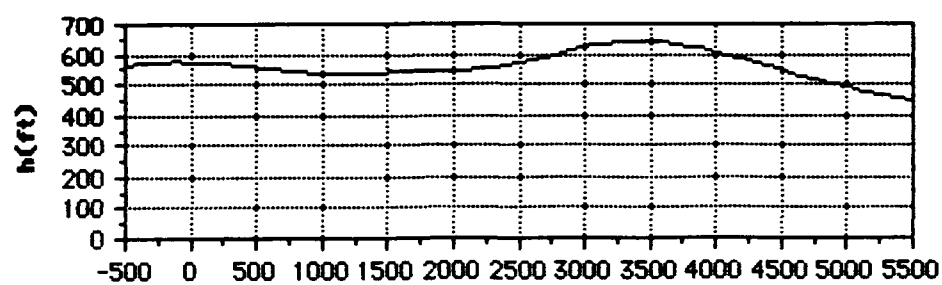


Figure F31. T-44 performing a constant 25 unit AOA escape.

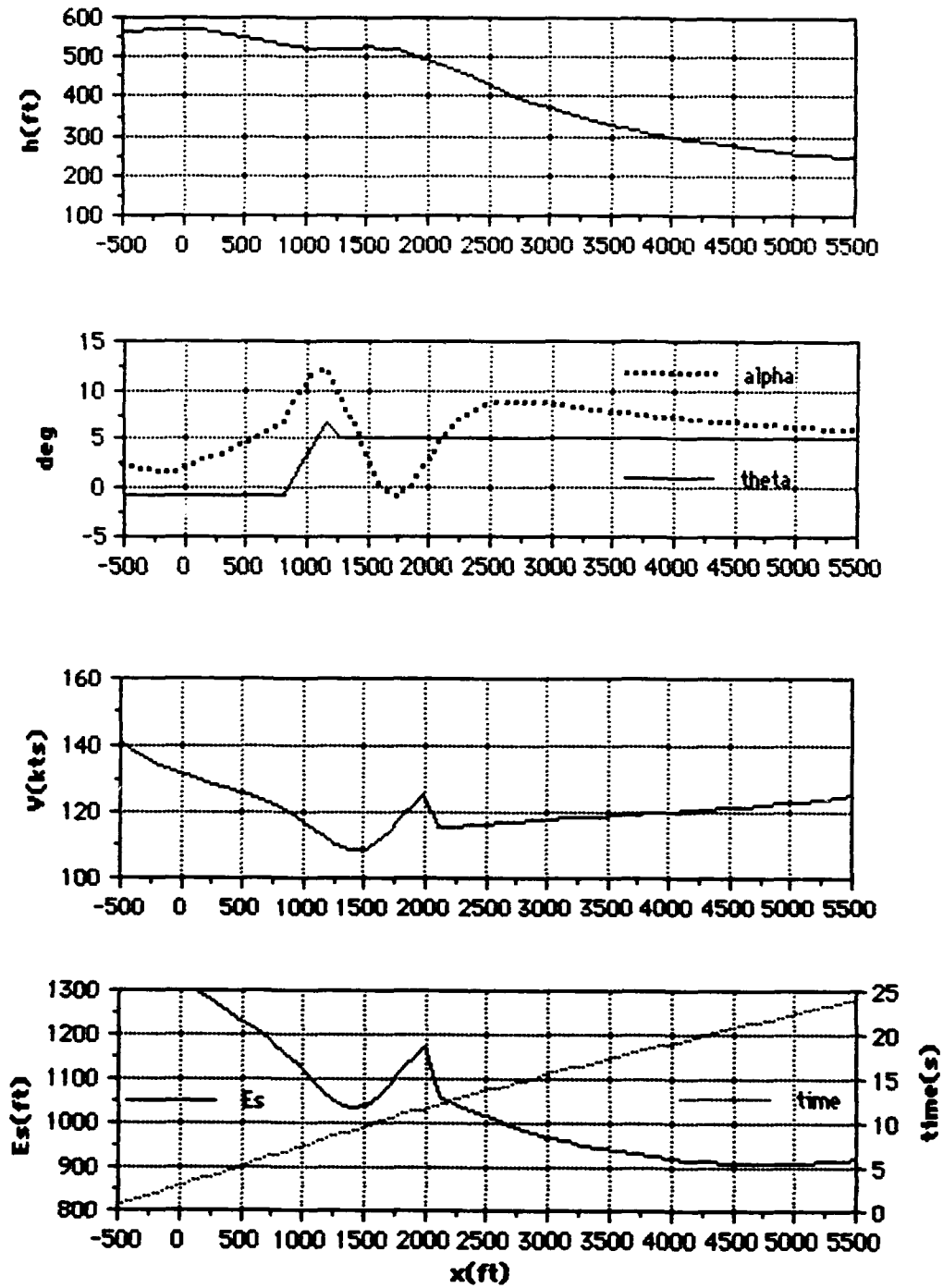


Figure F32. P-3 at 89,500lbs gross weight with three engines operating performing a constant 5° theta escape.

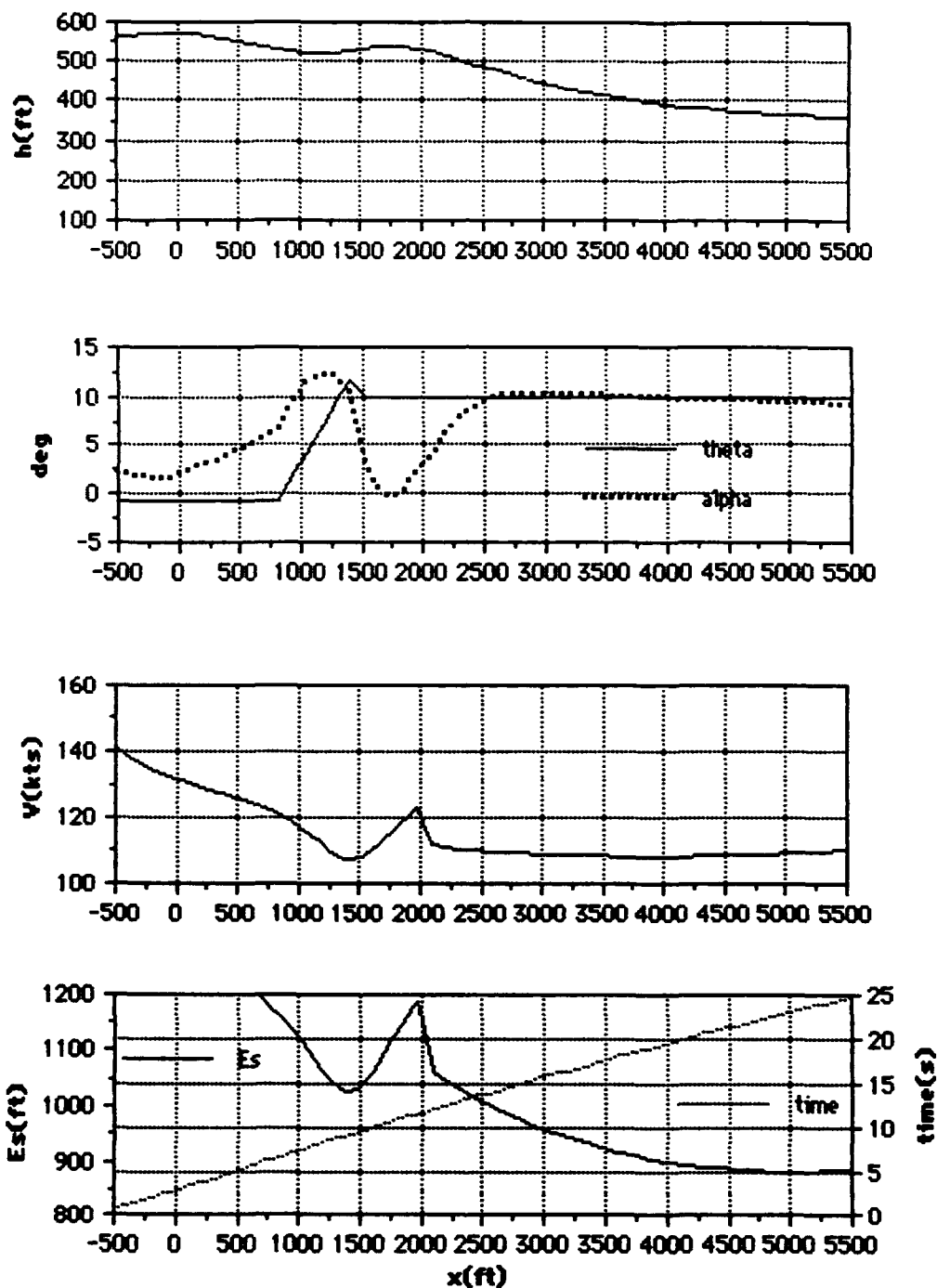


Figure F33. P-3 at 89,500lbs gross weight with three engines operating performing a constant 10° theta escape.

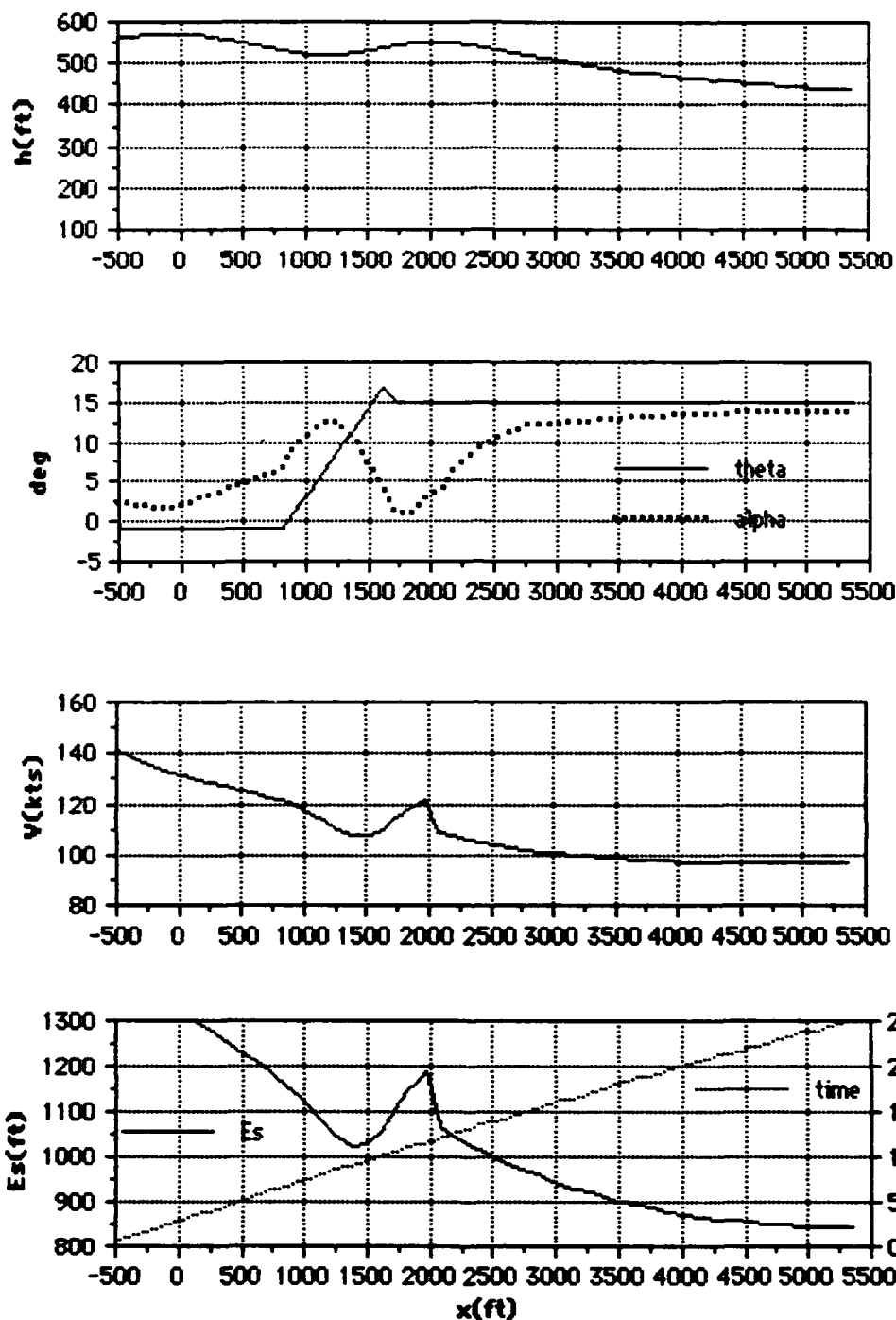


Figure F34. P-3 at 89,500lbs gross weight with three engines operating performing a constant 15° theta escape.

APPENDIX G

TAKEOFF ENCOUNTER GRAPHIC DATA

This appendix contains the calculated performance of different aircraft and weight combinations upon encountering a microburst windshear at or immediately after lift off. Each figure is for a particular aircraft performing a specified escape maneuver. Each figure contains four graphs depicting altitude, theta, alpha, airspeed, specific energy, and time. The abscissa in all graphs is x (distance from microburst center).

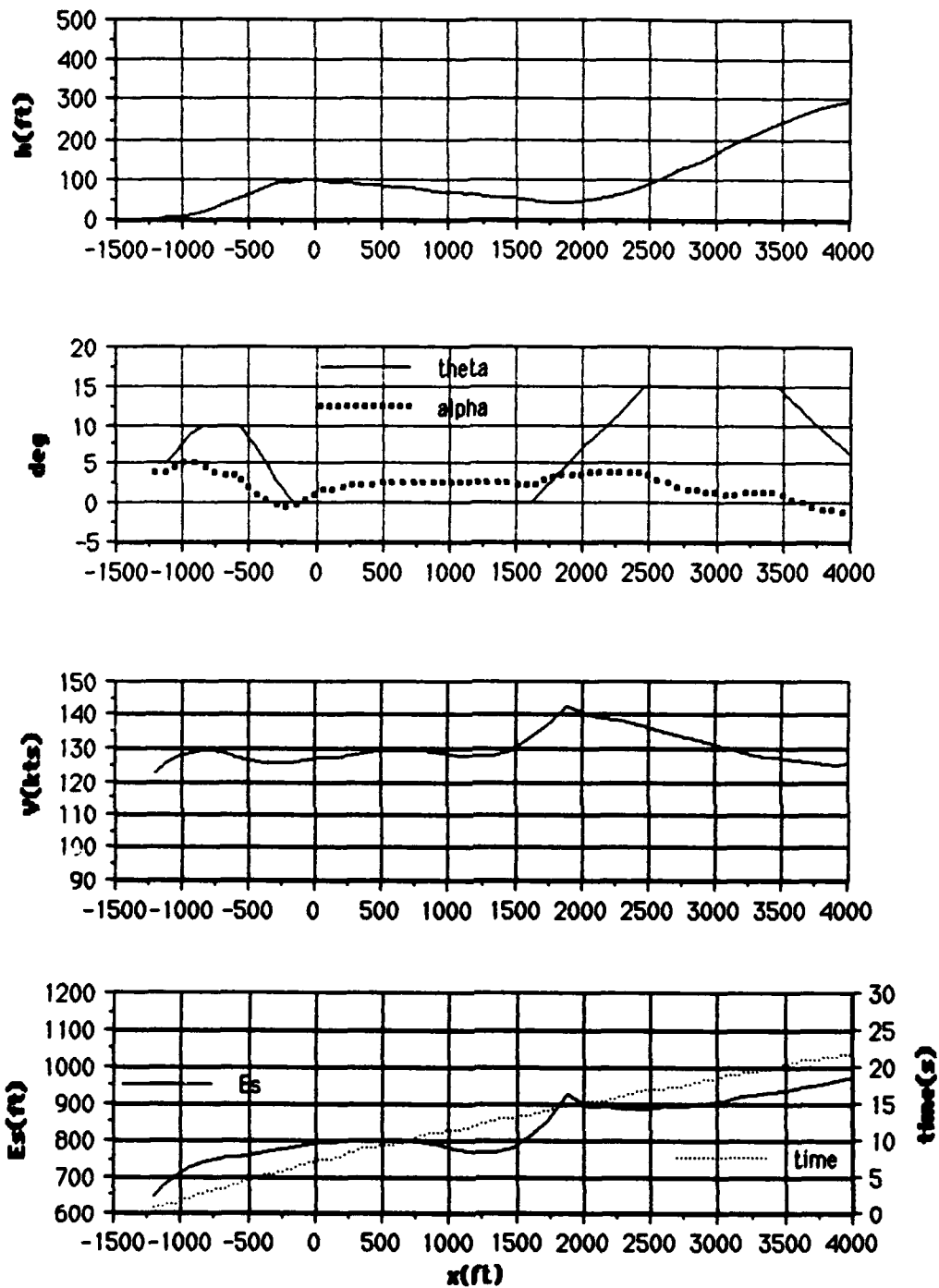


Figure G1. P-3 at 90,000lbs gross weight performing a constant airspeed maneuver during takeoff.

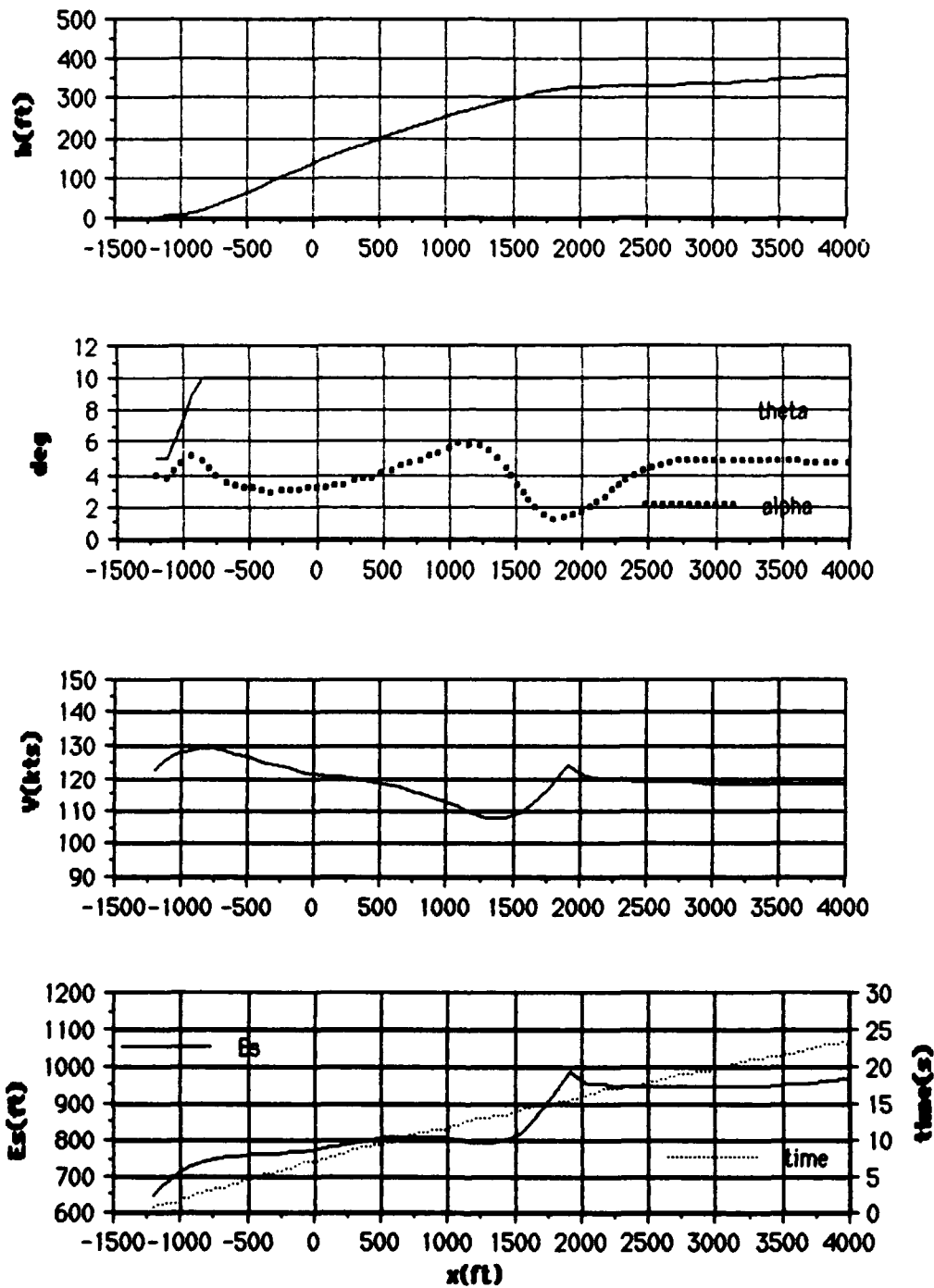


Figure G2. P-3 at 90,000lbs gross weight performing a constant 10° theta maneuver during takeoff.

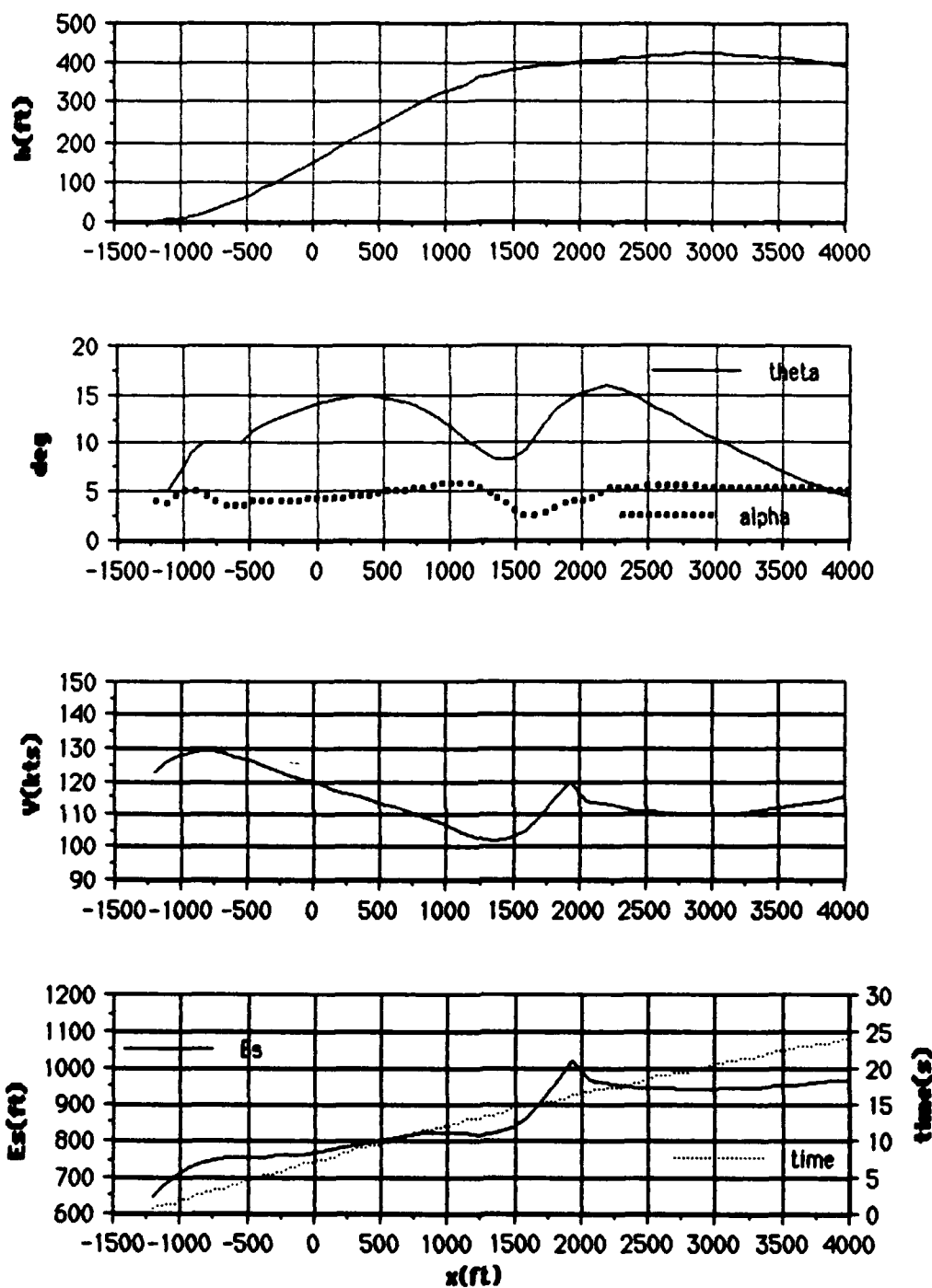


Figure G3. P-3 at 90,000lbs gross weight performing a constant 12 unit AOA maneuver during takeoff.

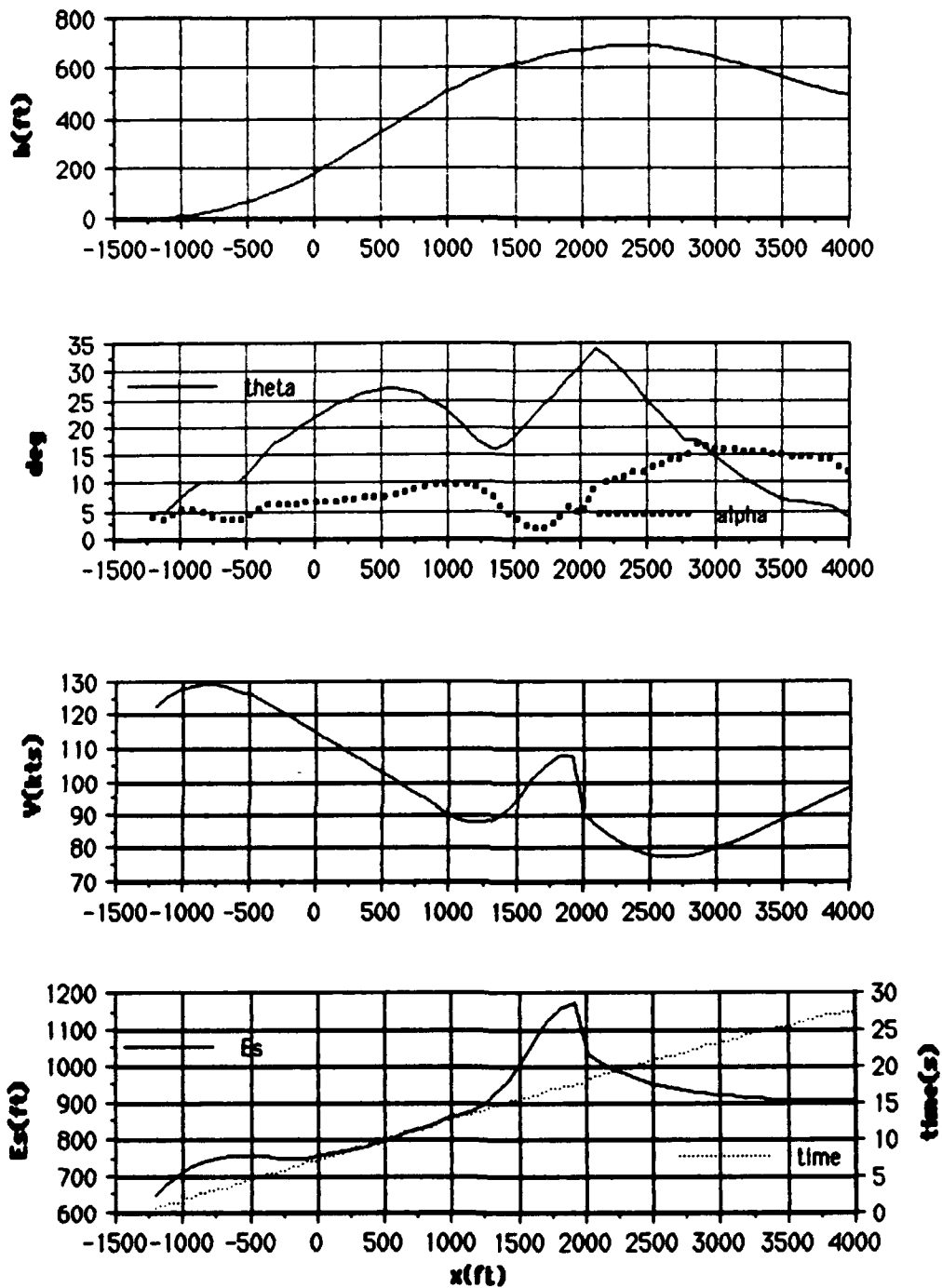


Figure G4. P-3 at 90,000lbs gross weight performing a constant 15 unit AOA maneuver during takeoff.

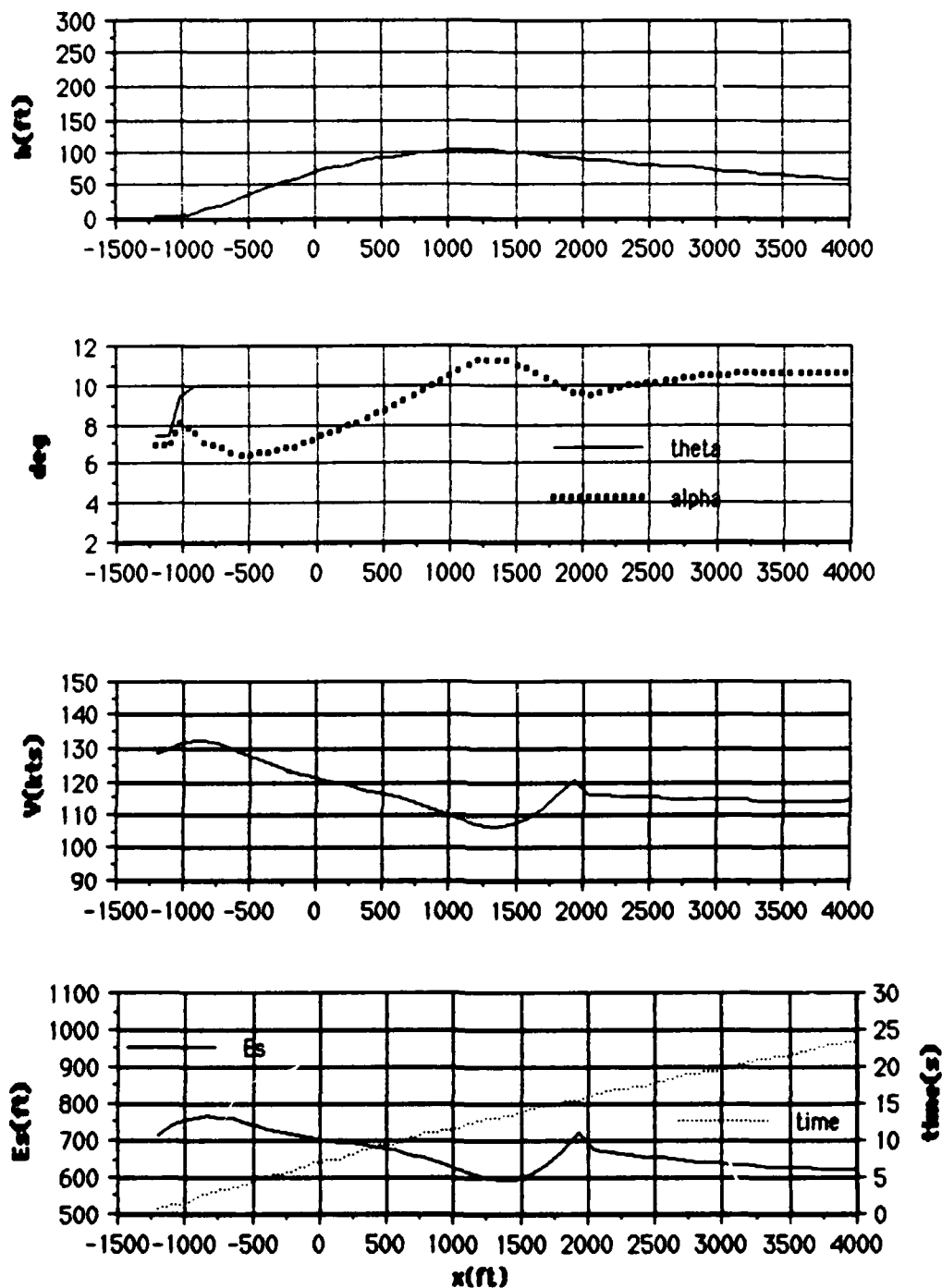


Figure G5. P-3 at 120,000lbs gross weight performing a constant 10° theta maneuver during takeoff.

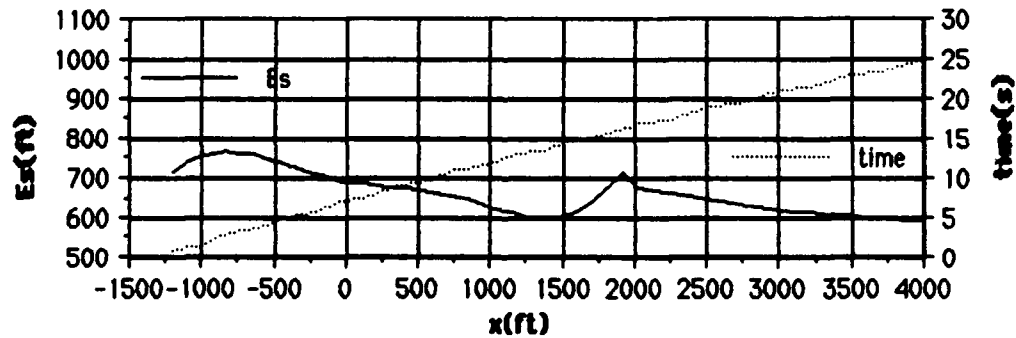
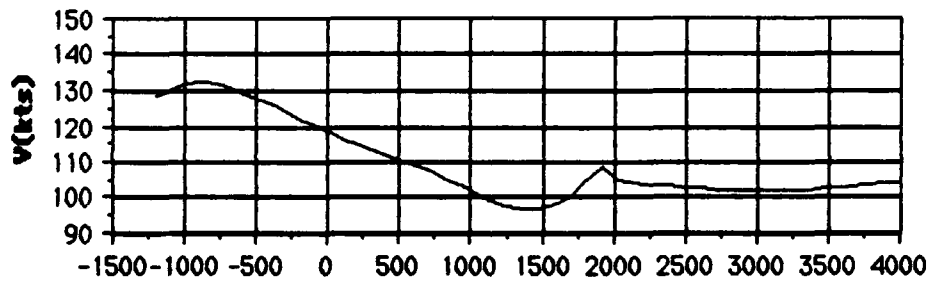
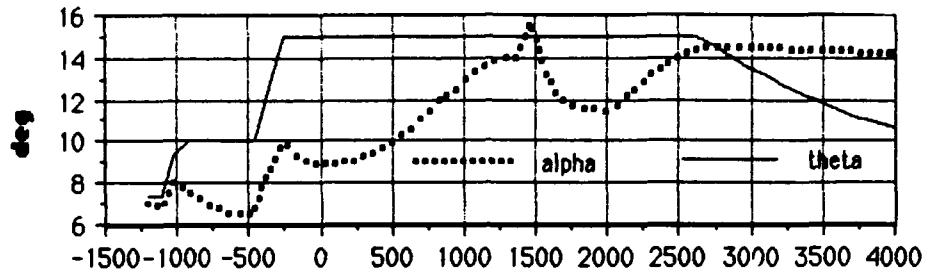
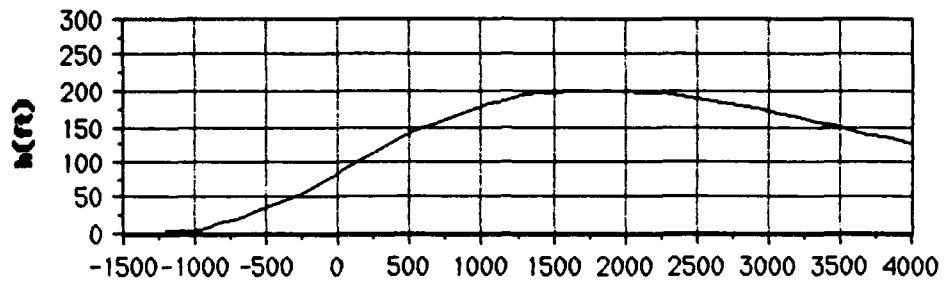


Figure G6. P-3 at 120,000lbs gross weight performing a constant 15° theta maneuver during takeoff.

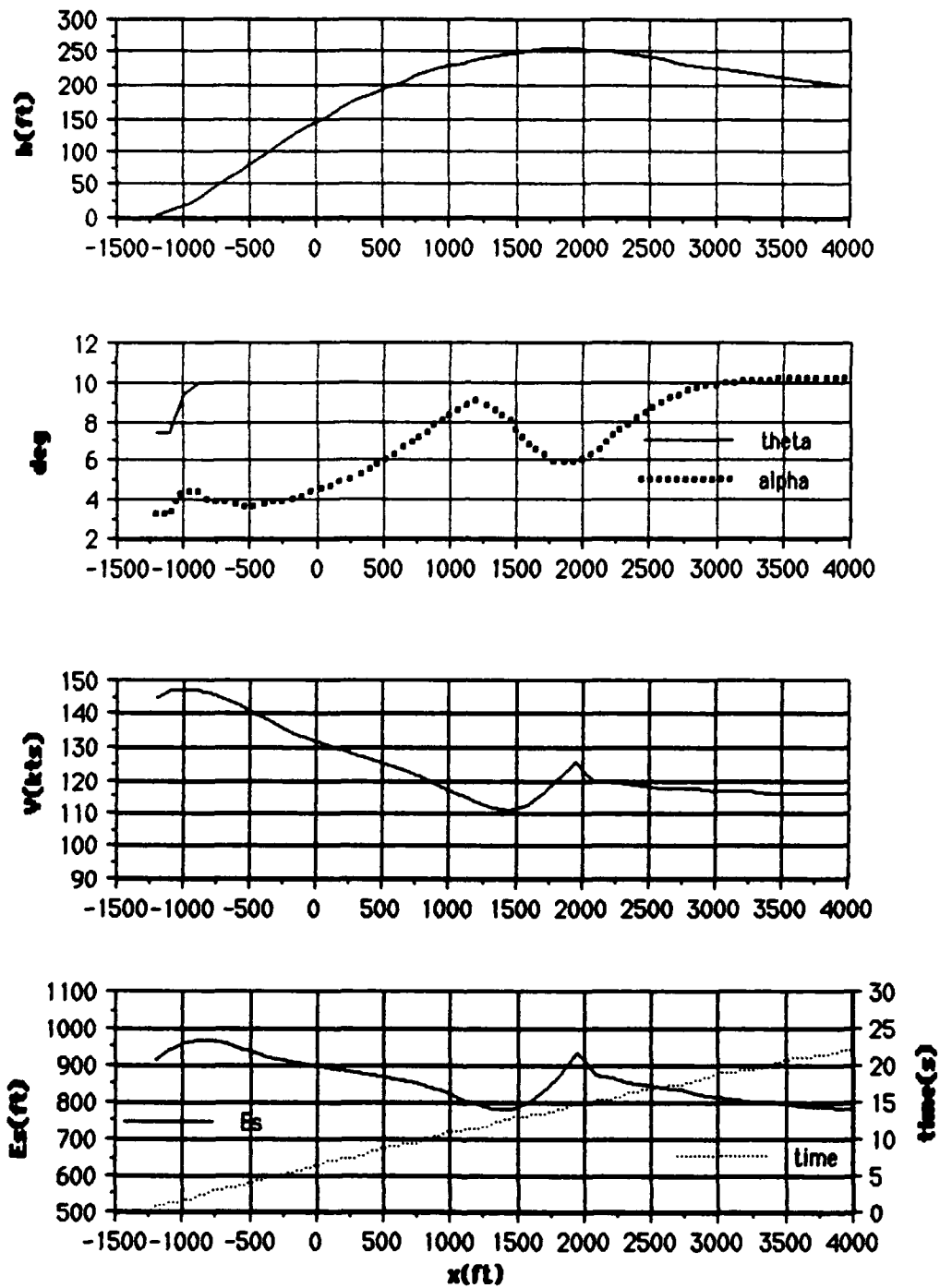


Figure G7. P-3 at 120,000lbs gross weight with an increased rotate speed followed by a constant 10° theta climb.

APPENDIX H

P-3 FLIGHT SIMULATOR DATA

FUEL TANK	FUEL LOAD	ENGINE	1	2	3	4	BRAKES
1	3937	SHP	483	484	499	597	PILOT
2	3937	TIT	549	549	551	564	COPILOT
3	3937	FUEL FLOW	849	849	855	893	FLIGHT
4	3935						IAS 115
5	996	RUNWAY- 100 MOFFETT NAS RWY 32R					ALT 490
							HDG 265.9

FLIGHT CONDITIONS PAGE

FLIGHT TIMER	00:00:00	MET TIMER	00:03:58
GROSS WEIGHT	89960	CONFIGURATION/CONDITIONS	
C.G.	20.00	PRESSURE ALTITUDE	524.0
FLAP POSITION	19.1	CALIBRATED AIRSPD	114.7
GEAR POSITION	1.0	EQUIVALENT AIRSPD	114.72
		TRUE AIRSPD (F/S)	195.41
		MACH NUMBER	0.18
		FLIGHT/AERO	
PITCH ANGLE	7.3	BANK ANGLE	-1.4
ANGLE OF ATTACK	6.4	SIDESLIP	-1.4
HEADING ANGLE	283.2	RATE OF CLIMB (FPM)	181
PITCH VELOCITY (D/S)	-0.156	PITCH ACCELERATION	0.0004
ROLL VELOCITY (D/S)	-0.164	ROLL ACCELERATION	-0.0024
YAW VELOCITY (D/S)	-0.273	YAW ACCELERATION	-0.0023
NORTH-SOUTH VELOCITY	111.71	NORTH-SOUTH ACCEL	-0.373
EAST-WEST VELOCITY	-160.32	EAST-WEST ACCELERATION	-0.138
VERTICAL VELOCITY	-2.99	VERTICAL ACCELERATION	0.579
LONGITUDINAL ACCEL	0.1216	TOTAL PITCHING MOMENT	336
LATERAL ACCEL	0.0117	TOTAL ROLLING MOMENT	-1664
VERTICAL ACCEL (G'S)	-0.9739	TOTAL YAWING MOMENT	-3575
		CONTROL LOADING	
ELEVATOR POSITION	-5.43	ELEVATOR TRIM TAB	12.69
COLUMN FORCE	16.06	COLUMN POSITION	3.24
RUDDER POSITION	-4.34	RUDDER TRIM TAB	3.79
PEDAL FORCE	-11.06	PEDAL POSITION	-0.47
AILERON POSITION	-0.30	AILERON TRIM TAB	0.42
WHEEL FORCE	-2.20	WHEEL POSITION	-1.16
		ENGINES	
TOTAL THRUST	5024	THRUST COEFFICIENT	0.09
THROTTLE ANGLE	46.4	LATERAL T.C.	0.08
ENGINE S.H.P.	460	ENGINE T.I.T.	549
		WEIGHT AND BALANCE	
IXX INERTIA (/ 1024)	725	IYY INERTIA (/ 1024)	862
IZZ INERTIA (/ 1024)	1549	CROSS PRODUCT/INERTIA	43240

NOTE: VALUES INVALID DURING ATG - TO USE COL MARKER SW FOR SNAPS SET COLSNP TRUE

FUEL TANK	FUEL LOAD	ENGINE	1	2	3	4	BRAKES
1	3929	SHP	485	486	496	600	PILOT
2	3929	TIT	550	550	551	564	COPILOT
3	3929	FUEL FLOW	848	848	853	893	FLIGHT
4	3927						IAS 108
5	996	RUNWAY- 100 MOFFETT NAS RWY 32R					ALT 490
							HDG 256.8

FLIGHT CONDITIONS PAGE

FLIGHT TIMER	00:00:00	MET TIMER	00:04:27
GROSS WEIGHT	89928	PRESSURE ALTITUDE	524.0
C.G.	20.00	CALIBRATED AIRSPD	108.6
FLAP POSITION	19.1	EQUIVALENT AIRSPD	108.59
GEAR POSITION	1.0	TRUE AIRSPD (F/S)	185.00
		MACH NUMBER	0.17

FLIGHT/AERO

PITCH ANGLE	11.9	BANK ANGLE	-0.3
ANGLE OF ATTACK	7.8	SIDESLIP	-1.0
HEADING ANGLE	273.8	RATE OF CLIMB (FPM)	804
PITCH VELOCITY (D/S)	0.195	PITCH ACCELERATION	-0.0002
ROLL VELOCITY (D/S)	0.086	ROLL ACCELERATION	0.0003
YAW VELOCITY (D/S)	-0.023	YAW ACCELERATION	-0.0007
NORTH-SOUTH VELOCITY	80.19	NORTH-SOUTH ACCEL	-0.056
EAST-WEST VELOCITY	-166.20	EAST-WEST ACCELERATION	0.108
VERTICAL VELOCITY	-13.38	VERTICAL ACCELERATION	0.455
LONGITUDINAL ACCEL	0.1999	TOTAL PITCHING MOMENT	-176
LATERAL ACCEL	0.0046	TOTAL ROLLING MOMENT	256
VERTICAL ACCEL (G'S)	-0.9636	TOTAL YAWING MOMENT	-1092

CONTROL LOADING

ELEVATOR POSITION	-6.40	ELEVATOR TRIM TAB	12.69
COLUMN FORCE	16.87	COLUMN POSITION	2.76
RUDDER POSITION	-4.98	RUDDER TRIM TAB	3.79
PEDAL FORCE	-14.28	PEDAL POSITION	-0.55
AILERON POSITION	0.44	AILERON TRIM TAB	0.42
WHEEL FORCE	0.03	WHEEL POSITION	1.46

ENGINES

TOTAL THRUST	5232	THRUST COEFFICIENT	0.10
THROTTLE ANGLE	46.4	LATERAL T.C.	0.10
ENGINE S.H.P.	461	ENGINE T.I.T.	550

WEIGHT AND BALANCE

IXX INERTIA (/ 1024)	725	IYY INERTIA (/ 1024)	862
IZZ INERTIA (/ 1024)	1549	CROSS PRODUCT/INERTIA	43230

NOTE: VALUES INVALID DURING ATG - TO USE COL MARKER SW FOR SNAPS SET COLSNP TRUE

FUEL TANK	FUEL LOAD	ENGINE	1	2	3	4	BRAKES
1	3923	SHF	486	487	505	604	PILOT
2	3923	TIT	549	549	551	564	COPILOT
3	3923	FUEL FLOW	850	850	856	894	FLIGHT
4	3921						IAS 117
5	996	RUNWAY- 100 MOFFETT NAS RWY 32R					ALT 490
							HDG 256.2

FLIGHT CONDITIONS PAGE

FLIGHT TIMER	00:00:00	MET TIMER	00:04:49
GROSS WEIGHT	89904	PRESSURE ALTITUDE	524.0
C.G.	20.00	CALIBRATED AIRSPD	117.4
FLAP POSITION	19.1	EQUIVALENT AIRSPD	117.37
GEAR POSITION	1.0	TRUE AIRSPD (F/S)	200.03
		MACH NUMBER	0.18

FLIGHT/AERO

PITCH ANGLE	2.4	BANK ANGLE	-0.2
ANGLE OF ATTACK	6.4	SIDESLIP	-0.6
HEADING ANGLE	273.3	RATE OF CLIMB (FPM)	-821
PITCH VELOCITY (D/S)	-0.016	PITCH ACCELERATION	-0.0000
ROLL VELOCITY (D/S)	0.000	ROLL ACCELERATION	-0.0000
YAW VELOCITY (D/S)	0.023	YAW ACCELERATION	-0.0000
NORTH-SOUTH VELOCITY	86.11	NORTH-SOUTH ACCEL	-0.025
EAST-WEST VELOCITY	-180.05	EAST-WEST ACCELERATION	0.210
VERTICAL VELOCITY	13.63	VERTICAL ACCELERATION	-0.482
LONGITUDINAL ACCEL	0.0376	TOTAL PITCHING MOMENT	-176
LATERAL ACCEL	0.0046	TOTAL ROLLING MOMENT	-640
VERTICAL ACCEL (G'S)	-1.0149	TOTAL YAWING MOMENT	-16

CONTROL LOADING

ELEVATOR POSITION	-5.43	ELEVATOR TRIM TAB	12.69
COLUMN FORCE	15.94	COLUMN POSITION	3.25
RUDDER POSITION	-3.51	RUDDER TRIM TAB	3.79
PEDAL FORCE	-8.97	PEDAL POSITION	-0.38
AILERON POSITION	0.19	AILERON TRIM TAB	0.42
WHEEL FORCE	-1.52	WHEEL POSITION	0.52

ENGINES

TOTAL THRUST	4848	THRUST COEFFICIENT	0.08
THROTTLE ANGLE	46.4	LATERAL T.C.	0.08
ENGINE S.H.P.	463	ENGINE T.I.T.	549

WEIGHT AND BALANCE

IXX INERTIA (/ 1024)	725	IYY INERTIA (/ 1024)	861
IZZ INERTIA (/ 1024)	1549	CROSS PRODUCT/INERTIA	43222

NOTE: VALUES INVALID DURING ATG - TO USE COL MARKER SW FOR SNAPS SET COLSNP TRUE

FUEL TANK	FUEL LOAD	ENGINE	1	2	3	4	BRAKES
		SHP	483	484	499	597	PILOT
1	3983	TIT	550	550	552	564	COPILOT
2	3983	FUEL FLOW	849	849	855	893	FLIGHT
3	3983						IAS 114
4	3983						ALT 490
5	997	RUNWAY- 100 MOFFETT NAS RWY 32R					HDG 321.6

FLIGHT CONDITIONS PAGE

FLIGHT TIMER	00:00:00	MET TIMER	00:01:13
GROSS WEIGHT	90144	PRESSURE ALTITUDE	524.0
C.G.	24.65	CALIBRATED AIRSPD	114.5
FLAP POSITION	19.1	EQUIVALENT AIRSPD	114.53
GEAR POSITION	1.0	TRUE AIRSPD (F/S)	195.12
		MACH NUMBER	0.18

FLIGHT/AERO

PITCH ANGLE	7.7	BANK ANGLE	-1.8
ANGLE OF ATTACK	6.6	SIDESLIP	-0.2
HEADING ANGLE	338.8	RATE OF CLIMB (FPM)	252
PITCH VELOCITY (D/S)	0.250	PITCH ACCELERATION	0.0025
ROLL VELOCITY (D/S)	-0.141	ROLL ACCELERATION	-0.0007
YAW VELOCITY (D/S)	-0.359	YAW ACCELERATION	0.0011
NORTH-SOUTH VELOCITY	195.01	NORTH-SOUTH ACCEL	-0.238
EAST-WEST VELOCITY	5.56	EAST-WEST ACCELERATION	-1.073
VERTICAL VELOCITY	-4.21	VERTICAL ACCELERATION	-0.013
LONGITUDINAL ACCEL	0.1284	TOTAL PITCHING MOMENT	2128
LATERAL ACCEL	-0.0010	TOTAL ROLLING MOMENT	-576
VERTICAL ACCEL (G'S)	-0.9914	TOTAL YAWING MOMENT	1837

CONTROL LOADING

ELEVATOR POSITION	-3.96	ELEVATOR TRIM TAB	12.69
COLUMN FORCE	8.94	COLUMN POSITION	4.05
RUDDER POSITION	-3.16	RUDDER TRIM TAB	3.79
PEDAL FORCE	-5.06	PEDAL POSITION	-0.34
AILERON POSITION	0.68	AILERON TRIM TAB	0.42
WHEEL FORCE	-0.72	WHEEL POSITION	2.15

ENGINES

TOTAL THRUST	5056	THRUST COEFFICIENT	0.09
THROTTLE ANGLE	46.4	LATERAL T.C.	0.08
ENGINE S.H.P.	460	ENGINE T.I.T.	550

WEIGHT AND BALANCE

IXX INERTIA (/ 1024)	728	IYY INERTIA (/ 1024)	862
IZZ INERTIA (/ 1024)	1551	CROSS PRODUCT/INERTIA	43270

NOTE: VALUES INVALID DURING ATG - TO USE COL MARKER SW FOR SNAPS SET COLSNP TRUE

FUEL TANK	FUEL LOAD	ENGINE	1	2	3	4	BRAKES
1	3917	SHP	484	483	500	597	PILOT
2	3917	TIT	549	549	551	564	COPILOT
3	3917	FUEL FLOW	849	849	855	893	FLIGHT
4	3915						IAS 114
5	996	RUNWAY- 100 MOFFETT NAS RWY 32R					ALT 490
							HDG 255.8

FLIGHT CONDITIONS PAGE

FLIGHT TIMER	00:00:00	MET TIMER	00:05:10
GROSS WEIGHT	89880	PRESSURE ALTITUDE	524.0
C.G.	30.00	CALIBRATED AIRSPD	114.7
FLAP POSITION	19.1	EQUIVALENT AIRSPD	114.72
GEAR POSITION	1.0	TRUE AIRSPD (F/S)	195.28
		MACH NUMBER	0.18

FLIGHT/AERO

PITCH ANGLE	8.1	BANK ANGLE	0.4
ANGLE OF ATTACK	6.2	SIDESLIP	-0.3
HEADING ANGLE	272.9	RATE OF CLIMB (FPM)	407
PITCH VELOCITY (D/S)	-0.039	PITCH ACCELERATION	0.0020
ROLL VELOCITY (D/S)	-0.086	ROLL ACCELERATION	-0.0011
YAW VELOCITY (D/S)	0.062	YAW ACCELERATION	-0.0014
NORTH-SOUTH VELOCITY	84.02	NORTH-SOUTH ACCEL	0.438
EAST-WEST VELOCITY	-176.15	EAST-WEST ACCELERATION	0.376
VERTICAL VELOCITY	-6.78	VERTICAL ACCELERATION	0.123
LONGITUDINAL ACCEL	0.1567	TOTAL PITCHING MOMENT	2384
LATERAL ACCEL	0.0002	TOTAL ROLLING MOMENT	-768
VERTICAL ACCEL (G'S)	-0.9844	TOTAL YAWING MOMENT	-2103

CONTROL LOADING

ELEVATOR POSITION	-1.54	ELEVATOR TRIM TAB	12.55
COLUMN FORCE	1.19	COLUMN POSITION	5.33
RUDDER POSITION	-3.10	RUDDER TRIM TAB	3.79
PEDAL FORCE	-5.31	PEDAL POSITION	-0.34
AILERON POSITION	0.19	AILERON TRIM TAB	0.42
WHEEL FORCE	-1.14	WHEEL POSITION	0.53

ENGINES

TOTAL THRUST	5056	THRUST COEFFICIENT	0.09
THROTTLE ANGLE	46.4	LATERAL T.C.	0.08
ENGINE S.H.P.	460	ENGINE T.I.T.	549

WEIGHT AND BALANCE

IXX INERTIA (/ 1024)	725	IYY INERTIA (/ 1024)	861
Izz INERTIA (/ 1024)	1548	CROSS PRODUCT/INERTIA	43214

NOTE: VALUES INVALID DURING ATG - TO USE COL MARKER SW FOR SNAPS SET COLSNP TRUE

FUEL TANK	FUEL LOAD	ENGINE	1	2	3	4	BRAKES
1	3911	SHP	486	485	496	601	PILOT
2	3911	TIT	550	550	551	564	COPILOT
3	3910	FUEL FLOW	848	848	853	893	FLIGHT
4	3908						IAS 108
5	996	RUNWAY- 100 MOFFETT NAS RWY 32R					ALT 490
							HDG 252.4

FLIGHT CONDITIONS PAGE

FLIGHT TIMER	00:00:00	MET TIMER	00:05:32
GROSS WEIGHT	89856	PRESSURE ALTITUDE	524.0
C.G.	30.00	CALIBRATED AIRSPD	108.6
FLAP POSITION	19.1	EQUIVALENT AIRSPD	108.59
GEAR POSITION	1.0	TRUE AIRSPD (F/S)	185.09
		MACH NUMBER	0.17

FLIGHT/AERO

PITCH ANGLE	12.8	BANK ANGLE	1.1
ANGLE OF ATTACK	7.3	SIDESLIP	0.7
HEADING ANGLE	269.5	RATE OF CLIMB (FPM)	1085
PITCH VELOCITY (D/S)	-0.109	PITCH ACCELERATION	0.0002
ROLL VELOCITY (D/S)	0.070	ROLL ACCELERATION	-0.0003
YAW VELOCITY (D/S)	0.062	YAW ACCELERATION	-0.0002
NORTH-SOUTH VELOCITY	71.96	NORTH-SOUTH ACCEL	0.255
EAST-WEST VELOCITY	-169.59	EAST-WEST ACCELERATION	-0.033
VERTICAL VELOCITY	-18.07	VERTICAL ACCELERATION	0.483
LONGITUDINAL ACCEL	0.2229	TOTAL PITCHING MOMENT	80
LATERAL ACCEL	-0.0112	TOTAL ROLLING MOMENT	-192
VERTICAL ACCEL (G'S)	-0.9587	TOTAL YAWING MOMENT	-276

CONTROL LOADING

ELEVATOR POSITION	-1.72	ELEVATOR TRIM TAB	12.42
COLUMN FORCE	1.41	COLUMN POSITION	5.23
RUDDER POSITION	-2.91	RUDDER TRIM TAB	3.79
PEDAL FORCE	-4.37	PEDAL POSITION	-0.32
AILERON POSITION	1.38	AILERON TRIM TAB	0.42
WHEEL FORCE	-1.17	WHEEL POSITION	4.28

ENGINES

TOTAL THRUST	5168	THRUST COEFFICIENT	0.10
THROTTLE ANGLE	46.4	LATERAL T.C.	0.10
ENGINE S.H.P.	463	ENGINE T.I.T.	550

WEIGHT AND BALANCE

IXX INERTIA (/ 1024)	724	IYY INERTIA (/ 1024)	861
IZZ INERTIA (/ 1024)	1548	CROSS PRODUCT/INERTIA	43206

NOTE: VALUES INVALID DURING ATG - TO USE COL MARKER SW FOR SNAPS SET COLSNP TRUE

FUEL TANK	FUEL LOAD	ENGINE	1	2	3	4	BRAKES
1	10000	SHF	4744	4744	4744	4744	PILOT
2	10000	TIT	1075	1075	1075	1075	COPILOT
3	10000	FUEL FLOW	2467	2466	2466	2467	FLIGHT
4	10000						IAS 125
5	995	RUNWAY- 100 MOFFETT NAS RWY 32R					ALT 490
							HDG 228.6

FLIGHT CONDITIONS PAGE

FLIGHT TIMER	00:00:00	MET TIMER	00:07:52
GROSS WEIGHT	114200	CONFIGURATION/CONDITIONS	
C.G.	26.01	PRESSURE ALTITUDE	524.0
FLAP POSITION	19.1	CALIBRATED AIRSPD	125.6
GEAR POSITION	1.0	EQUIVALENT AIRSPD	125.59
		TRUE AIRSPD (F/S)	213.97
		MACH NUMBER	0.19
		FLIGHT/AERO	
PITCH ANGLE	8.0	BANK ANGLE	-2.7
ANGLE OF ATTACK	4.6	SIDESLIP	-0.8
HEADING ANGLE	246.1	RATE OF CLIMB (FPM)	759
PITCH VELOCITY (D/S)	0.273	PITCH ACCELERATION	0.0000
ROLL VELOCITY (D/S)	-0.430	ROLL ACCELERATION	0.0010
YAW VELOCITY (D/S)	-0.500	YAW ACCELERATION	-0.0048
NORTH-SOUTH VELOCITY	-5.82	NORTH-SOUTH ACCEL	-1.923
EAST-WEST VELOCITY	-213.54	EAST-WEST ACCELERATION	0.015
VERTICAL VELOCITY	-12.72	VERTICAL ACCELERATION	-0.801
LONGITUDINAL ACCEL	0.1443	TOTAL PITCHING MOMENT	-176
LATERAL ACCEL	-0.0097	TOTAL ROLLING MOMENT	1344
VERTICAL ACCEL (G'S)	-1.0163	TOTAL YAWING MOMENT	-9720
		CONTROL LOADING	
ELEVATOR POSITION	-2.78	ELEVATOR TRIM TAB	10.69
COLUMN FORCE	6.28	COLUMN POSITION	4.66
RUDDER POSITION	-10.06	RUDDER TRIM TAB	5.08
PEDAL FORCE	-46.25	PEDAL POSITION	-1.12
AILERON POSITION	1.29	AILERON TRIM TAB	0.42
WHEEL FORCE	-1.56	WHEEL POSITION	4.04
		ENGINES	
TOTAL THRUST	29280	THRUST COEFFICIENT	0.42
THROTTLE ANGLE	90.0	LATERAL T.C.	0.42
ENGINE S.H.P.	4699	ENGINE T.I.T.	1075
		WEIGHT AND BALANCE	
IXX INERTIA (/ 1024)	1154	IYY INERTIA (/ 1024)	872
IZZ INERTIA (/ 1024)	1984	CROSS PRODUCT/INERTIA	47766

NOTE: VALUES INVALID DURING ATG - TO USE COL MARKER SW FOR SNAPS SET COLSNP TRUE

FUEL TANK	FUEL LOAD	ENGINE	1	2	3	4	BRAKES
1	10000	SHF	4720	4722	4722	4720	PILOT
2	10000	TIT	1075	1075	1075	1075	COPILOT
3	10000	FUEL FLOW	2459	2459	2459	2459	FLIGHT
4	10000						IAS 113
5	995	RUNWAY- 100 MOFFETT NAS RWY 32R					ALT 490
							HDG 203.1

FLIGHT CONDITIONS PAGE

FLIGHT TIMER	00:00:00	MET TIMER	00:08:32
GROSS WEIGHT	114208	CONFIGURATION/CONDITIONS	
C.G.	26.01	PRESSURE ALTITUDE	524.0
FLAP POSITION	19.1	CALIBRATED AIRSPD	112.7
GEAR POSITION	1.0	EQUIVALENT AIRSPD	112.72
		TRUE AIRSPD (F/S)	192.12
		MACH NUMBER	0.17

FLIGHT/AERO

PITCH ANGLE	12.9	BANK ANGLE	-0.5
ANGLE OF ATTACK	5.9	SIDESLIP	-2.3
HEADING ANGLE	220.1	RATE OF CLIMB (FPM)	1425
PITCH VELOCITY (D/S)	-0.297	PITCH ACCELERATION	0.0022
ROLL VELOCITY (D/S)	0.102	ROLL ACCELERATION	-0.0014
YAW VELOCITY (D/S)	0.039	YAW ACCELERATION	-0.0004
NORTH-SOUTH VELOCITY	-92.79	NORTH-SOUTH ACCEL	-0.024
EAST-WEST VELOCITY	-166.59	EAST-WEST ACCELERATION	-0.234
VERTICAL VELOCITY	-23.70	VERTICAL ACCELERATION	0.929
LONGITUDINAL ACCEL	0.2163	TOTAL PITCHING MOMENT	1872
LATERAL ACCEL	0.0105	TOTAL ROLLING MOMENT	-1728
VERTICAL ACCEL (G'S)	-0.9460	TOTAL YAWING MOMENT	-710

CONTROL LOADING

ELEVATOR POSITION	-3.15	ELEVATOR TRIM TAB	10.69
COLUMN FORCE	8.00	COLUMN POSITION	4.45
RUDDER POSITION	-12.70	RUDDER TRIM TAB	5.08
PEDAL FORCE	-48.78	PEDAL POSITION	-1.41
AILERON POSITION	0.75	AILERON TRIM TAB	0.42
WHEEL FORCE	-0.83	WHEEL POSITION	2.34

ENGINES

TOTAL THRUST	30176	THRUST COEFFICIENT	0.54
THROTTLE ANGLE	90.0	LATERAL T.C.	0.54
ENGINE S.H.P.	4671	ENGINE T.I.T.	1075

WEIGHT AND BALANCE

IXX INERTIA (/ 1024)	1154	IYY INERTIA (/ 1024)	872
IZZ INERTIA (/ 1024)	1984	CROSS PRODUCT/INERTIA	47766

NOTE: VALUES INVALID DURING ATG - TO USE COL MARKER SW FOR SNAPS SET COLSNP TRUE

FUEL TANK	FUEL LOAD	ENGINE	1	2	3	4	BRAKES
1	10000	SHP	4743	4742	4742	4743	PILOT
2	10000	TIT	1075	1075	1075	1075	COPILOT
3	10000	FUEL FLOW	2465	2465	2465	2465	FLIGHT
4	10000						IAS 124
5	995	RUNWAY- 100 MOFFETT NAS RWY 32R					ALT 490
							HDG 193.7

FLIGHT CONDITIONS PAGE

FLIGHT TIMER	00:00:00	MET TIMER	00:09:06
GROSS WEIGHT	114208	PRESSURE ALTITUDE	524.0
C.G.	21.00	CALIBRATED AIRSPD	124.2
FLAP POSITION	19.1	EQUIVALENT AIRSPD	124.16
GEAR POSITION	1.0	TRUE AIRSPD (F/S)	211.66
		MACH NUMBER	0.19

FLIGHT/AERO

PITCH ANGLE	8.5	BANK ANGLE	-1.2
ANGLE OF ATTACK	5.1	SIDESLIP	-4.1
HEADING ANGLE	210.7	RATE OF CLIMB (FPM)	757
PITCH VELOCITY (D/S)	0.086	PITCH ACCELERATION	-0.0016
ROLL VELOCITY (D/S)	0.250	ROLL ACCELERATION	-0.0037
YAW VELOCITY (D/S)	-0.180	YAW ACCELERATION	-0.0048
NORTH-SOUTH VELOCITY	-136.83	NORTH-SOUTH ACCEL	0.518
EAST-WEST VELOCITY	-160.99	EAST-WEST ACCELERATION	-0.250
VERTICAL VELOCITY	-12.68	VERTICAL ACCELERATION	-0.932
LONGITUDINAL ACCEL	0.1521	TOTAL PITCHING MOMENT	-1456
LATERAL ACCEL	0.0393	TOTAL ROLLING MOMENT	-4160
VERTICAL ACCEL (G'S)	-1.0176	TOTAL YAWING MOMENT	-9577

CONTROL LOADING

ELEVATOR POSITION	-4.99	ELEVATOR TRIM TAB	10.69
COLUMN FORCE	16.50	COLUMN POSITION	3.46
RUDDER POSITION	-14.61	RUDDER TRIM TAB	0.98
PEDAL FORCE	-52.44	PEDAL POSITION	-1.62
AILERON POSITION	0.17	AILERON TRIM TAB	0.42
WHEEL FORCE	-1.41	WHEEL POSITION	0.45

ENGINES

TOTAL THRUST	29376	THRUST COEFFICIENT	0.43
THROTTLE ANGLE	90.0	LATERAL T.C.	0.43
ENGINE S.H.P.	4693	ENGINE T.I.T.	1075

WEIGHT AND BALANCE

IXX INERTIA (/ 1024)	1154	IYY INERTIA (/ 1024)	872
IZZ INERTIA (/ 1024)	1984	CROSS PRODUCT/INERTIA	47766

NOTE: VALUES INVALID DURING ATG - TO USE COL MARKER SW FOR SNAPS SET COLSNP TRUE

FUEL TANK	FUEL LOAD	ENGINE	1	2	3	4	BRAKES
1	10000	SHF	4722	4721	4721	4722	PILOT
2	10000	TIT	1075	1075	1075	1075	COPILOT
3	10000	FUEL FLOW	2459	2459	2459	2459	FLIGHT
4	10000						IAS 113
5	995	RUNWAY- 100 MOFFETT NAS RWY 32R					ALT 490
							HDG 171.9

FLIGHT CONDITIONS PAGE

FLIGHT TIMER	00:00:00	MET TIMER	00:10:07
GROSS WEIGHT	114200	CONFIGURATION/CONDITIONS	
C.G.	21.00	PRESSURE ALTITUDE	524.0
FLAP POSITION	19.1	CALIBRATED AIRSPD	112.6
GEAR POSITION	1.0	EQUIVALENT AIRSPD	112.56
		TRUE AIRSPD (F/S)	191.91
		MACH NUMBER	0.17
		FLIGHT/AERO	
PITCH ANGLE	12.6	BANK ANGLE	-0.7
ANGLE OF ATTACK	6.8	SIDESLIP	-2.5
HEADING ANGLE	108.7	RATE OF CLIMB (FPM)	1169
PITCH VELOCITY (D/S)	-0.070	PITCH ACCELERATION	-0.0010
ROLL VELOCITY (D/S)	0.273	ROLL ACCELERATION	-0.0012
YAW VELOCITY (D/S)	0.055	YAW ACCELERATION	0.0032
NORTH-SOUTH VELOCITY	-166.58	NORTH-SOUTH ACCEL	-0.232
EAST-WEST VELOCITY	-93.36	EAST-WEST ACCELERATION	-0.130
VERTICAL VELOCITY	-19.51	VERTICAL ACCELERATION	-0.237
LONGITUDINAL ACCEL	0.2287	TOTAL PITCHING MOMENT	-944
LATERAL ACCEL	0.0112	TOTAL ROLLING MOMENT	-1600
VERTICAL ACCEL (G'S)	-0.9812	TOTAL YAWING MOMENT	6515
		CONTROL LOADING	
ELEVATOR POSITION	-6.02	ELEVATOR TRIM TAB	10.69
COLUMN FORCE	15.87	COLUMN POSITION	2.96
RUDDER POSITION	-14.19	RUDDER TRIM TAB	8.98
PEDAL FORCE	-41.87	PEDAL POSITION	-1.56
AILERON POSITION	0.90	AILERON TRIM TAB	0.42
WHEEL FORCE	1.61	WHEEL POSITION	3.13
		ENGINES	
TOTAL THRUST	30200	THRUST COEFFICIENT	0.54
THROTTLE ANGLE	90.0	LATERAL T.C.	0.54
ENGINE S.H.P.	4674	ENGINE T.I.T.	1075
		WEIGHT AND BALANCE	
IXX INERTIA (/ 1024)	1154	IYY INERTIA (/ 1024)	872
IZZ INERTIA (/ 1024)	1984	CROSS PRODUCT/INERTIA	47766

NOTE: VALUES INVALID DURING ATG - TO USE COL MARKER SW FOR SNAPS SET COLSNP TRUE

INITIAL DISTRIBUTION LIST

- | | |
|---|----------|
| <p>1. Deputy Chief of Naval Operations
 Air Warfare (Safety)
 Code OP-05F
 Washington, D.C.</p> | <p>1</p> |
| <p>2. Commander Patrol Wings
 U.S. Pacific Fleet
 Code 003
 NAS Moffett Field, CA 94035-5003</p> | <p>1</p> |
| <p>3. Commander Patrol Wings
 U.S. Atlantic Fleet
 Code 002
 Brunswick, ME 04011-5000</p> | <p>1</p> |
| <p>4. Commander Training Wing Four
 Attn: T-44 Model Manager
 Corpus Christi, TX 78419</p> | <p>1</p> |
| <p>5. Commander Naval Safety Center
 Code 00
 NAS Norfolk, VA 23511-5796</p> | <p>1</p> |
| <p>6. Commanding Officer Patrol Squadron Thirty
 Attn: CNAL Evaluator
 NAS Jacksonville, FL 32212</p> | <p>1</p> |
| <p>7. Commanding Officer Patrol Squadron Thirty-One
 Attn: P-3 Model Manager
 NAS Moffett Field, CA 94035</p> | <p>1</p> |
| <p>8. Aviation Safety Programs
 Code 034
 Naval Postgraduate School
 Monterey, CA 93943-5100</p> | <p>1</p> |

- | | |
|---|---|
| 9. Henry H. Smith ED. D.
Code 00A
Patrol Squadron Thirty-One
NAS Moffett Field, CA 94035 | 2 |
| 10. Herbert W. Schlickemaier
Federal Aviation Administration
Code ARD-200
800 Independence Ave. S.W.
Washington, D.C. 20591 | 2 |
| 11. Richard S. Bray
NASA Ames Research Center
Bldg. 211
NAS Moffett Field, CA 94035 | 1 |
| 12. Rod Wingrove
NASA Ames Research Center
Bldg. 210
NAS Moffett Field, CA 94035 | 1 |
| 13. Defense Technical Information Center
Cameron Station
Alexandria, VA 22304-6145 | 2 |
| 14. Library, Code 0142
Naval Postgraduate School
Monterey, CA 93943-5002 | 2 |
| 15. E.R. Wood
Code AA/WO
Naval Postgraduate School
Monterey, CA 93943-5000 | 1 |
| 14. Rick Howard
Code AA/HO
Naval Postgraduate School
Monterey, CA 93943-5000 | 1 |
| 15. Thomas Sponsler
Simuflight Training International
2929 W. Airfield Drive
Dallas/Ft. Worth Airport, TX 75261 | 1 |